2010

IN-VITRO METABOLISM AND PROTEIN BINDING OF 5-HMF, A POTENTIAL ANTISICKLING AGENT

Taghrid Obied
Virginia Commonwealth University

IN-VITRO METABOLISM AND PROTEIN BINDING OF 5-HMF, A POTENTIAL ANTISICKLING AGENT

A dissertation submitted in partial fulfillment of the requirements for the degree of Doctor of Philosophy at Virginia Commonwealth University.

by

TAGHRID YOUSEF RASHID OBIED

MS. Pharmaceutical Sciences, Virginia Commonwealth University, 2007

B.Sc. Pharmacy, University of Jordan, Jordan, 2003

Director: Jürgen Venitz, M.D., Ph.D.

Associate Professor, Department of Pharmaceutics

Virginia Commonwealth University
Richmond, Virginia
February 2010

ACKNOWLEDGEMENTS

I wish to cordially thank all of those who supported me and allowed me to establish my life in the USA.

First of all, I would like to express my grateful appreciation for my advisor Dr. Jürgen Venitz for his continuous valued mentorship through the past five years. I am very much thankful for his expert guidance and creative comments. His assistance in clarifying my thoughts and his challenging questions had led me through my entire dissertation project to explore novel ideas.

My gracious thanks to my committee members: Dr. Thomas Karnes, Dr. Patricia Slattum, Dr. Philip Gerk, Dr. Martin Safo, and Dr. John Roberts for their kind review and help in my dissertation project.

I would like to convey my gratitude to Dr. Philip Gerk and Dr. Thomas Karnes and their lab members for being generous in allowing me to use their instruments and for advising me regarding various issues and difficulties that I faced.

I am really indebted to my Pharmacokinetics/Pharmacodynamics research group members, in particular, David Lee, Satjit Brar, Prajakta Badri, Soniya Vaiyda, and Pankaj

Gupta who highlighted me with their knowledge and enthusiasm that motivated me to the end.

My heartfelt thanks to my beloved, Ahmad, my family, and friends for their continuous spiritual support and patience. Their assistance in immeasurable ways and their faith in me have enlightened my entire life.

TABLE OF CONTENTS

Page

LIST OF TABLES

LIST OF FIGURES

List of Abbreviations

AAG	α-Acid glycoprotein
AUC	Area under the curve
BCS	The biopharmaceutics classification system
B_{max}	Maximum binding capacity
CL	Clearance
CL_{int}	Intrinsic clearance
CL_{met}	Metabolic clearance
CL_{tot}	Total clearance
CV	Coefficient of variation

DFN	Difference from nominal
FDA	Food and drug administration
FDCA	2,5-Furan dicarboxylic acid
F_{oral}	Oral bioavailability
FTIM	First-time in man study
F_u	Fraction unbound to protein
Hemoglobin	Hemoglobin
HbA	Adult hemoglobin
HbF	Fetal hemoglobin
HbS	Sickled hemoglobin
5-HMF	5-Hydroxymethylfurfural
HMFA	5-Hydroxmethyl-2-furoic acid
HSA	Human serum albumin

IC_{50}	The concentration of the drug that causes a 50% inhibition in the substrate metabolism
IV	Intravenous route
K_1	Forward rate constant
K_{-1}	Backward rate constant
K_A	Equilibrium association constant
K_d	Equilibrium dissociation constant
K_i	Affinity constant
K_M	Metabolic affinity constant
Log P	Octanol-to-water partition coefficient
LLOQ	Lower limit of quantitation
LOD	Lower limit of detection
NAD^+	Nicotinamide adenine dinucleotide
NSB	Nonspecific binding

NTP	National toxicology program
O_2	Molecular oxygen
OEC	Oxygen equilibrium curve
PBS	Phosphate-buffered saline
PHARMACODYNAMICS	Pharmacodynamics
PHARMACOKINETICS	Pharmacokinetics
pKa	Negative log of the acid association constant
pK_i	Negative log of the affinity constant
pO_2	Oxygen affinity
QC	Quality control
r^2	Coefficient of determination
SB	Specific binding
SCD	Sickle cell disease

SD	Standard deviation
SS Cells	Red blood cells containing HbS
Vd_{ss}	Volume of distribution at steady state
V_{max}	Maximum metabolic capacity

Abstract

IN-VITRO METABOLISM AND PROTEIN BINDING OF 5-HMF,
A POTENTIAL ANTISICKLING AGENT

By Taghrid Yousef Rashid Obied, MS. Pharmaceutical Sciences

A dissertation submitted in partial fulfillment of the requirements for the degree of Doctor of Philosophy at Virginia Commonwealth University.

Virginia Commonwealth University, 2010

Major Director: Jürgen Venitz, M.D., Ph.D.
Associate Professor, Department of Pharmaceutics

Purpose. 5-HMF is a potential antisickling agent forming a Schiff-adduct with hemoglobin (Hb). *In-vitro* studies were designed to identify the metabolic pathways of 5-HMF in human hepatic cytosol, to assess inter-species differences in its hepatic metabolism, and to predict *in-vivo* PK properties. Moreover, metabolism of 5-HMF in human RBCs was investigated. Finally, *in-vitro* studies were done to characterize 5-HMF binding kinetics with human Hb and albumin (HSA).

Methods. NAD^+ reduction was monitored at 340 nm in human hepatic cytosol for 5-HMF (26 mM) and prototypical ADH and ALDH substrates in the presence or absence of their inhibitors. Furthermore, concentration-dependency studies were performed for 5-HMF (1.5-96 mM) in mouse, rat, dog, and human hepatic cytosol and fitted by Michaelis Menten (MM) model. *In-vitro-in-vivo*-extrapolation (IVIVE) was performed using the well-stirred model. Moreover, metabolic studies of 5-HMF (12-142 mM) in human RBCs were done under similar conditions.

Time- and concentration-dependent binding studies were conducted for 5-HMF (5 µM-5 mM), in Hb (217 µM) and HSA (6 3 and 202 µM) solutions. Ultrafiltered 5-HMF concentrations were measured by a validated HPLC-UV assay. After correction for nonspecific binding, rate constants, binding affinity, and capacity were estimated by nonlinear regression.

Results. In human hepatic cytosol, 5-HMF followed MM kinetics with K_m: 218(±74) mM and was mainly inhibited by the ALDH inhibitor. In all animal species, 5-HMF exhibited millimolar K_m values and is expected to have low hepatic extraction, high oral bioavailability, and first-order PK for relevant blood concentrations. The IVIVE-predicted *in-vivo* half-lives for 5-HMF were adequate for the mouse and dog but overestimated for humans. In RBCs, 5-HMF had $Cl_{int}^{in\text{-}vitro}$ of 0.34(± 0.02) ml/min/ml RBCs scaled-up to 9.9 ml/min/kg.

Time-dependent binding of 5-HMF was demonstrated for both Hb and HSA. Steady-state studies revealed saturable Hb binding and non-saturable HSA binding.

Conclusions. 5-HMF is an ALDH/ADH substrate in hepatic cytosol. Across animal species, 5-HMF is expected to be a low-hepatic-extraction-ratio drug with high oral bioavailability. 5-HMF is subject to RBCs metabolism in human. 5-HMF is expected to show fast association with, but slow dissociation from its drug target, Hb, which may lead to a prolonged *in-vivo* PD effect.

CHAPTER 1

INTRODUCTION

1.1 Sickle Cell Disease

1.1.1 Prevalence

Sickle cell disease (SCD) is one of the most common inheritable genetic diseases worldwide (Niscola 2009) (Wahl 2009). SCD is affecting 1 in every 375 African-American births in the USA, 100,000 patients in the general USA population, and it has an estimate of 20-25 million patients in the world (Aliyu 2008) (Driscoll 2007) (Bolaños-Meade 2009) (Field 2009). The frequency of SCD is becoming more uniform through the world because of the immigration of patients to countries with low SCD incidence history (Niscola 2009).

1.1.2 Pathogenesis

The pathogenesis of the disease reveals a substitution of the normal GAG codon with GTG resulting in the expression of sickled hemoglobin (HbS) rather than adult hemoglobin (HbA), where glutamic acid amino acid is replaced by valine amino acid at the sixth position of β-globin protein in patients with SCD (Niscola 2009) (Smiley 2008) (Wahl 2009). The resultant HbS is less stable and less soluble than the normal HbA (Niscola 2009). Consequently, the typically flexible doughnut shape of red blood cells (RBCs) is altered to stiff crescent-like RBCs, in which Hb is likely to polymerize upon uploading its oxygen content (Vekilov 2007). Furthermore, patients with SCD might be affected by other hemoglobin abnormalities, such as thalassemia, and the resultant syndrome is dependent of the accompanying defect (Niscola 2009).

1.1.3 Complications

The quality of life of SCD patients ranges from normal asymptomatic life to one with frequent hospitalization (Niscola 2009). Besides leading to anemia as a result of abnormal RBCs destruction, SCD is associated with other complications due to the abnormal shape of RBCs. Infection is an important problem faced by SCD patients and can be severe enough to cause death, e.g. pulmonary infections. Furthermore, the tendency of HbS to polymerize upon deoxygenation results in vascular occlusion (Driscoll 2007). Because of that, acute manifestations like acute splenic sequestration and vaso-occlusive pain crises occur, which is the predominant symptom in SCD patients (Niscola 2009). Niscola and co-workers reported that while 39% of SCD patients had no pain crises, 5.2% of the patients had 3-10 annual pain episodes (Niscola 2009). The pain crises were found more frequent in adults than in children and were associated with higher hematocrit and lower fetal hemoglobin (HbF) percentage (Field 2009). Overall, approximately 90% of SCD patients' hospitalizations are due to the pain episodes that they encounter (Niscola 2009). Other consequences of RBC deformation are chronic organ damage, cerebrovascular disease, and pulmonary hypertension (Smiley 2008) (Driscoll 2007). Because of the chronic nature of SCD and frequent hospitalization, some patients suffer from psychological illnesses as well (Niscola 2009).

1.1.4 Sickle Cell Disease Treatments

1.1.4.1 Non-Opioid Analgesics

Mild to moderate pain is managed by acetaminophen and non-steroidal anti-inflammatory drugs (NSAIDs) in a pathway that leads to desensitizing of the nociceptors responsible for pain, with an advantage of the latter in having an anti-inflammatory effect (Niscola 2009). In severe pain cases, these are combined with opioids to decrease the dose that would be required if opioids were used alone (Field 2009) (Niscola 2009). On the other hand, NSAIDs inhibit the basal levels of prostaglandin and may lead to renal and cardiovascular toxicity (Niscola 2009). Moreover, aspirin is avoided in children due to the risk of Reye's syndrome (Niscola 2009).

1.1.4.2 Opioids

Opioids represent an approach for providing an immediate relief of acute pain episodes (Field 2009). The presence of multiple choices in this class acting on different opioid receptors, ranging from weak agonists, e.g. codeine, to strong agonists, e.g. morphine, and formulated in different dosage forms offers an advantage that encourages clinicians to prescribe them for SCD patients (Niscola 2009) (Field 2009). However, the misuse of these drugs leading to drug dependence is an immense disadvantage in their therapy (Niscola 2009). In addition, if not cautiously administered, opioids may cause death by respiratory depression (Niscola 2009).

1.1.4.3 Hydroxyurea

Currently, hydroxyurea is the only Food and Drug Administration (FDA) approved therapeutic agent for the treatment of SCD (Charache 1997) (Lanzkron 2008). Its disease-modifying properties are a result of its ability to induce HbF production by unclear mechanism of action (Lanzkron 2008). HbF has a higher oxygen affinity than that of HbA (Lanzkron 2008). The protective effect of a relatively higher fraction of HbF in some SCD patients is demonstrated in lower pain episode rates, as discussed in Section 1.1.3 (Niscola 2009). In addition, a two-year study with a maximum hydroxyurea daily dose of 35 mg/kg resulted in 3.5% increase in HbF and a decrease in the annual rate of pain crises (Lanzkron 2008). Upon a seven-year follow-up, it was observed that the mortality rate decreased by 40% (Lanzkron 2008). Unfortunately, hydroxyurea was associated with reproductive toxicity in male mice and developmental toxicity in rat and mice fetuses (Lanzkron 2008). In addition, chronic administration of this agent was associated with leukemia, lymphoma, and skin hyperpigmentation (Lanzkron 2008).

1.1.4.4 Stem Cell Transplant

Other therapeutic approaches are mainly supportive and do not cure the disease with the exception of hematopoietic stem cell transplant, which is hindered by its eligibility criteria and the availability of suitable donors (Lanzkron 2008) (Driscoll 2007). The age of the ideal candidate for a bone marrow transplant is usually not more than 16 years and he should have suffered a major complication of SCD, such as stroke, neuropathy, and retinopathy. In addition, the donor should be a sibling having a matching lymphocyte antigen (Bolaños-Meade 2009). Besides, considering that children are the ones who are undergoing this surgery, families are often worried about the mortality rates and morbidities affecting their growth and development (Bolaños-Meade 2009).

1.1.4.5 Blood Transfusion:

Blood transfusion is indicated for the management of anemia in SCD. The aim of blood transfusion is to dilute HbS with normal blood and increase the life span of circulating RBCs (Wahl 2009). Yet, many complications are associated with this procedure, such as alloimmunization, infection, acute lung injury, and iron overload (Wahl 2009) (Porter 2007).

1.1.4.6 Non-Pharmacological Interventions

Non-pharmacological and behavioral interventions constitute an important part in SCD treatment. Massage and relaxation were reported to decrease the pain rate (Niscola 2009). In addition, optimism and cognitive strategies are used to cope with pain and alter its perception in SCD patients (Niscola 2009).

1.2 5-HMF

1.2.1 Exposure to 5-HMF

5-HMF is a versatile ubiquitous compound, to which humans are exposed in industry, food, and pharmaceutical formulations. As shown in Figure 1-1, 5-HMF is a small (MW: 126 D) molecule with a pKa value of 12.8 (ACS 2009) that behaves as a neutral molecule at physiological pH range.

The following are major areas, in which 5-HMF is involved:

1.2.1.1 5-HMF in Industry

As part of its utility, 5-HMF is used in the synthesis of resins, solvents, polymers, and plant protective agents (NTP 1994). In addition, 5-HMF is produced from biomass and is investigated as an alternative biofuel (Yong 2008). On the other hand, 5-HMF has a negative industrial interaction since it is considered as a potent inhibitor for ethanologenic bacteria growth and fermentation, which are used to produce ethanol (Liu 2006).

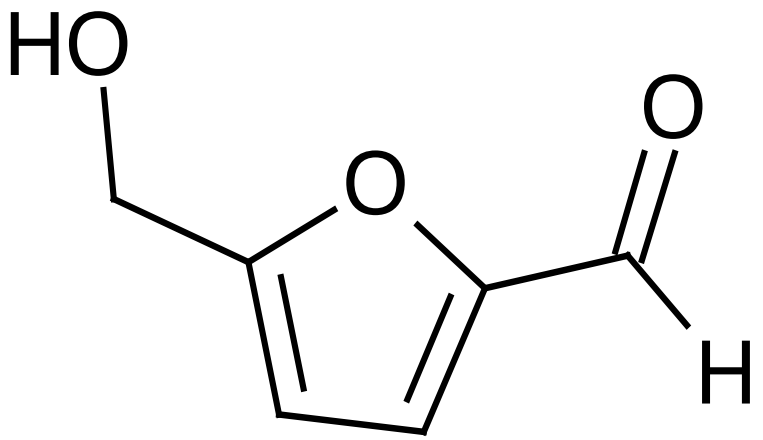

Figure 1-1. 5-HMF structure

1.2.1.2 5-HMF in Drug Formulations

Human exposure to 5-HMF can occur through cigarette smoke and pharmaceutical syrups (NTP 1994). In addition, 5-HMF is found in pharmaceutical products mainly as a degradation product. As a review for its inadvertent presence, 5-HMF concentration in parenteral preparations was reported by Ulbricht et al. In this review, 5-HMF was detected at a concentration of 10 mg/l (Ulbricht 1984) and at a range of 0.2-200 mg/l of 5-HMF in parenteral solutions (Germond 1987). In addition, 5-HMF was identified in a study investigating impurities in a morphine sulfate formulation as a result of including the carboxylate salt of opioids and/or having an acidic formulation (Kelly 2003).

Surprisingly enough, 5-HMF is an active ingredient of a microsupplement product, Sanopal (Matzi 2007). Currently, this product is marketed as a preoperative support for lung resection. Moreover, 5-HMF was identified as a therapeutic moiety in traditional Chinese medicines (Lin 2008) (Li 2005) (Xu 2007).

1.2.1.3 5-HMF in Food

1.2.1.3.1 5-HMF Formation

5-HMF can be found in foods as a result of Maillard reaction, which is a non-enzymatic reaction between free amino groups in protein and reducing sugars that is enhanced by high temperature. Moreover, caramelisation (dehydration) of reducing sugars catalyzed by high temperature and an acidic environment produces 5-HMF (Delgado-Andrade 2007) (M. P. Murkovic 2006) (Gaspar 2009).

5-HMF consumption is affected by food selection and cooking processes (Delgado-Andrade 2007). In a study conducted by Delgado-Andrade et. al., 5-HMF levels were correlated with thermal processing (frying vs. boiling) and sugar content (Delgado-Andrade 2007). It was found that the long heating time and temperature over 90 °C favor the production of furfurals, including 5-HMF (Cocchi 2008).

Along with 5-HMF, 5-methylfurfural (5-MF) and 2-furfural (2-F) are found in food as a result of the Maillard reaction (Gaspar 2009). These compounds were identified as structural analogs for 5-HMF by the National Toxicology Program (NTP) at NIH (NTP 1994). In addition, 5-hydroxymethyl-2-furoic acid (HMFA), which is an identified major metabolite of 5-HMF, was found in food along with 5-HMF (M. B. Murkovic 2007). A peak concentration of around 0.2 mg/g and 0.9 mg/g coffee of HMFA and 5-HMF, respectively, were formed during a roasting process. The fact that HMFA levels peaked after the 5-HMF peak suggested that HMFA is a degradation product of 5-HMF (M. B. Murkovic 2007). However, further investigations proposed an alternative for the production of HMFA (M. B. Murkovic 2007).

1.2.1.3.2 5-HMF CONSUMPTION IN FOOD

5-HMF is found in various types of food such as coffee, honey, biscuits, bread, juice, dried fruits, honey-wines, and cereals (Janzowski 2000) (Gaspar 2009) (Kahoun 2008) (Fallico 2008) at concentrations ranging between 300-1900 mg/kg (M. P. Murkovic 2006). Moreover, 5-HMF is present in traditional drinks such as barley tea, which is a common drink in Japan (Kulkarni 2008). Table 1-1 lists a number of foods with the estimated concentrations of 5-HMF and its primary metabolite (if data available). Considering its abundant presence, it is estimated that the daily consumption of 5-HMF ranges between 30-150 mg (Husøy 2008), which is within the reported acceptable daily intake of 2.5 mg/kg (Germond 1987). Furthermore, 5-HMF levels have been monitored in honey as an indicator for its quality with respect to overheating and aging (Gaspar 2009) (Fallico 2008). In addition, a limit of 0.08 mg/g of 5-HMF was reported to indicate potential adulteration (M. B. Murkovic 2007). Moreover, 5-10 mg/l and 25 mg/l are the recommendations by the International Federation of Fruit Juice Processors for 5-HMF concentration in fruit juice and fruit concentrate, respectively (Gaspar 2009).

Table 1-1. 5-HMF and HMFA concentrations in food.

Food	5-HMF Content (mg/kg)	HMFA Content (mg/kg)	Reference
Dried apricot	30-780	-	(M. P. Murkovic 2006)
Dried pear	100	-	(M. P. Murkovic 2006)
Dried Peach	40	-	(M. P. Murkovic 2006)
Dried plum	1600-2200	-	(M. P. Murkovic 2006)
Dried plum jam	1100-1200	-	(M. P. Murkovic 2006)
Dried date	1000	-	(M. P. Murkovic 2006)
Dried fig	1	-	(M. P. Murkovic 2006)
Dried pineapple	280	-	(M. P. Murkovic 2006)
Dried apple	80	-	(M. P. Murkovic 2006)
Bread with dried fruits	450	-	(M. P. Murkovic 2006)
Baby food	22	-	(M. P. Murkovic 2006)
Coffee (ground, roasted)	300-1900	-	(M. P. Murkovic 2006)
Whole wheat biscuit	0.16	0.18	(Husøy 2008)
Biscuits with chocolate and nuts	0.07	0.08	(Husøy 2008)
Cappuccino with added sugar, instant powder	1.72-143	0.23-17.2	(Husøy 2008)
Coffee instant	91.3-3060	5.6-174	(Husøy 2008)
Ground coffee	262-547	40.3-130	(Husøy 2008)
Bread	0.06-0.14	ND.07	(Husøy 2008)
Narwegian brown cheese	0.08-0.21	ND	(Husøy 2008)
Rasberry jam	0.08	ND	(Husøy 2008)
Honey	0.34	0.05	(Husøy 2008)
Dark beer	13.3	ND	(Husøy 2008)
Chocolate with nuts	ND	ND	(Husøy 2008)
Wine	0.84 g/l	-	(M. B. Murkovic 2007)
Dried plum juice	1.6 g/l	-	(Gaspar 2009)
Balsamic vinegar	1.2- 4.6 g/l	-	(Gaspar 2009)

ND: not detected

1.2.2 5-HMF Mechanism of Action and Pharmacodynamics in Sickle Cell Disease

Safo reported that 5-HMF is a potent agent in reducing the sickling of RBCs containing HbS (SS cells) (Safo 2004). The antisickling action of 5-HMF originates from its ability to form a Schiff base adduct through binding to the N-terminal α-valine amino acid (Abdulmalik 2005) (Safo 2004).

Upon preincubation of 5-HMF in SS cells suspension (haematocrit= 20%), a left-shift in oxygen equilibrium curve (OEC) was observed, shown in Figure 1-2, as a result of increased affinity to oxygen (O_2) in a dose-dependent manner (Abdulmalik 2005) (Safo 2004).

1, 2, and 5 mM of 5-HMF were added to suspensions of RBCs containing HbS (SS cells) (the concentration of SS cells was not specified) and incubated for an hour under air, after which they were exposed to hypoxic conditions for 5 hours. Samples were taken at 0, 1, 2, 3, and 5 hours to investigate the percentage of sickled cells using computer analysis (Abdulmalik 2005). 5-HMF added immediately before exposing the cells to the hypoxic conditions was associated with lower survival of cells in comparison to those pre-incubated with 5-HMF, as shown in Figure 1-3. This might be attributed to the notion that Hb adduct with aldehydes takes approximately an hour to form (Abdulmalik 2005).

The adduct formation in an *in-vivo* system was indicated by the appearance of a new peak in transgenic mice blood using anion-exchange chromatography at 215 nm after an oral administration of 5-HMF. 100% and 70% of Hb-adduct were formed in the transgenic mice after an hour of the oral administration of 100 and 50 mg/kg of 5-HMF, respectively. The peak remained for 3 hours followed by a gradual decrease. The peak was finally disappeared at 6 hours (Abdulmalik 2005). It should be noted that for *in-vitro* determination of Hb-adduct, cation

exchange chromatography along with detection at 410 nm were used, as shown in Figure 1-4 (Abdulmalik 2005).

Further analysis was performed on the data reported by Abdulmalik et. al. in transgenic mice (Abdulmalik 2005). Concentrations of free hemoglobin, 5-HMF plasma concentrations, and the adduct formed over time were combined in a semi-quantitative plot, as shown in Figure 1-5. It is observed that there was a lag-time between the peak plasma concentration and that for the adduct.

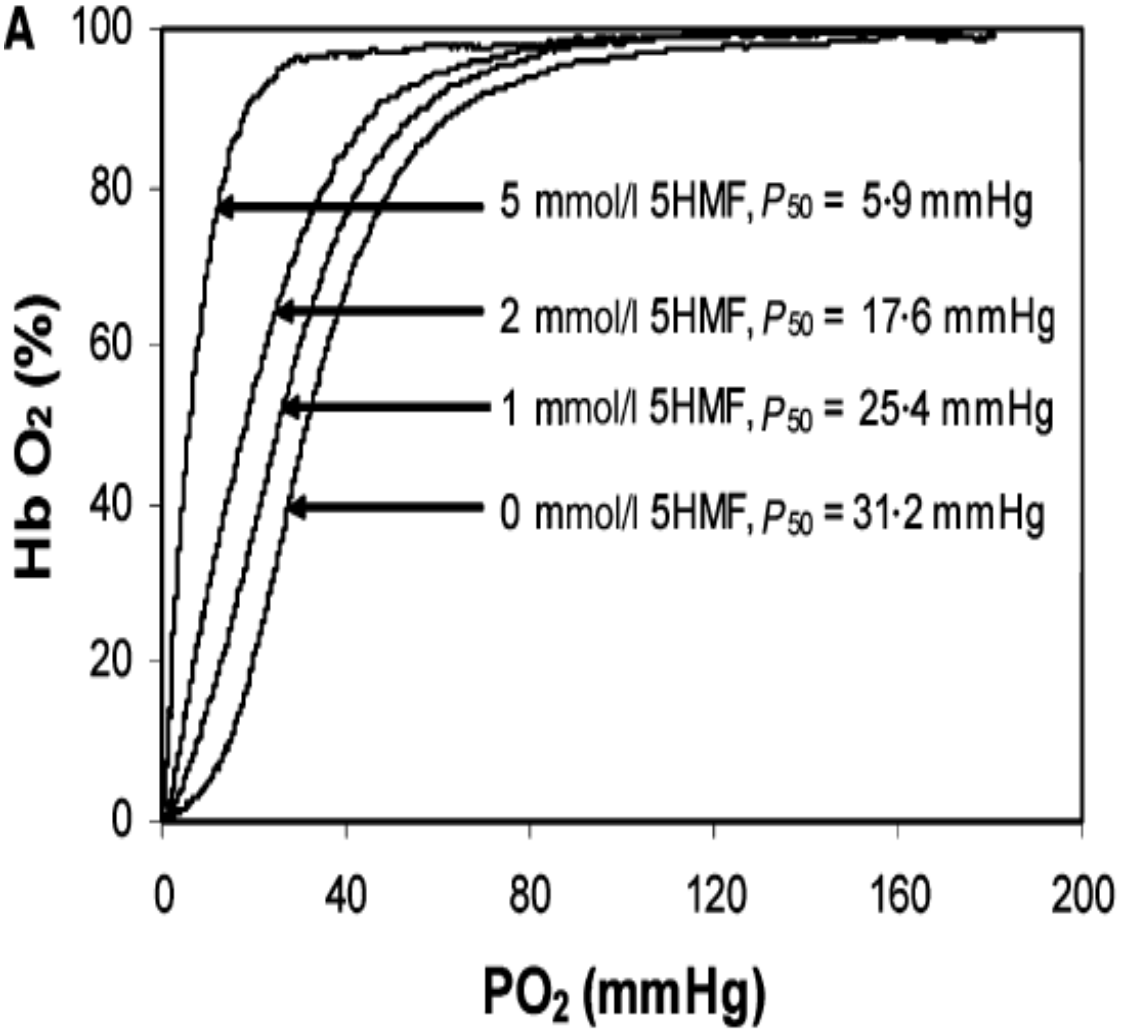

Figure 1-2. Left-shift in oxygen equilibrium curve upon incubation with 5-HMF. **(Abdulmalik 2005)**

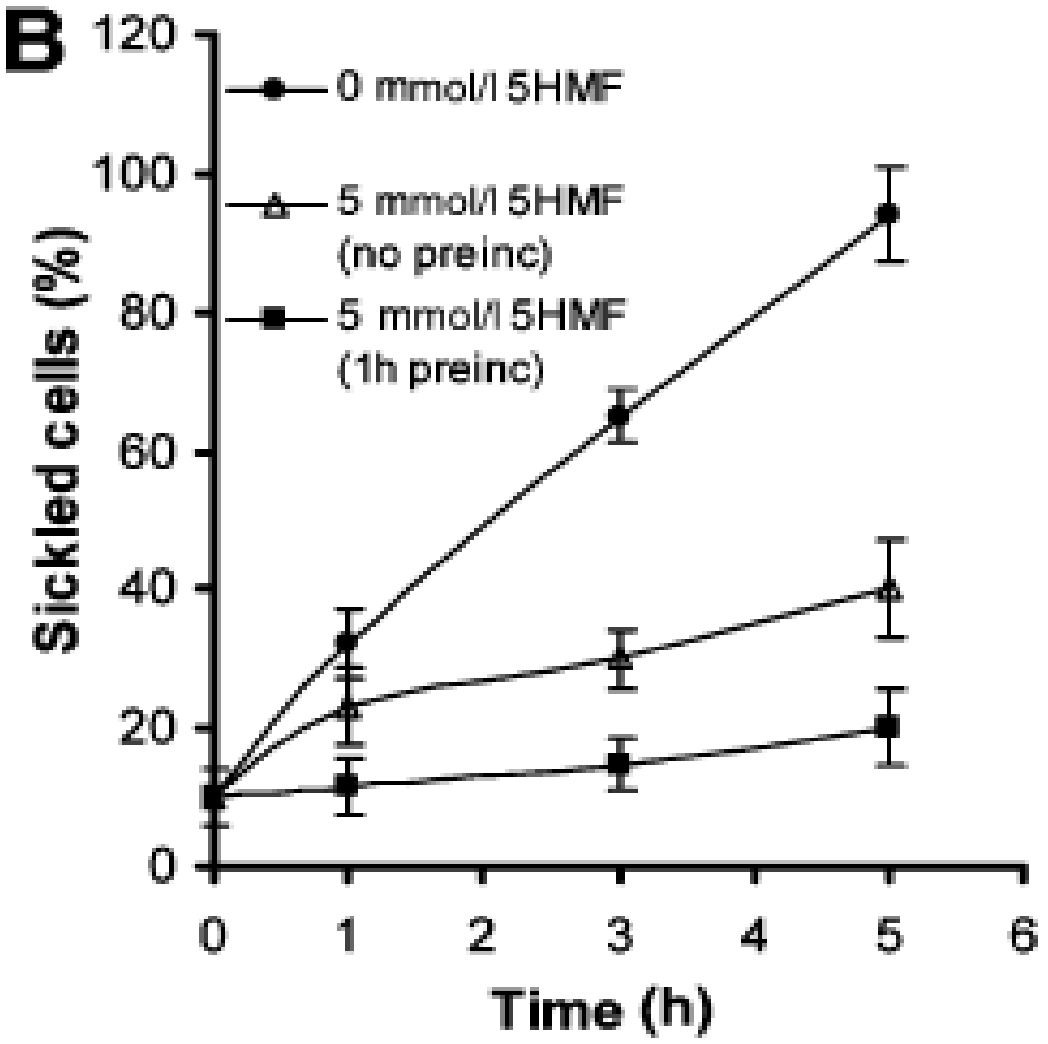

Figure 1-3. *In-vitro* increased survival of RBCs with 5-HMF preincubation. **(Abdulmalik 2005)**

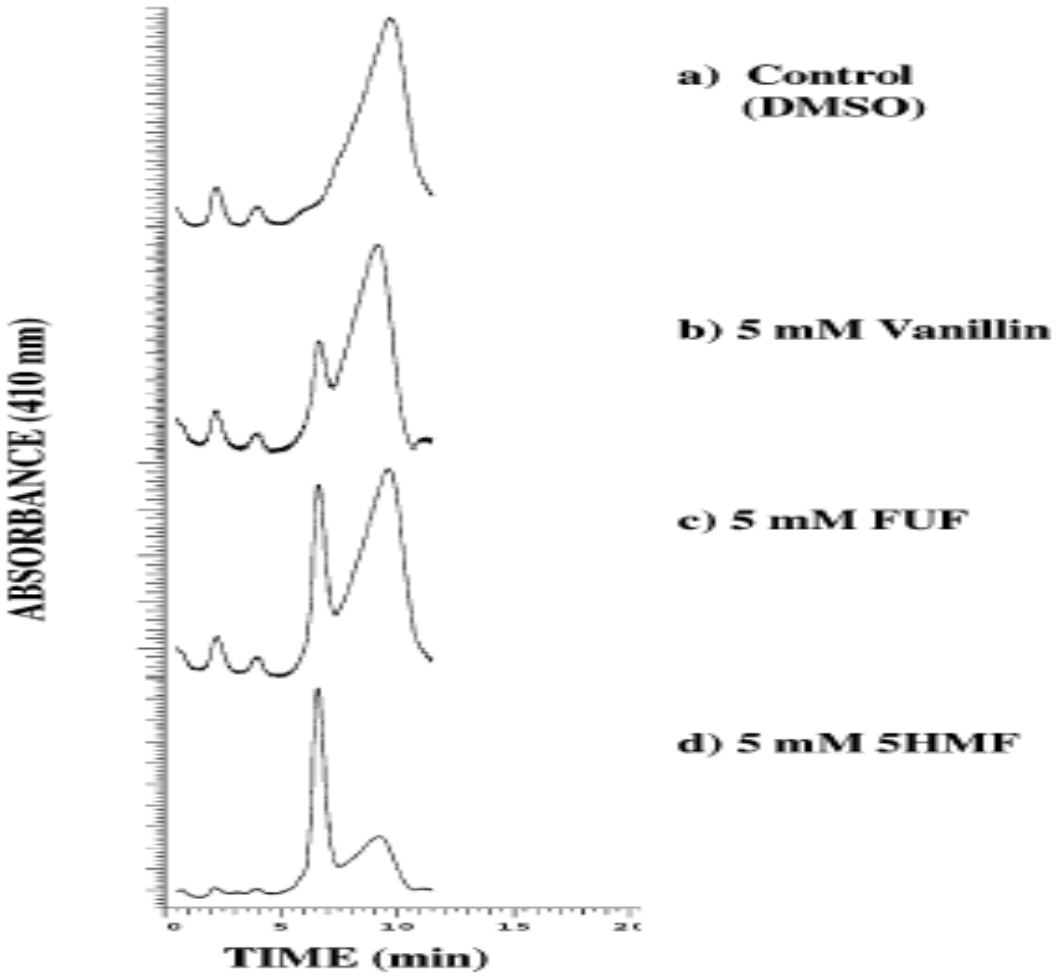

Figure 1-4. Hb-adduct formation. **(Safo 2004)**

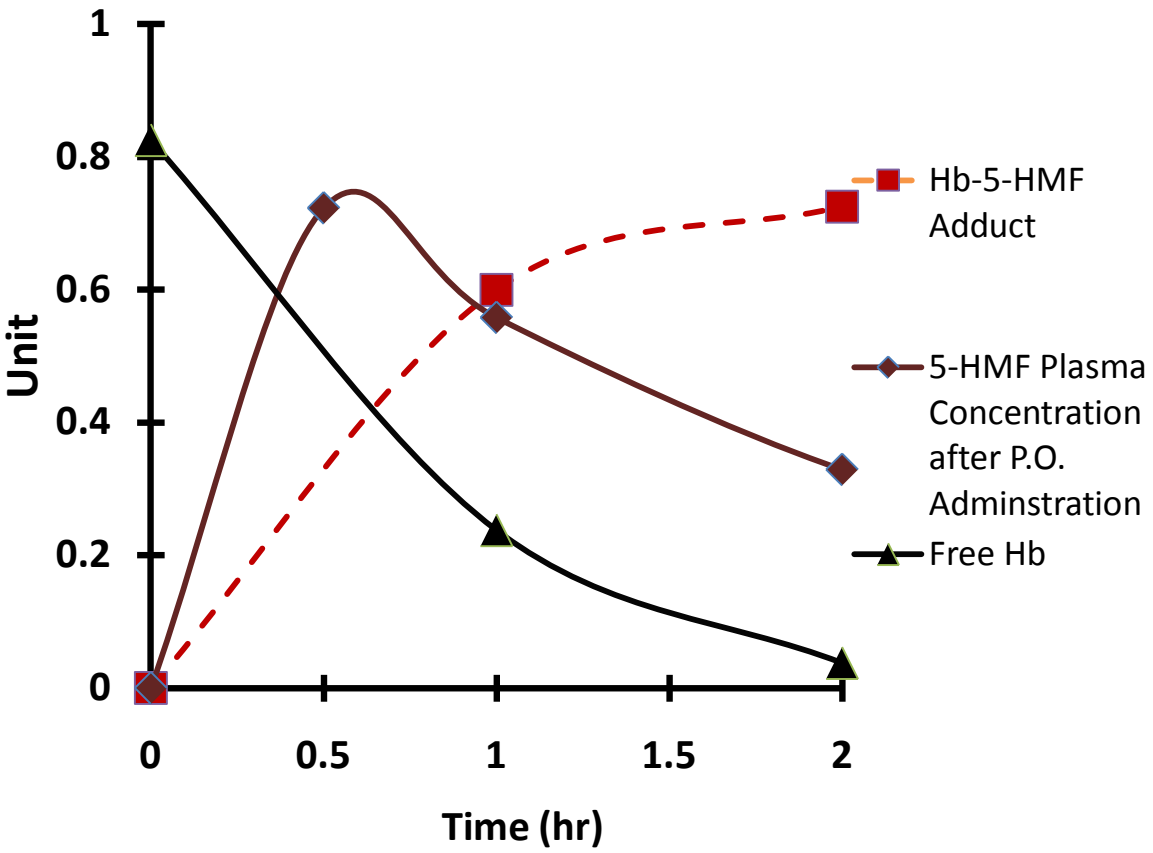

Figure 1-5. Hb-adduct concentration vs 5-HMF plasma concentration. Data taken from **(Abdulmalik 2005)**

Figure 1-6 shows a linear regression analysis that was performed on 5-HMF pharmacological effect versus the reported concentration. The pharmacological effects were the inhibition of *in-vitro* RBCs sickling (6A) and the change in oxygen affinity (pO_{50}) (6B). These effects were reported in suspensions of RBCs containing HbS that were pre-incubated for one hour with 0, 1, 2, and 5 mM of 5-HMF and exposed to hypoxic conditions (4% O_2) for 5 hours (Abdulmalik 2005). The inhibition of sickling and the change in pO_{50} were proportional to the concentration of 5-HMF in the RBCs suspension. Thus, if a shift of 5-10 mmHg in pO_2 is therapeutically targeted, a blood concentration of 1-2 mM (120-240 µg/ml) of 5-HMF would be required. This is supported by the results reported by Safo for *in-vitro* experiments, where 1 mM and 2 mM of 5-HMF were used and resulted in a shift of -6.6 mmHg and -10.8 mmHg in pO_2, respectively (Safo 2004). In concordance with that, a preliminary projection of a therapeutic 5-HMF IV dose was made as 0.8-1.5 g achieving 100-200 µg/ml blood concentration (Venitz 2006).

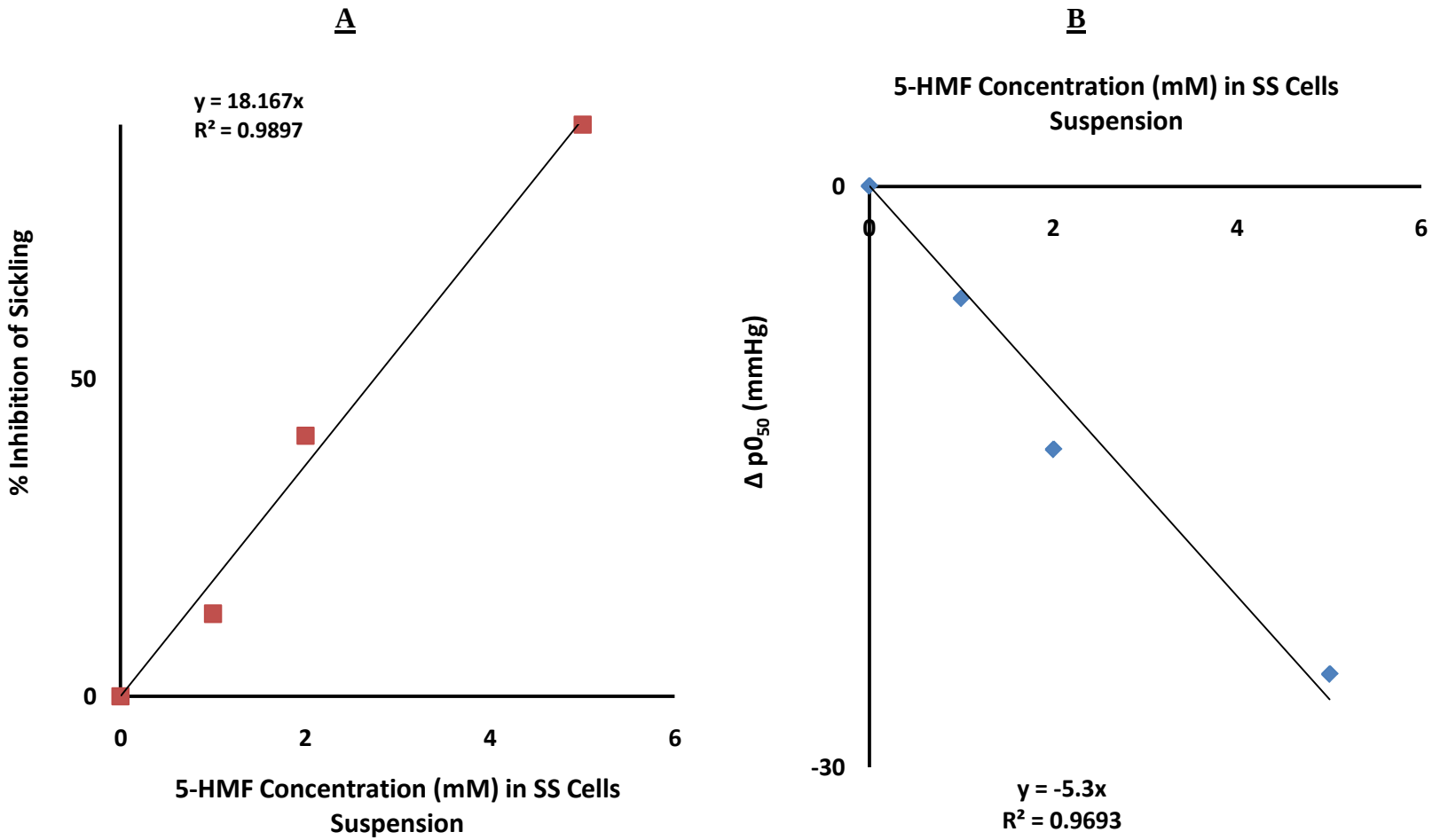

Figure 1-6. Blood PD after pre-incubation with 5-HMF. Estimated from **(Abdulmalik 2005) (Safo 2004)**.

1.2.3 1.2.3 Other 5-HMF Pharmacological Activities

Although 5-HMF occurs in herbs and fruits known to exhibit antioxidant effects, 5-HMF was reported not to have antioxidant activity (Prior 2006). On the other hand, a micronutrient supplement that contains 5-HMF along with α-ketoglutaric acid (α-KG) was reported to decrease oxidative stress and increase exercise capacity of athletes though they were declared to have no doping effect (Matzi 2007). Hence, its effectiveness as a pre-operative support for lung resection surgeries indicated by lung cancer was investigated (Matzi 2007). The pharmacological 5-HMF effect in this aspect was attributed to its ability to consume and interact with oxygen, hydroxyl, and superoxide radicals (Matzi 2007).

It was reported that 5-HMF inhibits interleukins-1 β expression together with the tumor necrosis factor α (Michail 2007). Consequently, 5-HMF was involved in phase II clinical studies in combination with other substances as a cytostatic agent (Michail 2007). This might be related to the ability of 5-HMF to selectively inhibit terminal deoxynucleotidyltransferase (TdT) with an IC_{50} of 5.5 μM and DNA polymerase λ with an IC_{50} of 26.1 μM in a competitive manner (Mizushina 2006). Mizushina et. al. reported that all of the investigated changes in the structure of 5-HMF resulted in activity loss (Mizushina 2006). This pharmacological activity of 5-HMF is relevant as an anticancer agent knowing that the inhibition of DNA polymerases is targeted by antitumor drugs (Miura 2004) and that TdT overexpression is reported in acute lymphocytic and myelocytic leukemias (Di Santo 2006). TdT is mainly expressed by the developing T and B-lymphocytes in bone marrow and thymus (Di Santo 2006). On the other hand, DNA polymerase λ is expressed mainly in human ovaries, testis, and fetal liver (Di Santo 2006).

5-HMF was extracted from *Dictyophora indusiata* mushroom and proved to have anti-tyrosinase activity. The mode of action was found through non-competitive inhibition of the enzyme with an ID_{50} of 0.98 mM that might be related to the formation of Schiff-base (Sharma 2004). In this study, mushroom tyrosinase was used for this assay (Sharma 2004). Tyrosinase enzymes are involved in many important functions as melanin synthesis and undesired enzymatic browning of vegetables and fruits upon post harvest damage (Sharma 2004).

1.2.4 5-HMF Pharmacokinetics

Following is an elaborate summary of the ADME properties for 5-HMF as described in the literature:

1.2.4.1 Oral Absorption and Bioavailability

Only 17% of a 100 mg/kg oral dose of 5-HMF was detected in mice intestine after 5 minutes of administration, which rapidly decreased to 1% by 60 minutes (Czok, Tolerance of 5-hydroxymethylfurfural (HMF). 2d communication: pharmacologic effects. 1970). This rapid disappearance indicated a rapid and complete absorption of 5-HMF assuming negligible chemical and metabolic degradation.

The intestinal absorption of 5-HMF was investigated using Caco-2 cell lines. Breakfast cereals were used as a source of 5-HMF in addition to a 5-HMF standard (Delgado-Andrade 2008). 5-HMF was subjected to stomach and intestinal digestion through continuous *in-vitro* mixing with gastric juice followed by intestinal enzymes and bile acids. This process was followed by assessment of 5-HMF concentration in the solution before adding it to the apical chamber of Caco-2 cell lines. It was found that only 13-56% of the 5-HMF content in the cereals was detected in the soluble fraction of the digest. When the digestion process was applied to 5-HMF standard, only 61% of the initial 5-HMF concentration was detected in the soluble fraction of the digest. Then, the concentration of 5-HMF in the basolateral side was measured after 2 hours of incubation. It was observed that 5-HMF did not affect the integrity of Caco-2 monolayer. 17-68% of the 5-HMF spiked test solutions was detected in the basolateral side. Breakfast cereals had only 24-32% transported through the cell lines. In this study, 5-HMF was

suggested to be transported in the intestine through passive diffusion and transporters (Delgado-Andrade, Estimation of hydroxymethylfurfural availability in breakfast cereals. Studies in Caco-2 cells 2008).

High oral bioavailability was pointed out by Abdulmalik et al. (Abdulmalik 2005), implying high fraction absorbed (f_{abs}) and low first-pass effect. In addition, the low value of the apparent clearance ($CL_{Tot/Foral}$), estimated in that study, indicated a high F_{oral} value and low first-pass effect unless the actual clearance value was so low. The absolute F_{oral} is calculated with reference to an IV administration of the drug, as illustrated by Equation 1-1, for the same dose (Hurst, 2007):

$$F_{oral} = \frac{AUC_{oral}}{AUC_{IV}} \quad \text{Equation 1-1}$$

Where, F_{oral} is a composite of the drug fraction absorbed through the GI (not metabolized, degraded, and/or subject to efflux transporters) (f_g) and the fraction that escapes the pre-systemic hepatic metabolism (f_h). Thus, F_{oral} can also be described by Equation 1-2 (Hurst, 2007):

$$F_{oral} = f_g \times f_h \quad \text{Equation 1-2}$$

5-HMF is probably a low hepatic-extraction ratio drug. Thus, f_h is probably high (>80%). The structure 5-HMF seems to be relatively stable to degradation in the GI and appears to be highly permeable. Unfortunately, the role of transporters in 5-HMF disposition has not yet been characterized. However, considering the structure of 5-HMF and assuming that 5-HMF can be classified as a class I BCS drug, transporters should not play a major part in its disposition.

Hence, we postulate that f_g is around 90%. Consequently, 72% is the value projected for the oral bioavailability (F_{oral}) of 5-HMF.

1.2.4.2 Distribution

5-HMF distribution in the body was investigated by assessing the concentration-time profiles of 5-HMF related radioactivity in rodent tissues studied by Godfrey et al (Godfrey 1999): it was observed that 5-HMF peak levels in various tissues were achieved before 2 hours post-administration of 100 and 500 mg/kg doses, suggesting a rapid distribution into most physiological compartments. In addition, liver and kidney had the largest tissue/blood partition coefficient (AUC_{48} ratio) in rats and mice, as evident in Table 1-2. This might be attributed to the fact that these organs not only act as distribution compartments, but also are elimination sites with relatively high blood supply.

Germond and co-workers investigated the distribution of 5-HMF using whole animal autoradiography in rats after oral and intravenous administration of [^{14}C]5-HMF (Germond 1987). After one hour of oral administration, most of the radioactivity was found in the bladder, kidney, and liver with little radioactivity detected in the stomach and small intestines and the lowest radioactivity detected in the nervous system (Germond 1987). Again, this supports the conclusion of rapid distribution and emphasize the importance of kidney and liver in the elimination of 5-HMF. On the other hand, a higher concentration was observed in the nervous system after intravenous administration (0.1% of the administered dose) and the radioactivity in the stomach, but not in the small intestine, was absent (Germond 1987). The radioactivity was

distributed uniformly in other organs (1-2% of radioactivity). Another point, the authors pointed out the discrepancy in almost complete recovery of 5-HMF related-radioactivity observed in this study and what was reported in earlier studies, summarized in by Ulbricht et al., in which only around 50% of 5-HMF was recovered and the unrecovered part was assumed to undergo covalent protein binding (Germond 1987). Germond et al. attributed this discrepancy to the ineffectiveness of the extraction method used in the previous studies, in which the glycine conjugate was not extractable (Germond 1987).

Further analysis of a study carried-out by Czok (Czok, Tolerance of 5-hydroxymethylfurfural (HMF). 2d communication: pharmacologic effects. 1970) observed a bixeponential decline of 5-HMF in rat plasma after an IV injection of 100 mg/kg. The volume of distribution (Vdcc) of 6.6 L/kg estimated for Czok is 10 fold higher than the anticipated 5-HMF Vd that is equivalent to total body water. The volume of distribution at pseudosteady-state (Vdpss), 7.2 L/kg, was similar to Vdcc. The same biphasic pattern was observed in mice after IV bolus injection of 100 mg/kg (Monien 2009). The Vdcc was estimated to be 0.55 L/kg (Monien 2009). This is equivalent to total body water as would be expected considering 5-HMF polar structure. On the other hand, the Vdpss was 7.7 L/kg (Monien 2009).

As far as plasma protein binding is concerned, *in-vitro* interaction of 5-HMF with intracellular Hb was similar when 5-HMF was incubated in plasma or RBC suspension in saline (Abdulmalik 2005). Therefore, the fraction of 5-HMF bound to plasma protein is anticipated to be low. Furthermore, the small molecular size and hydrophilic characteristics of 5-HMF support the notion of low plasma protein binding.

Table 1-2. AUC48 tissue/blood ratio of 5-HMF in rats and mice. Estimated from **(Godfrey 1999)**.

	Mice							
Dose (mg/kg)	**Blood**	**Liver**	**Kidney**	**Muscle**	**Skin**	**Adipose**	**Brain**	**Testes**
5	1	2.4	1.4	0.1	0.2	0.1	0.1	0.1
100	1	2.4	5.6	0.6	0.8	0.4	0.4	0.6
500	1	1.8	4.8	0.6	0.9	0.4	0.3	0.6
	Rats							
10	1	3.5	3.0	1.4	2.2	1.7	0.4	1.2
100	1	4.0	6.3	2.6	2.2	5.1	0.6	2.5
500	1	2.2	6.6	1.5	1.5	1.1	0.4	1.0

1.2.4.3 Metabolism

On the other hand, Godfrey and co-workers reported in a mass balance study conducted in rodents (mouse and rat) that the total radioactivity recovery within 48 hours after 5-HMF administration (5-500 mg/kg) by oral gavage was 80-92%, mostly (>70%) eliminated as metabolites in the urine (Godfrey 1999).

N-(5-hydroxymethyl-2-furoyl)glycine (HMFG), 5-Hydroxmethyl-2-furoic acid (HMFA), and 2,5-Furan dicarboxylic acid (FDCA), shown in Figure 1-7, were identified as metabolites in the urine of rodents, with HMFA accounting for approximately 80% of the metabolites (Godfrey 1999).

These results are concurred by the fact that two major metabolites were identified by Germond et al. as HMFA and HMFG, with the ratio of HMFA to HMFG increased from 1 to 18 with increasing the administered doses (Germond 1987). The ratio decreased when glycine was administered indicating the importance of its availability in the formation of HMFG (Germond 1987). The conjugation of glycine was proposed to occur in kidney, since this metabolite was only found in kidney homogenate (Germond 1987). Its note worthy, that HMFA, but not 5-HMF or HMFG, was extracted from liver homogenate (Germond 1987) and that 44-67% of 5-HMF administered to dogs, rabbits, and chickens were excreted as HMFA in the urine (NTP 1994).

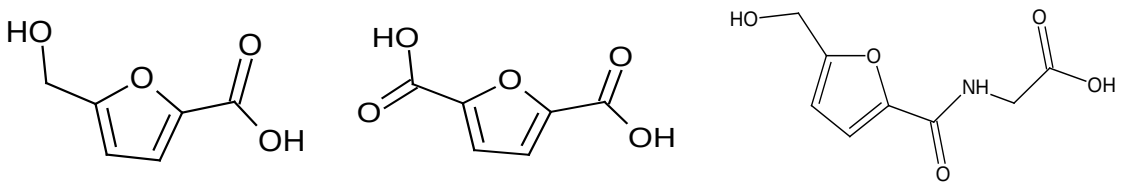

HMFA **FDCA** **HMFG**

I **II** **III**

Figure 1-7. Major metabolites of 5-HMF in rodents **(Godfrey 1999)**.

In humans, it was reported that the total recovery of 5-HMF in urine was 46% and 14% after 6 hours of oral administration of dried plum juice and dried plums as metabolites (Prior 2006). Likewise, 74% and 38% of the administered dose was recovered in the urine as HMFA and FDCA of parenterally fed human neonates exposed to 5-HMF as a hydrolysis product of fructose upon sterilization process of fructose solutions (E. B. Jellum 1973).

The above-mentioned study involved six healthy women volunteers who administered dried plum juice and dried plums after an overnight fast in a randomized cross-over clinical study (Prior 2006). The amount of 5-HMF was estimated as 497 mg (3.9 mmol) and 61.2 mg (0.5 mmol) in the dried plum juice and dried plums, respectively. In addition to the baseline sample, blood was sampled at 0.25, 0.5, 1, 2, 3, 4, and 6 hours post administration. Moreover, urine was collected at the baseline and every two-hour period up to six hours. Bioanalysis was performed using HPLC-MS/MS and HPLC-UV (Prior 2006). The analysis was focused on peaks that appeared in the plasma of those administered the dried plum products and was not in the control group (Prior 2006).

HMFA, compound I in Figure 1-7, was identified as the major metabolite of 5-HMF excreted in the urine accounting for 36.9% of 5-HMF dose (1.5 mmol/6 hrs). In addition, HMFA was detected in the urine of controls at levels of 0.006 mmol/6 hrs. The area under the curve of the plasma concentration-time profile for HMFA was 0.32 mmol/l.hr (Prior 2006). The reported plasma concentration-time profile for HMFA was used in the estimation of the pharmacokinetics parameters, as summarized in Table 1-3.

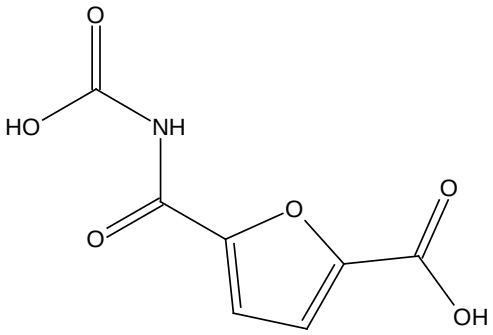

IV

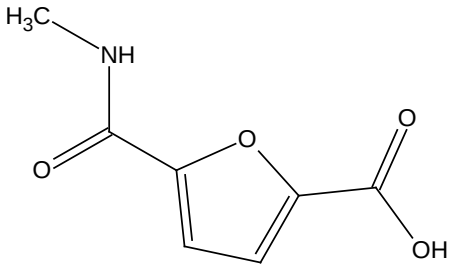

V

Figure 1-8. Potential metabolites of 5-HMF. **(Prior 2006)**

Table 1-3. Pharmacokinetics parameters of HMFA in humans.

Parameter	Value
AUC_{6hrs} (mM.hr)	0.316
AUC_{∞} (μM.hr)	0.328, reported 0.318
$t_{1/2}$ (min)	69
K_e (min^{-1})	0.01
Urinary clearance of unchanged drug (ml/min)	80

(5-Carboxylic acid-2-furoyl)glycine, compound IV in Figure 1-8, was identified as a metabolite of 5-HMF in urine with 0.168 mmol excreted in 6 hours (4.2% of 5-HMF dose). This compound was also found in one of the control urine (Prior 2006). This metabolite was not detected in murine studies after oral administration of 5-HMF (Germond 1987) (Godfrey 1999).

Moreover, N-(5-hydroxymethyl-2-furoyl)glycine, compound III in Figure 1-7, was identified as a metabolite in the urine accounting for 3.6% of 5-HMF dose (0.137 mmol/6 hrs). This metabolite was observed in urine earlier after oral administration of 5-HMF in rats and mice (Germond 1987) (Godfrey 1999).

Furthermore, 5-hydroxymethyl-2-furoylaminomethane, compound V in Figure 1-8, was identified as a metabolite for 5-HMF with small amounts excreted, which was 1.8% of 5-HMF dose. This compound was also detected in 50% of the controls excreted urine (Prior 2006). This metabolite was not detected in murine studies after oral administration of 5-HMF (Germond 1987) (Godfrey 1999).

In this study, the ratio of compound I to III was twofold higher with the administration of dried plum juice compared to dried plums, which is supported by Germond et al. observation that the proportion of excreted compound III decreased with the increase in the administered dose (Germond 1987) (Godfrey 1999).

Although compound II in Figure 1-7 was not detected in the study (Prior 2006), Godfrey et al. observed this metabolite in rats and mice (Godfrey 1999).

All of the above suggests that oxidation is the main biotransformation pathway of 5-HMF, is most likely by oxidoreductase enzymes; ALDH and ADH. The major metabolite, HMFA, implies that ALDH plays a crucial rule in 5-HMF detoxification. Besides the liver, these enzymes are found in stomach, kidney, erythrocytes, etc (Satre 1994) (Sládek 2003).

Recently, 5-sulfoxymethylfurfural (SMF) was detected in mice plasma after the I.V. bolus administration of 100 mg/kg 5-HMF (Monien 2009). SMF was reported as a carcinogenic and mutagenic compound, however, the AUC ratio of SMF to 5-HMF was 0.017% (Surh 1994) (Monien 2009).

ADH involvement in the formation of a primary metabolite was reported to happen only by yeast. 5-HMF was metabolized by ethanolgenic yeast to 2,5-bis-hydroxymethyl furan, shown in Figure 1-9, with a preference to the presence of NADPH as a cofactor in the redox reaction, which was observed at 222 nm with a total disappearance of 5-HMF after 48 hours of incubation (Liu 2006).

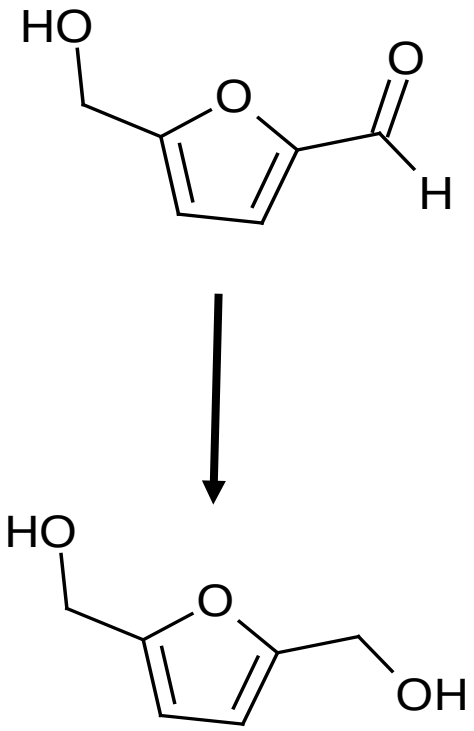

Figure 1-9. 2,5-bis-hydroxymethyl furan **(Lin 2008)**

In general, a drug is considered a low hepatic extraction-ratio drug if less than 20% of what enters the liver, through the hepatic artery and portal vein, is lost upon leaving the liver. As mentioned above, 5-HMF is highly metabolized with the metabolic clearance (Cl_{met}) accounting for more than 70% of total clearance (Cl_{tot}) in rats (Godfrey 1999). Stating that 5-HMF had high oral bioavailability in mice indicates that it is a low hepatic extraction-ratio drug (Abdulmalik 2005). The apparent clearance ($Cl_{tot/F}$) of less than 5 ml/min/kg in mice, reported by Abdulmalik and co-workers, is much less than the liver blood flow in mice (around 280 ml/min/kg) (Davies 1993). Knowing that this value as a clearance might have been overestimated, because of the unknown oral bioavailability (F_{oral}), provides us with more confidence in considering 5-HMF as a low hepatic extraction-ratio drug. When this apparent value was allometrically scaled to human, assuming it represents the true clearance, it was around 5% of the hepatic blood flow. However, this allometric scaling did not account for the differences in the metabolic enzymes expression and activity between human and animals (Venitz 2006).

1.2.4.4 Excretion

As a small molecule with a neutral structure at physiological pH range, it was anticipated that 5-HMF is freely filtered in the kidney and that it is subject to tubular reabsorption (Venitz 2006). However, only 12 mg of unchanged 5-HMF was excreted in urine after administration of 1 g of 5-HMF to rabbits (Lang 1970). This is in agreement with detecting 0.73% of the 5-HMF amount consumed by healthy volunteers in their urinary excretion as unchanged 5-HMF (M. P. Murkovic 2006). This study was conducted in seven healthy volunteers, in whom the urinary excretion of unchanged 5-HMF was investigated after administering 24 mg of 5-HMF in plum jam after an overnight fast (M. P. Murkovic 2006). Figure 1-10 shows the amount excreted in urine over time. The total of the average amounts of unchanged 5-HMF excreted over the 6 hours was 176 µg. Unfortunately, the metabolites were not investigated in this study. However, the presence of the sulfated metabolite was investigated but it was not detected in urine (M. P. Murkovic 2006).

More than 60% of the 5-HMF dose was eliminated in rodents urine, mainly as metabolites (~90%) (Godfrey 1999). In the studies performed by Germond, Jellum, and Godfrey, the urinary excretion of unchanged 5-HMF was not reported. Both Godfrey et al. and Jellum et al. stated clearly that 5-HMF was not detected in the urine (Godfrey 1999) (E. B. Jellum 1973). Germond and co-workers suggested that the kidney might contribute to the metabolism of 5-HMF by adding the glycine moiety to its carboxylic metabolite. Blood concentrations, reported by Godfrey et al. for the oral administration of 5-HMF in rodents, were used to estimate the exposure parameters of 5-HMF by non-compartmental analysis, as shown in Table 1-4. The values for the apparent clearance (Cl_{tot}/F) indicated higher bioavailability and/or lower

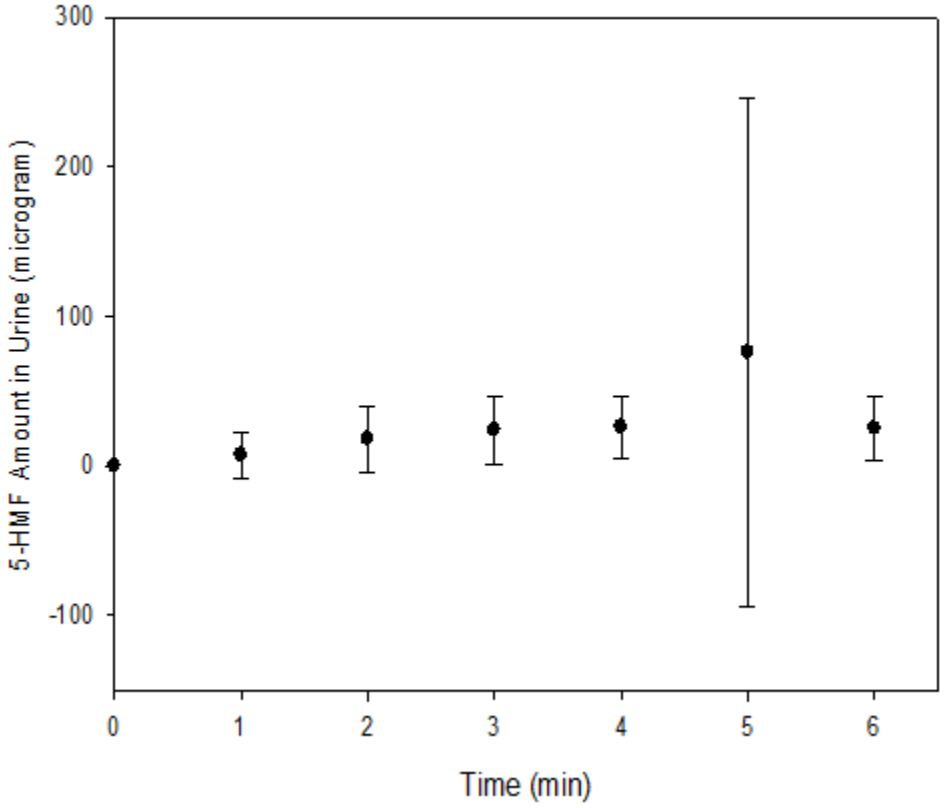

Figure 1-10. Unchanged 5-HMF excretion in human urine over time after administering 24 mg of 5-HMF in plum jam.

elimination rate of 5-HMF in rat compared to that in mice. The estimated parameters were compared to those reported by Abdulmalik et al. for the 100 mg/kg dose in mice, as shown in Table 4. In this study, the blood sampling schedule included seven time-points after the pre-dose sample from 30 minutes to 6 hours (Abdulmalik 2005), while Godfrey reported concentrations for four time points from 2 hours to 48 hours (Godfrey 1999). A discrepancy was noted in the estimate of the apparent clearance and the AUC reported by Abdulmalik et al.. Hence, the trapezoidal AUC (AUC_{trap}) was re-estimated for the concentration-time profile. The estimated AUC_{trap} was not similar to the reported value, as shown in Table 1-5.

Czok reported lower 5-HMF plasma concentrations in rats after I.V. injection of 100 mg/kg (Czok, Tolerance of 5-hydroxymethylfurfural (HMF). 2d communication: pharmacologic effects. 1970). Using non-compartmental analysis, the initial $t_{1/2}$ was estimated as 4.8 minutes and the terminal $t_{1/2}$ was 11 minutes with a total clearance of 446 ml/minute/kg, which is 10 fold higher than the apparent clearance estimated for Godfrey study. The findings are concurred by a recent study carried-out by Monien and co-workers (Monien 2009). The distribution $t_{1/2}$ after an I.V. bolus of 100 mg/kg in mice, was 1.7 minute and the terminal $t_{1/2}$ was 28 minutes with a total clearance of 190 ml/minute/kg after HPLC-MS/MS analysis of mice plasma (Monien 2009). In beagle dogs, 5-HMF was administered as 5 g/hour infusion (Klimmek 1978), and the pharmacokinetic parameters for it were summarized in Table 1-6.

In addition, in a mass balance study, 0-330 mg/kg of [C^{14}]5-HMF was administered to rats by both stomach tube and tail vein injection (Germond 1987). When 5-HMF administered through stomach tube, less than 1% was recovered as radioactivity in the expired air. The remaining activity, which accounted for around 85% of the radioactivity, was recovered in the

urine after 8 hours of administration (Germond 1987). Hence, it is postulated that at least 70% of 5-HMF is orally absorbed and is subject to extensive metabolism.

Table 1-4. Comparison of exposure parameter estimates in rats and mice in blood (n= 4). Estimated from **(Godfrey 1999)**

	Dose (mg/kg)					
	Rats			**Mice**		
	5	**100**	**500**	**10**	**100**	**500**
AUC_{48hrs} (µg/ml*min)	2071	8679	52005	159	2109	22877
Cl_{Tot}/F (ml/min/kg)	2.4	11.5	9.6	62.8	47.4	21.9

Table 1-5. Comparison of the exposure parameters for oral administration of 100 mg/kg in mice.

	Estimated from Godfrey et al., 1999	**Estimated from Abdulmalik et al., 2005**	**Reported by Abdulmalik et al., 2005**
AUC_{∞} (µg/ml*min)	2,109	22,680	412 ± 25
Cl_{tot}/F (ml/min/kg)	47.4	4.4	4.2 ± 0.3

Table 1-6. Pharmacokinetics parameters for IV infusion of 5 g/hour infusion to beagle dogs (n=7).

Parameter	Value
AUC_{120min} (µg/ml.min)	3503
AUC_{∞} (µg/ml.min)	7959
$t_{1/2}$ (min)	123.5
K_e (min^{-1})	0.006
CL (ml/min)	628.2
Vd (l)	112.0

As a conclusion, renal elimination contributes mainly to the elimination of drug metabolites. However, the kidney contribution to the unchanged drug elimination is minimal in the light of evidence that 5-HMF is highly metabolized and no 5-HMF was detected in the urine.

1.2.4.5 BCS Classification

The Biopharmaceutics Classification System (BCS) classifies drugs according to their solubility, dissolution, and permeability properties of the drug substance in the highest strength of their immediate release drug product (Wu 2005). The calculated solubility of 5-HMF, shown in Figure 1-1, is 48 g/l at 25 °C (ACS 2009), which means that up to 12 g of 5-HMF can be dissolved in 250 ml of aqueous media (pH 1-7.5 at 37 °C) as defined by the FDA (Wu 2005). This estimated solubility is based on the assumption that the solubility of 5-HMF is constant between 25-37 °C. 12 g is much larger than the proposed human dose of around 1.5 g 5-HMF (Venitz 2006) and probably the highest strength dose will be less than 12 g. Thus, 5-HMF can be considered as a highly soluble drug substance.

It is assumed in this case that other components in the formulation will not significantly decrease the dissolution of the dosage form. Hence, it is predicted that $\geq$ 85% of the labeled amount of 5-HMF will be dissolved in 900 ml buffer using apparatus I or II (FDA 2000). As far as permeability is concerned, a drug is considered to be highly permeable if it was proven that at least 90% of the administered dose is orally absorbed in humans. The intravenous (IV) reference dose or mass balance study can prove that (FDA 2000). Unfortunately, except for what was reported by Jellum et al. (E. B. Jellum 1973), where 5-HMF was administered intravenously, no *in-vivo* human study had 5-HMF administered intravenously. However, 46% recovery of HMFA in urine of healthy volunteers after administering dried plum juice (Prior 2006) indicates that at least 46% was absorbed through the gastrointestinal tract. If this value is compared to what was reported by Jellum regarding 36-73% recovery of 5-HMF metabolites in urine after parenteral administration of 5-HMF, it indicates that 5-HMF has high oral bioavailability.

The calculated log D value of 5-HMF equals -0.45 (ACS 2009) over a pH range of 1-10 and its small molecular weight (MW: 126 D) makes it a candidate for passive diffusion in the gastrointestinal tract (Hurst 2007). Germond and co-workers reported that 95-100% of the radioactivity was recovered in urine within 24 hours of oral and intravenous [14C]-5-HMF administration to rats (Germond 1987). The doses ranged between 0.8-330 mg/kg administered for two rats at each dose level (Germond 1987). This indicates that≥90% is orally absorbed in rats. If a similar absorption behavior is found in human, 5-HMF can be classified as a class I drug according to the BCS. However, although it was mentioned in this study that 5-HMF was administered both orally and intravenously; the AUC after IV administration was not reported. This prevents from calculating the absolute bioavailability in order to draw any informed conclusion regarding 5-HMF oral bioavailability. Abdulmalik et al. stated that 5-HMF had high oral bioavailability and achieved high levels in whole blood samples of mice (Abdulmalik 2005).

A mass balance study by Godfrey et al. reported 61-77% and 70-82% recovery of cumulative radioactivity in urine in mice and rats, respectively, after oral gavage of doses ranging between 5-500 mg/kg (Godfrey 1999). This indicates that at least 61% and 70% of 5-HMF is absorbed mice and rats, respectively. Assuming that there is no significant difference in the disposition of 5-HMF between human and rodents, 5-HMF might be classified as intermediate to high permeability drug in human. As a conclusion, 5-HMF was recognized to be highly metabolized in the above studies indicating that 5-HMF can be classified as a class I drug according to the Biopharmaceutics Drug Disposition Classification System (BDDCS) (Wu 2005). Thus, 5-HMF can be classified as either class I (high solubility, high permeability) or class III (high solubility, low permeability) drug according to the BCS.

The following points summarize the preclinical findings in rodents:

- A rapid distribution to physiological compartments was observed with the highest AUC tissue-to-blood ratios achieved in the kidney and liver. Plasma protein did not affect 5-HMF interaction with Hb.
- Metabolism was recognized as the major route of elimination for 5-HMF. Three metabolites were identified in the urine with HMFA as the primary one.
- There is a variation in the apparent clearance estimated for animals in the discussed studies. This complicates drawing any conclusion regarding bioavailability and clearance mechanism of 5-HMF.

1.2.5 5-HMF Toxicity

There is no epidemiological study relating 5-HMF to cancer, in neither a positive nor in a negative direction (NTP 1994).

1.2.5.1 *In-vitro*

Incubation of 5-HMF with RBCs did not cause any toxicity, when investigated through morphology, pumps, and transporters function of RBCs (Abdulmalik 2005). In another study, 0.07, 0.74, and 7.4 mM of 5-HMF were incubated with blood cells to investigate changes in the metabolic activity (Nässberger 1990). While the heat output increased by 60% in RBCs, a significant reduction in the heat output was observed in the granulocytes. On the other hand, no adverse effects were observed in thrombocytes (Nässberger 1990).

5-HMF present in light colored caramel resulted in colonic aberrant cryptic foci initiation and promotion in rats (X. C. Zhang 1993). However, upon conducting a statistical study on this work carried-out by Zhang et. al, it was found that 5-HMF had only a borderline significant effect in producing the aberrant cryptic foci (Minkin 1994).

Moderate carcinogenicity was induced by incubation of 5-HMF in cell lines for an hour at a concentration of 115 mM (Janzowski 2000). Also, at a high 5-HMF concentration (120 mM), a weak mutagenic effect was observed *in-vitro* (Janzowski 2000). However, DNA damage was not observed (Janzowski 2000). In addition, 5-[(sulfooxy)-methyl]furfural, a chemically synthesized derivative of 5-HMF was mutagenic adverse events, while another derivative, 5-(chloromethyl)furfural, was mutagenic and cytotoxic (Surh 1994).

1.2.5.2 *In-vivo*

1.2.5.2.1 HUMAN

5-HMF was administered in a clinical regimen as 720 mg/day subdivided into three doses to preoperative patients for 10 days with no apparent side effects (Matzi 2007). Furthermore, 5-HMF at concentrations normally encountered in parenteral solutions are not considered toxic (Ulbricht 1984).

1.2.5.2.2 DOG

5 g/hour and 50 mg/hour of 5-HMF were infused to beagle dogs in 0.9% sodium chloride (Klimmek 1978). An increase in lactate concentration, pO_2, and heart rate and a decrease in pCO_2, and pH to around 7.06 was observed with the infusion of 5 g/hour. On the other hand, no changes were observed in the haematocrit, electrolytes, creatinine, bilirubin, and enzyme activities (Klimmek 1978).

1.2.5.2.3 RABBIT

When 400 mg of 5-HMF was given twice daily for a week through subcutaneous injection to rabbits, no adverse effects were observed (Rasmussen 1982).

1.2.5.2.4 RAT

The LD_{50} in rats ranged between 2.5-5 g/kg when 5-HMF was administered through oral route (NTP 1994) (Janzowski 2000). 250 mg/kg of 5-HMF was fed to rats for 40 weeks without affecting their weights or the histological characteristics of liver, kidney, heart, spleen, and testes (Lang 1970). On the other hand, it was reported that 5-HMF showed some evidence of carcinogenicity in female mice at gavage doses of 188 and 375 mg/kg/day, while no evidence of carcinogenicity was reported for similar doses in rats or male mice up to 750 mg/kg doses in a two-year toxicity study. In addition, respiratory and olfactory epithelium degeneration was observed in this study (NTP, TR-554 Toxicology and Carcinogenesis Studies of 5-(Hydroxymethyl)-2-Furfural (CAS No. 67-47-0) in F344/N Rats and B6C3F1 Mice (Gavage Studies) 2008).

In a study aimed to find an association between the erectile dysfunction in renal failure and the increase in the glycation products, the levels of 5-HMF were measured in the penile tissue as an indicator of glycation products, which resulted from non-enzymatic reaction between sugars and free amino groups in proteins. A significant increase in 5-HMF levels was found in rats with induced renal failure in comparison to the control (Usta 2002).

In addition, 5-HMF is used as a measure of glycated proteins in diabetes and cataracts after being released by acid hydrolysis of the glycated proteins. A significant higher level of the released 5-HMF was estimated in diabetic rats with cataracts in comparison to non-diabetic rats (Turk 1997).

1.2.5.2.5 MICE

No lethal effects were observed upon oral administration of 5-HMF up to 2 g/kg (Czok, Tolerance of 5-hydroxymethylfurfural (HMF). 2d communication: pharmacologic effects. 1970). On the other hand, the LD_{50} was 0.84 g/kg through an intraperitoneal route (Czok, Tolerance of 5-hydroxymethylfurfural (HMF). 2d communication: pharmacologic effects. 1970). A slightly lower LD_{50} of 0.75 g/kg was estimated when 5-HMF was administered through an I.V. route (Czok, Tolerance of 5-hydroxymethylfurfural (HMF). 2d communication: pharmacologic effects. 1970). Gastrointestinal movements and bile secretion were increased with the increase in 5-HMF oral dose administered (50, 100, 200 mg/kg). In addition, 5-sulfoxymethylfurfural (SMF), a carcinogenic and mutagenic compound, accounted for 17 ppm of 5-HMF AUC in mice plasma after an I.V. bolus administration of 100 mg/kg 5-HMF (Monien 2009) (Surh 1994).

1.2.6 5-HMF in Humans

Despite the fact that 5-HMF is reported to be involved in clinical trials as anticancer agent and micronutrients, a shortage of literature for studies characterizing or predicting its PK in human is apparent. Moreover, the variation in the estimated *in-vivo* animal exposure parameters emphasizes the need for preclinical studies exploring the PK of 5-HMF.

720 mg/day of 5-HMF along with α-ketoglutaric acid (α-KG) divided into three doses were given to a study group (n=16) in a randomized prospective study involving 32 lung cancer patients undergoing lung resection surgery (Matzi 2007). The micronutrient supplement was given for 10 days before the surgery. The study group had a significant improvement in their exercise capacity and did not suffer from oxidative stress after the surgery as indicated by their carbonyl protein and isoprostane levels (Matzi 2007).

A study in seven healthy volunteers investigated the urinary excretion of unchanged 5-HMF after administering 1.2 mg/g of 5-HMF in 20 g of plum jam after an overnight fast. Volunteers were three females and four males with a wide age range between 18-45 years (M. P. Murkovic 2006).

Another study involved six healthy women volunteers aged between 65-70 years who administered dried plum juice and dried plums after an overnight fast in a randomized cross-over clinical study (Prior 2006). The amount of 5-HMF was estimated to be 497 mg (3.9 mM) and 61.2 mg (0.5 mM) in the dried plum juice and dried plums, respectively (Prior 2006).

Moreover, a study investigated the presence of furan compounds in the urine of healthy volunteers using gas chromatography and mass spectroscopy (Mrochek 1972). 2,5-furandicarboxylic acid with a total amount between 3-5 mg/24 hours, 2-Furoylglycine, 5-hydroxymethyl-2-furoic acid with a total amount between 1-25 mg/24 hours, were identified in

the urine of these healthy human. On the other hand, 5-hydroxymethyl-2-furoyl glycine was identified in a patient with chronic lymphocytic leukemia. Moreover, enhanced urinary excretion of the above compounds were observed in two patients with lymphocytic leukemia. The excreted amount of 2,5-furandicarboxylic acid in these patients reached 214 and 300 mg/24 hours (Mrochek 1972).

In a paper presented by Michail et. al., it was stated that 5-HMF is under phase II clinical studies in combination with other compounds for its anticytostatic activity (Michail 2007). In addition, it was mentioned that a dose of 3 g 5-HMF/day was given to cancer patients in a pilot study. 300 ng/ml was reported to be the approximate minimum concentration to characterize the pharmacokinetic profile of 5-HMF considering the required number of half-lives (Michail 2007).

The only systemic exposure to 5-HMF was reported in parenterally fed human neonates (n=2), who were exposed to 5-HMF as a hydrolysis product of fructose upon sterilization process of fructose solutions (E. B. Jellum 1973).

1.3 Aldehyde Dehydrogenase (ALDH)

ALDH is a potential enzyme in the metabolism of 5-HMF. Below is a description of its structure, function, substrates, isoenzymes, expression, polymorphism, and pharmacogenetics.

1.3.1 1.3.1 Structure

ALDH1 and ALDH2 are the main ALDH isoenzymes studied in the liver. Both of these are homotetramers with a total molecular weight of ~220-240 kDa (C. D. Cheung 2003) (A. R. Klyosov, Possible role of liver cytosolic and mitochondrial aldehyde dehydrogenases in acetaldehyde metabolism 1996) (Agarwal 1992). In general, other ALDH isoenzymes are homotetramers with few present as homodimers. Table 1-7 summarizes the quaternary structures of ALDH isoenzymes.

Based on human ALDH1, Cys-302 and Glu-268 were reported to be involved in the catalytic site, while Lys-192, Gly-245, Gly-250, Glu-399, and Phe-401 are important amino acids for the binding of the cofactor $NAD(P)^+$ (Manzer 2003). Consequently, inactive isoenzymes were characterized by the presence of arginine amino acid in their active site instead of cysteine (Manzer 2003).

Table 1-7. Quaternary protein structure of ALDH isoenzymes **(Marchitti 2008) (V. P. Vasiliou 2000)**

Quaternary Protein Structure	Isoenzyme
Tetramer	ALDH1A1, ALDH1A2, ALDH1B1, ALDH1L1, ALDH1L2, ALDH2, ALDH5A1, ALDH6A1, ALDH7A1, ALDH9A1
Dimer	ALDH1A3, ALDH3A1, ALDH3A2, ALDH4A1

1.3.2 Function

In general, ALDH catalyzes an irreversible oxidation of aliphatic and aromatic aldehydes into acids (C. D. Cheung 2003) (V. P. Vasiliou 2000). In conjunction with this irreversible oxidation of aldehydes, the enzymatic reaction involves the reduction of a cofactor, nicotinamide adenine dinucleotide, (NAD^+) into NADH.

The main isoenzymes studied are ALDH1 and ALDH2 because of their well-known function in acetaldehyde detoxification and converting it into acetic acid (Liao 1991) (Agarwal 1992) (Ricciardi 1983) (Klimmek 1978). Consequently, ALDH1A1 deficiency was associated with alcohol injury in mice while increased expression of ALDH1A1 in brain contributed to alcohol avoidance (Marchitti 2008). ALDH activity was proposed as an alcohol consumption indicator since the activity of ALDH in RBCs was found to be significantly less in alcoholics than teetotalers (Johnson 1992).

Hence, the role of ALDH is very important in detoxification processes. Besides alcohol, this includes many compounds causing skin sensitization and present in flavors and fragrances, such as cinnamaldehyde (C. D. Cheung 2003). While cinnamaldehyde might be present in the fragrance, it can be formed because of cinnamic alcohol activation through metabolism (C. D. Cheung 2003). Moreover, the cytosolic ALDH1A1 is involved in cyclophosphamide detoxification (V. P. Vasiliou 2000) (Beedham 1997). While ALDH1A1 decreases the toxicity of cyclophosphamide, it also causes resistance of tumors to cyclophosphamide in the case of its high expression in targeted tumor tissue (Marchitti 2008). Hence, the metabolism of anticancer drugs by ALDH contributes to the development of resistance to these drugs, especially where there is an increase expression of ALDH in the tumor tissue (Beedham 1997) (V. N. Vasiliou 2005).

In particular, it was fond that antineoplastic resistance is associated with an enhanced expression of ALDH3A1 (V. P. Vasiliou 2000). While ALDH3A1 has low expression level in healthy liver tissue, its expression increases in liver cancer cells since it contributes to cell regulation by downregulating transcription factors (Marchitti 2008). Relevant to this aspect, ALDH1A2 was reported to act as a tumor suppressor (Marchitti 2008).

On the other hand, the ALDH enzyme is essential for development and growth as they catalyze the oxidation of retinal to retinoic acid, which is an essential compound for gene expression (V. N. Vasiliou 2005). An ALDH1A2 knockout mice, dies in the early embryonic stages due to its key role in retinoic acid metabolism and its function as an important regulator in the development of organs including kidney, pancreas, forebrain, spinal cord, retina, spleen, and lung (Marchitti 2008) (V. P. Vasiliou 2000). ALDH decreased activity is observed in cirrhosis and can result in feminization due to its importance in retinal oxidation and androgen binding role in testis (Marchitti 2008) (Ricciardi 1983).

Besides detoxicification, ALDH plays a role in the bioactivation of GABA neurotransmitter and is involved in DNA repair and replication through catalyzing the formation of tetrahydrofolate that is required for purine synthesis (Marchitti 2008) (V. N. Vasiliou 2005).

In addition, ALDH1 and ALDH3 were proposed to have a role in the transparency of cornea since a reduced level of these enzymes was observed in cataract (Manzer 2003) (Marchitti 2008). It is thought that ALDH1A1 protects the eye from cataracts by oxidizing lipid peroxidation products, thus decreasing oxidative stress caused by aging and UVB exposure (Marchitti 2008) (Manzer 2003). This is supported by the notion that lipid peroxidation products, such as malondialdehyde and 4-hydroxynonenal, are substrates for ALDH (Manzer 2003). Moreover, ALDH acts as an antioxidant by producing NAD(P)H and scavenging free radicals

through its cysteine, sulfhydryl, and methionine groups (Marchitti 2008). On the other hand, some of the ALDH isoenzymes, which are present in the cornea have no metabolic capacity and thought to contribute only structurally to the transparency of cornea (Manzer 2003) (Sophos 2003) (V. N. Vasiliou 2005).

Other than its famous role in aldehydes oxidation, ALDH catalyzes ester hydrolysis and ALDH2 acts as a nitrate reductase, thus activating nitroglycerine (Marchitti 2008). Furthermore, in addition to their catalytic activity, ALDH function as binding proteins for endogenous moieties as androgen in human genital tissues and exogenous substances as acetaminophen (Sophos 2003) (V. N. Vasiliou 2005).

An advantageous outcome for the absence of ALDH1A1 was noticed in knockout mice, where a protection against insulin resistance and diet-induced obesity was observed (Marchitti 2008).

1.3.3 Substrates

Aldehydes are known to be very reactive compounds due to the presence of the highly electrophilic carbonyl group, for which they are related to carcinogenicity (Beedham 1997) (V. N. Vasiliou 2005). Inside the human body, they are generated from carbohydrates, amino acids, lipids, and neurotransmitters (Marchitti 2008). On the other hand, human exposure to aldehyde might be through exogenous sources, such as environmental acetaldehyde and formaldehyde and through intended exposure while ingesting ethanol, food flavors, and anticancer medications (e.g. cyclophosphamide and ifosfamide) (Marchitti 2008). Consequently, some aldehydes are essential for biological process in the body while others are toxic (Marchitti 2008).

Generally, aliphatic aldehydes with longer carbon chains have higher affinity toward ALDH than those with shorter chains (A. R. Klyosov, Possible role of liver cytosolic and mitochondrial aldehyde dehydrogenases in acetaldehyde metabolism 1996). Some aromatic aldehydes were also shown to have high affinity for ALDH with K_m values less than 100 nM (A. R. Klyosov, Possible role of liver cytosolic and mitochondrial aldehyde dehydrogenases in acetaldehyde metabolism 1996). In this aspect, naphthaldehydes have K_m values in the single nM range (A. R. Klyosov, Possible role of liver cytosolic and mitochondrial aldehyde dehydrogenases in acetaldehyde metabolism 1996). A substitution on benzaldehydes and naphthaldehydes did not significantly affect their affinity to ALDH whether the addition was an electropositive or electronegative group (A. R. Klyosov, Possible role of liver cytosolic and mitochondrial aldehyde dehydrogenases in acetaldehyde metabolism 1996). On the other hand, modification in the structure to make it more hydrophilic especially at the ortho-position, decreased the affinity toward ALDH with around 10 fold or more activity (A. R. Klyosov,

Possible role of liver cytosolic and mitochondrial aldehyde dehydrogenases in acetaldehyde metabolism 1996).

High affinity substrates for liver ALDH, such as cinnamaldehyde and benzaldehyde, have been identified with a K_m values less than 100 nM (A. R. Klyosov, Possible role of liver cytosolic and mitochondrial aldehyde dehydrogenases in acetaldehyde metabolism 1996). While hyperbolic non-linear regression using the Michaelis Menten equation is usually used to estimate the metabolic parameters, these low K_m values make it difficult to determine the metabolic parameters accurately (A. R. Klyosov, Possible role of liver cytosolic and mitochondrial aldehyde dehydrogenases in acetaldehyde metabolism 1996). Even with known substrates as acetaldehyde and retinal, different affinity values were reported that vary as much as 100 fold difference (A. R. Klyosov, Possible role of liver cytosolic and mitochondrial aldehyde dehydrogenases in acetaldehyde metabolism 1996). In addition, the K_m value for certain substrates was difficult to determine although the activity was observed (A. R. Klyosov, Possible role of liver cytosolic and mitochondrial aldehyde dehydrogenases in acetaldehyde metabolism 1996).

Consequently, for substrates having affinities in the nanomolar or subnanomolar range, a more complicated procedure that involved the addition of another substrate to the reaction was reported (A. R. Klyosov, Possible role of liver cytosolic and mitochondrial aldehyde dehydrogenases in acetaldehyde metabolism 1996). However, this procedure was deemed complicated and does not provide an advantage over measuring the kinetics using the substrate alone (A. R. Klyosov, Possible role of liver cytosolic and mitochondrial aldehyde dehydrogenases in acetaldehyde metabolism 1996).

Acetaldehyde is a prototypical substrate for ALDH. In human, the K_m value of cytosolic ALDH toward acetaldehyde is 180 µM (A. R. Klyosov, Possible role of liver cytosolic and mitochondrial aldehyde dehydrogenases in acetaldehyde metabolism 1996). In mice, acetaldehyde K_m was reported to be 0.9-5 µM and 0.8-1.4 mM in the mitochondrial fraction, while it was 10-50 µM and 0.1-0.6 mM in the cytosol (Tomita 1990). This variation in the K_m values in addition to what was reported with more than a 20 fold range (22-483 µM) estimated as the K_m value for acetaldehyde in humans is attributed to difficulties in measuring the initial velocities for low concentrations or variations in the enzyme or cell fraction purification processes (A. R. Klyosov, Possible role of liver cytosolic and mitochondrial aldehyde dehydrogenases in acetaldehyde metabolism 1996). Likewise, acetaldehyde experiments are difficult to carry on since the acetaldehyde boiling point is 21 °C. In addition, acetaldehyde oxidation products formed in the presence of air interferes with oxidoreductase activity measurement. Hence, redistillation of acetaldehyde under anaerobic conditions is recommended before conducting the experiments to remove interfering substances (Yan 1987). Moreover, acetaldehyde is not a high affinity substrate for all ALDH isoenzymes. Acetaldehyde is primarily metabolized by ALDH2 with a $K_m < 1$ µM (Marchitti 2008). ALDH1A1 is another isoenzyme that contributes to acetaldehyde metabolism, for which the K_m was estimated to be between 50-180 µM (Marchitti 2008). Besides, ALDH1B has high affinity toward acetaldehyde with a K_m of 30 µM (Marchitti 2008). On the other hand, the affinity of acetaldehyde toward ALDH3 is less than that for ALDH1 and ALDH2, hence, its role in the metabolism of ingested ethanol is minimal (Liao 1991). Likewise, ALDH1A2 does not seem to play an important role in acetaldehyde oxidation since it has a relatively low affinity with a K_m value of 650 µM (Marchitti 2008).

Other than acetaldehyde, retinal is an endogenous substrate for ALDH1 and an inhibitor for ALDH2 (A. R. Klyosov, Possible role of liver cytosolic and mitochondrial aldehyde dehydrogenases in acetaldehyde metabolism 1996). Furthermore, lipid peroxidation products, such as malondialdehyde and 4-hydroxynonenal, are substrates for ALDH enzyme (Manzer 2003). γ-aminobutyric acid represents another example of endogenous substrate for ALDH5A1 and ALDH9A1 (V. P. Vasiliou 2000). Table 1-8 lists some ALDH substrates.

Table 1-8. ALDH substrates.

Substrates	K_m (mM)	v_{max} (nmol/min/mg protein)	Species	ALDH Enzyme Source	Reference
Ethanol	4.7	20.2	Rat	Hepatic cytosol	(Gupta 2006)
	6	8.4	Rabbit	Hepatic cytosol	(Gupta 2006)
	1.7	33	Dog	Hepatic cytosol	(Gupta 2006)
	0.7	32.5	Human	Hepatic cytosol	(Gupta 2006)
Propylene glycol	19.7	9	Rat	Hepatic cytosol	(Gupta 2006)
	15.7	4.8	Rabbit	Hepatic cytosol	(Gupta 2006)
	13	24.5	Dog	Hepatic cytosol	(Gupta 2006)
	5.8	37.2	Human	Hepatic cytosol	(Gupta 2006)
Ethanol	1 to 2	-	Human	Liver purified enzyme	(Wagner 1983)
Methanol	6 to 150	-	Human	Liver purified enzyme	(Wagner 1983)
Ethylene glycol	13 to 220	-	Human	Liver purified enzyme	(Wagner 1983)
Benzyl alcohol	0.004 to 0.12	-	Human	Liver purified enzyme	(Wagner 1983)
Octanol	0.005 to 0.017	-	Human	Liver purified enzyme	(Wagner 1983)
16-HHA	0.007 to 0.026	-	Human	Liver purified enzyme	(Wagner 1983)
Cyclohexanol	0.005 to 23	-	Human	Liver purified enzyme	(Wagner 1983)
5-Bromo-1-naphthaldehyde	2.5 ± 0.3	2 ± 0.2*	Human	Liver cytosol purified enzyme (ALDH1)	(A. R. Klyosov, Possible role of liver cytosolic

					and mitochondrial aldehyde dehydrogenases in acetaldehyde metabolism 1996)
6-(Dimethylamino)-2-naphthaldehydec	6.3 ± 1.8	20 ± 5*	Human	Liver cytosol purified enzyme (ALDH1)	(A. R. Klyosov, Possible role of liver cytosolic and mitochondrial aldehyde dehydrogenases in acetaldehyde metabolism 1996)
5-Nitro-1-naphthaldehyde	11 ± 5	4.2 ± 0.6*	Human	Liver cytosol purified enzyme (ALDH1)	(A. R. Klyosov, Possible role of liver cytosolic and mitochondrial aldehyde dehydrogenases in acetaldehyde metabolism 1996)
Fluorene-2-carboxaldehyde	54 ± 6	46 ± 5*	Human	Liver cytosol purified enzyme (ALDH1)	(A. R. Klyosov, Possible role of liver cytosolic and mitochondrial aldehyde

					dehydrogenases in acetaldehyde metabolism 1996)
p-(Dimethylamino)benzaldehyde	60 ± 20	16 ± 2*	Human	Liver cytosol purified enzyme (ALDH1)	(A. R. Klyosov, Possible role of liver cytosolic and mitochondrial aldehyde dehydrogenases in acetaldehyde metabolism 1996)
4-Methoxy-1-naphthaldehyde	200 ± 20	34 ± 5*	Human	Liver cytosol purified enzyme (ALDH1)	(A. R. Klyosov, Possible role of liver cytosolic and mitochondrial aldehyde dehydrogenases in acetaldehyde metabolism 1996)
Indole-3-acetaldehydec	310 ± 20	86 ± 2*	Human	Liver cytosol purified enzyme (ALDH1)	(A. R. Klyosov, Possible role of liver cytosolic and mitochondrial aldehyde dehydrogenases in acetaldehyde metabolism

					1996)
Trans-cinnamaldehyde	400 ± 40	59 ± 5*	Human	Liver cytosol purified enzyme (ALDH1)	(A. R. Klyosov, Possible role of liver cytosolic and mitochondrial aldehyde dehydrogenases in acetaldehyde metabolism 1996)
p-(Dimethylamino)cinnamaldehyde	900 ± 200	62 ± 5*	Human	Liver cytosol purified enzyme (ALDH1)	(A. R. Klyosov, Possible role of liver cytosolic and mitochondrial aldehyde dehydrogenases in acetaldehyde metabolism 1996)
7-(Dimethylamino)coumarin-4-carboxaldehydec	1420 ± 230	60 ± 10*	Human	Liver cytosol purified enzyme (ALDH1)	(A. R. Klyosov, Possible role of liver cytosolic and mitochondrial aldehyde dehydrogenases in acetaldehyde metabolism 1996)
Phenylacetaldehyde	5500 ± 1200	380 ± 40*	Human	Liver cytosol purified enzyme	(A. R. Klyosov, Possible role of

				(ALDH1)	liver cytosolic and mitochondrial aldehyde dehydrogenases in acetaldehyde metabolism 1996)
Phenanthrene-9-carboxaldehyde	9400 ± 800 2700 ± 700	<4*	Human	Liver cytosol purified enzyme (ALDH1)	(A. R. Klyosov, Possible role of liver cytosolic and mitochondrial aldehyde dehydrogenases in acetaldehyde metabolism 1996)
Acetaldehyde	0.18 ± 0.10	-	Human	Liver cytosol purified enzyme (ALDH1)	(A. R. Klyosov, Possible role of liver cytosolic and mitochondrial aldehyde dehydrogenases in acetaldehyde metabolism 1996)
Propanal	$4.5 \pm 0.3 \times 10^{-3}$	-	Human	Liver cytosol purified enzyme (ALDH1)	(A. R. Klyosov, Possible role of liver cytosolic and mitochondrial

					aldehyde dehydrogenases in acetaldehyde metabolism 1996)
Pentanal	$0.16 \pm 0.03 \times 10^{-3}$	-	Human	Liver cytosol purified enzyme (ALDH1)	(A. R. Klyosov, Possible role of liver cytosolic and mitochondrial aldehyde dehydrogenases in acetaldehyde metabolism 1996)
Hexanal	$0.041 \pm 0.002 \times 10^{-3}$	-	Human	Liver cytosol purified enzyme (ALDH1)	(A. R. Klyosov, Possible role of liver cytosolic and mitochondrial aldehyde dehydrogenases in acetaldehyde metabolism 1996)
Heptanal	$0.018 \pm 0.002 \times 10^{-3}$	-	Human	Liver cytosol purified enzyme (ALDH1)	(A. R. Klyosov, Possible role of liver cytosolic and mitochondrial aldehyde dehydrogenases in acetaldehyde

					metabolism 1996)
Octanal	$0.012 \pm 0.002 \times 10^{-3}$	-	Human	Liver cytosol purified enzyme (ALDH1)	(A. R. Klyosov, Possible role of liver cytosolic and mitochondrial aldehyde dehydrogenases in acetaldehyde metabolism 1996)
Decanal	$2.9 \pm 0.4 \times 10^{-6}$	-	Human	Liver cytosol purified enzyme (ALDH1)	(A. R. Klyosov, Possible role of liver cytosolic and mitochondrial aldehyde dehydrogenases in acetaldehyde metabolism 1996)
Retinal	$0.99\text{-}1.3 \times 10^{-3}$	-	Human	Liver cytosol purified enzyme (ALDH1)	(A. R. Klyosov, Possible role of liver cytosolic and mitochondrial aldehyde dehydrogenases in acetaldehyde metabolism 1996)
Formaldehyde	0.32 ± 0.08	-	Human	Liver mitochondria	(A. R. Klyosov,

				purified enzyme (ALDH2)	Possible role of liver cytosolic and mitochondrial aldehyde dehydrogenases in acetaldehyde metabolism 1996)
Acetaldehyde	$0.20 \pm 0.02 \times 10^{-3}$	-	Human	Liver mitochondria purified enzyme (ALDH2)	(A. R. Klyosov, Possible role of liver cytosolic and mitochondrial aldehyde dehydrogenases in acetaldehyde metabolism 1996)
Propanal	$95 \pm 5 \times 10^{-6}$	-	Human	Liver mitochondria purified enzyme (ALDH2)	(A. R. Klyosov, Possible role of liver cytosolic and mitochondrial aldehyde dehydrogenases in acetaldehyde metabolism 1996)
Pentanal	$34 \pm 2 \times 10^{-6}$	-	Human	Liver mitochondria purified enzyme (ALDH2)	(A. R. Klyosov, Possible role of liver cytosolic and

					mitochondrial aldehyde dehydrogenases in acetaldehyde metabolism 1996)
Hexanal	$30 \pm 5 \times 10^{-6}$	-	Human	Liver mitochondria purified enzyme (ALDH2)	(A. R. Klyosov, Possible role of liver cytosolic and mitochondrial aldehyde dehydrogenases in acetaldehyde metabolism 1996)
Heptanal	$27 \pm 4 \times 10^{-6}$	-	Human	Liver mitochondria purified enzyme (ALDH2)	(A. R. Klyosov, Possible role of liver cytosolic and mitochondrial aldehyde dehydrogenases in acetaldehyde metabolism 1996)
Octanal	$28 \pm 4 \times 10^{-6}$	-	Human	Liver mitochondria purified enzyme (ALDH2)	(A. R. Klyosov, Possible role of liver cytosolic and mitochondrial aldehyde dehydrogenases

					in acetaldehyde metabolism 1996)
Decanal	$22 \pm 3 \times 10^{-6}$	-	Human	Liver mitochondria purified enzyme (ALDH2)	(A. R. Klyosov, Possible role of liver cytosolic and mitochondrial aldehyde dehydrogenases in acetaldehyde metabolism 1996)
Retinal	$<100 \times 10^{-6}$	-	-	ALDH1A1	(Marchitti 2008)
Acetaldehyde	$0.9\text{-}5 \times 10^{-3}$ 0.8-1.4	-	Mouse	Mitochondrial fraction	(A. R. Klyosov, Possible role of liver cytosolic and mitochondrial aldehyde dehydrogenases in acetaldehyde metabolism 1996)
Acetaldehyde	$10\text{-}50 \times 10^{-3}$ 0.1-0.6	-	Mouse	Cytosol	(A. R. Klyosov, Possible role of liver cytosolic and mitochondrial aldehyde dehydrogenases in acetaldehyde metabolism

					1996)

*% Relative to acetaldehyde

1.3.4 Isoenzymes and Expression

250 genes under the ALDH superfamily were identified in different species (V. P. Vasiliou 2000). Out of these genes, 16 genes were identified in human (V. P. Vasiliou 2000) and transcriped into around 20 families. Each family consists of enzymes having at least 40% of similarity in their sequence, symbolized by an Arabic number. If more than 60% of sequence similarity exists, these enzymes are categorized under the same subfamily indicated by a letter (Sophos 2003) (V. N. Vasiliou 2005). For example, ALDH1L2 has 72% homology with ALDH1L1 and ALDH3B2 has 83% similarity with ALDH3B1 (Marchitti 2008). In addition, ALDH1B shares 75% of homology with ALDH2 (Marchitti 2008). There is around 68% positional identity between ALDH1 and ALDH2 (Agarwal 1992). It is noteworthy that when 145 ALDH proteins aliened, only Gly-245, Gly-299, Glu-399, and Phe-401 were the amino acids conserved among these proteins (Manzer 2003).

With respect to their subcellular expression, ALDH are expressed in all cell components (Marchitti 2008). However, the majority of the isoenzymes are located in the cytosol followed by mitochondria as shown in Table 1-9. For instance, ALDH2 is mainly present in mitochondria while ALDH1 and ALDH3 are present in the cytosol (C. D. Cheung 2003).

In the body, ALDH are widely distributed in tissues (Marchitti 2008). While ALDH isoenzymes are abundant in the liver, as shown in Table 1-10, it is also expressed in different parts of the body. Even though the main isoenzymes, ALDH1-3, are expressed in liver, they are present in extrahepatic tissues (C. D. Cheung 2003). For example, ALDH1 and ALDH3 are expressed in cornea (Manzer 2003). Moreover, the expression of some ALDH enzymes increases in tumor tissues as a response for oxidative stress (Gaspar 2009).

Table 1-9. Subcellular locations of ALDH isoenzymes **(Marchitti 2008) (V. P. Vasiliou 2000)**

Subcellular Location	Isoenzyme
Cytosol	ALDH1A1, ALDH1A2, ALDH1A3, ALDH1L1, ALDH1L2, ALDH3A1, ALDH3B1, ALDH3B2, ALDH7A1, ALDH8A1, ALDH9A1
Mitochondria	ALDH1B1, ALDH2, ALDH4A1, ALDH5A1, ALDH6A1, ALDH7A1, ALDH18A1
Nucleus	ALDH3A1, ALDH7A1
Microsomes, peroxisomes	ALDH3A2

Table 1-10. Tissue expression of ALDH isoenzymes.

Isoenzyme	Expression	Reference
ALDH1A1	Highest in liver but also present in eye lens, brain (dopaminergic neurons) kidney, lung, hematopoietic stem cells, red blood cells, genital tissues Androgen-inducible protein Highly conserved	(V. P. Vasiliou 2000) (Marchitti 2008)
ALDH1A2	Intestine, testis, lung, kidney, liver, brain, and retina.	(Marchitti 2008)
ALDH1A3	Salivary glands, stomach, breast, kidney, nasal mucosa, eye, olfactory bulbs, hair follicles, forebrain, and cerebral cortex.	(Marchitti 2008)
ALDH1A6	kidney, salivary glands, and stomach	(V. P. Vasiliou 2000)
ALDH1B1	Liver, kidney, muscle, heart, placenta, cornea, testis, and brain.	(V. P. Vasiliou 2000) (Marchitti 2008)
ALDH1L1	Mainly in liver, pancreas, and kidney. Also in lung, prostate, brain, muscle, thymus, ovary, and testis. Downregulated by xenobiotics as acetaminophen and methotrexate	(Marchitti 2008)
ALDH1L2	Spleen	(Marchitti 2008)
ALDH2	Liver, brain, heart, lung, leukocytes, and hair roots	(V. P. Vasiliou 2000) (Yamamoto 1993) (Marchitti 2008)

ALDH3A1	Cornea, stomach, lung, skin, esophagus Inducible by cortisone and xenobiotics (e.g. polycyclic aromatic hydrocarbons) and cancers. Can be downregulated by progesterone	(V. P. Vasiliou 2000) (Marchitti 2008) (Liao 1991)
ALDH3A2	Liver, kidney, stomach, intestine, muscle, skin, lung, pancreas, heart, brain, and placenta.	(V. P. Vasiliou 2000) (Marchitti 2008) (Liao 1991)
ALDH3B1	Mainly in liver and kidney and in lesser amounts in lung and brain.	(Marchitti 2008)
ALDH3B2	Salivary glands, lung, brain, liver, kidney, and prostate.	(Marchitti 2008)
ALDH4A1	Liver, muscle, and kidney.	(Marchitti 2008)
ALDH5A1	Mainly in brain but also present in liver, pituitary, muscle, heart, and ovary	(V. P. Vasiliou 2000) (Marchitti 2008)
ALDH6A1	Mainly in liver, kidney, heart, and to a less extent in muscle and brain	(V. P. Vasiliou 2000) (Marchitti 2008)
ALDH7A1	Heart, liver, and kidney	(Marchitti 2008)
ALDH8A1	Liver, kidney mainly and moderately in brain, spinal cord	(Marchitti 2008)
ALDH9A1	Liver, kidney, muscle, and brain	(V. P. Vasiliou 2000) (Marchitti 2008)
ALDH18A1	Pancreas, ovary, testis, and kidney.	(Marchitti 2008)

Despite the fact that a particular ALDH isoenzyme might be expressed in more than one tissue, its activity might be different from one tissue to another. An example of that is shown in Table 1-11 for ALDH2 enzyme.

Table 1-11. ALDH activity in human tissues relative to that in liver. **(Yin 1994)**

	Liver	**Lung**	**Esophagus**	**Stomach**	**Colon**	**Rectum**
ALDH2	100	2.8	2.8	12	3.8	4.0

1.3.5 Polymorphism and Pharmacogenetics

Nine of 16 ALDH genes identified in humans are polymorphic and appear to play an important role in human development and neurological health (V. P. Vasiliou 2000). Consequently, this genetic mutation is associated with metabolic diseases having neurological manifestations, such as hyperprolinemia, where the increase in proline levels is associated with seizures and mental retardation, Sjogren-Larsson syndrome (SLS), and cancer (V. N. Vasiliou 2005) (V. P. Vasiliou 2000). Moreover, a manipulation in the ALDH1 genes led to death of mice at their midgestational stage (V. P. Vasiliou 2000). In addition, ALDH deficiency is investigated as a contributing factor in Alzheimer disease (V. N. Vasiliou 2005). Table 1-12 summarizes diseases associated with ALDH polymorphism and deficiency. The importance of ALDH enzymes is evident by the diseases caused by mutations in its isoenzymes.

A well-known pharmacogenetic issue that is associated with ALDH is alcoholism. While familial history is an important factor in alcoholism because of environmental and cultural issues, the inheritance of ALDH polymorphism is another factor in familial trends in alcoholism where ALDH polymorphism is thought to be protective against alcoholism (Agarwal 1992). In mice, acute alcohol intoxication affected the activity of ALDH2 but not ALDH1 (Tomita 1990). The loss of ALDH2 activity might be a consequence of a point mutation in the ALDH2 gene, which is common among Asian populations who are not alcoholics (48% vs 12%) (Thomasson 1991) (Beedham 1997). This mutation causes sensitivity to alcohol consumption in 50% of Orientals and 40% of American Indians since they lack the activity of ALDH2 causing slower metabolism of acetaldehyde (Liao 1991) (Agarwal 1992) (Yamamoto 1993). Consequently, persons with ALDH2 deficiency suffer from aversive reactions including, facial flushing, nausea,

and palpitation as a result of catecholamine and kinins release (Thomasson 1991) (Beedham 1997) (Hatake 1990) (Agarwal 1992). ALDH2 deficient population are characterized by the presence of ALDH2*1/ALDH2*2 and ALDH2*2/ ALDH2*2 alleles (Yamamoto 1993). The difference between ALDH2*1 and ALDH2*2 involves an alteration of a single base, where guanine is replaced by adenine (Yamamoto 1993). Consequently, this point mutation results in the expression of lysine in the 14 position from the C-terminus instead of glutamic acid (Agarwal 1992). Moreover, alcohol flushing syndrome is associated with alcohol related cancer and hypertension (V. N. Vasiliou 2005) (V. P. Vasiliou 2000). Nevertheless, this polymorphism has an advantage through protecting against alcoholism (V. P. Vasiliou 2000). On the other hand, flushing in Caucasian population is due to several mutations leading to ALDH1 activity decrease (Agarwal 1992).

Table 1-12. Diseases associated with ALDH polymorphism and deficiency.

ALDH Isoenzyme	Disease	Reference
ALDH1A1	Increased the likely risk of ethanol-induced cancers Decreased the likely risk of alcoholism Lower expression levels: Down's syndrome. Testicular feminization Parkinson Disease Schizophrenia	(V. P. Vasiliou 2000) (Marchitti 2008)
ALDH1A2	Spina bifida Congenital diaphragmatic hernia Alcohol-induced toxicity in liver and eye lens	(Marchitti 2008)
ALDH1A3	Congenital diaphragmatic hernia Downregulated in breast cancer	(Marchitti 2008)
ALDH2	Increased risk of ethanol-induced cancers (esophageal and upper aerodigestive tract cancers) Decreased risk of alcoholism Increased DNA damage in polyvinyl chloride workers who smoke. A decrease in nitroglycerin efficiency Myocardial infarction, and hypertension Late onset Alzheimer disease Parkinson disease	(V. P. Vasiliou 2000) (Marchitti 2008)
ALDH1L1	Decrease reproductive efficiency Imbalances in tetrahydrofolate Increased risk of methanol toxicity Increased or decreased risk of postmenopausal breast cancer Downregulated in pancreas, liver, prostate, ovarian, and lung cancers	(Marchitti 2008)
ALDH3A1	Susceptibility to cataract upon UV exposure	(Marchitti 2008)
ALDH3A2	Sjögren-Larsson syndrome Preterm birth	(V. P. Vasiliou 2000) (Marchitti 2008)
ALDH3B1	Mutation is associated with paranoid and schizophrenia	(Marchitti 2008)
ALDH4A1	Type II hyperprolinemia	(V. P. Vasiliou 2000) (Marchitti 2008)
ALDH5A1	4-hydroxybutyric aciduria	(V. P. Vasiliou 2000)
ALDH6A1	Developmental delay	(V. P. Vasiliou 2000)

1.3.6 Similarities between Species

ALDH activity was observed in the liver of rat, rabbit, dog, monkey, cow, sheep, and pig (Deitrich 2007). In addition, ALDH was studied in the lung and kidneys of rat, rabbit, dog, and monkey (Deitrich 2007). Nevertheless, the expression, structure, presence of isoenzymes, catalytic activity, and inhibition sensitivity are factors that contributes to the differences observed between species with respect to ALDH activity. Hence, similarities between species ALDH1 enzyme was studied through its activity in metabolizing acetaldehyde and other compounds (A. R. Klyosov, Possible role of liver cytosolic and mitochondrial aldehyde dehydrogenases in acetaldehyde metabolism 1996). In addition, human, hamster, and rat liver homogenates were compared using agarose gel electrophoresis (A. R. Klyosov, Possible role of liver cytosolic and mitochondrial aldehyde dehydrogenases in acetaldehyde metabolism 1996). Such studies demonstrated that there is a high similarity (91%) in ALDH1 between human and horse (Agarwal 1992).

Although rodents are used for investigating ADH and ALDH activities assuming similarity in of these enzyme to the isoenzymes present in human (A. R. Klyosov, Possible role of liver cytosolic and mitochondrial aldehyde dehydrogenases in acetaldehyde metabolism 1996), the cytosolic fraction for human liver was characterized by the presence of ALDH1 while the hamster and rat cytosolic fraction contained three isoenzymes of ALDH (A. R. Klyosov, Possible role of liver cytosolic and mitochondrial aldehyde dehydrogenases in acetaldehyde metabolism 1996). In addition, rodents' cytosolic ALDH1 enzyme exhibits more basic character, lower molecular weight (120000-150000) than human ALDH1 (230000-240000) and are presumed to be dimeric in contrast to the tetrameric human ALDH1 enzyme (A. R. Klyosov, Possible role of liver cytosolic and mitochondrial aldehyde dehydrogenases in acetaldehyde

metabolism 1996). Furthermore, it was found that human cytosolic ALDH1 is different from rodents' ALDH1 in its catalytic activity toward acetaldehyde (A. R. Klyosov, Possible role of liver cytosolic and mitochondrial aldehyde dehydrogenases in acetaldehyde metabolism 1996).

With respect to isoenzyme expression, rabbits express ALDH1 in the cornea rather than ALDH3 that is expressed in the cornea of human, pigs, baboon, bovine, sheep, rat, and mice (Manzer 2003).

1.3.7 ALDH in RBCs

A tetramer ALDH enzyme has been characterized in human RBCs (Inoue 1979) (Rawles 1987) (Ueshima 1993). Similarities between this enzyme and human cytosolic enzyme in the liver were reported including their sensitivity to acetaldehyde and disulfiram along with their optimum pH (Inoue 1979) (Rawles 1987). The physiological function for ALDH in RBCs is not known, however, it is thought to contribute to the metabolism of the acetaldehyde fraction that escapes liver metabolism (Rawles 1987). During a study conducted by Ueshima et. al., one subject out of 16 subjects had no expression of ALDH in his RBCs (Ueshima 1993). With the exception of that subject, ALDH activity was estimated as 25 nmol NADH/minute/g hemoglobin (Ueshima 1993). The same group conducted an *in-vitro* study, in which acetaldehyde was added at a concentration of 0.1 mM to 1 ml of heparinized blood and measured over 14 minutes by gas chromatography. Approximately 60-70% of the added acetaldehyde disappeared within the 14 minutes, while only 20% disappeared in the person with ALDH deficiency (Ueshima 1993). At the physiological concentration of Mg^{+2}, it inhibited ALDH probably by decreasing the rate of enzyme-NADH dissociation rate (Rawles 1987). Hence, while diluting the RBC matrix to conduct metabolic studies, the inhibitory effect of Mg^{+2} will be diluted. Hence, the activity of the

enzyme will be overestimated (up to 6-fold as implied by Rawles et al.) upon extrapolating the *in-vitro* activity to its corresponding *in-vivo* value.

ALDH activity decreased upon storage of RBCs at 4, -20, -70 °C (Johnson 1992). Addition of sucrose at 40 g/l concentration increased ALDH stability upon storage at -20 °C (Johnson 1992). Lactate dehydrogenase might interfere in the results but can be inhibited by oxalate (Johnson 1992). It is noteworthy that ALDH activity was not observed in rat blood (Deitrich 2007).

1.4 Alcohol Dehydrogenase (ADH)

ADH is a potential enzyme in the metabolism of 5-HMF. Below is a description of its structure, function, substrates, isoenzymes, expression, polymorphism, and pharmacogenetics.

1.4.1 Structure

ADH is an 80 kDa dimeric-enzyme that catalyzes an interconversion reaction between alcohol and aldehydes (Agarwal 1992) (C. D. Cheung 2003). Each subunit contains two zinc molecules and is consisted of around 374 amino acids (Yin 1994) (Agarwal 1992) (Liao 1991). There are seven structural genes encoding for the subunits of ADH, namely; α, β, γ, π, x, and μ (Liao 1991) (Agarwal 1992) (Ricciardi 1983) (Yin 1994). These subunits are the basis for the six identified mammalian classes, which are ADH1 through ADH6 (C. D. Cheung 2003).

1.4.2 Function

ADH catalyzes the interconversion of alcohols and their corresponding aldehydes, including primary, secondary, and tertiary alcohols that are primarily aliphatic in nature and to a lesser degree are cyclic (Agarwal 1992). ADH is involved in the metabolism of endogenous compounds, such as retinol, bile acid, and steroids (Agarwal 1992). Likewise, ADH catalyzes the bioconversion of xenobiotics, like food flavors and digoxin (Agarwal 1992). Ethanol is one of the most studied substrates, for which ADH is significantly responsible for converting it to acetaldehyde (Liao 1991) (Agarwal 1992) (Yin 1994). Besides its known function in the

oxidation of aliphatic and aromatic alcohol, it was reported to have aldehyde dismutase function transferring aldehydes into acids (C. D. Cheung 2003).

1.4.3 Substrates

The K_m for ethanol was determined between 0.049-4.2 mM for class I ADH while it was 30 mM for Class II, IV, V. Class III does not seem to be involved in ethanol metabolism (Yin 1994).

1.4.4 Isoenzymes and Expression

ADH1-2 are predominantly expressed in liver while ADH3 is present in liver and extrahepatic tissues (C. D. Cheung 2003). With respect to extrahepatic tissues, ADH is expressed in stomach with 20% of ingested ethanol metabolized there (Liao 1991). The γ ADH is the predominant isoenzyme in the gastrointestinal tract with small amounts of β ADH present (Liao 1991). In addition, ADH2 is also present in leukocytes (Yamamoto 1993). Table 1-13 summarizes ADH activities in human tissue relative to liver.

Table 1-13. ADH activities in human tissue relative to liver **(Yin 1994)**

	Liver	**Lung**	**Esophagus**	**Stomach**	**Colon**	**Rectum**
ADH1	100	2.1	26	8.2	7.2	10

1.4.5 Polymorphism and Pharmacogenetics

There is 90% similarity in enzymes with the same class and 60% between the enzymes from different classes (Yin 1994). Genetic polymorphism that is associated with ADH occurs in β_1, β_2, β_3 and γ_1, γ_2 genes of ethnic groups (Liao 1991) (Yamamoto 1993) (Yin 1994). Particularly, polymorphism in β and γ subunits of ADH2 and ADH3, respectively, are thought to be responsible for the genetic part that accounts for up to 50% of the three-fold difference in alcohol metabolism observed in different populations (Thomasson 1991). This polymorphism in ADH2 and ADH3 were more frequent in non-alcoholic Chinese when compared to alcoholics Chinese (Thomasson 1991). Non-alcoholic populations have ADH with higher capacity to metabolize ethanol since they have the ADH2*2 allele with β_2 subunit, which has a higher enzymatic activity in comparison to the wild ADH2*1 allele with β_1 subunit (Thomasson 1991) (Ricciardi 1983). However, it was shown later that a significant higher acetaldehyde concentration in the blood of individuals who are homozygous for ALDH2*2 in comparison to those who are homozygous for ADH2*2 (Yamamoto 1993) (Ricciardi 1983). The frequency of ADH 2*2 in Japanese and Chinese was found to be around 69%-85% while it was 20% in Swiss population (Yamamoto 1993) (Agarwal 1992) (Ricciardi 1983). Table 1-14 shows the frequency of ADH polymorphism in different population.

Table 1-14. ADH polymorphism in different population **(Yin 1994)**

	ADH2[1]	**ADH2[2]**	**ADH2[3]**	**ADH3[1]**	**ADH3[2]**
Orientals	0.30	0.70	0	0.90	0.10
Caucasian	0.90	0.10	0	0.60	0.40
African-American	0.84	0	0.16	0.85	0.15
American Indian	1.00	0	0	0.41	0.59
Taiwanese Aborigines	0.09	0.91	0	0.99	0.01

1.4.6 Similarities between Species

ADH1 is present in mouse, rat, guinea pig, and human liver and skin (C. D. Cheung 2003). However, its expression level is dependent on the developmental stage, as shown in rat and mice (C. D. Cheung 2003). On the other hand, it was shown that ADH2 is not expressed in mouse, rat, guinea pig skin but expressed their livers and the liver and the skin of humans (C. D. Cheung 2003). The v_{max} determined for ADH in human skin was lower than that for rodents and guinea pig although their intrinsic clearance (v_{max}/K_m) values were similar (C. D. Cheung 2003).

In addition, Gupta reported different K_m and v_{max} values ranging between 0.8-14 mM and 0.05-2.8 mmol/min, respectively, for *in-vivo* ethanol metabolism, mediated by ADH, in rat, rabbit, dog, and human (Gupta 2006). Besides, Cheung and co-workers observed that the cytosolic ADH of rodents had a lower metabolic efficiency of ethanol metabolism than that of human (C. D. Cheung 2003).

1.5 Blood Composition

Blood is a connective tissue that safeguards living cells in the body by delivering oxygen and nutrients as well as getting rid of toxins (Rhoades 1996). Blood is confined to the blood vessels and heart compartments (Rhoades 1996). Figure 1-21 shows the main components of sedimented blood layers. The average viscosity of an adult blood is 4.5-fold higher than water (Rhoades 1996).

1.5.1 Plasma

Plasma is a transparent fluid that carries blood platelets, cells, and proteins (Rhoades 1996). Upon fractionation of blood, plasma is separated from the blood cells and platelets. When fractionated, plasma is mainly composed of water (93%) that contains proteins, organic, and inorganic substance (Rhoades 1996). Plasma proteins regulate the osmotic pressure of blood, which controls the exchange of substances between blood and interstitial fluid (Rhoades 1996). In addition, it acts as a reservoir for amino acids and as a buffering agent to keep the slightly alkaline environment of blood (Rhoades 1996). A well-known function of plasma proteins is the transport of endogenous substances, such as hormones and the otherwise insoluble fat (Rhoades 1996). Moreover, exogenous material exemplified by drugs can bind to plasma proteins (Rhoades 1996).

1.5.2 Red Blood Cells

Approximately 5000 million RBCs exist in each milliliter of the blood (Rhoades 1996). RBCs (erythrocytes) originates from the bone marrow through the erythropoiesis process (Rhoades 1996). In contrast to other cells in the body, mature RBCs do not contain a nucleus and are anchored by a cytoskeleton that is connected to the inner membrane of RBCs (Rhoades 1996). They are characterized by their flexibility, which allow them to pass through blood vessels regaining their biconcave shape, after bending and twisting (Rhoades 1996). In addition, their distinct shape increases their main function efficiency, which involves gases exchange, because it maximizes the surface area to volume ratio (Rhoades 1996).

Unfortunately, the flexibility and the doughnut shape of RBCs are impaired in genetic diseases like sickle cell anemia. Table 1-15 lists the differences between normal RBCs and sickled RBCs.

Table 1-15. Differences between normal and sickled RBCs.

	Sickled RBCs relative to Normal RBCs	Reference
Reticulocytes	Increased	(Hebbel 1991)
Abnormally dense RBCs	5-50%	(Hebbel 1991)
Water content	Dehydrated	(Hebbel 1991)
Mean cell hemoglobin concentration (MCHC)	Increased	(Hebbel 1991)
Irreversible sickled RBCs	Present	(Hebbel 1991)
Monovalent cations	Increased Na^{+} Decreased K^{+}	(Hebbel 1991)
Ca^{+2}	10 fold increase in total Ca^{+2}	(Hebbel 1991)
Lipid bilayer	Phospholipid destabilization Adducts with malondialdehyde	(Hebbel 1991)
Strength and flexibility	Decreased	(Hebbel 1991)
Hemoglobin	Decreased stability and solubility	(Hebbel 1991)

1.5.3 White Blood Cells (WBCs)

Approximately 7 to 10 million WBCs are present in each one milliliter of whole blood (Rhoades 1996). WBC types are distinguished by the shape of their nuclei and the presence or the absence of granulated vesicles (Rhoades 1996). WBCs need staining for differentaion purposes since they do not contain coloring molecules in contrast to RBCs (Rhoades 1996). Besides the blood stream, WBCs are found in the lymphatic system and connective tissues (Rhoades 1996). Their general function is defense against toxins and foreign substance entering the body (Rhoades 1996). As part of the immune system, they produce antibodies against and engulf invading bacteria (Rhoades 1996).

1.5.4 Platelets

Platelets (thrombocytes) are membrane bounded cell fragments that lack nuclei (Rhoades 1996). There are approximately 150-350 million platelets in each milliliter of blood (Rhoades 1996). Their main function is concerned with decreasing blood loss in injuries by playing a role in blood vessel contraction and blood coagulation at the site of injury (Rhoades 1996).

1.5.5 Blood Proteins

Albumin and α-acid glycoprotein (AAG) are involved in drug binding. There are other proteins present in plasma at low concentration, such as lipoproteins, C-reactive proteins and are thought to have a minimal contribution to drug binding (Routledge 1986). The overall concentration of albumin and globulins in the blood are regulated to keep a constant total concentration with a variant albumin/globulin ratio depending on the health status of the patient.

1.5.5.1 Albumin

Albumin accounts for 60% of plasma proteins, thus represents the most abundant protein in plasma and it is a main contributor to the osmotic pressure of blood (Rhoades 1996). Hence, a decrease in its concentration, because of malnutrition or liver disease, results in a fluid shift from the blood compartment into interstitial fluid (Rhoades 1996). Albumin is a single chain peptide protein with a molecular weight of 66,478 Da (Sigma-Aldrich n.d.). Human serum albumin solubility is 50 g/l (Sigma-Aldrich n.d.). Although albumin concentration is relatively stable, 35-50 g/l, it can decrease in disease states, such as renal and hepatic failures (Corti 1994). Nevertheless, changes in the concentration are less than two fold of the normal concentration. This concentration stability in addition to the fact that albumin has low affinity, high capacity of binding make drugs binding to albumin less susceptible to variations (Routledge 1986).

1.5.5.2 Hemoglobin

Hemoglobin (Hb) is a tetramer protein that is soluble in water at a concentration of 20 g/l (Sigma-Aldrich n.d.). The molecular weight of hemoglobin is 64,677 Da (Sigma-Aldrich n.d.). The average concentration of hemoglobin in blood is 150 g/l (2.3 mM) (Dixon 1997), while the average normal mean corpscular hemoglobin concentration (MCHC), i.e. concentration of hemoglobin in erythrocytes, is 340 g/l (5.3 mM) (Clark 1989). Hemoglobin is major carrier of oxygen in the body and the absence of this function requires the heart to pump around 80 l/minute since only a small percentage of oxygen is dissolved in blood (Sladen 1981). Hemoglobin is known for its cooperativety in binding to oxygen, as described by Hill, with conformational changes facilitating this binding (Riggs 1998). Upon oxygen binding to the heme groups in hemoglobin, it destabilizes salt bridges in the quaternary structure of hemoglobin leading to an increase in the affinity to oxygen that appears in the sigmoidal shape of oxygen saturation curve (Sladen 1981). This curve is characterized by the P_{50} value, which represent the oxygen pressure achieving 50% saturation of hemoglobin. The typical P_{50} value in healthy individuals is 26.5 mmHg (Sladen 1981). However, the P_{50} is affected by temperature and organic and inorganic ligands, such as proton ions (H^+), carbon dioxide (CO_2), and 2,3 diphosphoglycerate (2,3-DPG). While the increase in CO_2 and 2,3-DPG concentration is associated with an increase in the P_{50} (right-shift in the oxygen saturation curve), the increase in the pH affects the P_{50} inversely (left-shift in the oxygen saturation curve). The concentration of 2,3-DPG is approximately 4 mM inside the RBCs and doubling its concentration has a major effect oxygen curve resulting a P_{50} of 37 mmHg (Sladen 1981). The decrease in hemoglobin affinity toward oxygen is a result of 2,3-DPG salt bridging interaction between the β–chains (Safo 2004).

1.5.5.3 AAG

The molecular weight of AAG is 40,000 Da and it has an acidic pKa. The concentration of albumin is approximately 100 times more than AAG (Routledge 1986). Its physiological function of this acidic protein is not clear but it can contribute to immunological and repair processes (Routledge 1986). Hydrophobic rather than electrostatic interactions are mainly involved in drugs binding to AAG (Routledge 1986). AAG does not significantly contribute to the binding of acidic drugs, which are more attracted to human serum albumin. Propranolol and disopyramide are examples of drugs bound to AAG (Routledge 1986). AAG is present in both plasma and extra-vascular space (Routledge 1986). AAG concentration is affected by environmental conditions more than hereditary factors (Routledge 1986). Since the concentration of AAG differs according to the health status, drug binding to this protein is associated with variability (Routledge 1986). For example, the concentration of AAG increases in infections, obese subjects, and in subjects on anticonvulsant therapy while it has lower levels in patients with nephrotic syndrome (Routledge 1986). Besides, AAG is characterized by a low capacity, high affinity binding interaction and subject to saturation (Routledge 1986).

CHAPTER 2

HYPOTHESES, SPECIFIC AIMS, AND SIGNIFICANCE

2.1 Hypotheses

The main objective of this research is to help predict human *in-vivo* PK of 5-HMF using *in-vitro-in-vivo* extrapolation (IVIVE). The results will be useful in determining a non-toxic and biologically relevant dosage regimen to be used in phase I clinical trials. Therefore, the hypotheses guiding this research are as follows:

- In hepatic cytosol:
  - 5-HMF is subject to ALDH- and ADH-mediated metabolism.
  - Significant species differences in 5-HMF disposition exist among mouse, rat, dog, and human.
- In human blood:
  - 5-HMF is subject to ALDH-mediated metabolism.
  - 5-HMF demonstrates a time- and a concentration-dependent binding to Hb.
  - 5-HMF demonstrates a time- and a concentration-dependent binding to HSA.

2.2 Specific Aims

In order to test the hypotheses specified in section 2.1, the following specific aims are proposed in this research project:

1. To review the available literature on the physiochemical properties, PK, and PD of 5-HMF, as a potential antisickling agent.
2. To optimize the experimental conditions needed to investigate 5-HMF metabolism and binding in blood and hepatic cytosol.
3. To develop and validate an assay method for the quantitation of 5-HMF in neat solution, human plasma, and human RBCs.
4. To identify the metabolic pathways of oxidative 5-HMF metabolism in human hepatic cytosol.
5. To determine the *in-vitro* affinities and metabolic capacities of 5-HMF in mouse, rat, dog, and human hepatic cytosol.
6. To perform IVIVE of hepatic metabolism for 5-HMF in mouse, rat, dog, and human hepatic cytosol and compare it with published data.
7. To determine the *in-vitro* affinity and metabolic enzyme capacity of 5-HMF in human RBCs.
8. To perform IVIVE for 5-HMF metabolism in human RBCs and compare it with published data.
9. To investigate the time-dependent kinetics of 5-HMF binding to human hemoglobin and serum albumin.
10. To determine the steady-state concentration-dependent parameters of 5-HMF binding to human hemoglobin and serum albumin.

11. To develop a PK model that combines both hemoglobin binding and RBC metabolism of 5-HMF to explain its disposition in blood.

2.3 Significance

Sickle cell disease is classified as the most common inherited disease in the world (Howard 2009). The susceptibility of HbS to polymerize upon deoxygenation is severe enough to decrease the life expectancy of patients with this disease to 45-55 years (Howard 2009). Moreover, sickle cell disease is accompanied with a decrease in the quality of life of the patient and their families because of the recurring and unpredictable pain episodes and other chronic and acute complications related to obstruction of blood vessels by sickled RBCs (Howard 2009). Bone marrow transplantation represent a cure for this disease, however, it is hindered by the having a suitable donor and the eligibility of the patient for this procedure (Bolaños-Meade 2009). The only treatment that specifically targets pathophysiology of sickle cell disease is hydroxyurea, through stimulating the production of HbF, which has higher oxygen affinity (Lanzkron 2008). Consequently, hydroxyurea decreases the fraction of hemoglobin that is susceptible to polymerization at certain oxygen pressure. Yet, hydroxyurea toxicities mire its use, especially in children (Lanzkron 2008). Therefore, there is an apparent need for having a curative and a relatively safe treatment for this disease. Besides, none of the current therapeutic approaches prevents the polymerization of HbS that precedes sickling of RBCs. In the process of searching for an agent targeting the pathophysiology of SCD, 5-HMF was found to reduce RBCs sickling in rodents though increasing the affinity of HbS to oxygen (Safo 2004). Consequently,

less HbS exists in the deoxygenated state at any specific oxygen pressure, therefore, 5-HMF decreases HbS polymerization. An attractive fact about 5-HMF, with regard to its safety, that 5-HMF is found constitutively in food such as coffee, dried fruits, and traditional Chinese medicines (Lin 2008) (Janzowski 2000). In addition, 5-HMF is an adulteration product in honey, beer, fruit juice, and glucose infusion solutions (Godfrey 1999).

Despite the long history of 5-HMF research, the literature is scarce with respect to studies fully characterizing its human PK. 5-HMF was dosed to different animal species, rodents, dogs, rabbits, and chickens, with the oral route being the method of administration in most of the studies (Klimmek 1978) (Rasmussen 1982) (Godfrey 1999) (Czok, Tolerance of 5-hydroxymethylfurfural (HMF). 2d communication: pharmacologic effects 1970) (Germond 1987) (NTP 1994) (NTP 2008). In addition, 5-HMF was administered orally to humans in three clinical studies without elaborating its PK properties (Prior 2006) (Matzi 2007) (M. P. Murkovic 2006). Differences in the estimated half-life and systemic clearance were found between and among species in the reported studies. Furthermore, 5-HMF oral bioavailability was not evaluated by a simultaneous administration of 5-HMF through systemic and oral routes.

In studies with the radiolabeled molecule, 5-HMF was shown to be extensively metabolized and the metabolites were mainly excreted in urine, however, the metabolic pathways were not identified (Godfrey 1999) (Germond 1987). Moreover, the metabolic affinity and capacity were not characterized along with any relevant differences and/or similarities among species. Furthermore, extra-hepatic metabolism was not investigated as a potential contributor for the overall clearance.

On the other hand, 5-HMF was reported to bind to hemoglobin by transient covalent binding to form a Schiff base (Safo 2004). However, the kinetics of this binding was not studied;

including the expected time to equilibrium and extent of binding. In addition, binding to the major serum protein, albumin, was not investigated to explore its interaction with hemoglobin binding.

Consequently, 5-HMF stability in human blood was investigated using a validated HPLC-UV assay in human plasma, where a decrease in 5-HMF concentration over time was observed. In addition, experiments were performed to evaluate the metabolic stability of 5-HMF in human hepatic cytosol. A concentration-dependent increase in nicotinamide adenine dinucleotide (NADH) formation was demonstrated, indicating the involvement of ALDH/ADH enzymes in the metabolism of 5-HMF. Hence, as a part of this research, the mechanistic basis behind 5-HMF metabolism in human hepatic cytosol was explored. In addition, this research intended to evaluate 5-HMF metabolic properties in hepatic cytosol of human, dog, rat, and mouse. These properties were compared among species to evaluate any similarities or variations. Furthermore, metabolism in human RBCs was studied as a potential source of extra-hepatic metabolism. More to the point, time- and concentration dependency studies were carried-out in human serum albumin and hemoglobin solutions. The overall objective of these in-vitro studies was to support first-time-in-human phase I studies with 5-HMF as a part of its development as antisickling agent.

CHAPTER 3

DEVELOPMENT AND VALIDATION OF HPLC ASSAY METHODS

3.1 Introduction

A number of analytical methods for the quantification of 5-HMF were described in the literature, as summarized in Table 3-1. The lowest reported concentration is listed in Table, except where indicated, since the LLOQ was not reported in most of these analytical methods. However, most of these were dedicated for the determination of 5-HMF in non-biological matrices. Other methods measured 5-HMF as a hydrolysis product of glycosylated RBCs and plasma proteins. Although few assay methods in biological matrices were reported, complex or tedious sample preparation was utilized in these. Hence, the need to a simple and a sensitive bioanalytical assay method was pointed-out to determine 5-HMF concentration in biological matrices involved in potential future clinical and animal studies. It is noteworthy that 5-HMF was investigated in a pilot study, which employed cancer patients with a dose of 3 g/l/day of 5-HMF. The minimum concentration of 5-HMF in plasma in that study was anticipated to be around 2.4 µM (Michail 2007).

Table 3-1. 5-HMF literature-reported assays

Author	Matrix	Method	Lowest Reported Concentration (µM)
(Coco 1996)	Honey	HPLC-UV/VIS	0.008 mg/kg (LOD)
(Drifield 2005)	Honey	HPLC-UV	1.4 mg/kg (LOD)
(E. B. Jellum 1973)	Intravenous nutrition and urine	GC-MS	NA
(Standefer 1983)	RBC (HbA_1)	Colorimetric spectrophotometry	~ ≥19.8
(Menez 1984)	RBC (HbA_1)	HPLC-UV	0.50
(Sampietro 1987)	Plasma (glycosylated protein)`	HPLC-UV	0.50
(Godfrey 1999)	Tissues (including whole blood) and urine	HPLC-UV and HMF-derived radioactivity	~ 0.16 in blood ~ 0.013 µg/g brain
(Abdulmalik 2005)	Whole blood and plasma	HPLC-UV	~ 23.8
(Michail 2007)	Plasma	HPLC-UV	2.4 (LLOQ)

3.2 Methods

3.2.1 Materials and Reagents

1. Mobile Phase for 5-HMF Assay Method in Plasma and RBCs:

   - 93.5% Milli-Q® water (Virginia Commonwealth University, PK/PD Laboratory)

   - 6.2% Methanol, HPLC grade (Burdick and Jackson, Morristown, NJ)

   - 1% Acetic acid, glacial, > 99% (Sigma, Milwaukee, WI)

   - 0.3 % Tetrahydrofuran, HPLC grade (Burdick and Jackson, Morristown, NJ)

2. Mobile Phase for HMFA Assay Method in Human Hepatic Cytosol:

   - 83% Milli-Q® water (Virginia Commonwealth University, PK/PD Laboratory)

   - 17% Methanol, HPLC grade (Burdick and Jackson, Morristown, NJ)

   - Tetrabutylammonium iodide, 99% (Sigma, St. Louis, MO)

3. 5-Hydroxymethyl-2-furfural (5-HMF) Stock Solution:

   - 5-Hydroxymethyl-2-furfural (Sigma, St. Louis, MO)

   - Milli-Q® water (Virginia Commonwealth University, PK/PD Laboratory)

4. 2-Furfuraldehyde (2F) Stock Solution:

   - 2-Furfural (Sigma, St. Louis, MO)

   - Milli-Q® water (Virginia Commonwealth University, PK/PD Laboratory)

5. Acetylfuran (AF) Stock Solution:

   - Acetylfuran (Sigma, St. Louis, MO)

   - Milli-Q® water (Virginia Commonwealth University, PK/PD Laboratory)

6. 5-Methyl-2-furfuraldehyde (MF) Stock Solution:

   - 5-Methyl-2-furfural (Sigma, St. Louis, MO)

   - Milli-Q® water (Virginia Commonwealth University, PK/PD Laboratory)

7. 5-Hydroxymethyl-2-furoic Acid (HMFA) Stock Solution:

   - 5-Hydroxymethyl-2-furoic Acid (Toronto Research Chemicals, Inc., North York, On.Canada)

   - Milli-Q® water (Virginia Commonwealth University, PK/PD Laboratory)

8. Furan-2,5-dicarboxylic Acid (FDCA) Stock Solution:

   - Furan-2,5-dicarboxylic acid (Toronto Research Chemicals, Inc., North York, On.Canada)

   - Milli-Q® water (Virginia Commonwealth University, PK/PD Laboratory)

9. SPE Conditioning:

   - Methanol, HPLC grade (Burdick and Jackson, Morristown, NJ)

   - Milli-Q® water (Virginia Commonwealth University, PK/PD Laboratory)

10. SPE Washing Solution: Phosphate-buffered Saline (PBS), pH 7.4:

    - Phosphate-buffered saline (PBS) tablets, pH 7.4 (Sigma, St. Louis, MO)

    - Milli-Q® water (Virginia Commonwealth University, PK/PD Laboratory)

11. SPE Eluting Solution: 50% Methanol:

    - Methanol, HPLC grade (Burdick and Jackson, Morristown, NJ)

    - Milli-Q® water (Virginia Commonwealth University, PK/PD Laboratory)

3.2.2 Equipment

1. 25-µl, 50-µl, and 250-µl positive displacement pipettes and corresponding pipette tips (Microman, Rainin Instruments, Oakland, CA).
2. 10-µl, 100-µl, and 1000-µl VWR pipettes and corresponding pipette tips (VWR, West Chester, PA).
3. 0.5-5 ml Finnpipette (Thermo Scientific, Waltham, MA).
4. Vortex (Vortex-Genie, VWR, West Chester, PA).
5. Sonicator (American Brand Products C6450-11, VWR, West Chester, PA).
6. pH meter (Corning, Glendale, AZ).
7. Balance (Fisher Scientific A 250, Pittsburgh, PA).
8. Oasis HLB cartridge, 1 cc/ 30 mg (Waters).
9. Centrifuge 5804-R (Eppendorf, Hauppauge, NY).
10. Glass vials with caps, 1 ml (Waters, Milford, MA).
11. UV detector (Shimadzu, AV-10, Columbia, MA).
12. C_{18} Zorbax Rx column, 4.6 X 150 mm (Agilent, Santa Clara, CA).
13. C_{18} guard column, 12.5 mm x 4.6 mm (Agilent, Santa Clara, CA).
14. 717 plus autosampler (Waters, Milford, MA).
15. 600 Multisolvent controller (Waters, Milford, MA).
16. Empower 2 software (Waters, Milford, MA).

3.2.3 Preparation of Solutions

- Mobile Phase for 5-HMF Assay Method in Plasma and RBCs (1 L):

  935 ml water, 62 ml methanol, 10 ml acetic acid glacial, and 3 ml tetrahydrofuran were mixed to prepare the mobile phase.

- Mobile Phase for HMFA Assay Method in Human Hepatic Cytosol (1 L):

  2 g of tetrabutylamonium iodide were dissolved in 830 ml water mixed with 170 ml methanol.

- 5-Hydroxymethyl-2-furfural (5-HMF) Stock Solution, 39.6 mM

  20 mg of 5-hydroxymethyl-2-furfural (M.W.: 126.11 Da) in 4 ml of water.

- 2-Furfuraldehyde (2F) Stock Solution, 12.1 mM.

  11.6 mg of 2-furfural (M.W.: 96.08 Da) was added to 10 ml of water.

- Acetylfuran (AF) Stock Solution, 9.97 mM.

  10.1 mg of acetylfuran (M.W.: 110.11 Da) was added to 10 ml of water.

- 5-Methyl-2-furfuraldehyde (MF) Stock Solution, 10.1 mM.

  11.1 mg of 5-methyl-2-furfural (M.W.: 110.11 Da) was added to 10 ml water.

- 5-Hydroxymethyl-2-furoic Acid (HMFA) Stock Solution, 1.41 mM.

  2 mg of 5-hydroxymethyl-2-furoic acid (M.W.: 142.11 Da) was added to 10 ml water.

- Furan-2,5-dicarboxylic acid (FDCA) Stock Solution, 12.8 mM.

  10 mg of furan-2,5-dicarboxylic acid (M.W.: 156.09 Da) was added to 5 ml water.

- SPE Washing Solution: Phosphate-buffered Saline (PBS), pH 7.4

  One tablet of phosphate-buffered saline was added to 200 ml of water.

- SPE Eluting Solution: 50% Methanol.

  25 ml of methanol was mixed with 25 ml of water.

3.2.4 Procedures

0.3 ml of plasma and 0.1 ml of thawed RBCs (after freezing at -80 °C) were diluted to 0.6 ml and 1.2 ml, respectively. 0.6 ml of the diluted sample was loaded into preconditioned (with methanol and water) HLB (hydropilic-lipophilic balance) solid phase extraction cartridges. The undesired impurities were washed with PBS and the sample was finaly eluted with 0.5 ml of 50% methanol in water. The extraction procedure is summarized in Table 3-2. Reference was made to Michail and co-workers, with minor amendments, for the sample prepartion by solid phase extraction (Michail 2007). However, the extract was injected directly into the HPLC-UV system with satisfactiory results without including the tedious and time-cosumimg dervitization step reported in that method.

The mobile phase for the analysis of 5-HMF in plasma and RBCs was prepared in an identical way to that reported by Menez et al., where an isocratic mobile phase was prepared by mixing water, methanol, acetic acid, tetrahydrofuran, 93.5:6.2:1:0.3, respectively, were mixed and used in (Menez 1984). A UV scan was performed between 200 nm to 330 nm to check if the mobile phase contributes to the absorbance measured at 285 nm. Figure 3-1 demonstrates that the mobile phase absorbance is insignificant at that wavelength window.

10 µl of the extracted samples were injected into Zorbax C_{18} analytical column (150 x 4.6 mm) protected by a C_{18} guard column (12.5 mm x 4.6 mm) through an autosampler at 4 °C and the mobile phase flowed at 0.75 ml/minute rate. 5-HMF peak was detected using Shimadzu 10 AV UV absorbance detector a at 285 nm.

Another method was developed for the detection of the metabolite HMFA in the presence of the parent compound 5-HMF in human hepatic cytosol. 0.2 ml of hepatic cytosol reaction mixture was diluted with 1 ml ice-cold acetonitrile. Then, 0.15 ml of the mixture was diluted

further with 0.65 ml ice-cold water. 10 µl of the diluted samples was injected directly into HPLC. The mobile phase was a mixure of water and methanol, 87:13, respectively. In addition, 0.2% w/v tetrabutylammonium iodide was added an ion-pairing agent. The flow ratewas 1 ml/minute though Zorbax C_{18} analytical column (150 x 4.6 mm) protected by a C_{18} guard column (12.5 mm x 4.6 mm). HMFA peak was detected using Shimadzu 10 AV UV absorbance detector a at 260 nm.

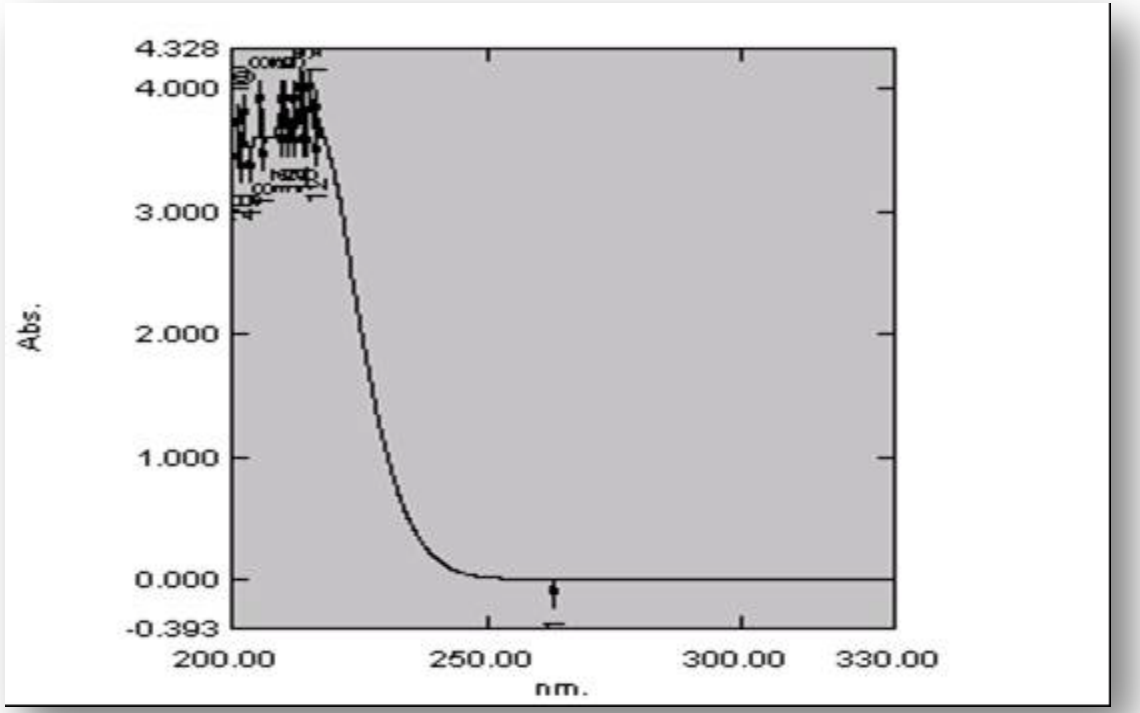

Figure 3-1. UV spectrum for the mobile phase.

Table 3-2. Solid phase extraction procedure

Step	Solvent	Volume (ml x times)	Minimum centrifuge speed (rpm) – time (min)
Conditioning	Methanol	1 x 2	400-2
	Water	1 x 2	400-2
Loading	Plasma (diluted one fold) or RBCs suspension (diluted 6 folds)	0.6 x 1	400-7
Washing	Phosphate buffer saline pH 7.4	1 x 2	700-5
Elution	50% methanol in water	0.5 x 1	400-5

3.3 Method Validation

3.3.1 5-HMF in Human Plasma

A summary of the 5-HMF assay method in human plasma is described in Table 3-3. In addition, representative chromatograms of 5-HMF in human plasma are shown in Figures 3-2, 3-3, 3-4, 3-5, 3-6, and 3-7.

To ensure the suitability and reliability of the developed method for the intended measurements, validation of this analytical method in human plasma was evaluated through the following:

3.3.1.1 Recovery

The response of extracted samples at low, medium, and high concentrations was compared to the response of unextracted known concentrations that represent 100% recovery. The efficiency of extraction was reproducible with a CV less than 4% and a recovery of more than 78%. Moreover, the recovery at the LLOQ was determined to be 84% with a CV not exceeding 1%, as summarized in Table 3-4.

Table 3-3. 5-HMF assay descriptive summary.

Type of assay	HPLC-UV
Sample preparation	Solid phase extraction of diluted plasma by Oasis HLB cartridges (Waters)
Detector	Shimadzu 10 AV Absorbance Detector
LC pump	Waters 600E Multisolvent Delivery System
LC column	Zorbax Rx C_{18}, 80 A^o, 150 mm x 4.6 mm, 5 µm (Agilent, Serial # USDU010028)
Guard column	C_{18}, 12.5 mm x 4.6 mm (Agilent, Serial # USCI042710)
Detection	UV at 285 nm
Autosampler temperature	4 °C
Flow rate	0.75 ml/minute
Regression algorithm	Linear, weighted 1/X
Sample volume and matrix	0.3 ml of plasma diluted with water to a total volume of 0.6 ml. The 0.6 ml diluted sample is extracted to 0.5 ml sample using HLB cartridges
Mobile phase	Water-methanol-acetic acid-tetrahydrofuran (93.5:6.2:1:0.3)
Injection volume	10 µL
Chromatographic run time	10 minutes
Calibration curve range	0.16 – 158.6 µM
LLOQ	0.16 µM
Quality control levels	0.48, 15.9, 126.9 µM

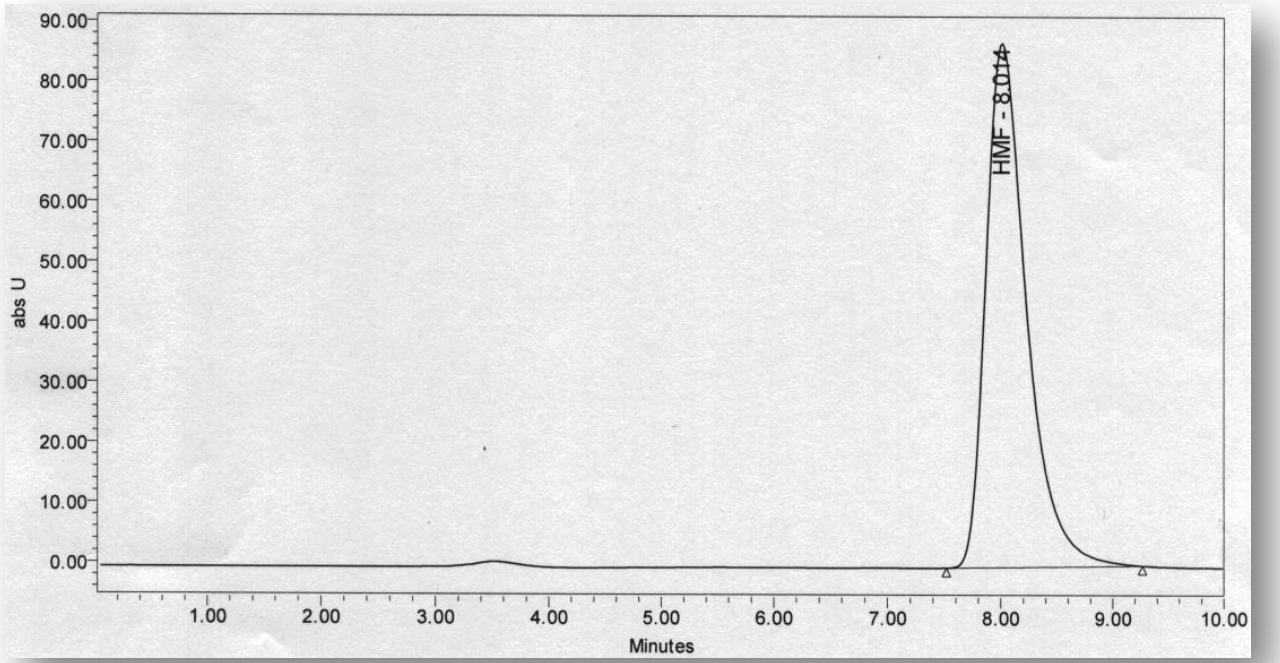

Figure 3-2. Representative chromatogram of 5-HMF standard in mobile phase.

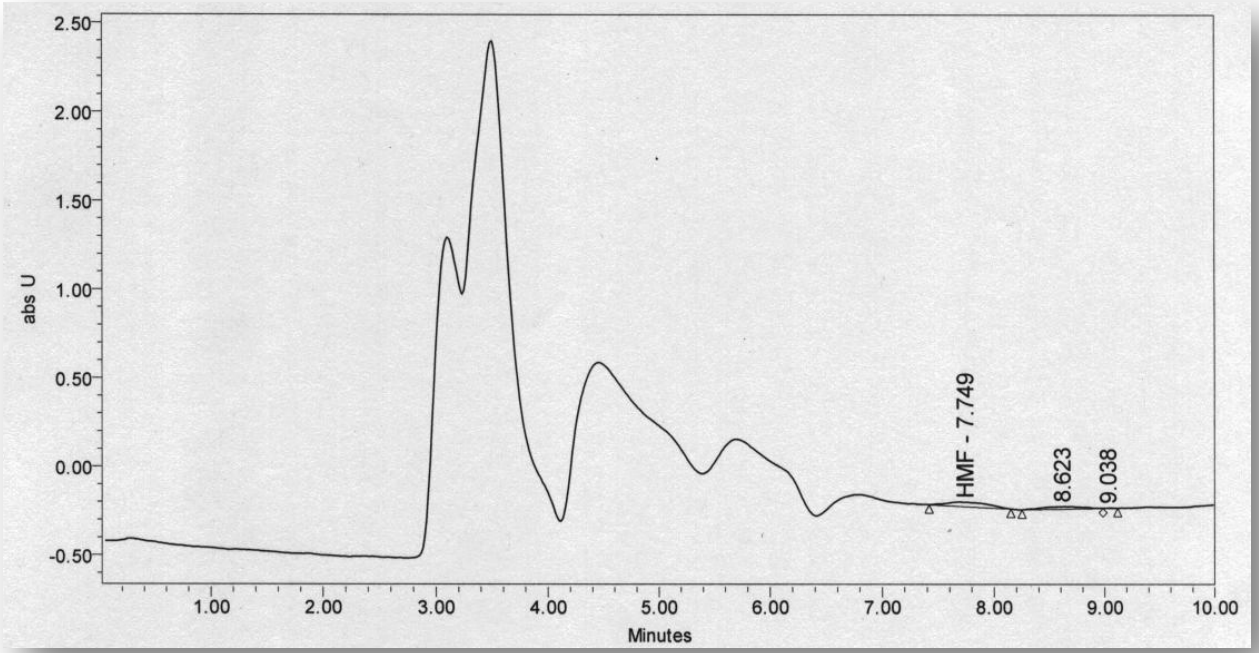

Figure 3-3. Representative chromatogram of individual human plasma blank.

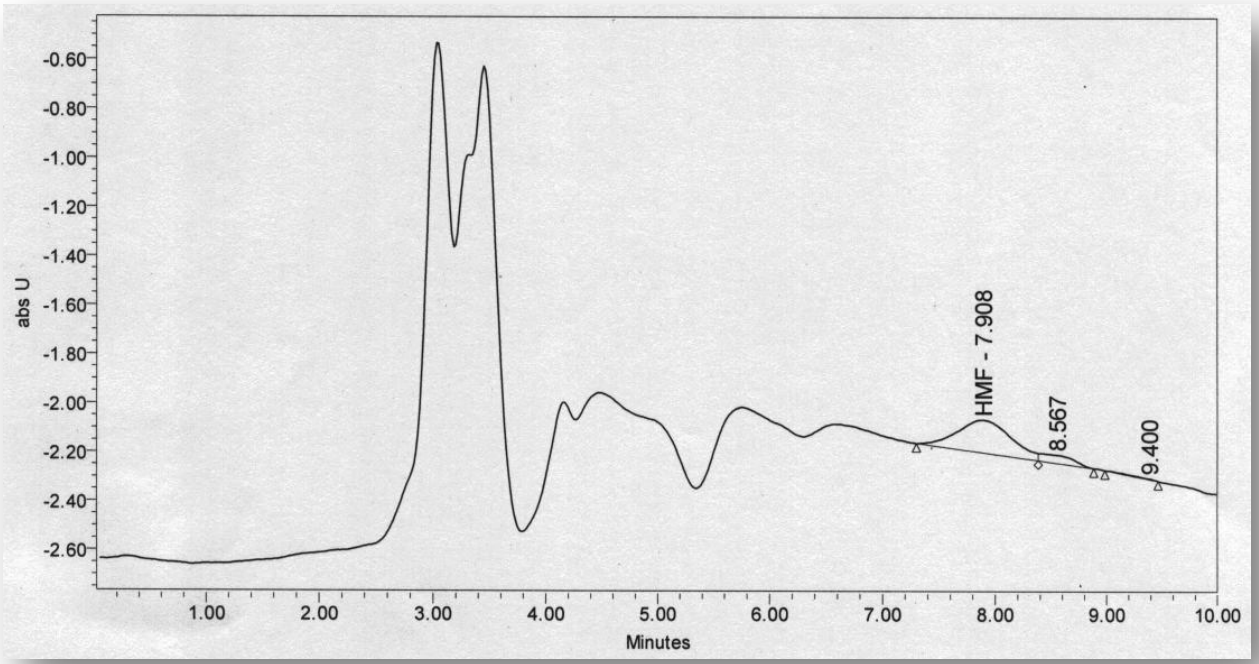

Figure 3-4. Representative chromatogram of LLOQ concentration.

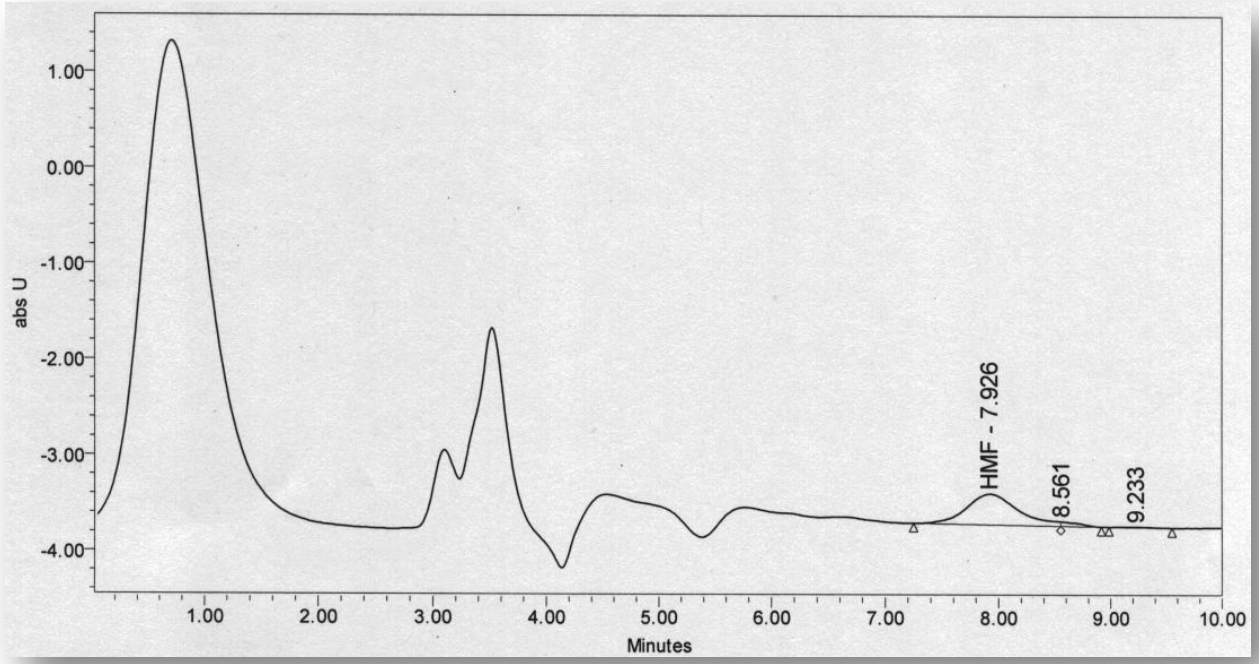

Figure 3-5. Representative chromatogram of low QC concentration.

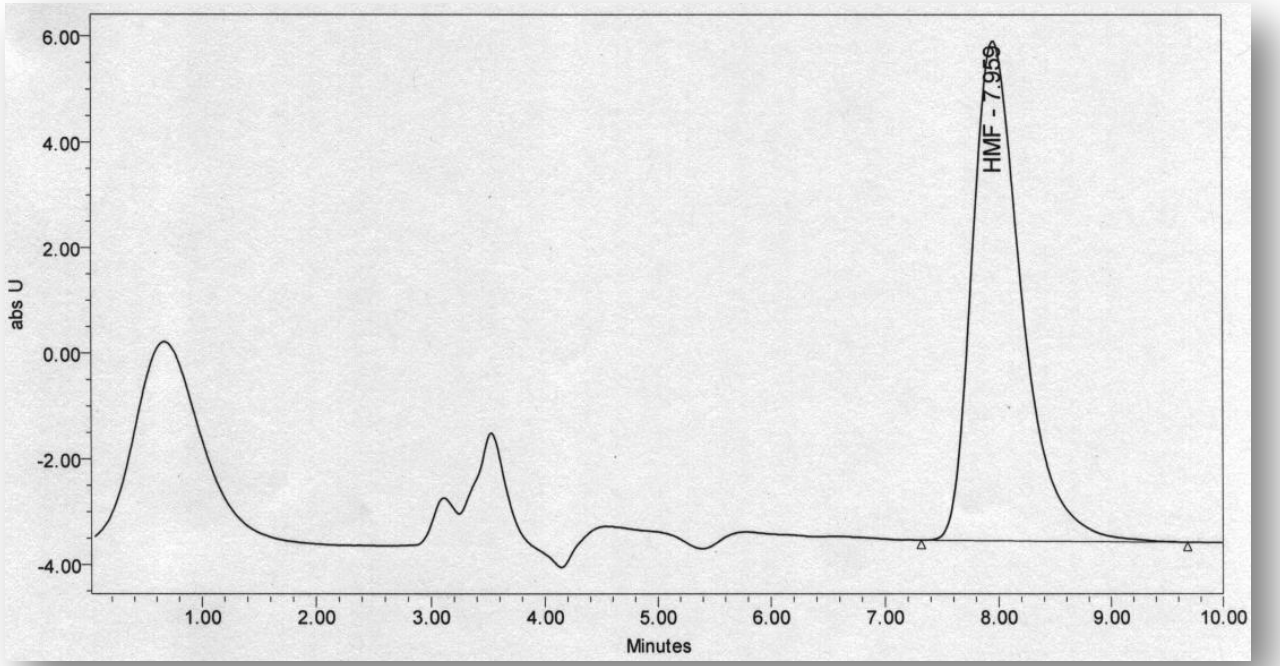

Figure 3-6. Representative chromatogram of mid QC concentration.

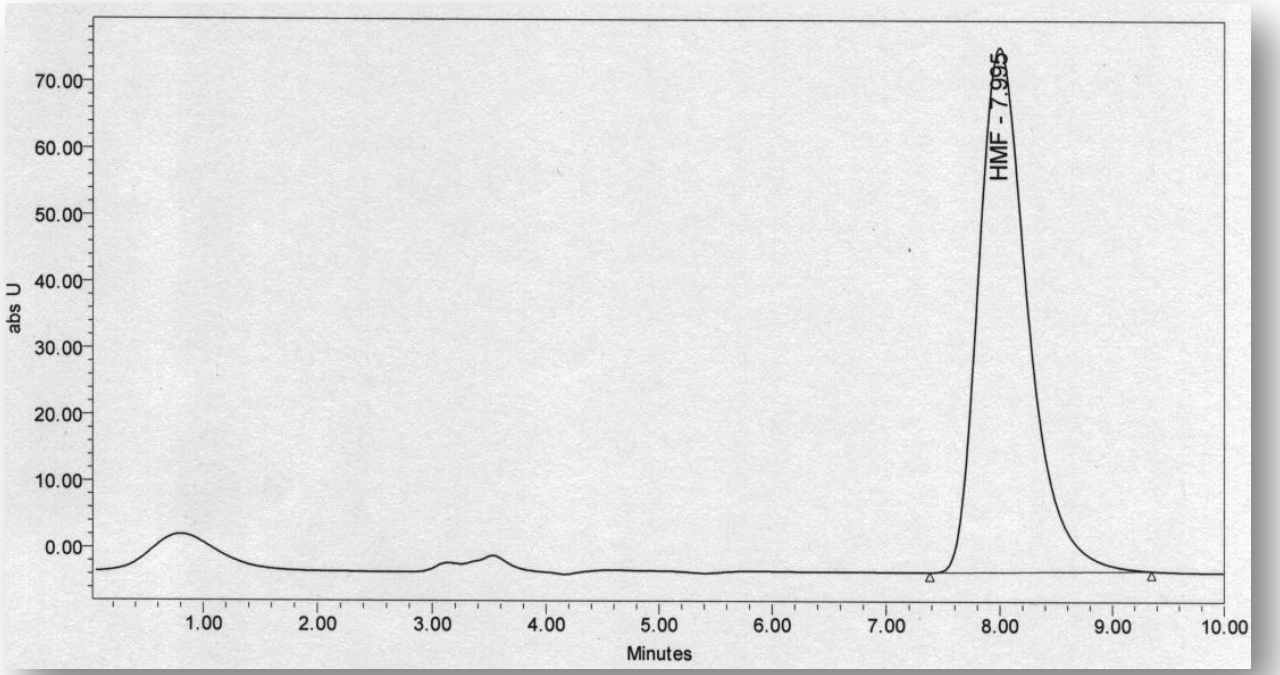

Figure 3-7. Representative chromatogram of high QC concentration.

Table 3-4. 5-HMF recovery in human plasma.

Concentration (µM)	R1	R2	R3	Mean	CV
0.16	85	84	85	84	0.9
0.48	75	81	79	78	3.7
15.9	105	108	109	107	1.9
126.9	107	108	111	109	1.9

3.3.1.2 Accuracy

Within-assay accuracy was determined for six replicate measurements at four different concentrations, in addition to the LLOQ. The mean deviation from the nominal value was used as a measure of accuracy in the analytical range (DFN). The DFN did not exceed 15% at any of these concentrations including the LLOQ, as shown in Table 3-5. 1/X weighted linear regression was used in the calibration curve.

Inter-assay accuracy was determined at three levels with twelve replicates at each concentration, as summarized in Table 3-6. The accuracy was deemed acceptable as per the FDA guidance for industry "Bioanalytical Method Validation" criteria, with no more than 15% DFN for the selected concentrations and 20% as the DFN at the LLOQ.

3.3.1.3 Precision

The analysis was applied repeatedly at three levels with twelve replicates at each concentration to evaluate the between-run repeatability, as summarized in Table 3-6. Within-run precision was determined for six replicates, shown in Table 3-5, at four concentrations in the analysis range. To measure the repeatability of the method with time, three different runs were analyzed. The FDA guidance for industry "Bioanalytical Method Validation" criteria was used as a reference, with no more than 15% coefficient of variation (CV) for the selected concentrations and $\leq$ 20% as a CV at the LLOQ.

Within the expected range of concentrations, the method produced satisfactory results without the use of an internal standard. In addition, sample preparative procedure did not diminish the recovery of 5-HMF. Consequently, an internal standard was deemed unnecessary.

3.3.1.4 Selectivity

As shown in Table 3-6, six sources of plasma were analyzed to test for interferences and to investigate the ability to differentiate and quantify 5-HMF in the presence of other endogenous components in the extracted plasma. The chromatograms for these are shown in Figures 3-8, 3-9, 3-10, 3-11, 3-12, and 3-13. The ratio of the average area response of six replicates at the LLOQ concentration to that of six blank sources was 5.5.

Table 3-5. 5-HMF intra-run accuracy and precision in human plasma.

Concentration (µM)	R1	R2	R3	R4	R5	R6	Mean	CV	DFN%
0	848	145	1028	705	1175	886.5	798	44.9	
0.16	4522	4131	4359	4357	4518	4405	4382	3.3	-11.8
0.32	7080	7788	6609	7128	4936	6933	6746	14.3	7.5
0.48	10006	10256	10084	9678	10358	9911	10049	2.4	4.3
15.9	283536	281470	286576	282973	284034	286408	284166	0.7	14.6
126.9	2716556	2454494	2391176	2404352	2387093	2415976	2461608	5.2	5.6

Table 3-6. 5-HMF inter-run accuracy and precision in human plasma.

		0.16 µM	0.48 µM	15.9 µM	126.9µM
First run	**R1**	4348	10139	337282	3021407
	R2	3964	10051	343673	3041115
	R3	4410	9997	346116	3147102
Second run	**R1**	4522	10006	283536	2716556
	R2	4131	10256	281470	2454494
	R3	4359	10084	286576	2391176
	R4	4357	9678	282973	2404352
	R5	4518	10358	284034	2387093
	R6	4405	9911	286408	2415976
Third run	**R1**	4825	12182	334845	2412090
	R2	5907	13063	341995	2409259
	R3	6510	13016	336680	2426958
Mean		4688	10728	312132	2602298
CV		16.0	11.7	9.4	11.4
DFN%		-18.6	-2.8	4.4	-0.1

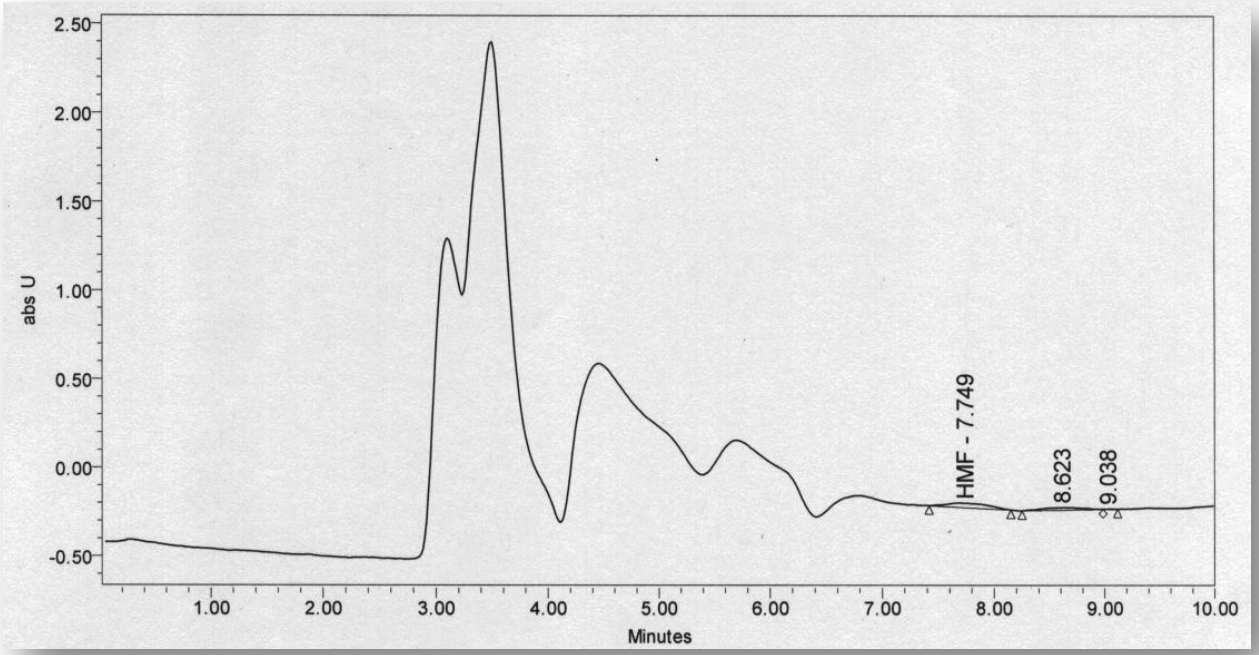

Figure 3-8. Individual human plasma chromatogram (blank 1).

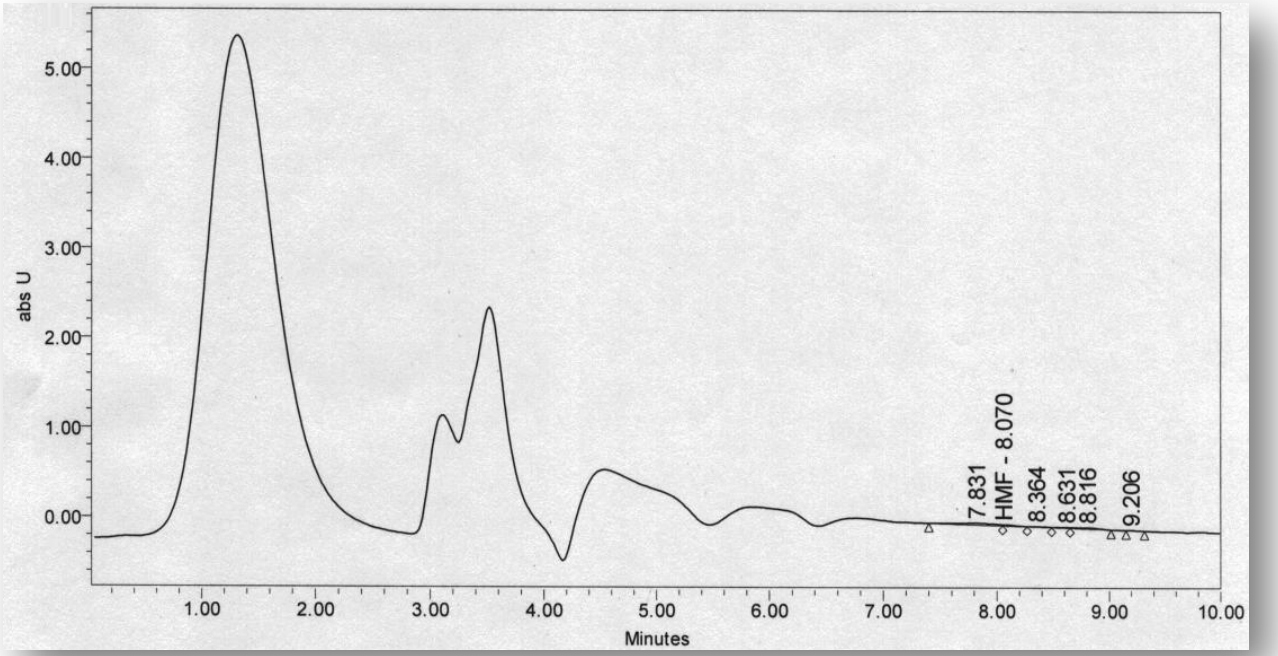

Figure 3-9. Individual human plasma chromatogram (blank 2).

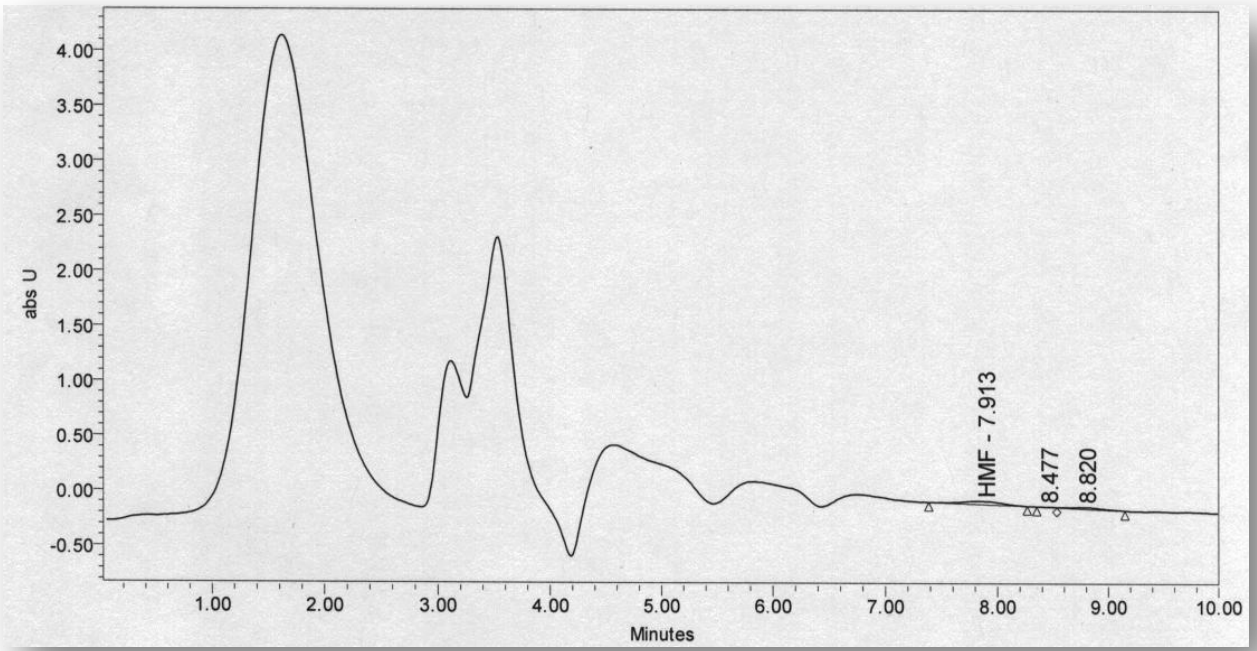

Figure 3-10. Individual human plasma chromatogram (blank 3).

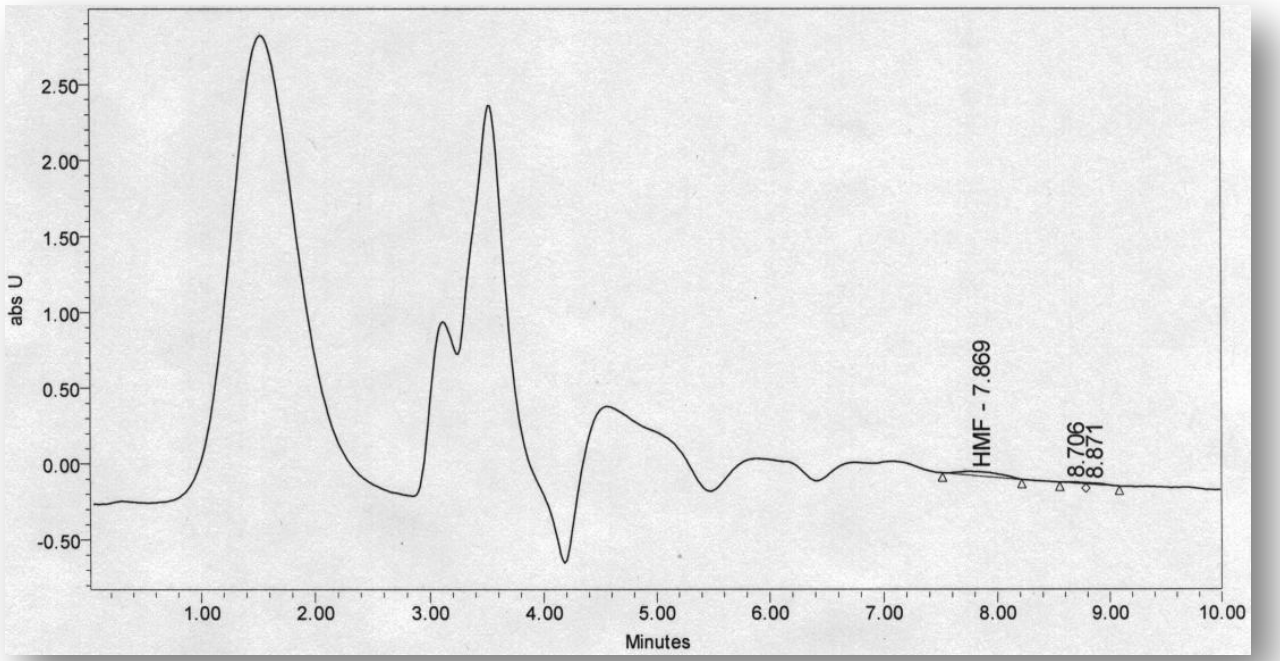

Figure 3-11. Individual human plasma chromatogram (blank 4).

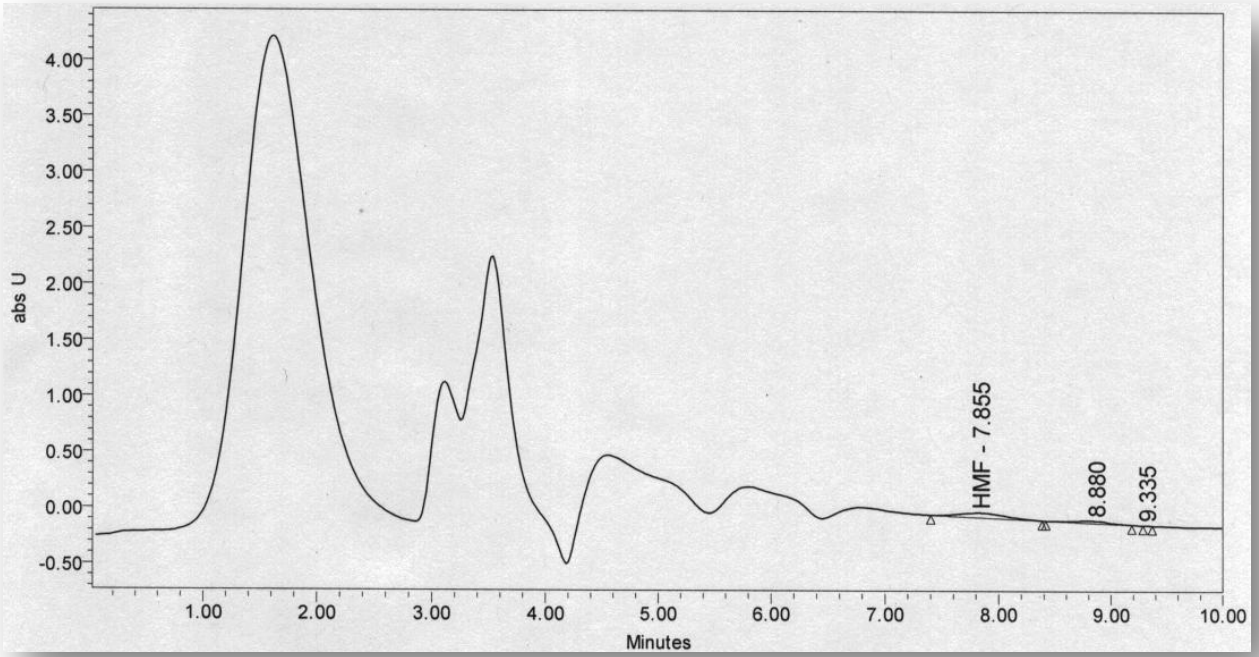

Figure 3-12. Individual human plasma chromatogram (blank 5).

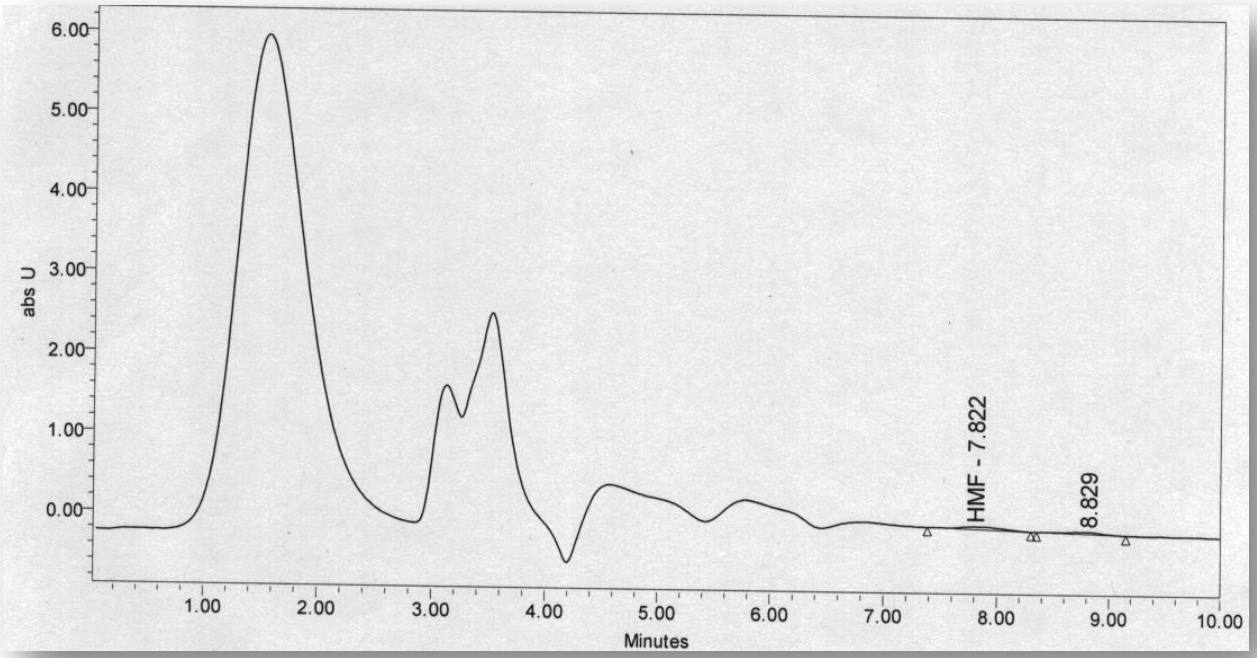

Figure 3-13. Individual human plasma chromatogram (blank 6).

In addition, three structurally related compounds, along with potential metabolites, namely, 5-hydroxymethylfuran-2-carboxylic acid (HMFA), and furan-2,5-dicarboxylic acid (FDCA), were studied to investigate the selectivity of this bioanalytical method. The three other compounds, named in Table 3-7, were reported to co-exist with 5-HMF in some infants dietary products as a result of excessive heat exposure of the protein and carbohydrates during the sterilization process of these products (Ferrer 2002). The absorbance of these compounds was scanned between 200 nm to 330 nm as demonstrated in Figure 3-14. As evident in Table 3-7, the calculated molar absorptivity and λ_{max} indicates a potential interference of these compounds in case of their presence in the sample if they are co-eluted with 5-HMF. Consequently, the compounds were injected separately into the HPLC column and in a mixture along with 5-HMF under the same chromatographic conditions of this analytical method. The chromatogram for the mixture is shown in Figure 3-15 below.

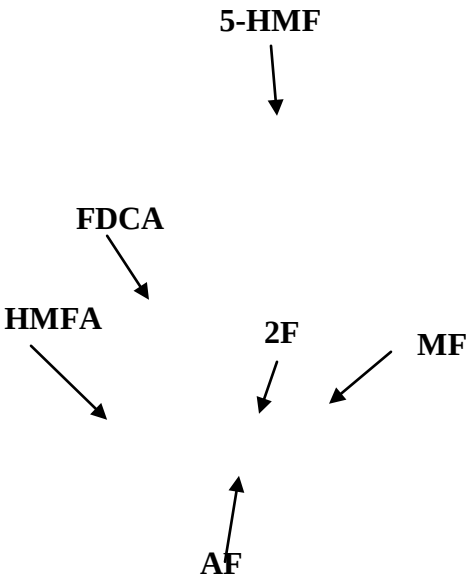

Figure 3-14. Furan carboxylic acids and furfurals UV spectrum.

Table 3-7. Molar absorptivity of furan carboxylic acids and furfurals.

	λ_{max} (nm)	ε (AbsU/M/cm)	
		λ_{max}	285 nm
5-HMF	283.8	19913	19452
5-Hydroxymethyl)furan-2-carboxylic acid (HMFA)	256.7	12854	817
Furan-2,5-dicarboxylic acid (FDCA)	265.4	18692	3430
Acetylfuran (AF)	274.4	11843	12224
5-Methylfuran-2-carbaldehyde (MF)	292.3	15785	5473
2-Furfural (2F)	276.9	12022	11748

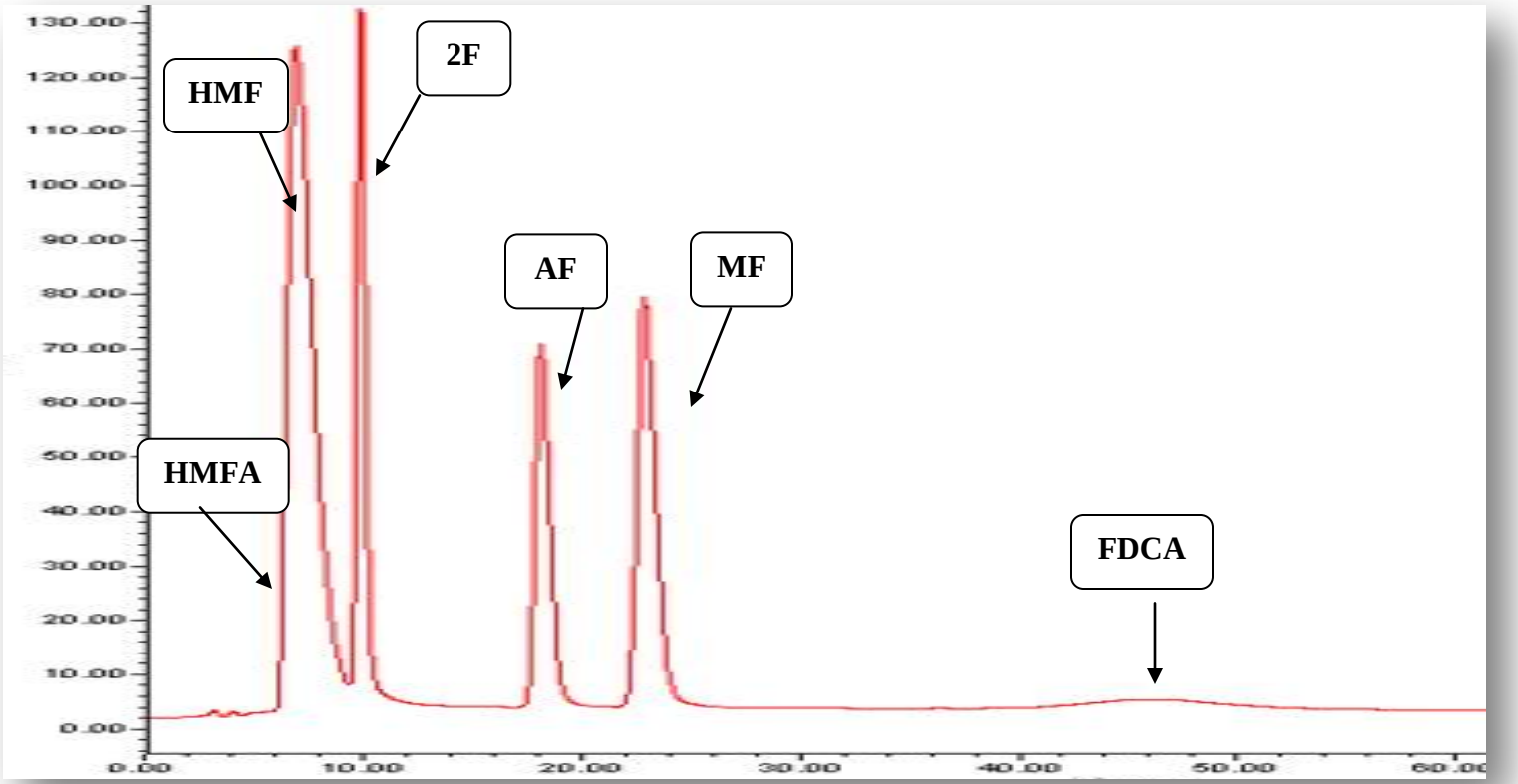

Figure 3-15. Furan carboxylic acids and furfurals chromatogram.

The relationship between these compounds' logP values, calculated via ChemSketch (ACD Labs), vs their retention factors (k') was plotted in Figure 3-16. The k' values were calculated according Equation 3-1 and are listed in Table 3-8. t_R' in Equation 3-1 was calculated according to Equation 3-2, where the mobile phase retention time (t_M) was estimated to be 3.1 minutes. A positive trend was observed with increasing the hydrophobicity of the compounds relative to their retention time (t_R). However, the slope for the linear regression model was not significant (p-value > 0.05).

$$k' = t_R'/t_M \quad \text{Equation } 3-1$$

$$t_R' = t_R - t_M \quad \text{Equation } 3-2$$

The insignificant model might be due to the small number of compounds incorporated in this relationship. In addition, considering the structure of 2-furfural, the calculated logP value seemed higher than what is expected. This calculated logP for 2-furfural is higher than that for acetylfuran although the latter has an additional methyl group. Therefore, the assigned logP value appears to be overestimated for 2-furfural. Moreover, FDCA was retained in the column to a greater extent than what is predicted using its logP value. The pH of the mobile phase is 3 and FDCA should be mainly unionized at that pH, which might increased its lipophilic characteristics. Unfortunately, we were not able to obtain a pka values for these compounds. Consequently, the compounds with acidic were excluded from the group and the relationship was re-plotted in Figure 3-17. An improvement in the association was observed, however, the slope remained insignificant.

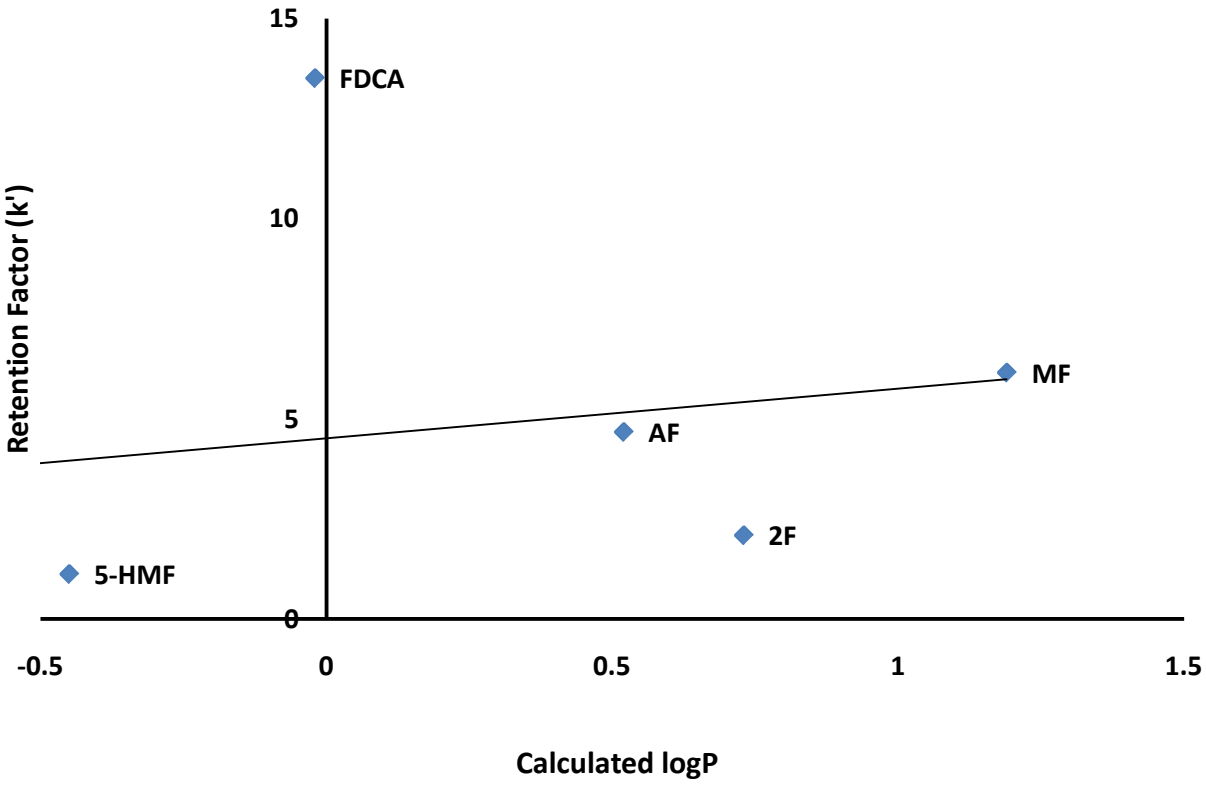

Figure 3-16. Furan carboxylic acids and furfurals calculated logP vs k'.

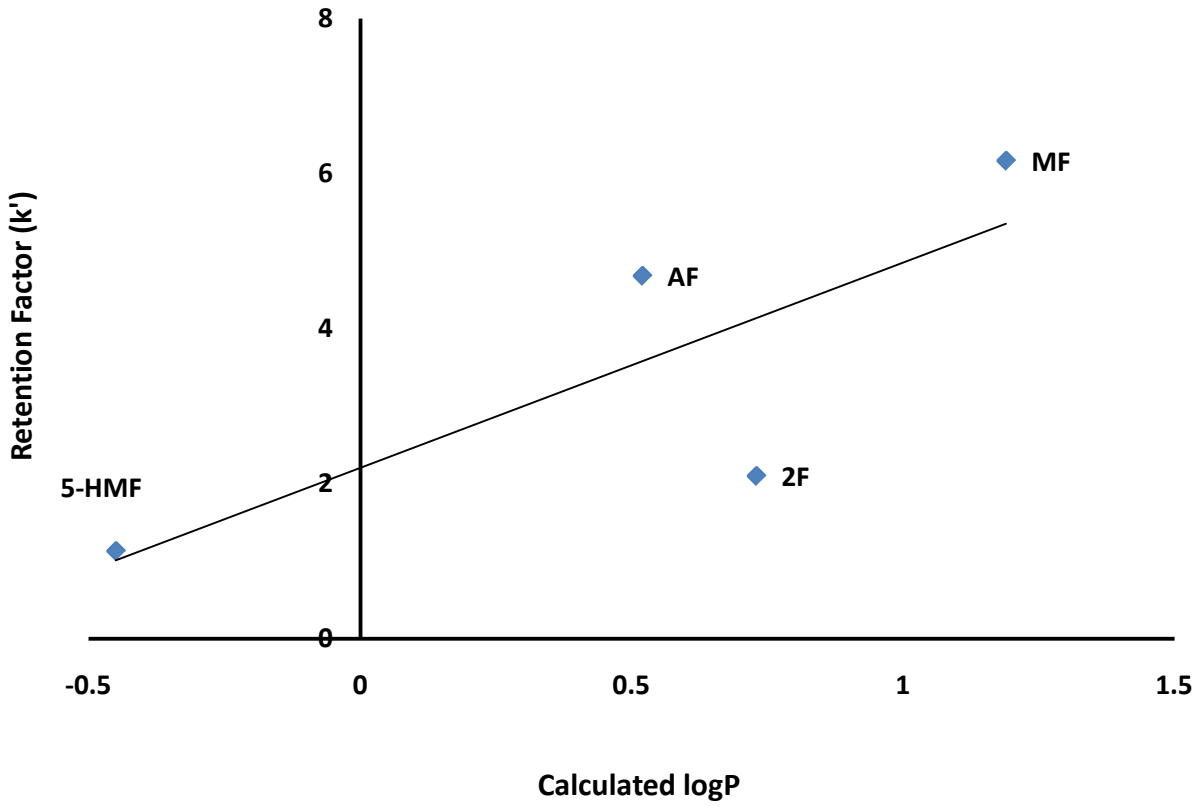

Figure 3-17. Furfurals calculated logP vs k'.

Table 3-8. 5-HMF and its metabolites along with structurally related furfurals calculated logP and retention properties.

Compound Name	Structure	Calculated logP	Retention time (min)	k'
5-HMF	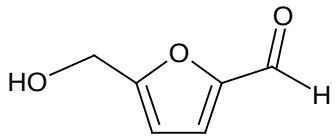	-0.45 ± 0.27	6.6	1.1
HMFA	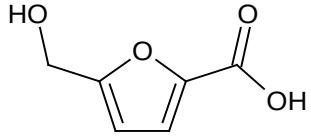	-0.55 ± 0.33	7.1	1.3
FDCA	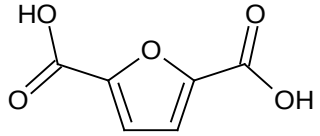	-0.02 ± 0.41	45.0	13.5
AF	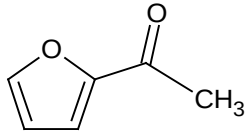	0.52 ± 0.31	17.6	4.7
2F	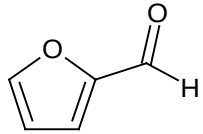	0.73 ± 0.26	9.6	2.1
MF	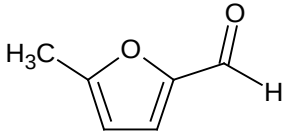	1.19 ± 0.26	22.2	6.2

After the exclusion of acids from the correlation between the logP and the corresponding retention factor (k') for the compounds, shown in Figure 3-17, the r value increased from 0.18 to 0.79. Equation 3-3 describes the relationship between k' and logP in this HPLC system.

$$k' = 2.6*(\log P) + 2.2 \quad \text{Equation } 3-3$$

The use of logP value as a factor affecting the retention of the compounds is based on the partitioning properties of these compounds between the hydrophobic C_{18} stationary phase and the hydrophilic mobile phase. However, secondary hydrogen bonding interactions with the free silanol groups might have existed. A change in the column to one with better end capping quality to minimize the secondary interactions might result in an improved relationship between the logP and the retention properties.

Both UV absorptivity and retention properties, summarized in Table 3-9, can potentially cause an interference in 5-HMF analysis if the compounds happened to coexist with 5-HMF in the sample. The interference of FDCA in this assay method is not expected due to the difference in the retention time between FDCA and 5-HMF. On the other hand, as shown in the chromatogram, HMFA and 5-HMF peaks overlap. In the presence of equimolar amounts of HMFA and 5-HMF, it will be difficult to recognize the presence of HMFA since 5-HMF absorption at 285 is 23.8 times higher than HMFA. Nevertheless, HMFA is not expected to survive the extraction method since the washing solution is PBS with a pH of 7.4, at which HMFA is expected to be fully ionized and washed away.

Table 3-9. HPLC-UV selectivity contributors of furfurals.

	λ_{max} (nm)	R_t (min)
5-HMF	**283.8**	**6.6**
5-Hydroxymethylfuran-2-carboxylic acid (HMFA)	256.7	**7.1**
Furan-2,5-dicarboxylic acid (FDCA)	265.4	45.0
Acetylfuran (AF)	**274.4**	17.6
2-Furfural (2F)	**276.9**	9.6
5-Methylfuran-2-carbaldehyde (MF)	**292.3**	22.2

3.3.1.5 Calibration Curve

The relationship between 5-HMF concentrations in plasma and the UV detector response was modeled by a linear regression algorithm in the range of 0.16 – 158.9 µM, as demonstrated in Figure 3-18. Three replicates were used to define the analytical relationship. As evident in Table 3-10, all the concentrations (excluding the blank) in the defined analytical range were within 92.6-104.4% of the nominal concentrations and did not exceed 7% in their coefficient of variation.

The lowest value in the calibration curve, which is 0.16 µM, was deemed as the LLOQ. The response of the blank at the retention time of 5-HMF, was not more than the 20% of the LLOQ response at the specified retention time. The ratio of the average response of six replicates at the LLOQ to that of the six sources of blanks was 5.5. The average of the analytical results for a minimum of six replicates at the LLOQ had DFN value of 7.4 %. The CV at the LLOQ did not exceed 5.7% as a measure of precision.

Due to the wide analytical range, a weighing factor of (1/X) was used in the established linear model. All the individual calibration curves had significant slopes and non-significant intercepts. The residual plot, shown in Figure 3-19, demonstrates over- and underestimation of the values predicted by the linear regression when compared with the observations. The residuals were distributed above and below the zero-line. Hence, the linear regression with a weighting factor of 1/X was deemed as a suitable model to describe and interpolate the response associated with 5-HMF analytical concentrations.

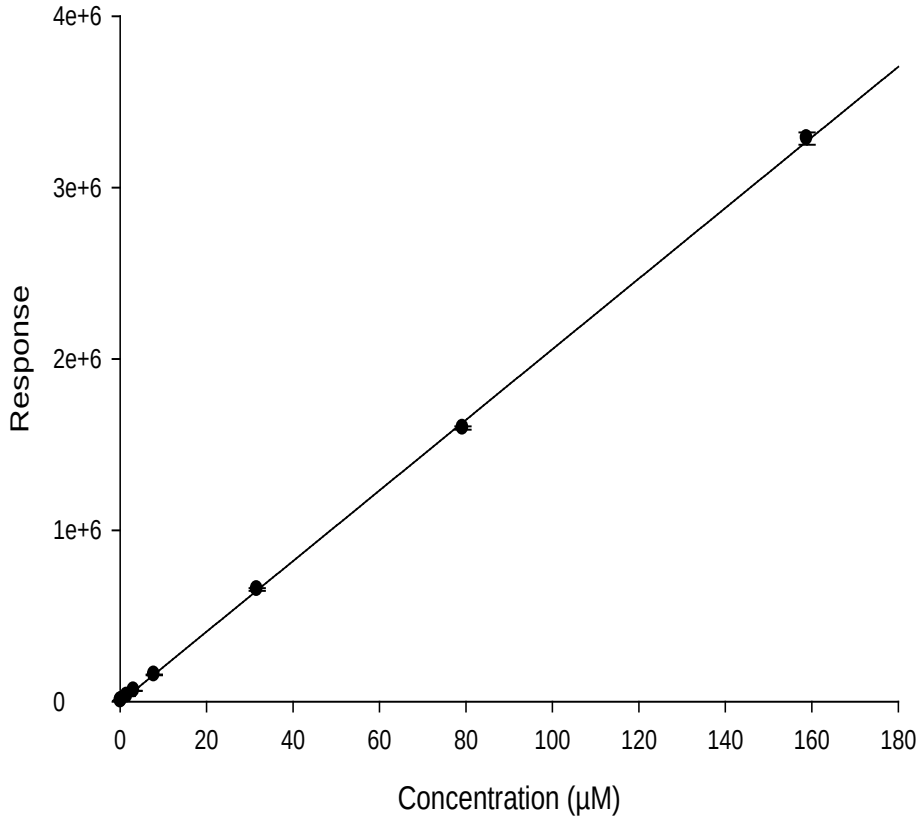

Figure 3-18. 5-HMF response-concentration curve in human plasma.

Table 3-10. 5-HMF standard curve.

Concentration (µM)	R1	R2	R3	Mean	CV	Average DFN%
0.16	4348	3964	4410	4241	5.7	7.4
0.32	7328	7737	6732	7266	7.0	1.0
1.6	32592	32385	32873	32617	0.8	-1.7
3.2	62716	63458	63556	63243	0.7	-3.7
7.9	156979	153307	157812	156033	1.5	-4.4
31.7	649542	650343	663931	654605	1.2	0.6
79.3	1606296	1595854	1586900	1596350	0.6	-1.8
158.9	3251346	3283051	3322955	3285784	1.1	1.1
Slope	20364.9	20437.1	20611.2	20471.1	0.6	
Intercept	782.0	594.3	568.3	697.5	18.0	
r^2	0.9999	0.9997	0.9995	0.9997	0.02	

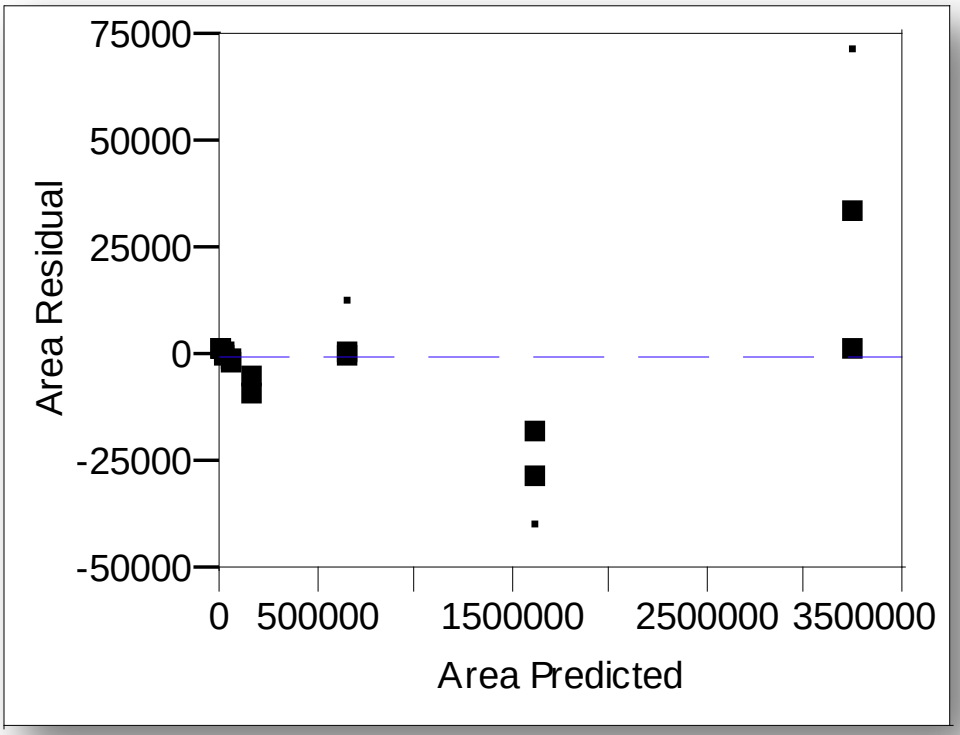

Figure 3-19. Area residuals by the predicted area.

3.3.1.6 Dilution Integrity

A solution was prepared at 7.9 mM of 5-HMF in the plasma matrix and then diluted with the blank plasma matrix to 158.9 µM. Triplicates were analyzed in three different runs. The results are shown in Table 3-11.

3.3.1.7 Stock Solution Stability

A solution of 15.8 µM of 5-HMF was analyzed using the HPLC method. Then, the solution was left at RT for about 5.5 hours. After that, triplicates of that solution were reanalyzed and compared to the measurement when freshly prepared. The 95% confidence intervals of the means, shown in Table 3-12, were compared and were considered equivalent. The working solution was deemed stable at RT for 5.5 hours.

3.3.1.8 Post-Preparative Stability

Triplicates of processed samples at low, mid, and high QC concentrations were kept in the autosampler for around 48 hours and then reanalyzed. Their results were compared to those freshly analyzed, as shown in Table 3-13. A null hypothesis (H_0) of $\mu_{fresh} \geq \mu_{48\ hrs\ in\ autosampler}$ at each concentration was tested using a paired t-test. In each case the p-value was greater than 0.05. Hence, the processed samples were considered stable for 48 hours residence-time in the autosampler.

Table 3-11. Accuracy and precision for diluted samples.

First run	**R1**	2898187
	R2	3114074
	R3	2992520
Second run	**R1**	3080501
	R2	2973592
	R3	3036628
Third run	**R1**	3160578
	R2	3099857
	R3	2962983
Mean		3035436
CV		2.6
DFN%		7.1

Table 3-12. Working-solution stability at RT results.

	Freshly prepared	**After 5.5 hours at RT**
R1	256105	263072
R2	260565	263659
R3	264585	268184
Mean	260418	264972
CV	1.6	1.1
95% Confidence interval	249881- 270956	258023- 271921

Table 3-13. Short-term stability results.

	0.48 µM		15.8 µM		126.9 µM	
	Fresh	**After autosampler storage**	**Fresh**	**After autosampler storage**	**Fresh**	**After autosampler storage**
R1	10139	11264	337282	379305	3021407	3402782
R2	10051	12425	343673	381153	3041115	3254875
R3	9997	10993	346116	389284	3147102	3359762
Mean	10062	11561	342357	383247	3069875	3339140
CV	0.7	6.6	1.3	1.4	2.2	2.3
Prob< t	> 0.05		> 0.05		> 0.05	

3.3.2 5-HMF in Rat, Mouse, and Dog Plasma

The same HPLC-UV assay method validated in human plasma was investigated for the determination of 5-HMF in rat, mouse, and dog plasma. A descriptive summary of the method is shown in Table 3-14.

To ensure the suitability and reliability of the developed method for the intended measurements, validation of this analytical method in rat, mouse, and dog plasma was evaluated through the following:

3.3.2.1 Accuracy

Within-assay accuracy was determined for six replicate measurements at three different concentrations, in addition to the LLOQ, were determined. The DFN value was used as a measure of accuracy in the analytical range. The absolute DFN value did not exceed 15% at any of these concentrations including the LLOQ, as shown in Tables 3-15, 3-16, and 3-17.

Table 3-14. 5-HMF assay descriptive summary in species plasma.

Type of assay:	HPLC-UV
Sample preparation:	Solid phase extraction of diluted Plasma by Oasis HLB cartridges (Waters)
Detector:	Shimadzu 10 AV Absorbance Detector
LC pump:	Waters 600E Multisolvent Delivery System
LC column:	Zorbax Rx C_{18}, 80 A^o, 150 mm x 4.6 mm, 5 µm (Agilent, Serial # USDU010028)
Guard column:	C_{18}, 12.5 mm x 4.6 mm (Agilent, Serial # USCI042710)
Detection:	UV at 285 nm
Autosampler temperature:	4 °C
Flow rate:	0.75 ml/min
Regression algorithm:	Linear, weighted 1/X
Sample volume and matrix:	0.3 ml of plasma suspension, extract to 0.5 ml sample
Mobile phase	Water-methanol-acetic acid-tetrahydrofuran (93.5:6.2:1:0.3)
Injection volume:	10 µl
Chromatographic run time:	10 minutes
Calibration curve range:	Mouse: 1.6 – 158.9 µM, Rat: 1.6 – 158.9 µM, Dog: 0.16 – 158.9 µM
Lower limit of quantitation:	Mouse: 1.6 µM, Rat: 1.6 µM, Dog: 0.16 µM
Quality control levels:	Mouse: 2.4, 15.8, 126.9 µM, Rat: 2.4, 15.8, 126.9 µM, Dog: 0.48, 15.8, 126.9 µM

Table 3-15. 5-HMF intra-run accuracy and precision in mouse plasma.

Concentration (µM)	R1	R2	R3	R4	R5	R6	Mean	CV	DFN%
0	6603	2209	6982				5265	50.4	
1.6	21363	21757	21323	23279	18398	22461	21430	7.8	1.1
2.4	34029	30138	27702	37173	34145	35892	33180	10.8	6.9
15.8	174194	179427	174667	187060	183122	179418	179648	2.7	-9.4
126.9	1550036	1669814	1502977	1542189	1654157	1635667	1592473	4.3	1.0

Table 3-16. 5-HMF intra-run accuracy and precision in rat plasma.

Concentration (µM)	R1	R2	R3	R4	R5	R6	Mean	CV	DFN%
0	4470	4024	3558				4017	11.4	
1.6	24934	21537	20593	18901	19997	19795	20960	10.2	-3.8
2.4	34530	35786	33950	35969	34698	35574	35085	2.3	7.7
15.8	192685	199316	214060	212831	221287	199441	206947	3.4	-4.3
126.9	1638235	1729048	1783345	1665379	1908818	1679190	1734003	5.8	0.4

Table 3-17. 5-HMF intra-run accuracy and precision in dog plasma.

Concentration (µM)	R1	R2	R3	R4	R5	R6	Mean	CV	DFN%
0	772	805	416				664	32.5	
1.6	4516	4255	4531	3647	5158	3428	4256	14.9	-1.8
2.4	8226	9775	9346	9709	8746	9588	9232	6.7	3.8
15.8	217652	227034	229274	232000	247277	204856	226349	6.3	-1.6
126.9	1732705	1730375	1995461	1795253	1870952	1851862	1829435	5.5	0.2

3.3.2.2 Precision

Within-run precision was determined for six replicates, shown in Tables 3-15, 3-16, and 3-17 at four concentrations in the analysis range including the LLOQ. The FDA guidance for industry "Bioanalytical Method Validation" criteria were considered for acceptance with no more than 15% coefficient of variation for the selected concentrations and 20% as CV at the LLOQ.

3.3.2.3 Selectivity

As shown in Tables 3-15, 3-16, and 3-17, pooled plasma blank from at least six different sources were analyzed to test for interferences and to investigate the ability to differentiate and quantify 5-HMF in the presence of other endogenous components in the extracted plasma.

3.3.3 5-HMF in Human RBCs

An HPLC-UV assay was developed for the determination of 5-HMF in human RBCs. A descriptive summary of the method is shown in Table 3-18. In addition, representative chromatograms are shown in Figures 3-20, 3-21, 3-22, and 3-23.

To ensure the suitability and reliability of the developed method for the intended measurements, validation of this analytical method in human RBCs was evaluated through the following:

3.3.3.1 Recovery

The response of the extracted samples at low, medium, and high concentrations was compared to the response of unextracted known concentrations that represent 100% recovery. The efficiency of the extraction was reproducible with a CV less than 4% at each concentration. The CV was 17% through the calibration range with a recovery mean of 75.7%. The variability might be due to the big range (approximately 500 fold range) that can cause a difference in the in the performance of the extraction cartridges. Moreover, the recovery at the LLOQ was determined to be 80% with a CV not exceeding 3%, as summarized in Table 3-19.

Table 3-18. 5-HMF assay descriptive summary in human RBCs.

Type of assay:	HPLC-UV
Sample preparation:	Solid phase extraction of diluted RBCs by Oasis HLB cartridges (Waters)
Detector:	Shimadzu 10 AV Absorbance Detector
LC pump:	Waters 600E Multisolvent Delivery System
LC column:	Zorbax Rx C_{18}, 80 A^{o}, 150 mm x 4.6 mm, 5 µm
Guard column	C_{18}, 12.5 mm x 4.6 mm
Detection:	UV at 285 nm
Autosampler temperature:	4 °C
Flow rate:	0.75 ml/min
Regression algorithm:	Linear, weighted 1/X
Sample volume and matrix:	0.1 ml of RBCs suspension, extracted to 0.5 ml sample
Mobile phase	Water-methanol-acetic acid-tetrahydrofuran (93.5:6.2:1:0.3)
Injection volume:	10 µL
Chromatographic run time:	10 minutes
Calibration curve range:	4.3 – 2379 µM
Lower limit of quantitation:	4.3 µM
Quality control levels:	9.5, 47.6, 1903 µM

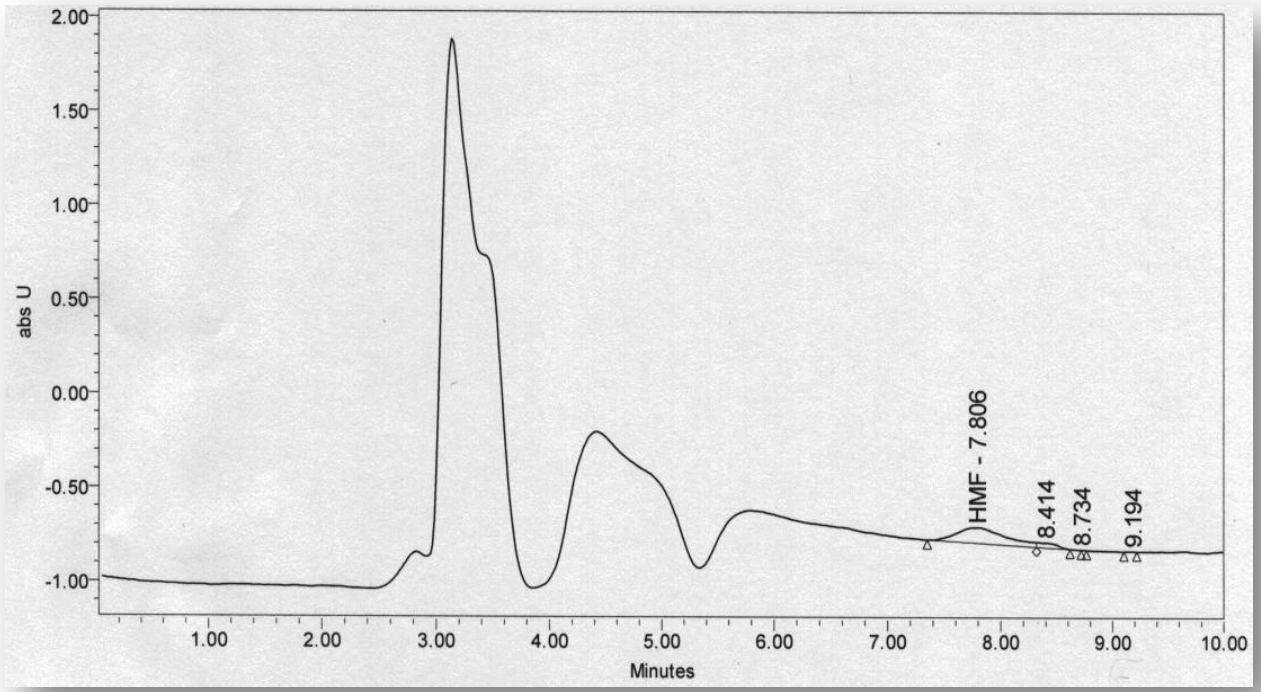

Figure 3-20. Representative chromatogram of individual human RBCs blank.

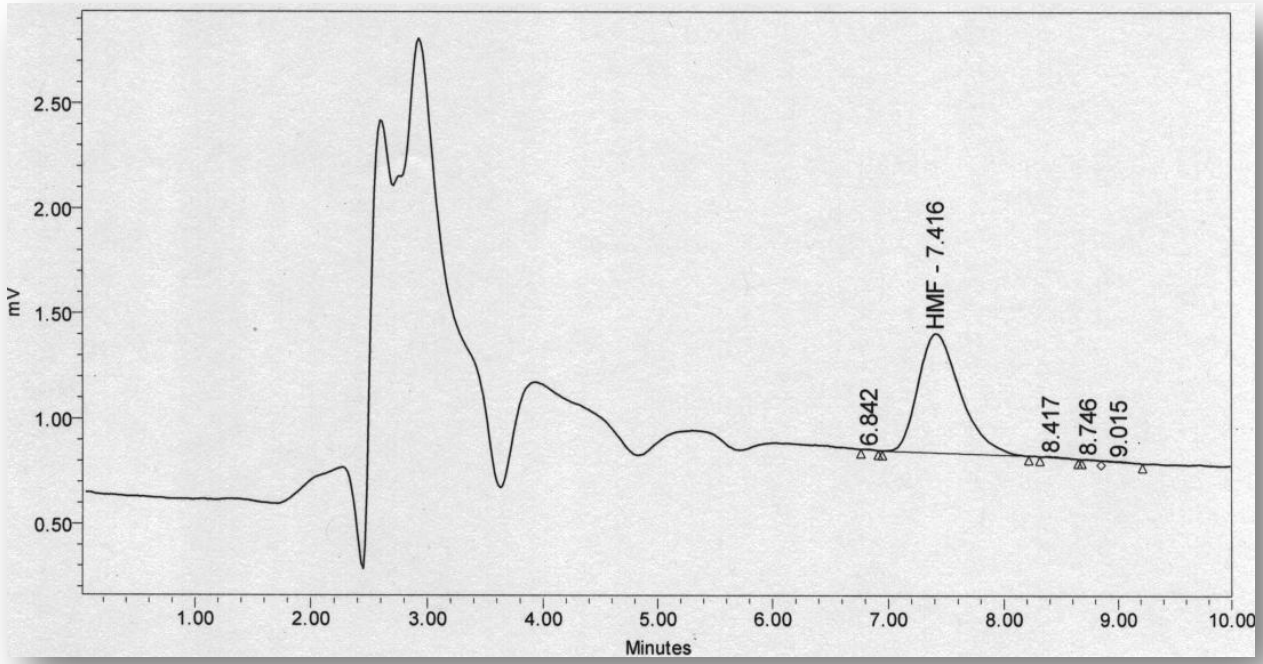

Figure 3-21. Representative chromatogram of the LLOQ concentration.

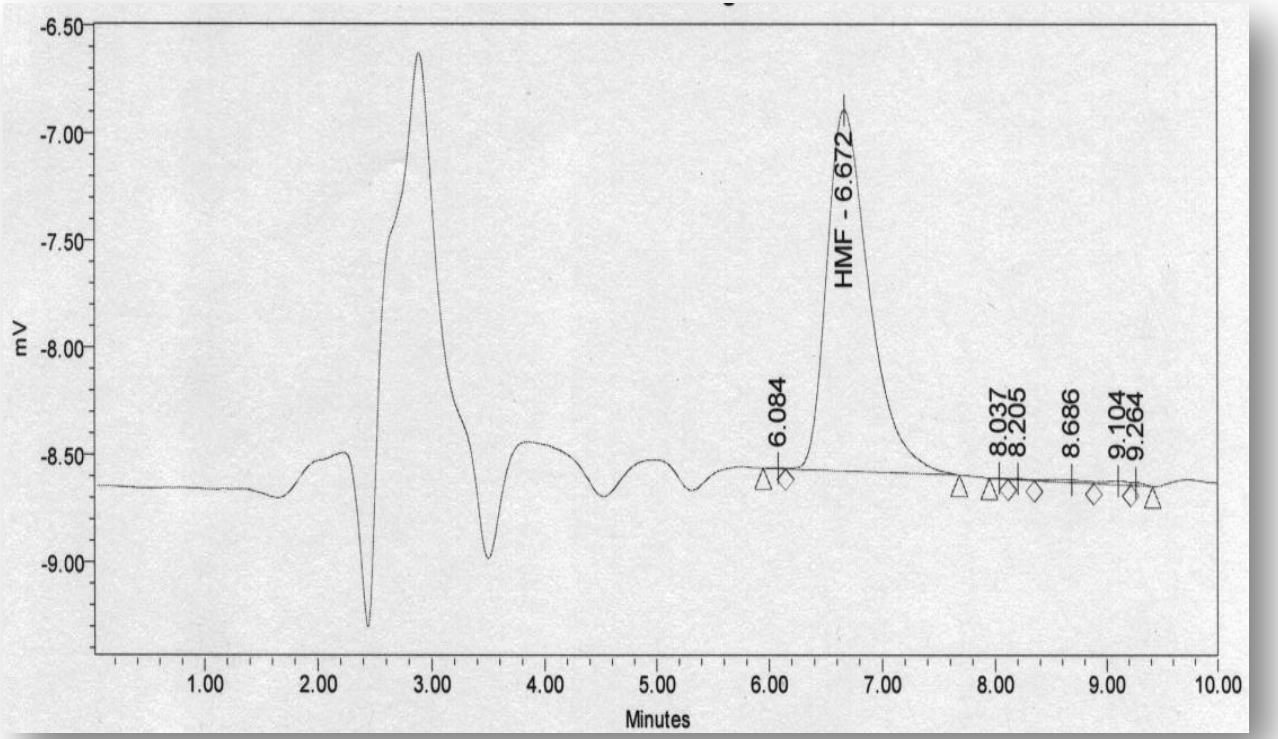

Figure 3-22. Representative chromatogram of low QC concentration.

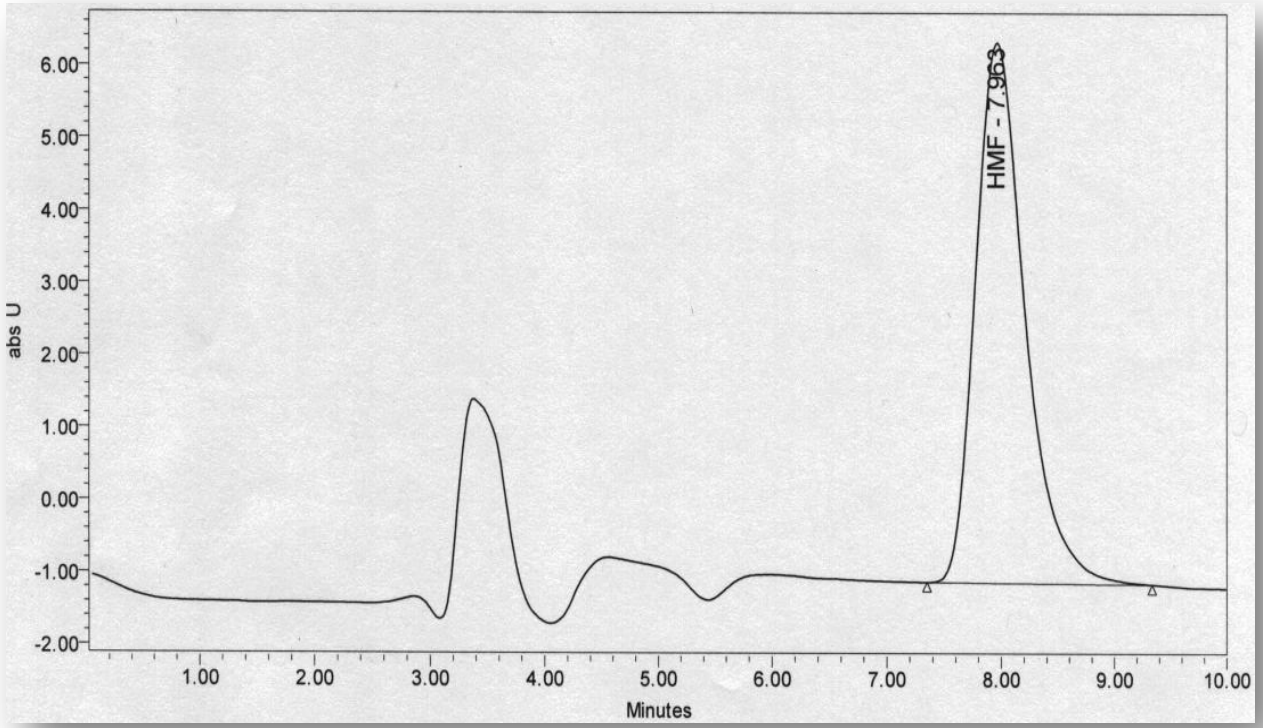

Figure 3-23. Representative chromatogram of mid QC concentration.

Table 3-19. 5-HMF recovery in human RBCs.

Concentration (µM)	R1	R2	R3	Mean	CV%
4	81.2	77.4	81.5	80.0	2.9
10	90.9	91.7	89.4	90.7	1.3
48	69.7	74.0	73.6	72.4	3.2
1903	59.7	59.7	60.1	59.8	0.4

3.3.3.2 Accuracy

Within-assay accuracy was determined for six replicate measurements at three different concentrations and at the LLOQ. The DFN value was used as a measure of the accuracy in the analytical range. The absolute DFN value did not exceed 15% at any of these concentrations including the LLOQ, as shown in Table 3-20.

3.3.3.3 Precision

Within-run precision was determined for six replicates, shown in Table 3-20, at four concentrations in the analysis range including the LLOQ. The FDA guidance for industry "Bioanalytical Method Validation" criteria were considered for acceptance with no more than 15% CV for the selected concentrations and 20% or less as the CV at the LLOQ.

3.3.3.4 Selectivity

As shown in Table 3-20, six different sources of RBCs were analyzed to test for interferences and to investigate the ability to differentiate and quantify 5-HMF in the presence of other endogenous components in the extracted RBCs. The ratio of the average area response of six replicates at the LLOQ concentration to that of six blank sources was 5.1.

Table 3-20. 5-HMF intra-run accuracy and precision in human RBCs.

Concentration (µM)	R1	R2	R3	R4	R5	R6	Mean	CV	DFN%
0	2934	2514	2552	2594	3001	3897	2915	17.9	
4	15287	14555	15341	14730	14394	14350	14776	3.0	-3.2
10	42751	43151	42055	43816	43857	42589	43037	1.7	-12.6
48	211185	224117	222822	221966	220153	225901	221024	2.4	-7.8
1903	7598597	7603656	7649638	8279831	8025133	7950308	7851194	3.6	6.0

3.3.3.5 Calibration curve

The relationship between 5-HMF concentration in RBCs and the UV detector response was modeled by a linear regression algorithm in the range of 4-2379 µM, as demonstrated in Figure 3-24. Three replicates were used to define the analytical relationship. As evident in Table 3-21, the concentrations in the defined analytical range were within 88.2-114.6% of the nominal concentrations and did not exceed 3% in their coefficient of variation. These results meet the acceptance criteria of having at least four of six concentrations within the accuracy and precision limits including the lowest and highest concentration.

The lowest value in the calibration curve, which is 4 µM, was deemed as the LLOQ. The response of the blank at the retention time of 5-HMF, was not more than the 20% of the LLOQ response at the specified retention time. The ratio of the average response of six replicates at the LLOQ to that of the six sources of thee blanks was 5.1. The average of the analytical results for a minimum of six replicates at the LLOQ had DFN value of 13.6%. The CV at the LLOQ did not exceed 3% as a measure of precision. The intercept of the equation was not statistically significant.

Due to the wide analytical range, a weighing factor of (1/X) was used in the established linear model. The calibration curve had a significant slope and a non-significant intercept.

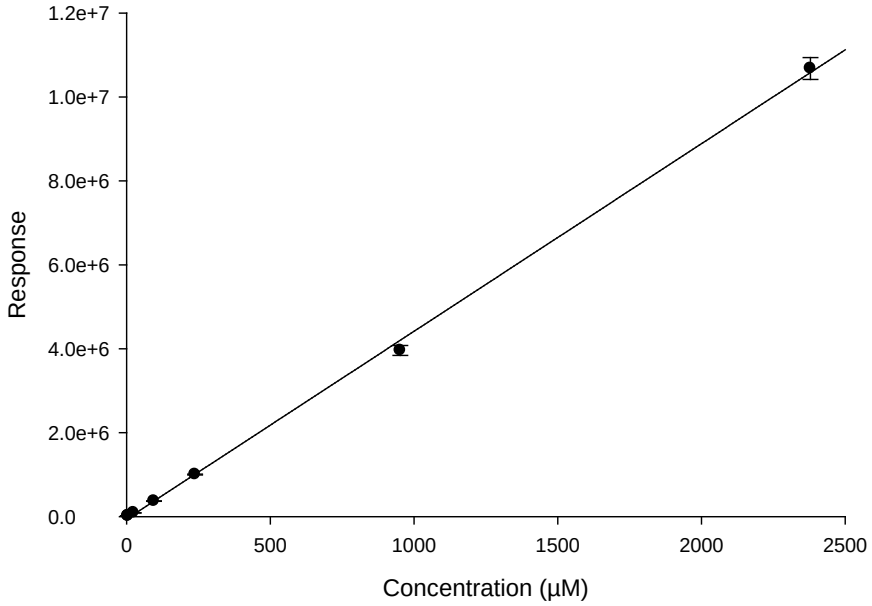

Figure 3-24. 5-HMF response-concentration curve.

Table 3-21. 5-HMF standard curve.

Concentration (µM)	R1	R2	R3	Mean	CV	Average DFN%
4	15287	14555	15341	15061	2.9	13.6
5	20287	20134	20635	20352	1.3	14.6
24	90157	88275	91153	89862	1.6	-11.8
95	367338	366141	376163	369881	1.5	-11.1
238	995900	1013878	999394	1003057	1.0	-3.3
952	3995286	3827174	4055532	3959331	3.0	-5.0
2379	10763231	10884655	10384749	10677545	2.4	2.6

	Value	p-value
Intercept	-4479.3	0.52
Slope	4372.9	<0.0001
r^2	0.998	

3.3.4 5-HMF in Rat, Mouse, and Dog RBCs

An HPLC-UV assay was developed for the determination of HMF in rat, mouse, and dog RBCs. A descriptive summary of the method is shown in Table 3-22.

To ensure the suitability and reliability of the developed method for the intended measurements, validation of this analytical method in rat, mouse, and dog RBCs was evaluated through the following:

3.3.4.1 Accuracy

Within-assay accuracy was determined for six replicate measurements at three different concentrations and at the LLOQ. The DFN value was used as a measure of accuracy in the analytical range, as shown in Tables 3-23, 3-24, and 3-25.

Table 3-22. 5-HMF assay descriptive summary in species RBCs.

Type of assay:	HPLC-UV
Sample preparation:	Solid phase extraction of diluted RBCs by Oasis HLB cartridges (Waters)
Detector:	Shimadzu 10 AV Absorbance Detector
LC pump:	Waters 600E Multisolvent Delivery System
LC column:	Zorbax Rx C_{18}, 80 A^o, 150 mm x 4.6 mm, 5 µm (Agilent, Serial # USDU010028)
Guard column	C_{18}, 12.5 mm x 4.6 mm (Agilent, Serial # USCI042710)
Detection:	UV at 285 nm
Autosampler temperature:	4 °C
Flow rate:	0.75 ml/min
Regression algorithm:	Linear, weighted 1/X
Sample volume and matrix:	0.1 ml of RBCs suspension, extracted to 0.5 ml sample
Mobile phase	Water-methanol-acetic acid-tetrahydrofuran (93.5:6.2:1:0.3)
Injection volume:	10 µL
Chromatographic run time:	10 minutes
Calibration curve range:	Mouse: 8.6 – 4757.8 µM, Rat: 8.6 – 4757.8 µM, Dog: 8.6 – 4757.8 µM
Lower limit of quantitation:	Mouse: 8.6 µM, Rat: 8.6 µM, Dog: 8.6 µM
Quality control levels:	Mouse: 19.0, 95.2, 3806.2 µM, Rat: 19.0, 95.2, 3806.2 µM, Dog: 19.0, 95.2, 3806.2 µM

Table 3-23. 5-HMF intra-run accuracy and precision in mouse RBCs.

Concentration (µM)	R1	R2	R3	R4	R5	R6	Mean	CV	DFN%
0	1851	2029	1379				1753	19.2	
8.6	4055	3427	3637	4058	3072	4878	3854	16.3	-492.4
19	9084	8992	8641	11221	8397	9679	9336	10.9	-46.2
95	135741	126266	127200	132624	125519	123645	128499	3.6	-14.1
3806	6437939	6537972	6681089	6647384	6923159	6542404	6628325	2.5	0.3

Table 3-24. 5-HMF intra-run accuracy and precision in rat RBCs.

Concentration (µM)	R1	R2	R3	R4	R5	R6	Mean	CV	DFN%
0	2686	1215	1174				1692	50.9	
8.6	26021	23840	26034	24697	24542	24981	25019	3.5	11.6
19	33723	35661	33846	31389	26440	-	32212	11.1	-24.8
95	208477	215522	202883	209306	210404	195089	206947	3.4	8.1
3806	7442537	7419570	7552769	7304463	7151040	7679852	7425039	2.5	-0.1

Table 3-25. 5-HMF intra-run accuracy and precision in dog RBCs.

Concentration (µM)	R1	R2	R3	R4	R5	R6	Mean	CV	DFN%
0	0	1060	822				627	88.7	
8.6	24142	21922	22295	23465	22352	23009	22864	3.7	-3.5
19	44696	45340	43986	42051	46204	46407	44781	3.6	3.0
95	206939	188630	179375	188713	191056	178310	128499	3.6	2.1
3806	7445653	6887127	6821685	6933841	6663242	7780804	6628325	2.5	-0.1

3.3.4.2 Precision

Within-run precision was determined for at least five replicates, shown in Tables 3-23, 3-24, and 3-25 at four concentration levels in the analytical range including the LLOQ. The FDA guidance for industry "Bioanalytical Method Validation" criteria were considered for acceptance with no more than 15% coefficient of variation for the selected concentrations and 20% or less as the CV at the LLOQ.

3.3.4.3 Selectivity

As shown in Tables 3-23, 3-24, and 3-25, pooled RBCs from at least six different sources were analyzed to test for interferences and to investigate the ability to differentiate and quantify 5-HMF in the presence of other endogenous components in the extracted RBCs.

3.3.5 Other Matrices

The development of this analytical method involved 5-HMF analysis in neat solution, as shown in to Table 3-26. In addition, the same method was used in the measurement of 5-HMF in the ultrafiltrate of human serum albumin and hemoglobin PBS solutions. For each study, a calibration curve in PBS was analyzed in conjunction with the samples. Samples and calibration curve standards were injected directly into HPLC. Table 3-27 is showing some of the PBS calibration curves.

Table 3-26. 5-HMF standards in neat solution.

Concentration (µM)	R1	R2	R3	Mean	CV
0.08	20280	21533	21900	21238	4
0.40	111678	112737	113100	112505	0.7
0.79	218133	218354	218880	218456	0.2
11.9	3330060	3322928	3319840	3324276	0.2
47.6	13349916	13302739	13323871	13325509	0.2
79.3	21462393	21492723	21453369	21469495	0.1

Table 3-27. 5-HMF standards in PBS.

Concentration (µM)	R1	R2	R3	R4	Mean	CV
0.2	6312	6764	6904	5165	6286	13
0.8	21454	20635	22599	19085	20943	7
4.0	97756	90331	99556	91037	94670	5
7.9	216324	185712	175796	172020	187463	11
39.6	1142549	958669	837630	866326	951294	14
79.3	2175225	1753218	1687014	1727478	1835734	12

3.3.6 HMFA in Human Hepatic Cytosol

In order to supplement 5-HMF metabolic stability studies in hepatic cytosol, a method was developed to qualitatively detect HMFA in human hepatic cytosol incubated with 5-HMF. 5-HMF and HMFA peaks overlapped, as shown previously in Figure 3-15, using the above described method. Consequently, a new mobile phase was prepared of water and methanol, in which tetrabutylammonium was dissolved. A summary of the method is described in Table 3-28 and a chromatogram showing the peaks of both 5-HMF and HMFA standards in Tris buffer, is shown in Figure 3-25. Response-concentration curves for 5-HMF and HMFA in buffer are shown in Figures 3-26 and 3-27, respectively. In addition, the chromatograms of a blank cytosol and two concentrations of HMFA added to the cytosol are shown in Figures 3-28, 3-29, and 3-30. As demonstrated in Figure 3-28, a peak in the blank cytosol is present in the retention window of 5-HMF, and in particular HMFA. However, for a qualitative purpose, the method was deemed satisfactory. A standard curve of HMFA was investigated in the cytosol and is shown in Figure 3-31.

Table 3-28. 5-HMF assay descriptive summary in human hepatic cytosol

Type of assay:	HPLC-UV
Sample preparation:	Dilution of with ice-cold acetonitrile and water.
Detector:	Shimadzu 10 AV Absorbance Detector
LC pump:	Waters 600E Multisolvent Delivery System
LC column:	Zorbax Rx C_{18}, 80 A^{o}, 150 mm x 4.6 mm, 5 µm (Agilent, Serial # USDU010028)
Guard column	C_{18}, 12.5 mm x 4.6 mm (Agilent, Serial # USCI042710)
Detection:	UV at 260 nm
Autosampler temperature:	4 °C
Flow rate:	1 ml/minute
Sample volume and matrix:	100 µl diluted to 800 µl (650 µl water and 50 µl acetonitrile)
Mobile phase	Water-methanol (83:17), 0.2% w/v tetrabutylammonium iodide
Injection volume:	10 µL
Chromatographic run time:	10 minutes

`

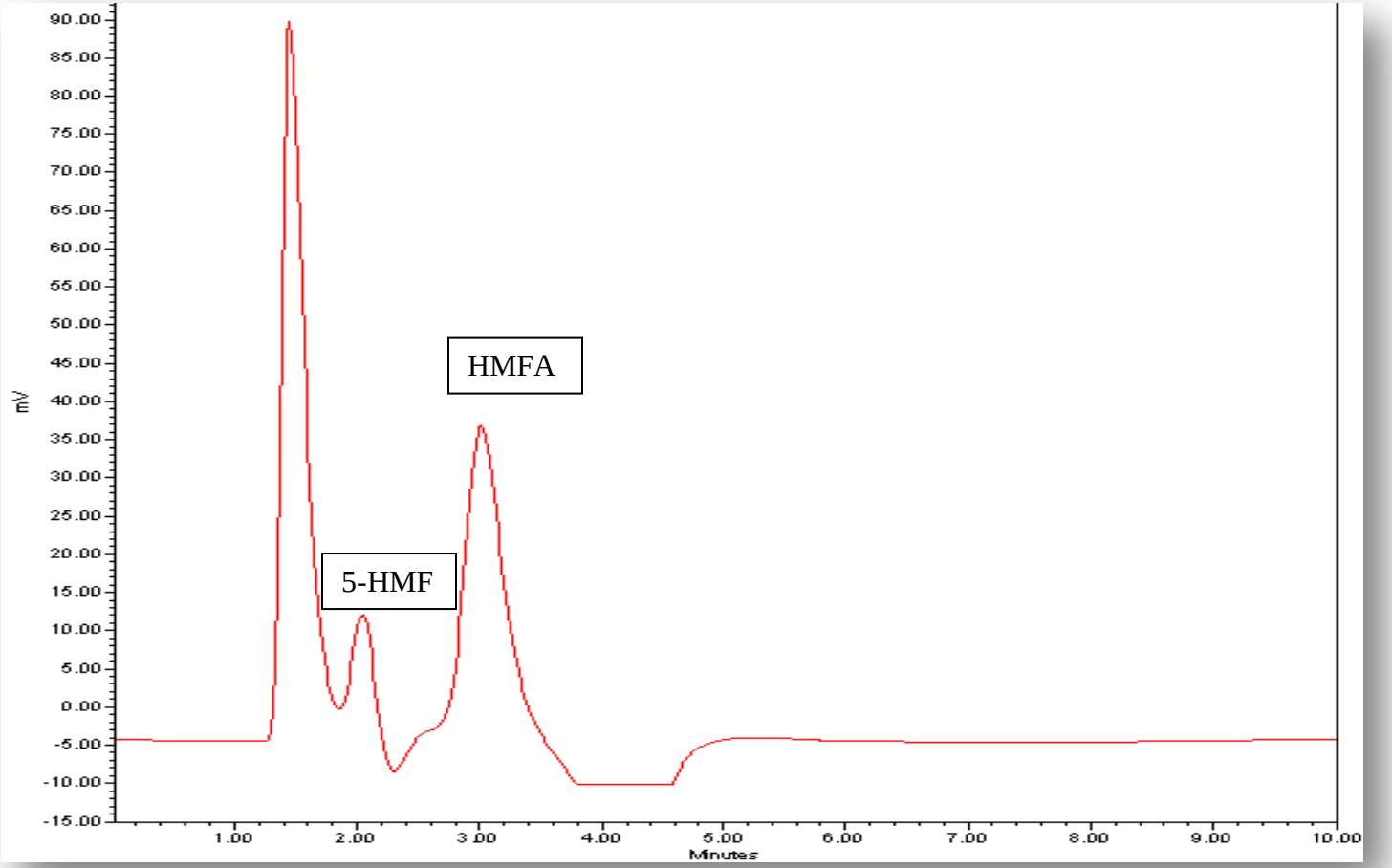

Figure 3-25. 5-HMF (0.79 mM) and HMFA (0.90 mM) chromatogram.

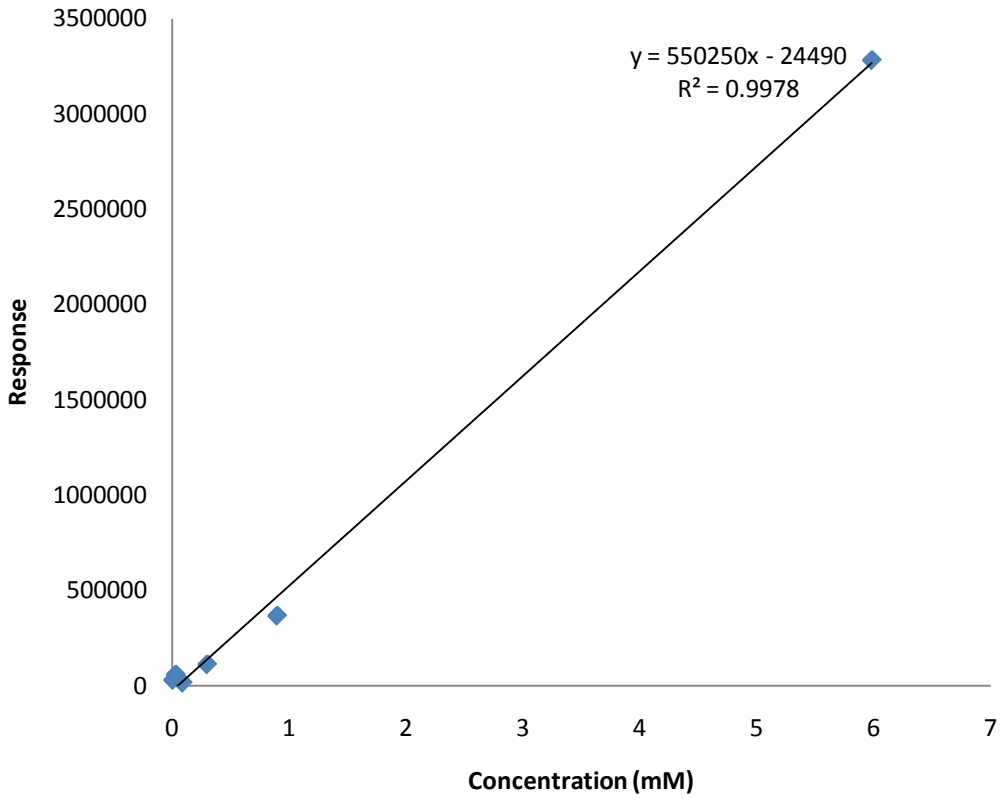

Figure 3-26. HMFA response-concentration curve.

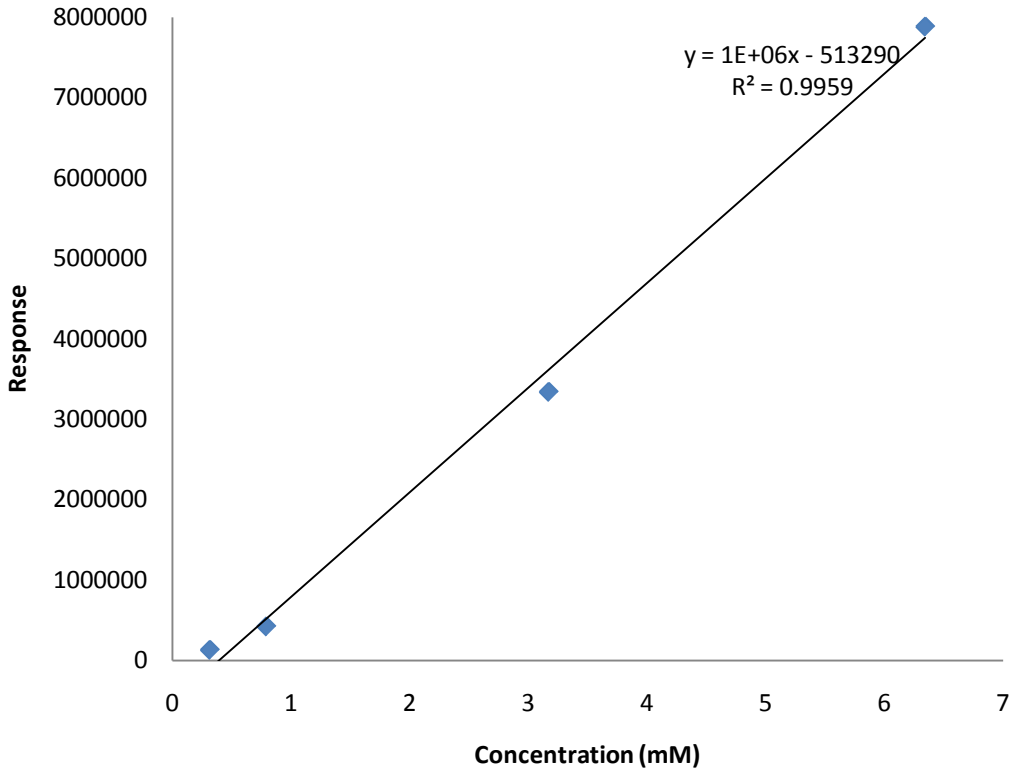

Figure 3-27. 5-HMF response-concentration curve.

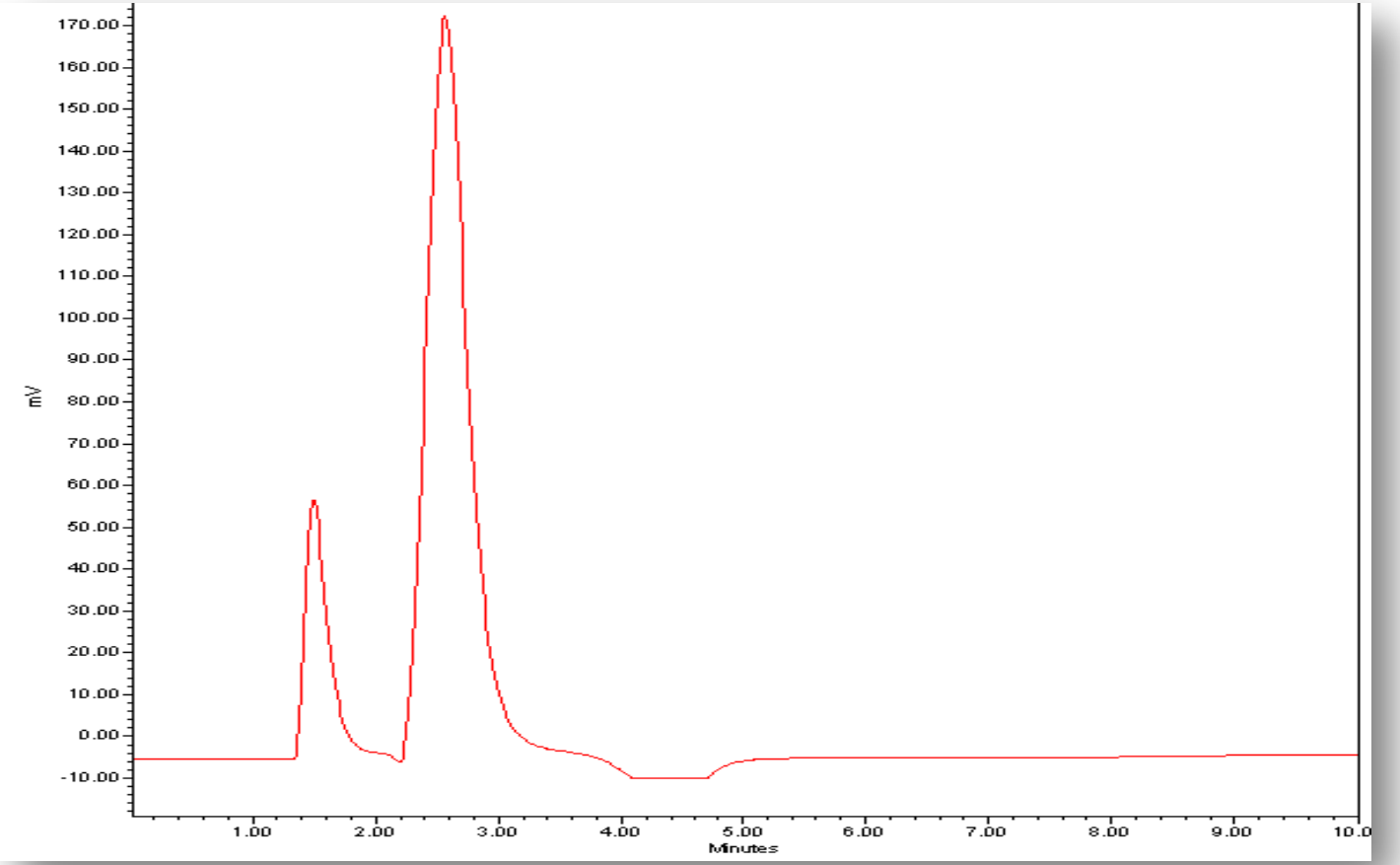

Figure 3-28. Cytosol blank chromatogram.

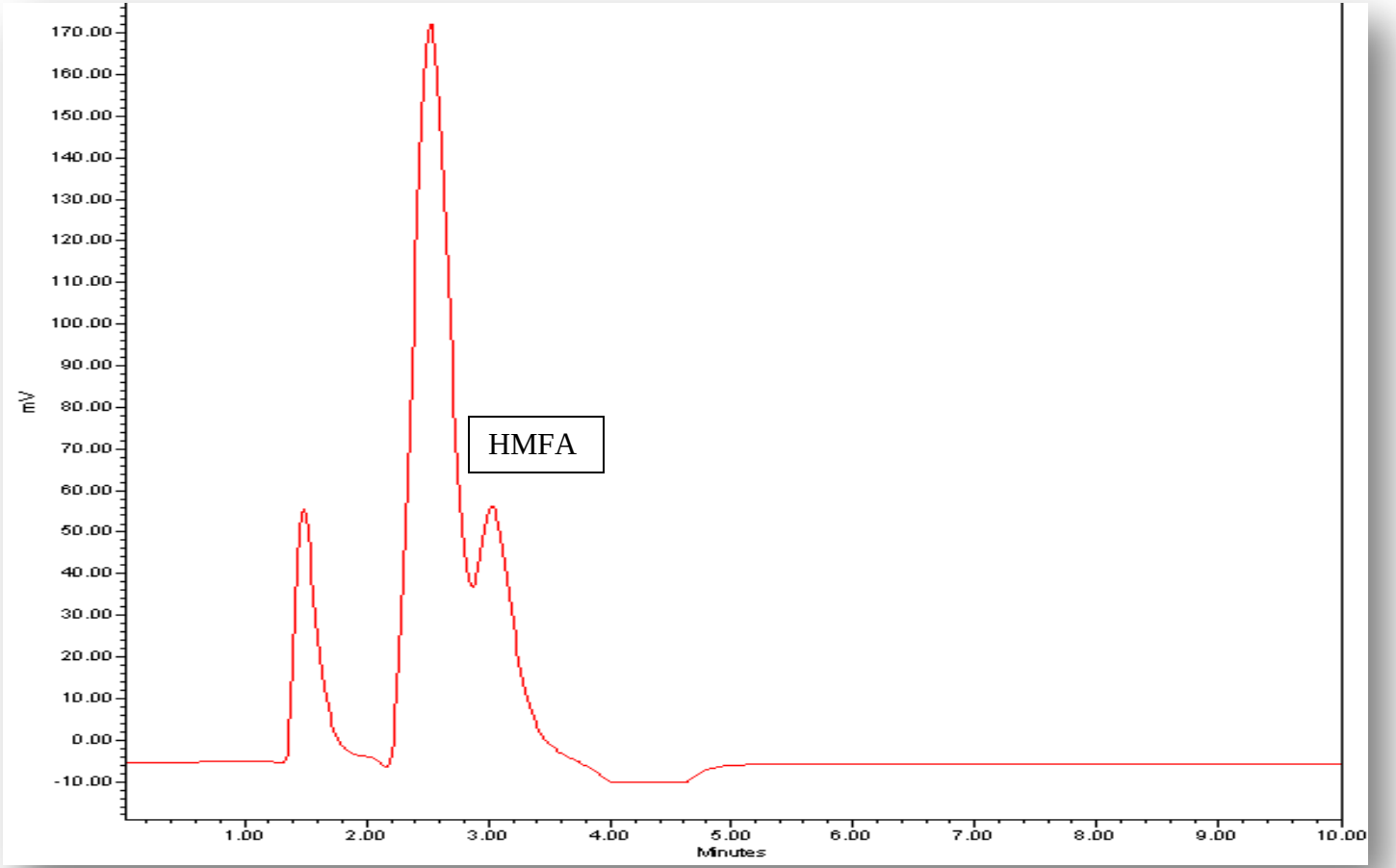

Figure 3-29. HMFA standard in hepatic cytosol (0.9 mM)

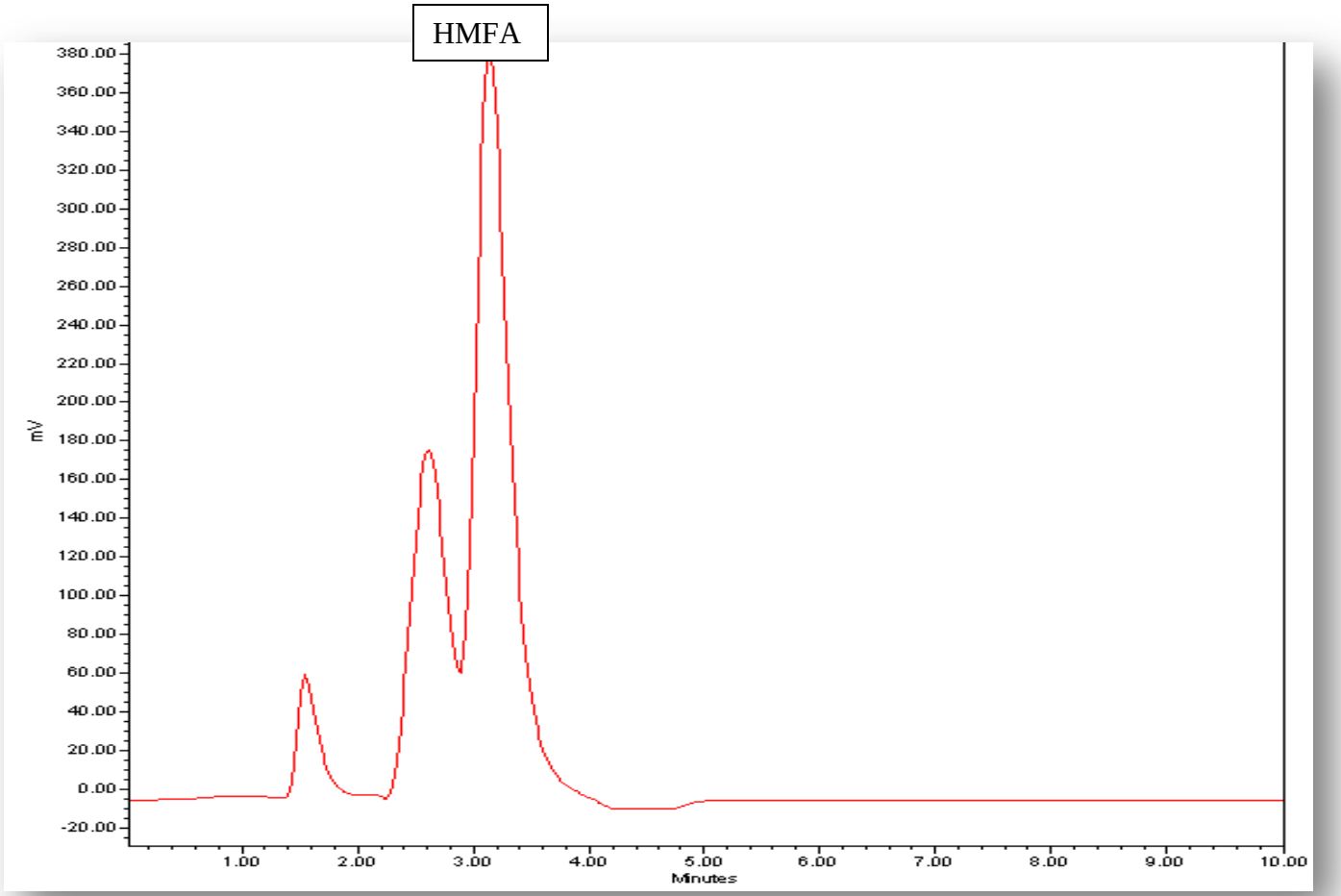

Figure 3-30. HMFA standard in hepatic cytosol (6.0 mM).

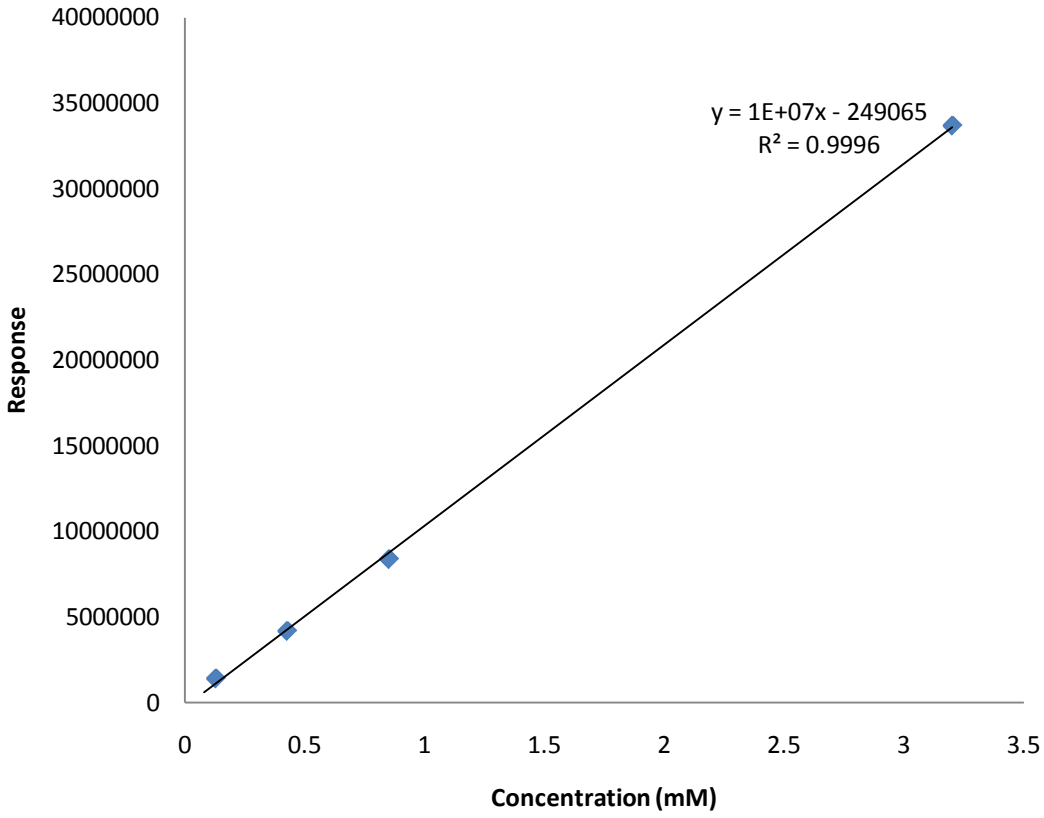

Figure 3-31. HMFA calibration curve in human cytosol.

CHAPTER 4

5-HMF *IN-VITRO* METABOLISM IN HEPATIC CYTOSOL OF DIFFERENT SPECIES

4.1 Introduction

Different *in-vitro* methodologies are used to predict human clearance. An example of that is recombinant enzymes; however, the artificial nature of this matrix represents a drawback of the recombinant system (Hallifax 2009). Hepatocytes are considered more physiological and give an idea about the cumulative metabolic rate for a drug if detoxified by different enzymes. However, identifying the exact metabolic pathway is challenging with the use of hepatocytes (Gupta 2006).

In general, metabolic stability studies follow the scheme introduced in Figure 4-1. These studies investigate the disappearance of the parent drug or the formation of the metabolite (Houston 2008). Initially, they result in pseudo-zero order kinetics that is estimated over a period of time (Houston 2008). Non-linear regression modeling is used to estimate the *in-vitro* metabolic parameters from the concentration-dependent initial metabolic rate profile. Then the metabolic parameters are used in the *in-vitro* intrinsic clearance calculation. Physiological

scaling variables are used to predict the *in-vivo* intrinsic clearance value from the *in-vitro* intrinsic clearance. This is further extrapolated to organ clearance using different models such as the well-stirred model to incorporate the hepatic blood flow limitation. The use of well-stirred model for projecting the hepatic clearance was justified by its mathematical simplicity and applicability for drugs with low intrinsic clearance (Houston 2008). This model assumes a uniform distribution of the relevant enzymes in the liver tissues and that merely the unbound drug fraction is subject to metabolism, which is made available to enzymes by hepatic perfusion (Houston 2008).

5-HMF structure and the known metabolites indicate its *in-vivo* oxidation rather than reduction, which might, otherwise, utilized the aldo/keto reductase enzymes (Marchitti 2008). Alternatively, aldehyde group oxidation can be carried-out by different enzymes, such as xanthine oxidase, aldehyde oxidase, and aldehyde dehydrogenase (ALDH) (Marchitti 2008). Nevertheless, xanthine oxidase, as its names indicates, is involved in the oxidation of purines (Beedham 1997). Thus, its role in 5-HMF metabolism is assumed to be minimal. On the other hand, aldehyde oxidase is implicated in the oxidation of N-containing heterocyclic compounds, such as antiviral drugs (Beedham 1997). Nevertheless, aldehyde oxidase metabolizes other aromatic aldehydes such as vanillin (Sahi 2008). The other moiety of 5-HMF that is susceptible to metabolism is the alcohol group, which is most likely metabolized by alcohol dehydrogenase (ADH) after excluding the other oxidizing enzymes and considering its structural similarity with ethanol. Table 4-1 lists these oxidizing enzymes and their respective cofactors.

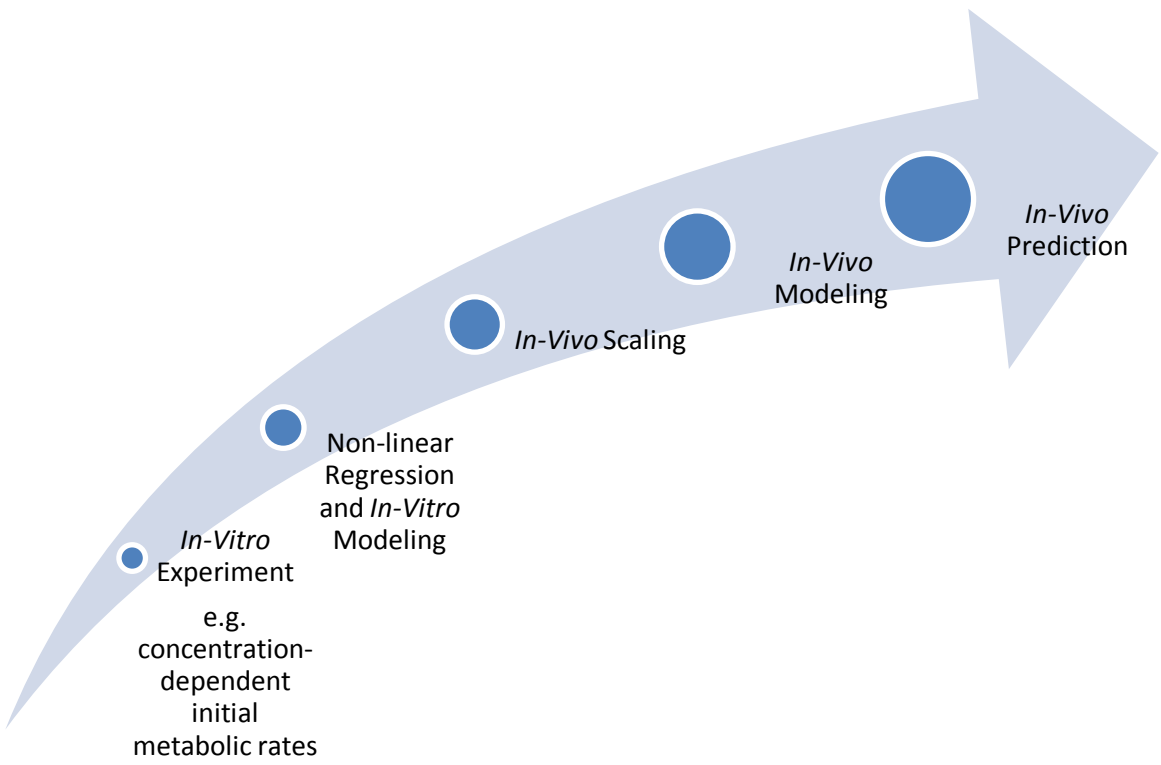

Figure 4-1. In-vitro-in-vivo extrapolation steps. Adapted from **(Hallifax 2009)**

Table 4-1. Oxidative enzymes **(Beedham 1997)**

Enzyme	Oxidative Reaction	Cofactor
ALDH	Aldehyde oxidation	$NAD(P)^+$
ADH	Alcohol oxidation	NAD^+
Aldehyde oxidase	Aldehyde oxidation, C-oxidation of N-heterocycles	O_2
Monoamine oxidase	Oxidative deamination	O_2
Flavine monooxygenase	N-oxidation	NADPH, O_2
Xanthine oxidase	C-oxidation of purines	NAD^+, O_2

Hepatic cytosol was selected for the purpose of predicting the intrinsic clearance of 5-HMF in humans and other species for the following reasons:

- The liver was reported to have high 5-HMF- related radioactivity in mice and rats after oral administration of 5-HMF (Godfrey 1999).
- It is a rich resource of ALDH and ADH enzymes (Gupta 2006).
- Human and other species cytosol is commercially available (Brandon 2003).
- It is an ethically acceptable medium for investigating enzyme kinetics (Brandon 2003).
- Studies with hepatic cytosol from different species were carried-out in the PK/PD laboratory at VCU and the following were demonstrated (Gupta 2006):
    - Successful prediction of *in-vivo* clearance of other substrates, such as ethanol and propylene glycol.
    - Demonstration of inter-species differences in hepatic cytosol metabolism.
- The metabolism by both ALDH and ADH enzymes can be measured simultaneously by a simple spectrophotometric method. NADH is measured as a common product for both enzymes at 340 nm.

The specificity of NADH production is assumed since none of the other oxidizing enzymes, if present in this system, has the potential to oxidize 5-HMF and produce NADH simultaneously.

Since NADH is a common product for both of ALDH and ADH enzymes, selective inhibitors were used to determine the individual contribution of each enzyme. 4-methylpyrazole and disulfiram were selected as the selective inhibitors for ADH and ALDH, respectively. 4-methylpyrazole, known as fomepizole, is used clinically as an antidote to treat alcohol and

ethylene glycol intoxication (Druteika 2002) (Bestic 2009). 4-methylpyrazole was shown to be a competitive reversible inhibitor for ADH enzyme (Bestic 2009) (C. D. Cheung 2003) (Plapp 1984). In comparison with ethanol, its affinity for ADH was reported to be approximately 8000 fold greater than that of ethanol (Bestic 2009). Its mechanism of action was found to involve the formation of a ternary complex involving NAD^+, ADH Zinc element, and 4-methylpyrazole preventing the substrate from the interaction with the enzyme (Bestic 2009). In a study conducted by Cheung, 38% of the control ADH activity remained in rat liver cytosol after using 1 M of 4-methylpyrazole as the highest inhibitory concentration (C. D. Cheung 2003).

On the other hand, disulfiram (tetraethylthiuram disulfide, Antabuse) is also used clinically for the treatment of alcoholism by inducing obnoxious effects of drinking, termed as "aversion therapy" (Kitson 1975) (Shena 2001). Although it is well agreed that these effects are due to the accumulation of acetaldehyde as a consequence of ALDH inhibition after the administration of disulfiram (Keung 1993), its mode of inhibition is controversial. The interaction with ALDH was stated to be a rapid, strong, non-competitive, and reversible inhibition (A. R. Klyosov, Possible Role of Liver Cytosolic and Mitochondrial Aldehyde Dehydrogenases in Acetaldehyde Metabolism 1996). Cheung et. al. used disulfiram as an inhibitor of ALDH enzyme stating that it is a competitive, reversible inhibitor (C. H. Cheung 2003). On the other hand, when tested with cytoplasmic ALDH of sheep liver, disulfiram caused an initial inhibition, after which an increase in the inhibition was observed over time, indicating an irreversible mode of inhibition (Kitson 1975). Cytosolic ALDH is believed to be "disulfiram sensitive" with a K_i of 13, 15, and 200 nM in hamster, rat, and human, respectively (A. R. Klyosov, Possible Role of Liver Cytosolic and Mitochondrial Aldehyde Dehydrogenases in Acetaldehyde Metabolism 1996).

In addition to human, the metabolic studies were conducted in mouse, rat, and dog hepatic cytosol to explore potential differences in 5-HMF metabolism and consequently disposition among these species. Gupta reported different K_m and v_{max} values ranging between 0.8-14 mM and 0.05-2.8 mmol/min, respectively, for *in-vivo* ethanol metabolism, mediated by ADH, in rat, rabbit, dog, and human (Gupta 2006). Cheung and co-workers also observed that the cytosolic ADH of rodents had a lower metabolic efficiency of ethanol than that of human (C. D. Cheung 2003). Moreover, interspecies differences in ALDH enzyme were also reported. Klyosov and co-workers found that human cytosolic ALDH is more acidic than that of rat and hamster (A. R. Klyosov, Possible Role of Liver Cytosolic and Mitochondrial Aldehyde Dehydrogenases in Acetaldehyde Metabolism 1996). In addition, human ALDH appears to be tetrameric with a molecular weight exceeding 1.5 fold of that in rodents, which is probably dimeric (A. R. Klyosov, Possible Role of Liver Cytosolic and Mitochondrial Aldehyde Dehydrogenases in Acetaldehyde Metabolism 1996). All of these findings emphasize the complementary role of *in-vitro* approaches in explaining the results of *in-vivo* animal studies in the preclinical phase. Hence, the objective of the proposed *in-vitro* studies is to mechanistically investigate 5-HMF disappearance in human hepatic cytosol and to identify and compare the metabolism of 5-HMF in human, dog, rat, and mouse hepatic cytosol.

.

4.2 Methods

4.2.1 Materials and Reagents

1. BD Gentest™ TRIS buffer 0.5 M, pH 7.5 (BD Bioscience, San Jose, CA).
2. 4-Dimethylaminonaphthaldehyde, (DN) Solution:
   - 4-Dimethylaminonaphthaldehyde 97% (Aldrich, Milwaukee, WI)
   - BD Gentest™ TRIS buffer 0.5 M, pH 7.5 (BD Bioscience, San Jose, CA).
3. Ethanol Solution:
   - Ethanol 200 proof, 99.5% (Aldrich, Milwaukee, WI).
   - BD Gentest™ TRIS buffer 0.5 M, pH 7.5 (BD Bioscience, San Jose, CA).
4. Acetaldehyde Solution:
   - Acetaldehyde, ACS 99% (Sigma-Aldrich, Milwaukee, WI).
   - BD Gentest™ TRIS buffer 0.5 M, pH 7.5 (BD Bioscience, San Jose, CA).
5. 5-Hydroxymethyl-2-furfural (5-HMF) Solution:
   - 5-Hydroxymethyl-2-furfural (Sigma, St. Louis, MO).
   - BD Gentest™ TRIS buffer 0.5 M, pH 7.5 (BD Bioscience, San Jose, CA).
6. 4-Methylpyrazole (4-MP) Solution:
   - 4-MP, 99% (Sigma-Aldrich, Milwaukee, WI).
   - BD Gentest™ TRIS buffer 0.5 M, pH 7.5 (BD Bioscience, San Jose, CA).
7. Tetraethylthiuram Disulfide (Disulfiram) Solution:
   - Disulfiram, purum 97% (Sigma-Aldrich, Milwaukee, WI).
   - BD Gentest™ TRIS buffer 0.5 M, pH 7.5 (BD Bioscience, San Jose, CA).

8. Liver Cytosol: 10 mg protein/ml (XenoTech, Lenexa, KS):

   - human: mixed gender, pool of 50 (Hispanic (8), Caucasian (41), Asian (1), 50 ± 14 years old).

   - dog: pooled Beagle males.

   - rat: pooled Fischer 344 males.

   - mouse: pooled B6C3F1 males.

9. Cytosol Diluent:

   - Bovine serum albumin (BSA) (Sigma, St. Louis, MO).

   - BD Gentest™ TRIS buffer 0.5 M, pH 7.5 (BD Bioscience, San Jose, CA).

10. Cofactor Solution, β-Nicotinamide Adenine Dinucleotide (NAD^+) Solution:

    - NAD^+ from yeast (Sigma, St. Louis, MO).

    - BD Gentest™ TRIS buffer 0.5 M, pH 7.5 (BD Bioscience, San Jose, CA).

4.2.2 Equipment

1. 25-µl, 50-µl, and 250-µl positive displacement pipettes and corresponding pipette tips (Microman, Rainin Instruments, Oakland, CA).
2. 10-µl, 100-µl, and 1000-µl VWR pipettes and corresponding pipette tips (VWR, West Chester, PA).
3. 0.5-5 ml Finnpipette (Thermo Scientific, Waltham, MA).
4. Vortex (Vortex-Genie, VWR, West Chester, PA).
5. Sonicator (American Brand Products C6450-11, VWR, West Chester, PA).
6. pH meter (Corning, Glendale, AZ).
7. Balance (Fisher Scientific A 250, Pittsburgh, PA).
8. Synergy™ 2 multi-mode microplate reader (BioTek, Winooski, VT).
9. Falcon assay plate, 96 reaction wells (VWR, West Chester, PA).

4.2.3 Preparation of Solutions

- Cofactor solution, β-nicotinamide adenine dinucleotide (β-NAD^+) solution

22.3 g of NAD^+ (M.W.: 663.43 Da) was dissolved in 3 ml of Tris buffer to prepare 1.4 mM solution.

- Cytosol diluent

BSA (M.W.: 66 kDa) was dissolved in Tris buffer to prepare 0.1% w/v. Solutions were kept cold during the experiment.

- Cytosol solution

Concentrated cytosol protein solution (10 mg/ml) was mixed with the cytosolic diluents to prepare a 4 mg/ml solution. For DN concentration-dependency experiments, a 2 mg/ml solution was prepared. Fresh solutions were prepared and kept cold during the experiment.

- Substrates solution

Solution at different concentrations of 5-HMF were prepared in Tris buffer. The measurement of NADH at low substrate concentration was limited by the assay sensitivity in some cases. In addition, the measurement of NADH at a high substrate concentration was limited by the solubility of 5-HMF and its high baseline absorbance. Since the K_m for other substrates: ethanol (M.W. 46.07 Da), acetaldehyde (M.W. 44.05 Da), and DN (M.W. 199.25 Da) were reported in the literature, their solutions were

perpared considering a range of ten-times lower and ten-times higher concentration relative to their reported K_m values, as summarized in Table 4-2.

- Inhibitor solutions

Solution of inhibitors, 4-methylpyrazole (M.W. 82.10 Da) and disulfiram (M.W. 296.54 Da) were prepared to achieve a maximum inhibition of the relevant enzymes taking into consideration their reported K_i values, as shown in Table 4-3.

Table 4-2. Selective Substrates.

Substrate	Ethanol	DN	Acetaldehyde
Structure	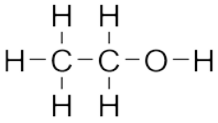	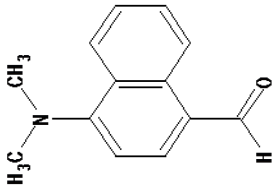	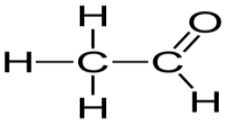
Reported K_m	0.7 mM (Gupta 2006)	1.9 nM (A. R. Klyosov 1996)	180 µM (A. Klyosov 1996)
Concentration Range	Up to 24 mM	Up to 66 nM	Up to 333 µM in the presence of 244 µM 4-MP

Table 4-3. Selective inhibitors.

	4-Methylpyrazole	**Disulfiram**
Structure	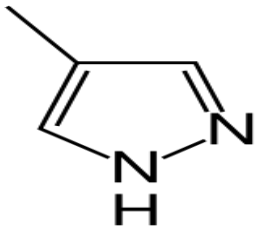	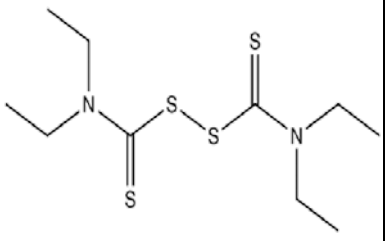
Reprted K_i (µM)	0.1-5 (Bestic 2009)	0.2 (A. R. Klyosov 1996)
Concentration range (µM)	0.03-281	0.03-33.8

4.2.4 Procedures

Cytosolic protein, NAD^+ cofactor, and substrates at different concentrations in Tris buffer (pH 7.5) were mixed at a final volume of 0.2 ml. The reaction was initiated by the addition of cytosolic protein solution after allowing the mixture to equilibrate for approximately 5 min. Then, the increase in the absorbance at 340 nm at 37 °C was monitored over time. The change in the absorbance was converted to NADH concentration using Beer's law, that relates the change in the absorbance to the concentration of absorbing species, as described by Equation 4-1.

$$\Delta A = \varepsilon \times b \times \Delta c \quad \text{Equation } 4-1$$

Where

ΔA: measured absorbance change

ε: the extenction coefficient of NADH at 340 nm

b: pathlenght of the cell

Δc: the concentration change of the absorbing species (NADH)

The change in the concentration of NADH over time represents the velocity at which the enzyme is forming NADH and simulatenously oxidizing 5-HMF, assuming 1:1 reaction. For each concentration, the reaction time and the points used for charcterization of the intitial velocity were selected where a linear increase in the absorbance over time existed, demonstrating a pseudo-zero order reaction. At each concentration, a minumum of duplicate reactions were included in the data analysis.

4.2.5 Optimization Experiments

The incubation conditions for the reaction were optimized through preliminary experiments. The concentration of the cofactor and the cytosol were selected after several experiments, so that the initial reaction rate could be observed at a zero-rate order increase in the absorbance, reflecting the NADH formation.

4.2.6 Concentration-Dependency Studies

These initial velocities were plotted against their corresponding substrate concentrations and were evaluated using Michaelis Menten kinetics. Michaelis Menten kinetics is characterized by a maximum velocity and an affinity constant, as shown in Equation 4-2.

$$v_i = \frac{v_{max} \times C}{K_m + C} + v_0 \quad \text{Equation } 4-2$$

Where

v_i: the observed velocity

v_0: the baseline velocity observed in the absence of the substrate

C: the substrate concentration

v_{max}: the maximum velocity

K_m: the affinity constant

The data were fitted to Equation 4-2 using nonlinear regression (SigmaPlot® 10.0, Systat) to obtain the model parameter estimates. The goodness of fit was evaluated through the coefficient of determination (r^2) values.

In addition, linearization graphing methods, namely: a Lineweaver-Burk (double-reciprocal) plot, a Eadie-Hofstee plot, and a Hanes-Woolf (half-reciprocal) plot, were used to inspect 5-HMF metabolic reaction in different species hepatic cytosol. The methods are described in Table 4-4.

Table 4-4. Linearization graphing methods to assess Michaelis Menten kinetics.

Lineweaver-Burk (double-reciprocal)	**Eadie-Hofstee**	**Hanes-Woolf (half-reciprocal)**
$\frac{1}{v} = \frac{K_m}{V_{max}} x \frac{1}{[S]_0} + \frac{1}{V_{max}}$	$v = -K_m x \frac{v}{[S]_0} + V_{max}$	$\frac{[S]_0}{v} = \frac{1}{V_{max}} x[S]_0 + \frac{K_m}{V_{max}}$
1/v against $1/[S]_0$ giving intercepts at $1/v_{max}$ and $-1/K_m$	v against $v/[S]_0$ giving intercepts at v_{max} and v_{max}/K_m	$[S]_0/v$ against $[S]_0$ giving intercepts at K_m/v_{max} and K_m

4.2.7 Inhibition Studies

Taking into consideration their reported K_i values, different concentrations of inhibitors of 4-methylpyrazole and disulfiram were used. All reaction components except 5-HMF were incubated for approximately 15 minutes and 25 minutes with 4-methylpyrazole and disulfiram, respectively, after which 5-HMF (26 mM) was added. Reactions were run in triplicate and monitored at 340 nm. In addition, 26 mM of 5-HMF was incubated with 273 µM 4-methylpyrazole and 17.4 µM disulfiram, simultaneously, using the same incubation conditions described previously.

The same approach was used for investigation of the inhibitory effect on ethanol and acetaldehyde at 1.8 mM and 5.3 mM, respectively. 257 µM of 4-methylpyrazole was used in the acetaldehyde experiment.

The data were modeled using Equation 4-3 by non-linear regression (SigmaPlot® 10.0, Systat) to estimate the maximum inhibition, as shown in Equation 4-3. IC_{50} is the concentration at which half of the maximum inhibition is achieved.

$$\%\ \text{inhibition} = \frac{\text{Maximum Inhibition} \times \text{Inhibitor Concentration}}{IC_{50} + \text{Inhibitor Concentration}} \quad \text{Equation } 4-3$$

4.2.8 *In-Vitro-In-Vivo* Extrapolation

The i*n-vitro* intrinsic clearance ($CL_{int}^{in\text{-}vitro}$) was calculated according to Equation 4-5:

$$CL_{int}^{in-vitro} = \frac{V_{max}}{K_m} \quad \text{Equation } 4-5$$

Where $CL_{int}^{in\text{-}vitro}$ is a measure of the innate ability of each milligram of cytosolic protein to clear a substrate (at concentrations below K_m). This *in-vitro* measure was extrapolated to the *in-vivo* intrinsic clearance (CL_{int}) using the cytosolic protein content per gram liver and the total liver weight. The values of these are listed in Table 4-5 as reported in the literature. CL_{int} refers to the innate ability of the whole liver cytosol to clear the substrate without flow restrictions.

Table 4-5. Physiological reference values for mouse, rat, dog, and human **(Bogaards 2001) (Gupta 2006)**.

	Cytosolic Protein Concentration (mg/g liver)	**Liver Weight (g)**	**Hepatic Blood Flow (ml/min)**	**Hepatic Blood Flow (ml/min/kg)**	**Body Weight (kg)**	**Total Body Water (l)**
Mouse	83	2.2	9.7	280.2	0.03	0.02
Rat	108	12.5	22.4	89.7	0.25	0.15
Dog	67	320	309	30.9	10	6
Human	45	1799	1502	21.5	70	42

In order to scale-up the estimated intrinsic clearance to total body clearance and estimate the hepatic extraction ratio, the following assumptions were made:

- 5-HMF is subject to oxidative metabolism in hepatic cytosol, only; no other significant hepatic metabolism, or biliary excretion.
- 5-HMF has negligible renal excretion.

This assumption of negligible biliary and renal excretion was based on the extensive metabolism reported in different studies with a minimum amount of unchanged 5-HMF excreted in feces or urine, as discussed in Chapter 1. In addition, the hydrophilic 5-HMF structure with a small molecular weight implies that 5-HMF is not a substrate for biliary excretion.

CYP-450 is the other potential class of enzymes that might be involved in 5-HMF metabolism. However, CYP-450 enzyme substrates have affinity in the single micromolar range. If this is the case with 5-HMF, the enzymes will be saturated at the proposed therapeutic concentration of 5-HMF (1-2 mM) and their contribution will be minimal to the over metabolism of 5-HMF.

- 5-HMF has no extrahepatic metabolism.

Extraheptic metabolism was not indicated by the reported studies. In addition, most of the drugs in the market do not undergo hepatic extraction.

- Fraction unbound of 5-HMF in plasma (f_u)= 1.

The hydrophilic 5-HMF structure supports the assumption of insignificant unbound fraction. Moreover, it was reported that binding to hemoglobin was not affected in the presence or absence of plasma protein (Abdulmalik 2005).

The hepatic extraction ratio (ER_{hep}) was estimated using the well-stirred model as shown in Equation 4-5 involving the hepatic blood flow (Q_{hep}):

$$ER_{hep} = \frac{f_u \times CL_{int}}{Q_{hep} + f_u \times CL_{int}} \ldots\ldots\ldots\

– Distribution along total body water compartment (as ethanol), i.e., Vd=0.6 l/kg in all species.

This assumption was based on the small, neutral, and hydrophilic structure of 5-HMF, as discussed above, and its similarity to ethanol structure.

ER_{hep} was used in the calculation of oral bioavailability (F_{oral}) as per Equation 4-7.

$$F_{oral} = 1 - ER_{hep} \quad \text{Equation } 4-7$$

The elimination half-life ($t_{1/2}$) was calculated according to Equation 4-8:

$$t_{1/2} = \frac{0.693 \times Vdss}{CL_{hep}} \quad \text{Equation } 4-8$$

The predicted 5-HMF elimination half-life was then compared to the half-life reported in or extrapolated from *in-vivo* studies. The *in-vitro-in-vivo* prediction accuracy was evaluated through calculating the ratio of the predicted value to the observed value.

In addition, 5-HMF AUC_{∞} was estimated after oral dosing using Equation 4-9 that involves the oral bioavailability and hepatic clearance assuming the equivalency of the latter to the total clearance.

$$AUC_{\infty} = \frac{F_{oral} \times Dose}{CL_{tot}} \quad \text{Equation } 4-9$$

The above equation was used in predicting the AUC after 100 mg/kg oral dose administered in mice. Then, this value was compared to the estimated value from *in-vivo* study reported by Abdulmalik and co-workers. Moreover, the predictions were performed for the AUC after oral administration of 5-HMF for the First-Time in Man (FTIM) Study in a dose-escalating study with proposed doses (100-10,000 mg).

4.2.9 Detection of HMFA in Human Hepatic Cytosol

Cytosolic protein, NAD^+ cofactor, and 5-HMF at 0.8 and 3.2 mM in Tris buffer (pH 7.5) were mixed at a final volume of 0.2 ml. The reaction was incubated at 36.5±1 °C between 20-80 minutes. The reaction was stopped by the addition of 0.1 ml ice-cold acetonitrile. Then, 0.15 ml of the mixture was further diluted with 0.65 ml ice-cold water and was subject to HPLC analysis, as described in Chapter 3.

4.3 Results

Upon incubation of the selective substrates of ALDH and ADH enzymes, ethanol, DN, and acetaldehyde with human hepatic cytosol, an increase in the absorbance at 340 nm was observed. This increase was expected due to the production of NADH in conjunction with NADH-dependent oxidation of these substrates by ADH and ALDH enzymes. Initial velocities (v_i) were estimated from the slope of the linear portion representing the pseudo-zero order increase in the absorbance for each concentration within a ten-minute frame during spectrophotometric monitoring. These initial velocities, when plotted against concentration resulted in a hyperbolic relationship that was modeled by the Michaelis Menten kinetics by non-linear regression, as shown in Figures 4-2, 4-3, and 4-4 for ethanol, DN, acetaldehyde.

An increase in the absorption was observed when 5-HMF was incubated with human hepatic cytosol and it was modeled by non-linear regression, as shown Figure 4-5. The maximum metabolic capacity and enzyme affinity are summarized in Table 4-6 along with the *in-vitro* intrinsic clearance. The *in-vitro* intrinsic clearance is expressed in µl/min/mg cytosolic protein.

The metabolic activity of ethanol in human hepatic cytosol was inhibited to a higher extent by 4-methylpyrazole than by disulfiram, as demonstrated in Figures 4-6 and 4-7. On the other hand, Figure 4-8 shows that acetaldehyde metabolism was inhibited to a great extent by disulfiram. 5-HMF metabolism was inhibited by both 4-methylpyrazole and disulfiram, However, the inhibition was larger with disulfiram as shown in Figures 4-9 and 4-10. The increase in the absorbance diminished in the presence of the two inhibitors. The results of the inhibition studies are listed in Tables 4-7, 4-8, and 4-9.

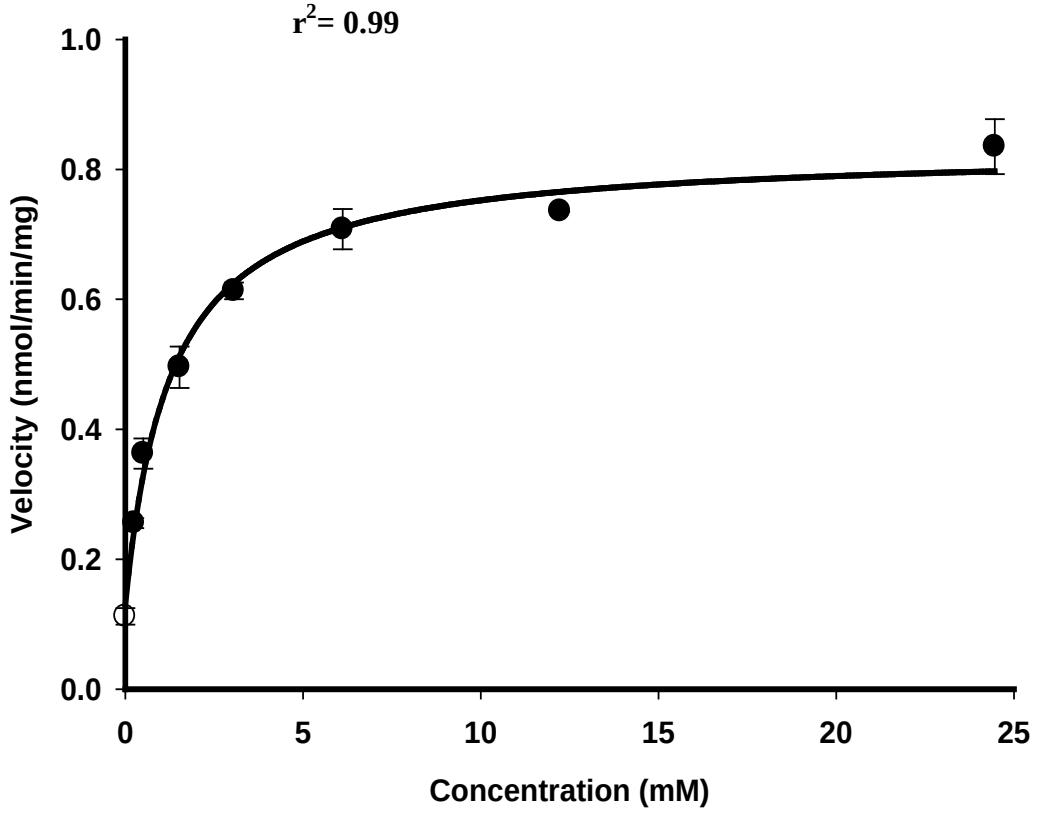

Figure 4-2. Concentration-dependent human hepatic cytosol metabolism of ethanol.

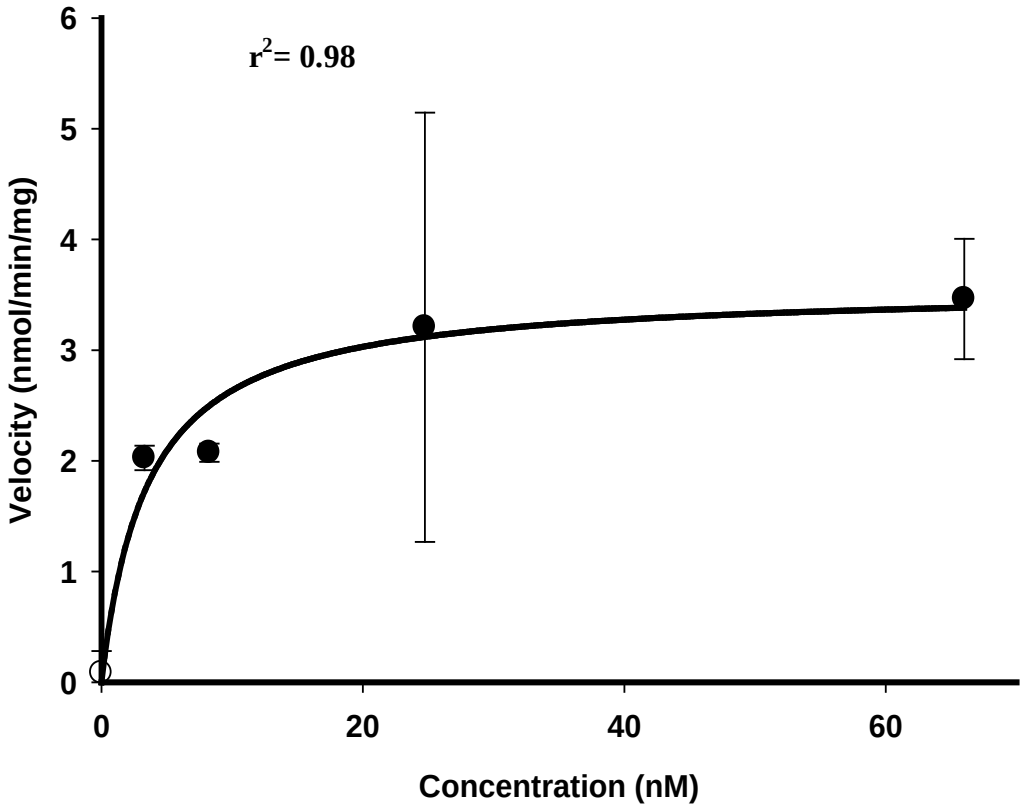

Figure 4-3. Concentration-dependent human hepatic cytosol metabolism of DN.

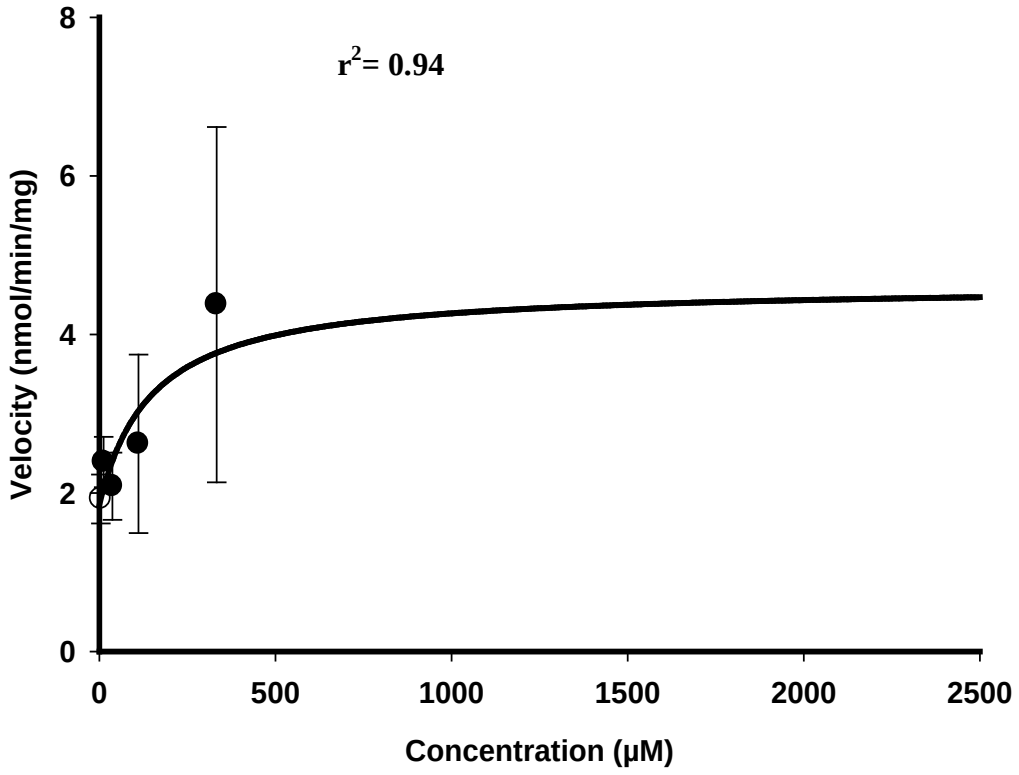

Figure 4-4. Concentration-dependent human hepatic cytosol metabolism of acetaldehyde.

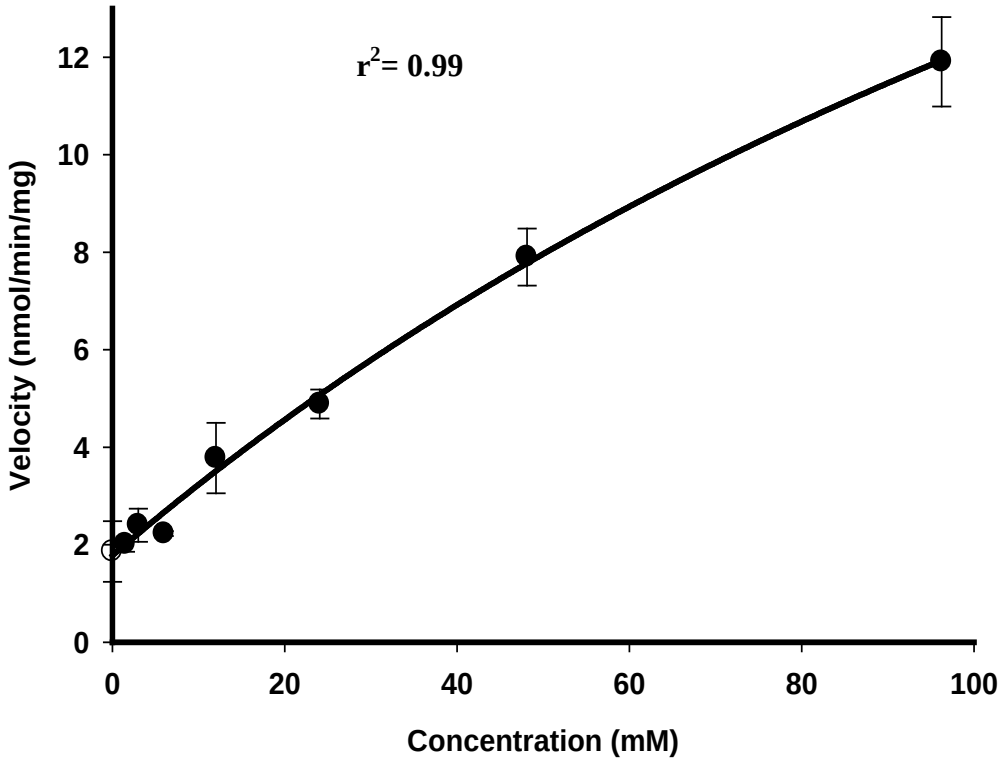

Figure 4-5. Concentration-dependent human hepatic cytosol metabolism of 5-HMF.

Table 4-6. Final Michaelis Menten metabolic parameter estimates (SE) for various substrates in human hepatic cytosol.

Substrate	Ethanol	DN	Acetaldehyde	5-HMF
v_0 (nmol/min/mg)	0.13 (0.03)	-	1.8 (0.4)	1.78 (0.15)
v_{max} (nmol/min/mg)	0.70 (0.03)	3.6 (0.3)	2.8 (0.6)	33.2 (8.0)
K_m (µM)	1.27 (0.23).10^3	3.5 (1.4).10^{-3}	149 (123)	218 (74).10^3
$CL_{int}^{in\text{-}vitro}$ (µl/min/mg)	0.55	1.0 X 10^6	18.8	0.15

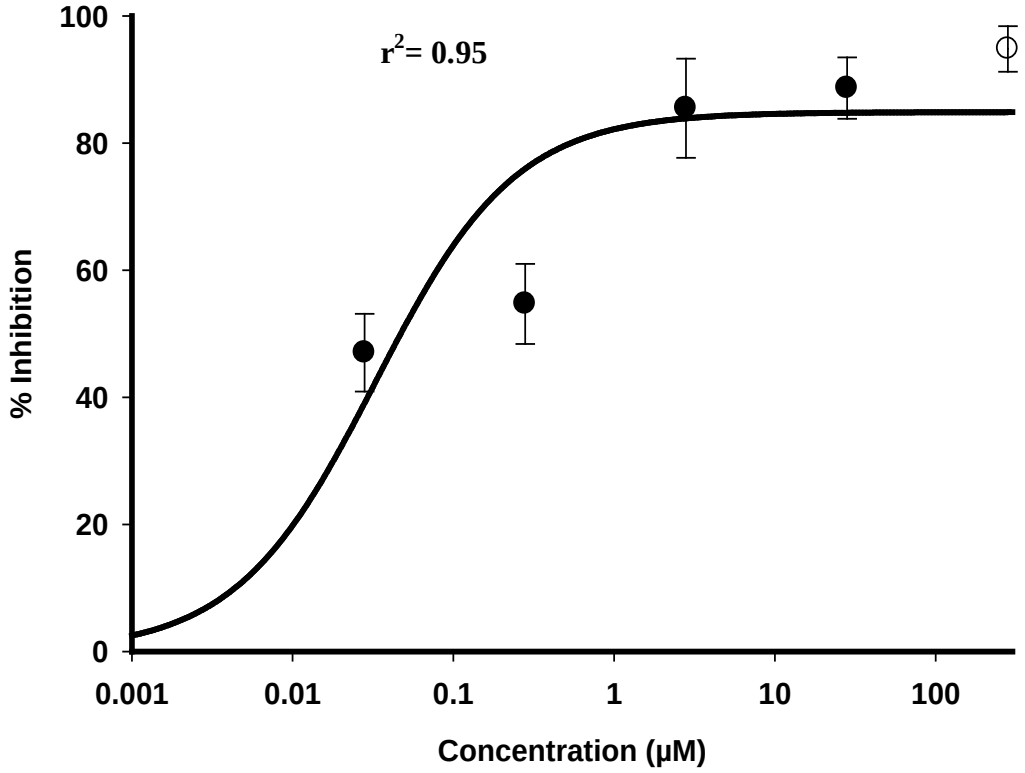

Figure 4-6. Inhibition of NADH-mediated human hepatic cytosol metabolism of ethanol by 4-methylpyrazole.

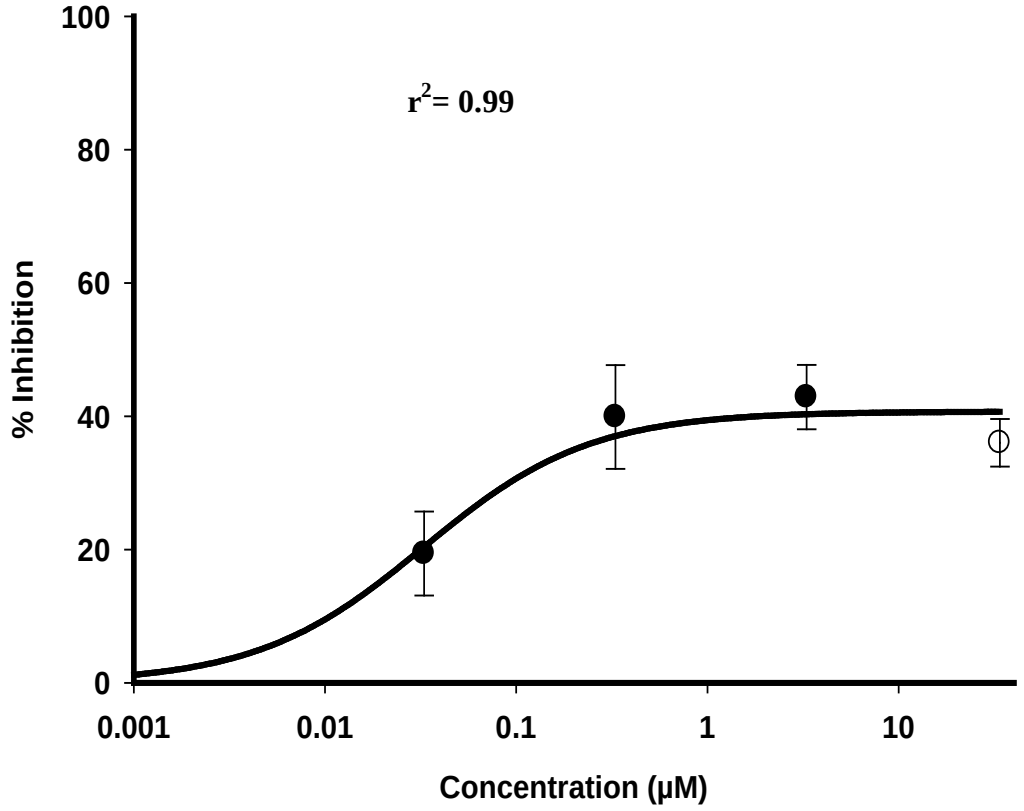

Figure 4-7. Inhibition of NADH-mediated human hepatic cytosol metabolism of ethanol by disulfiram.

Table 4-7. Inhibition metabolism of NADH-mediated human hepatic cytosol of ethanol by 4-methylpyrazole and disulfiram (SE).

	4-Methylpyrazole	**Disulfiram**
Maximum inhibition (%)	84.9 (6.9)	40.7 (2.3)

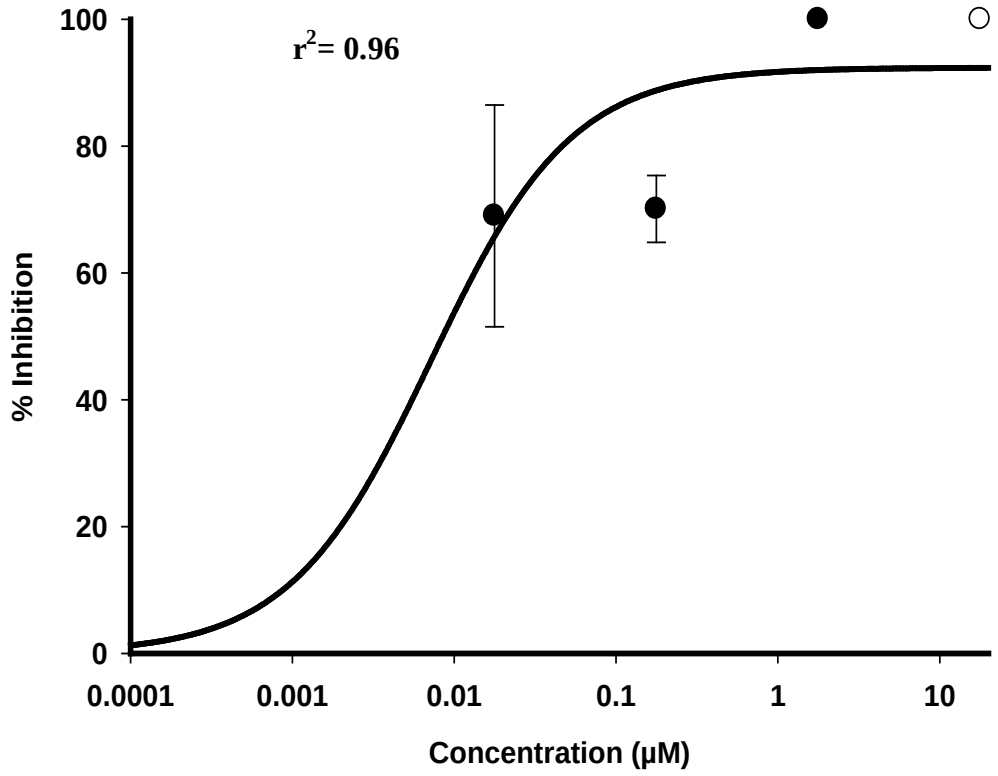

Figure 4-8. Inhibition of NADH-mediated human hepatic cytosol metabolism of acetaldehyde by disulfiram.

Table 4-8. Inhibition of NADH-mediated human hepatic cytosol metabolism of acetaldehyde by disulfiram (SE).

	Disulfiram
Maximum inhibition (%)	92.4 (7.8)

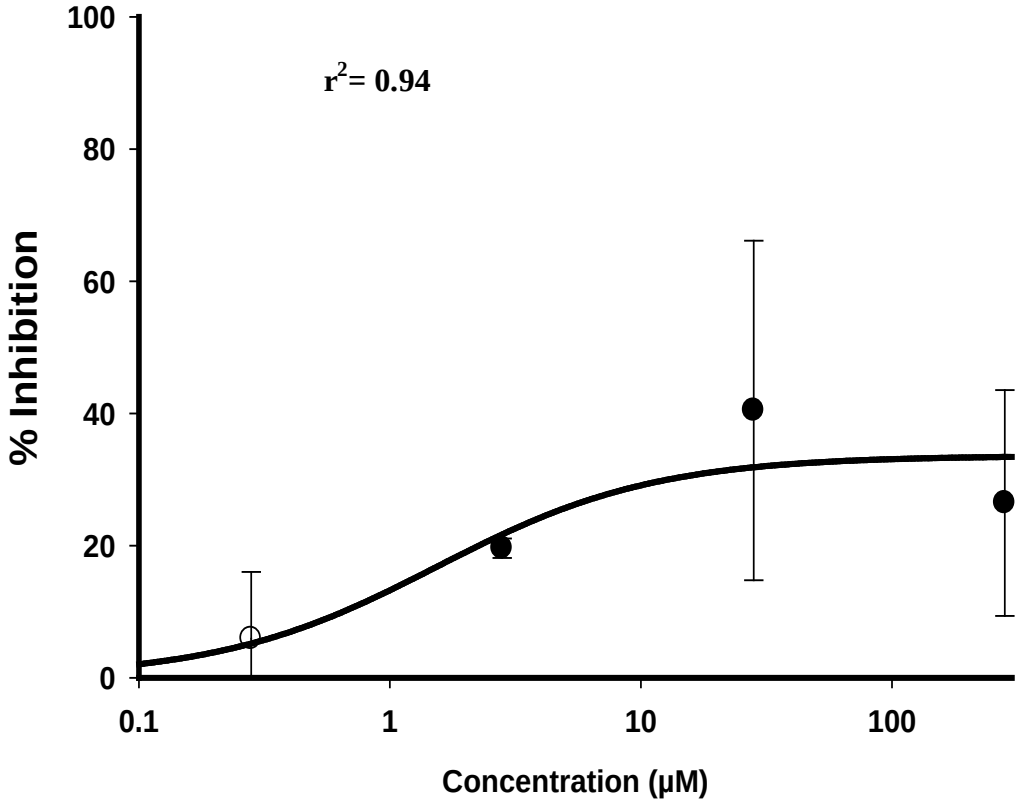

Figure 4-9. Inhibition of NADH-mediated human hepatic cytosol metabolism of 5-HMF by 4-methylpyrazole.

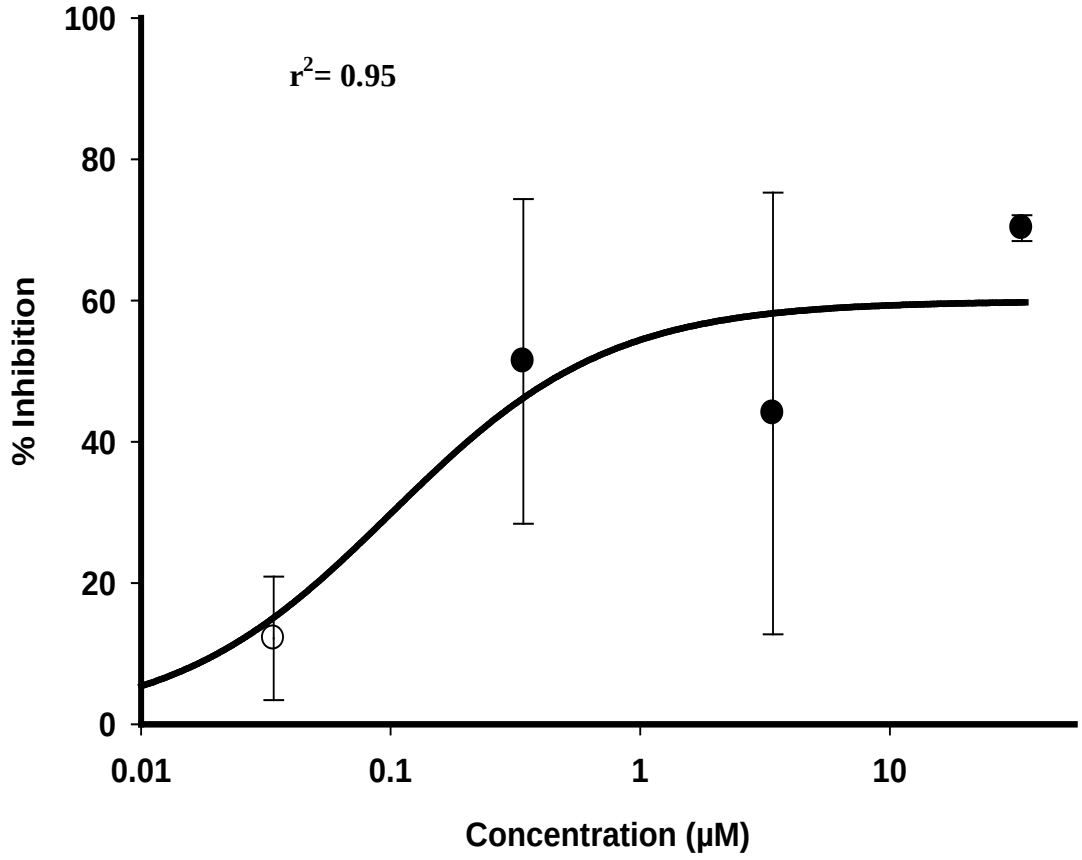

Figure 4-10. Inhibition of NADH-mediated human hepatic cytosol metabolism of 5-HMF by disulfiram.

.

Table 4-9. Inhibition of NADH-mediated human hepatic cytosol of 5-HMF metabolism by 4-methylpyrazole and disulfiram (SE).

	4-Methylpyrazole	**Disulfiram**
Maximum inhibition (%)	33.6 (5.1)	59.9 (7.8)

The increase in the absorption was also observed when 5-HMF was incubated in mouse, rat, and dog hepatic cytosol: The resulting Michaelis Menten curves for 5-HMF in different species hepatic cytosol are shown in Figures 4-11, 4-12, 4-13, and the parameters are summarized in Table 4-10. The estimated v_0 in the metabolism of 5-HMF in the mouse and human hepatic cytosol might indicate the involvement of high affinity/low capacity enzymes in the metabolism of 5-HMF. In addition, the corresponding linearization graphs are shown in Figures 4-14, 4-15, 4-16, 4-17, and 4-18 for 5-HMF metabolism in mouse, rat, dog, and human hepatic cytosol along with ethanol in human hepatic cytosol.

The final IVIVE results are summarized in Table 4-11, including $CL_{int}^{in\text{-}vivo}$, CL_{met}, ER_{hep}, F_{oral}, and $t_{1/2}$. In addition, a half-life comparison between that predicted by IVIVE and that obtained from *in-vivo* studies along with the projected AUC(s) after oral administration of 5-HMF for the First-Time in Man (FTIM) Study are shown in Tables 4-12 and 4-13.

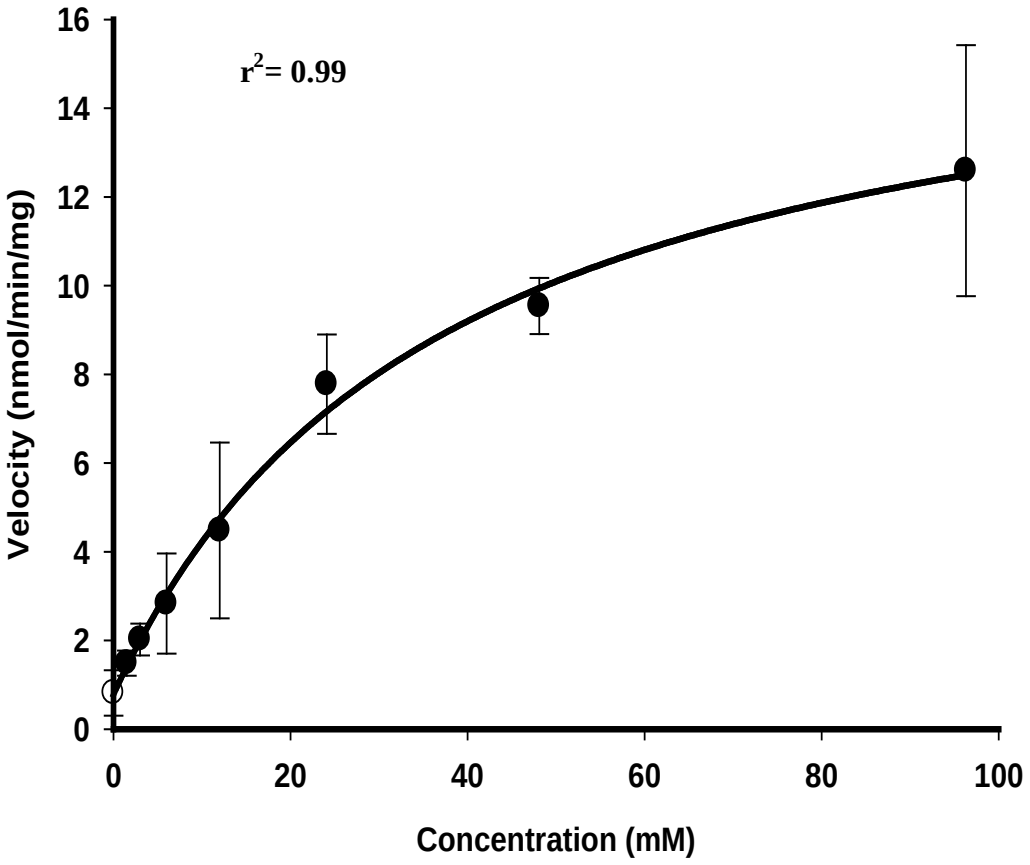

Figure 4-11. Concentration-dependent metabolism of 5-HMF in mouse hepatic cytosol.

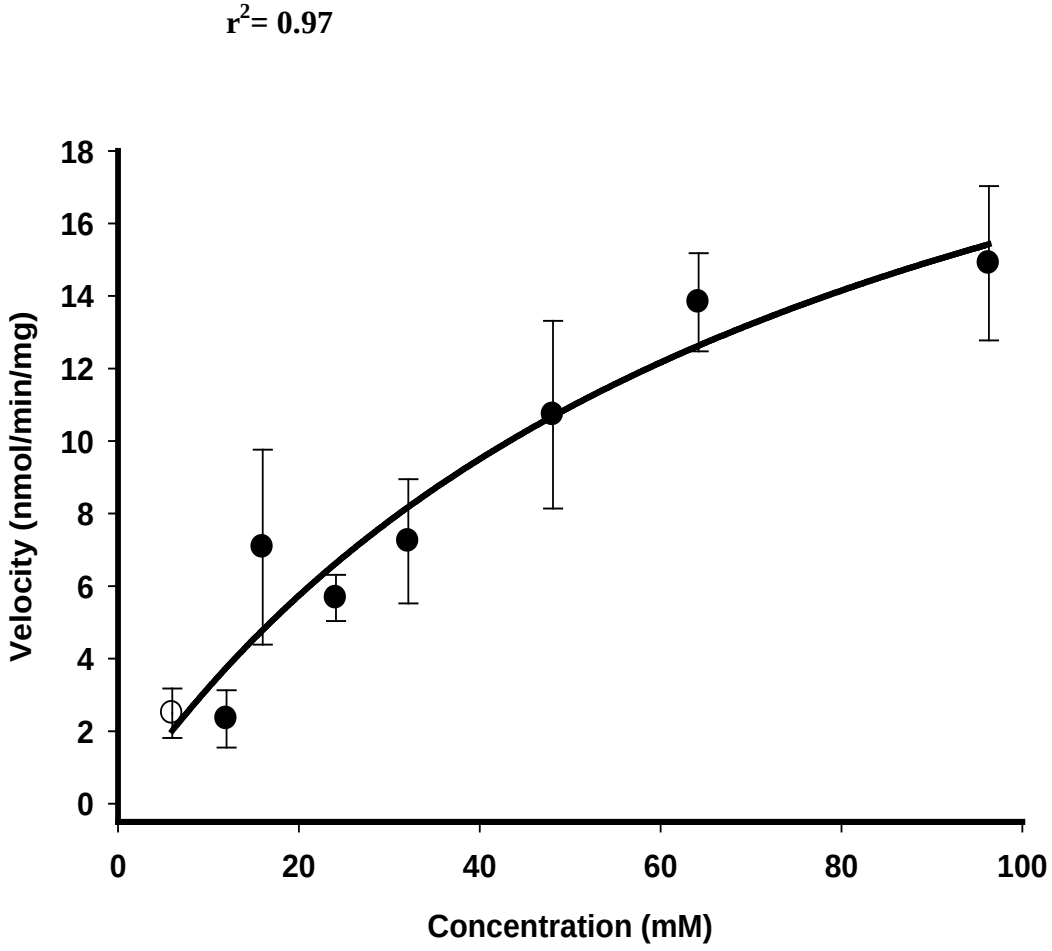

Figure 4-12. Concentration-dependent metabolism of 5-HMF in rat hepatic cytosol.

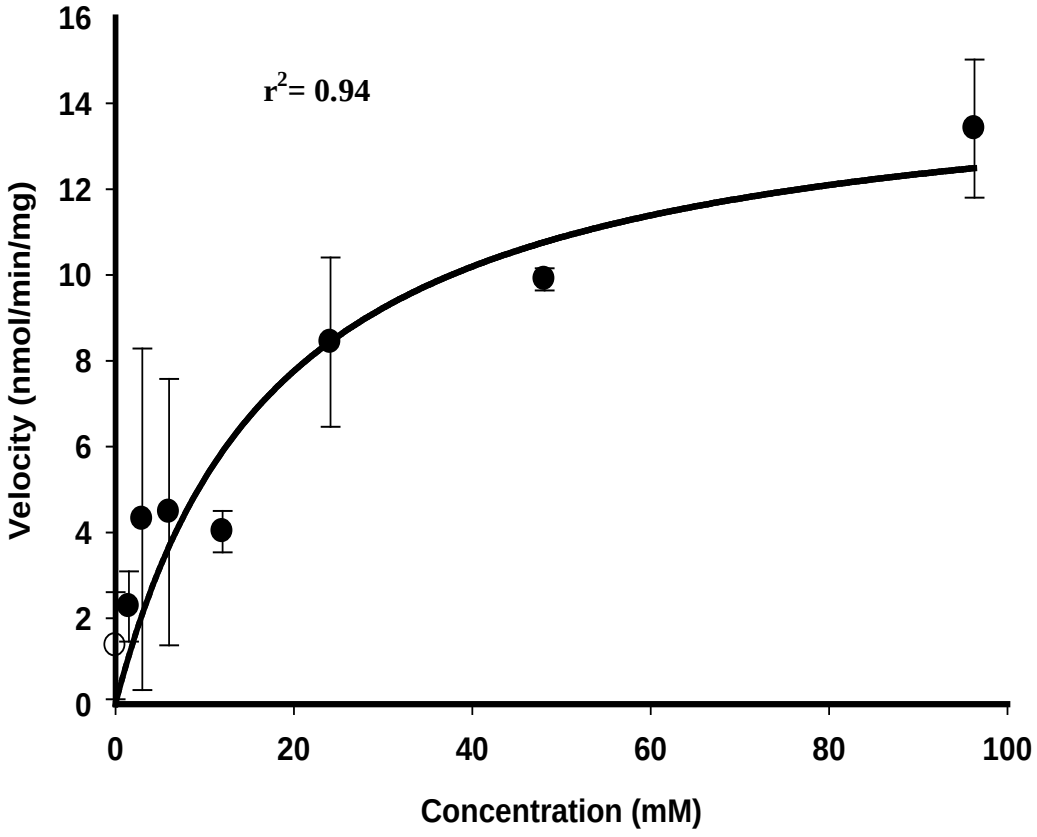

Figure 4-13. Concentration-dependent metabolism of 5-HMF in dog hepatic cytosol.

Table 4-10. Final Michaelis Menten metabolic parameter estimates (SE) for 5-HMF in hepatic cytosol from various animal species.

	Mouse	**Rat**	**Dog**	**Human**
v_0 (nmol/min/mg)	0.78 (0.24)			1.78 (0.15)
v_{max} (nmol/min/mg)	16.2 (1.0)	27.7 (6.8)	14.9 (2.3)	33.2 (8.0)
K_m (mM)	37.1 (6.3)	76.6 (32.4)	18.3 (8.0)	218 (74)
$CL_{int}^{in\text{-}vitro}$ (µl/min/mg)	0.44	0.36	0.81	0.15

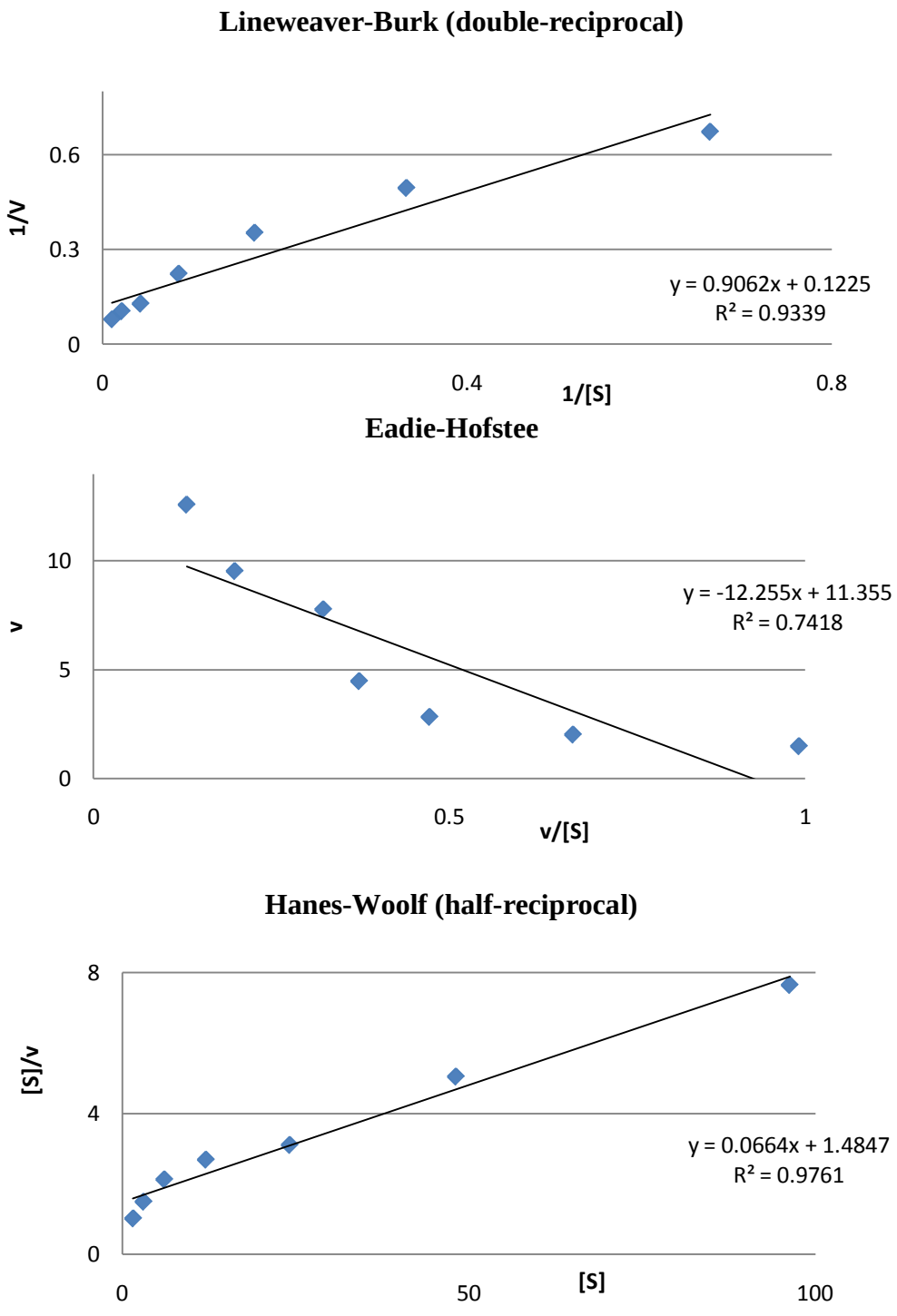

Figure 4-14. Linearization graphs for concentration-dependent metabolism of 5-HMF in mouse hepatic cytosol.

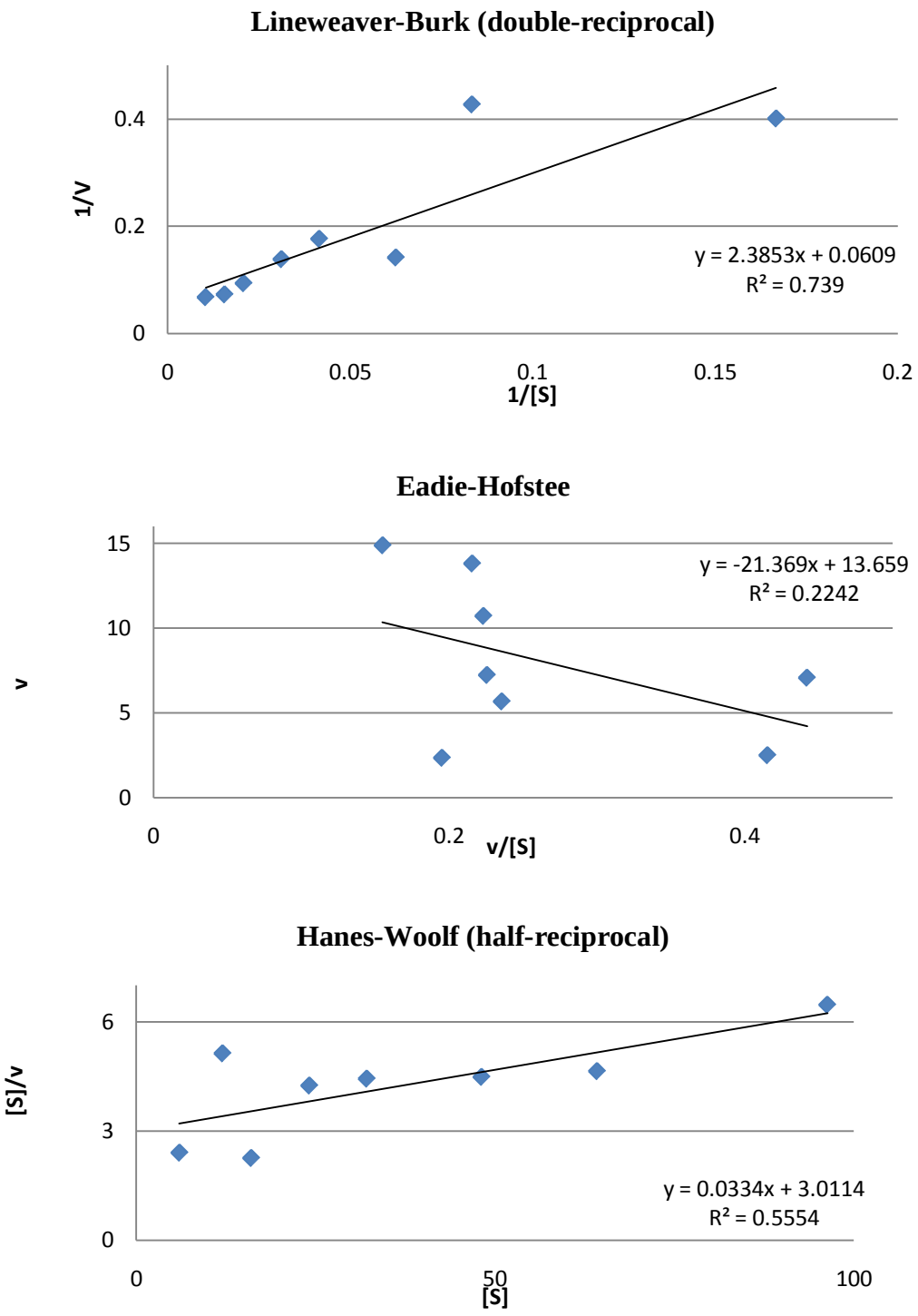

Figure 4-15. Linearization graphs for concentration-dependent metabolism of 5-HMF in rat hepatic cytosol.

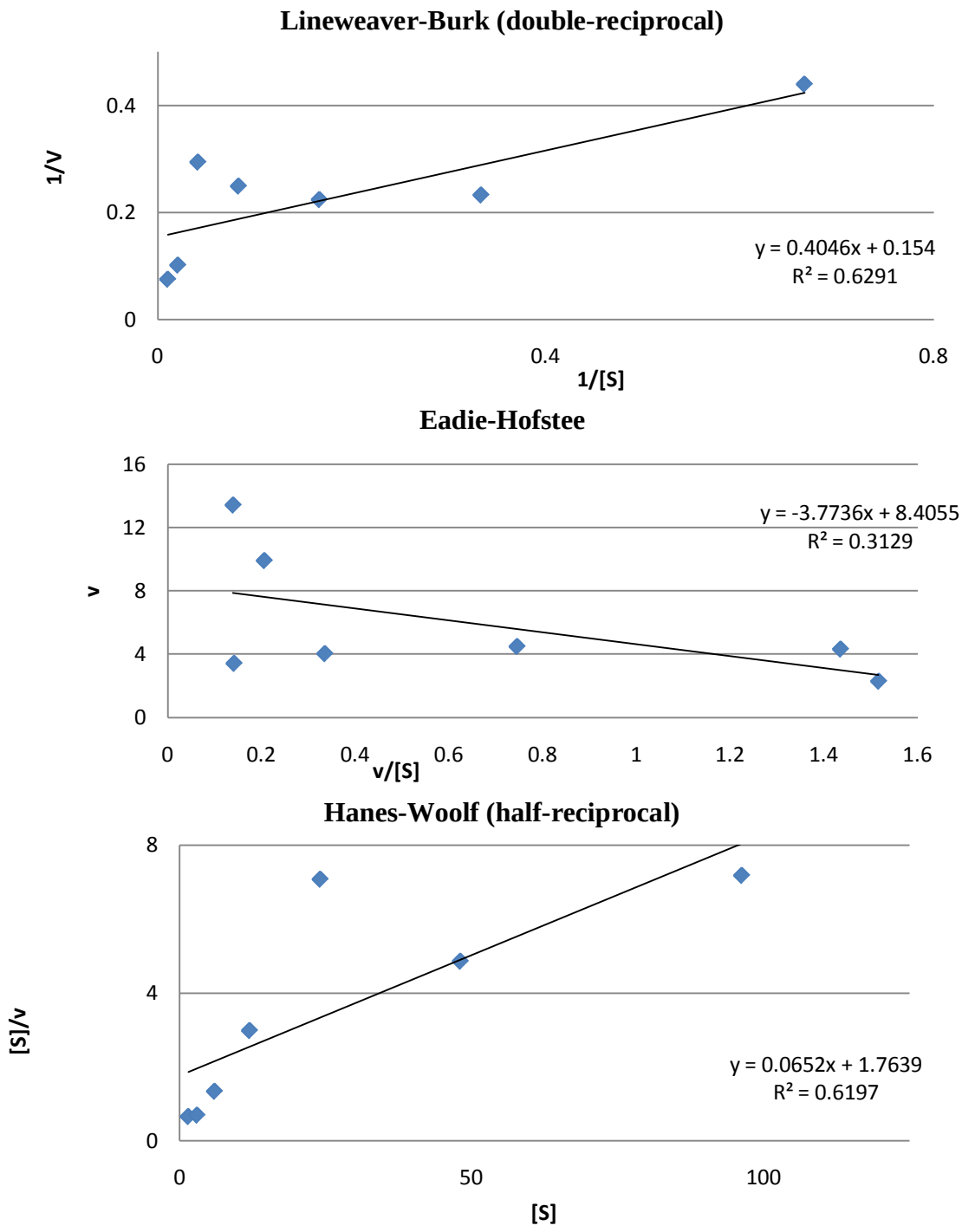

Figure 4-16. Linearization graphs for concentration-dependent metabolism of 5-HMF in dog hepatic cytosol.

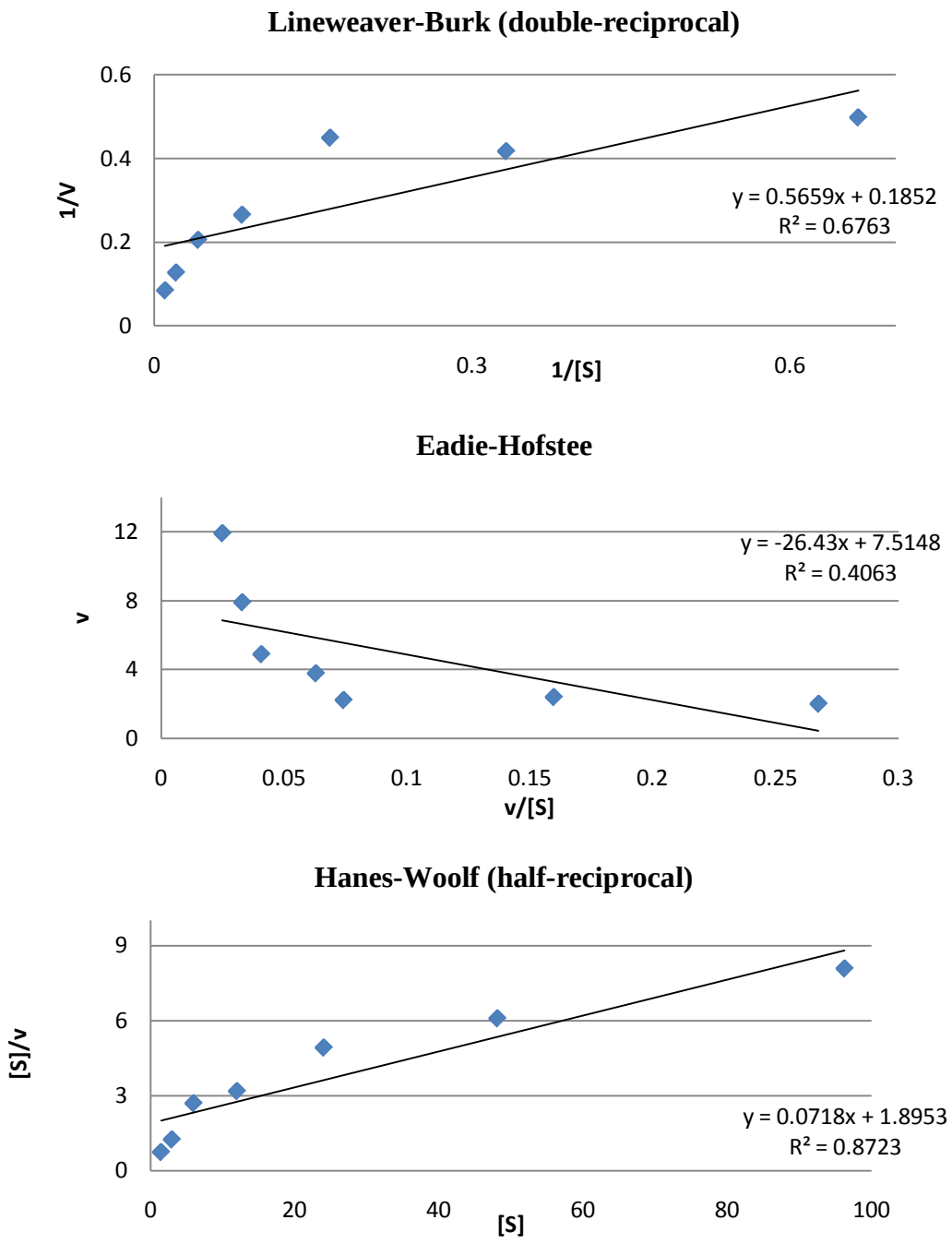

Figure 4-17. Linearization graphs for Concentration-dependent metabolism of 5-HMF in human hepatic cytosol.

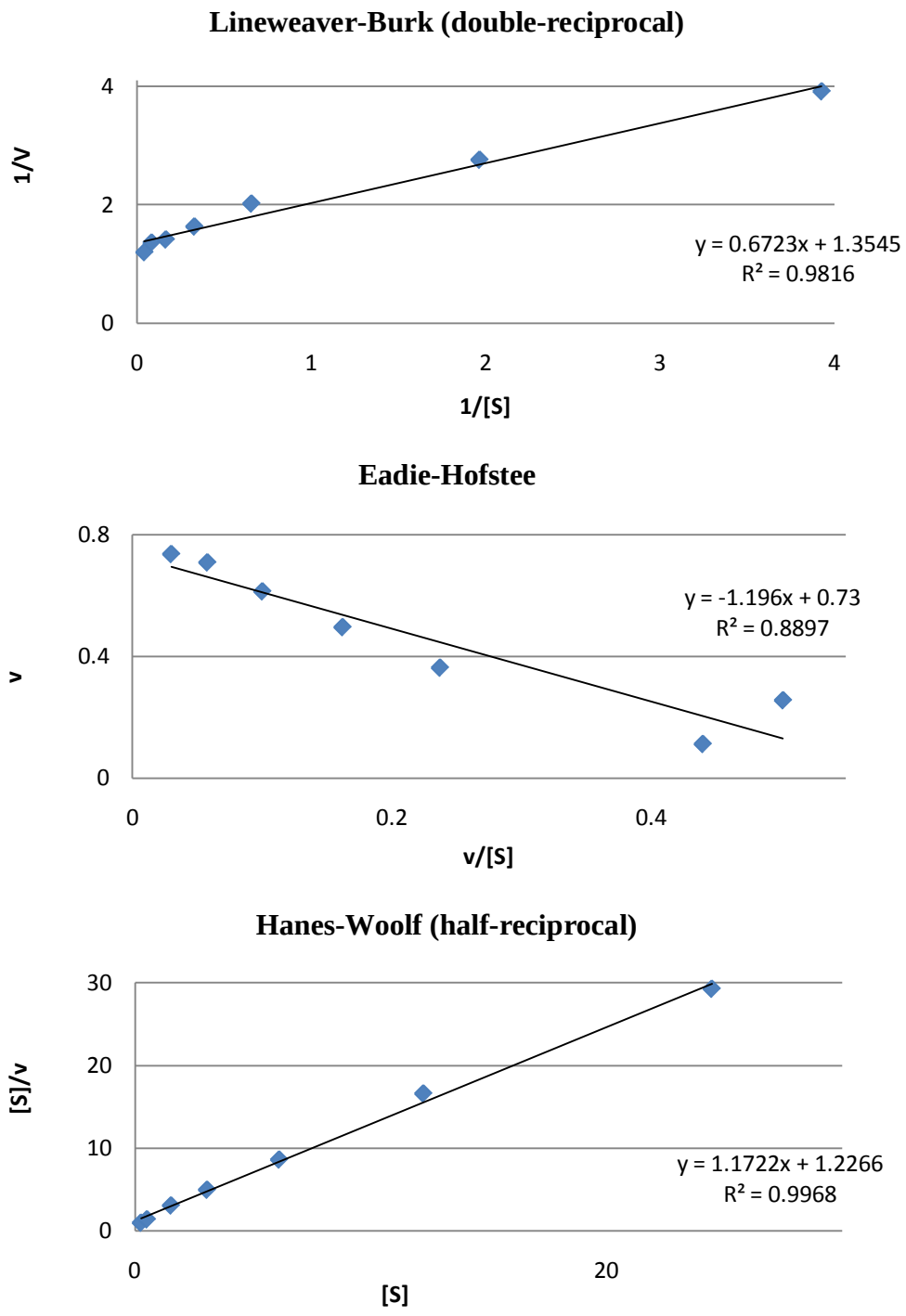

Figure 4-18. Linearization graphs for concentration-dependent metabolism of ethanol in human hepatic cytosol.

Table 4-11. IVIVE for 5-HMF in mouse, rat, dog, and human using physiological variables listed in Table 4-5.

	CL_{int} (ml/min)	CL_{int} (ml/min/kg)	CL_{hep} (ml/min)	CL_{hep} (ml/min/kg)	ER_{hep} (%)	F_{oral} (%)	$t_{1/2}$ (hour)
Mouse	0.08	2.3	0.08	2.3	0.8	99	3.1
Rat	0.49	2.0	0.48	1.9	2.1	98	3.6
Dog	17.4	1.7	16.5	1.7	5.0	95	4.2
Human	12.3	0.18	12.2	0.17	0.8	99	39.7

Table 4-12. Comparison of IVIVE predictions for 5-HMF with the reported values.

	IVIVE Predictions		**Literature**				
	$t_{1/2}$ (hr)	**AUC (mg/ml*min)**	**$t_{1/2}$ (hr)**	**AUC (mg/ml*min)**	**Dose**	**Species**	**Reference**
Mouse	3.1	44	1.5	26	100 mg/kg orally	Transgenic mice	(Abdulmalik 2005)
Dog	4.2		2.1		397 mg/kg infused over an hour	Male beagles	(Klimmek 1978)
Human	39.7		1.2 (for HMFA metabolite)		7.5 mg/kg of 5-HMF in dried plum juice	65-70 yrs old women	(Prior 2006)

Table 4-13. Predicted AUC∞ after oral administration of 5-HMF FTIM study.

Dose (mg)	Projected AUC_{∞} (mg/ml.min)
100	8
300	24
1000	81
3000	244
6000	487
10000	812

HMFA was detected in human cytosol after incubation of 5-HMF at different concentrations for different periods. Unfortunately, the peak of HMFA overlapped with a peak present in the blank, as discussed in Chapter 3. Nevertheless, it is demonstrated in Figures 4-19, 4-20, 4-21, 4-22, and 4-23 that the peak height increased with the increase in the concentration of 5-HMF and with the increase in the incubation period indicating the formation of HMFA in human hepatic cytosol after the addition of NAD^+.

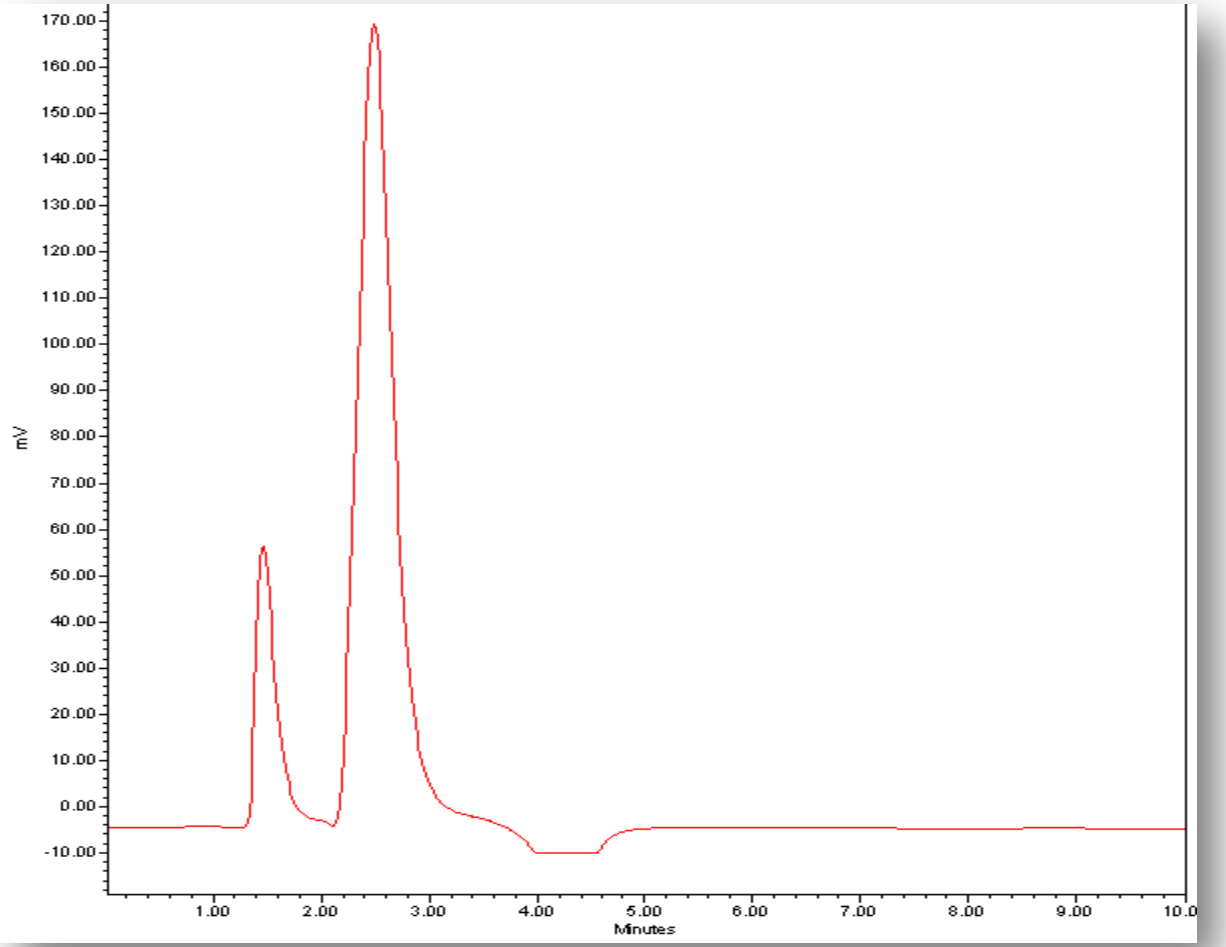

Figure 4-19. HPLC chromatogram for blank human hepatic cytosol, no 5-HMF added.

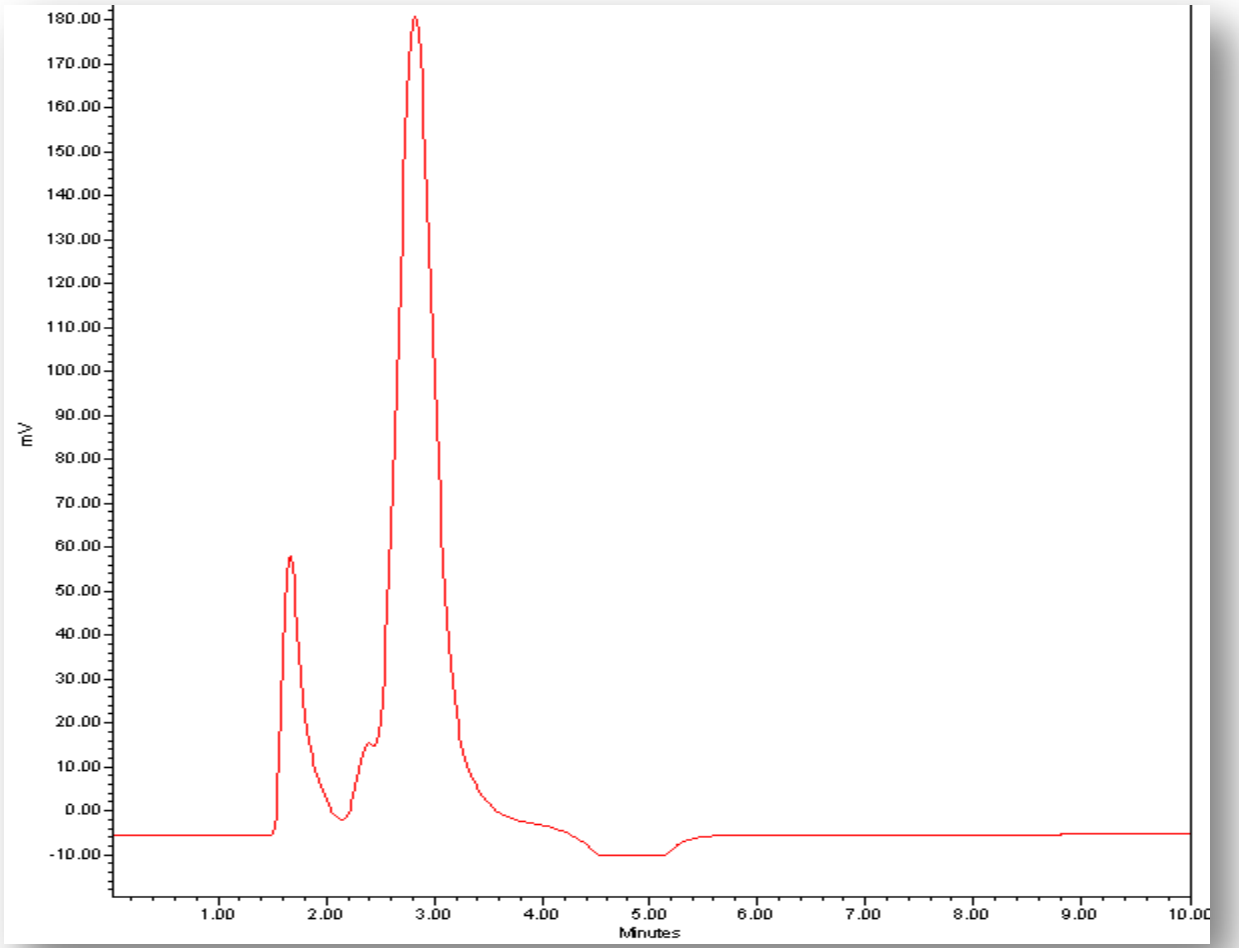

Figure 4-20. HPLC chromatogram for 0.8 mM of 5-HMF incubated in human hepatic cytosol for 20 minutes.

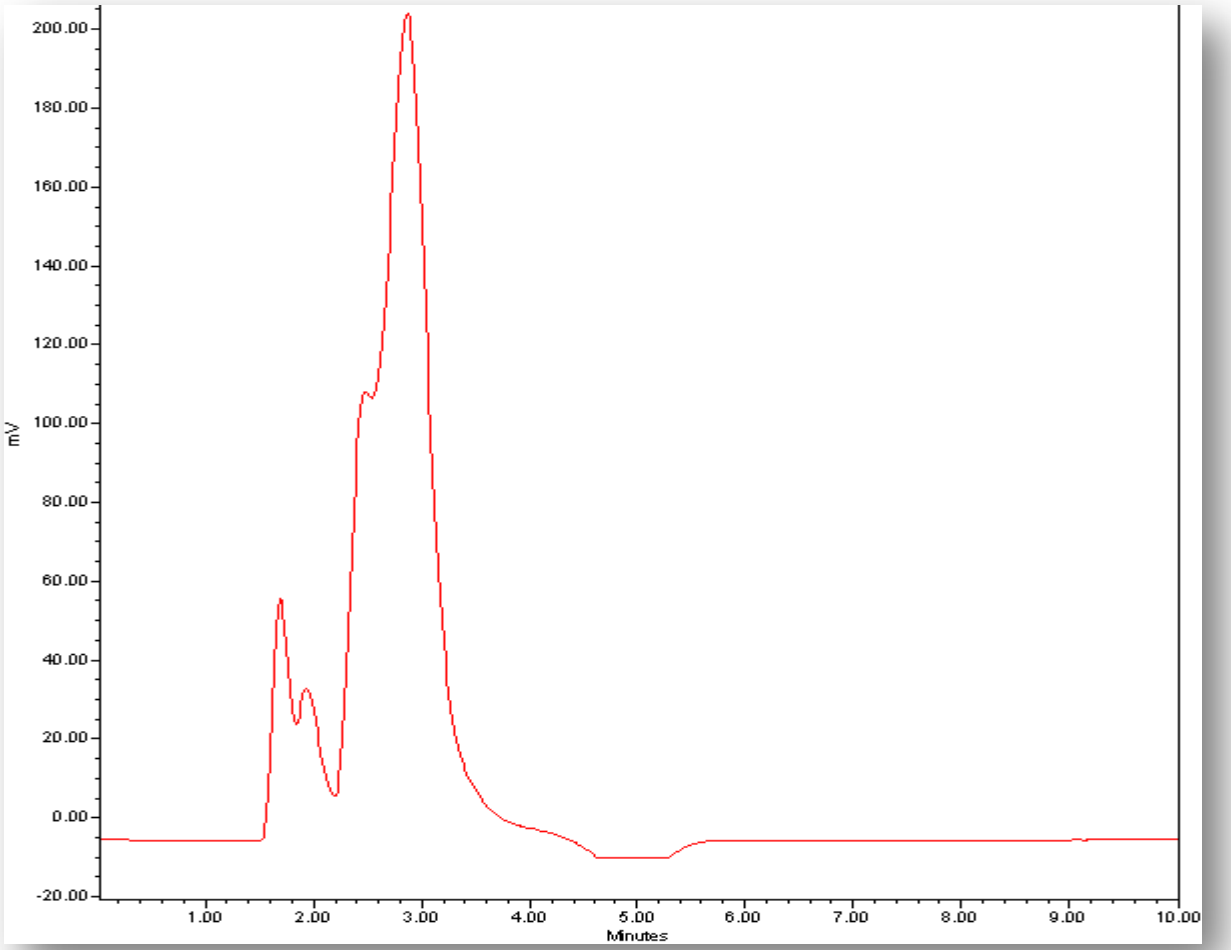

Figure 4-21. HPLC chromatogram for 0.8 mM 5-HMF incubated in human hepatic cytosol for 40 minutes.

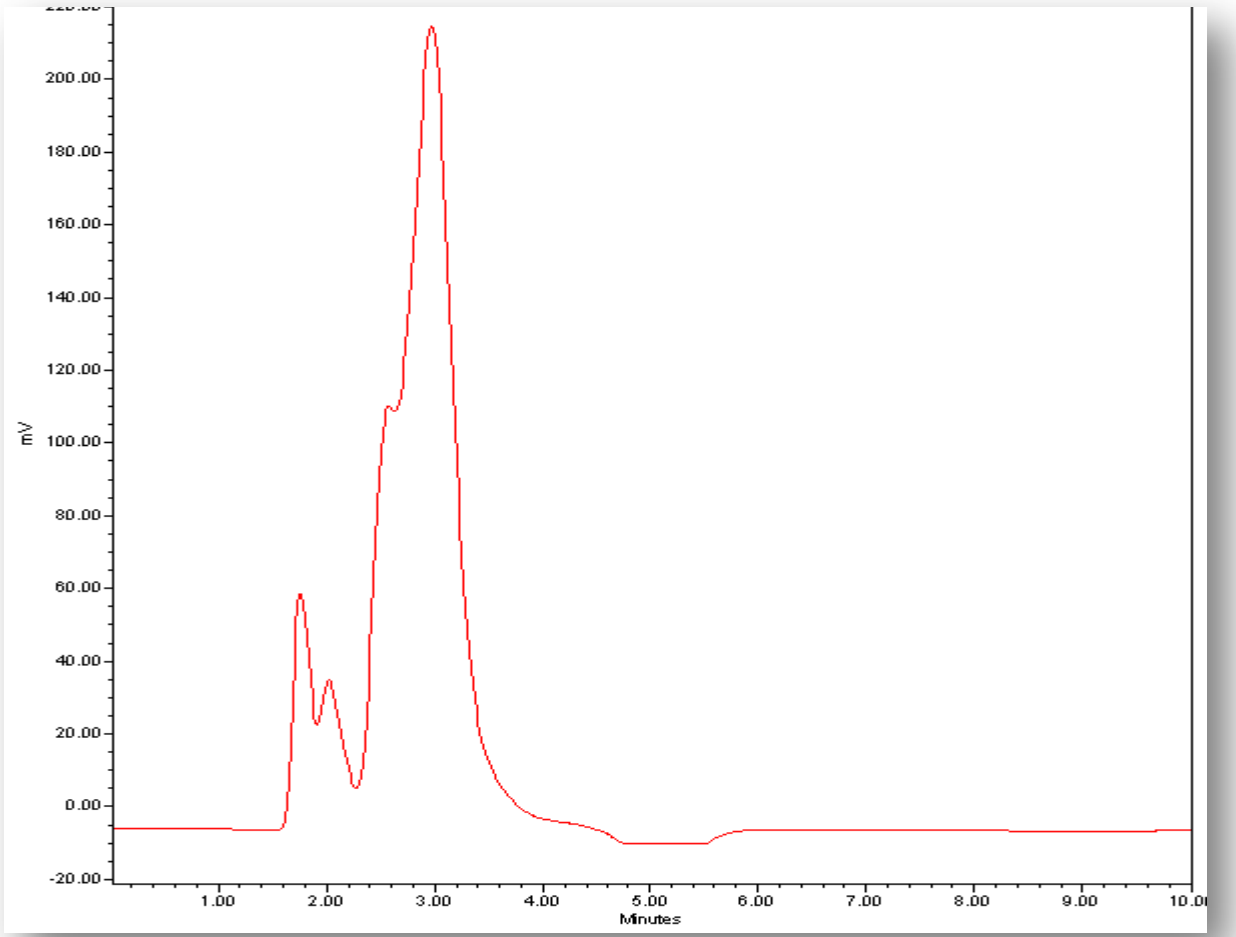

Figure 4-22. HPLC chromatogram for 3.2 mM 5-HMF incubated in human hepatic cytosol for 20 minutes.

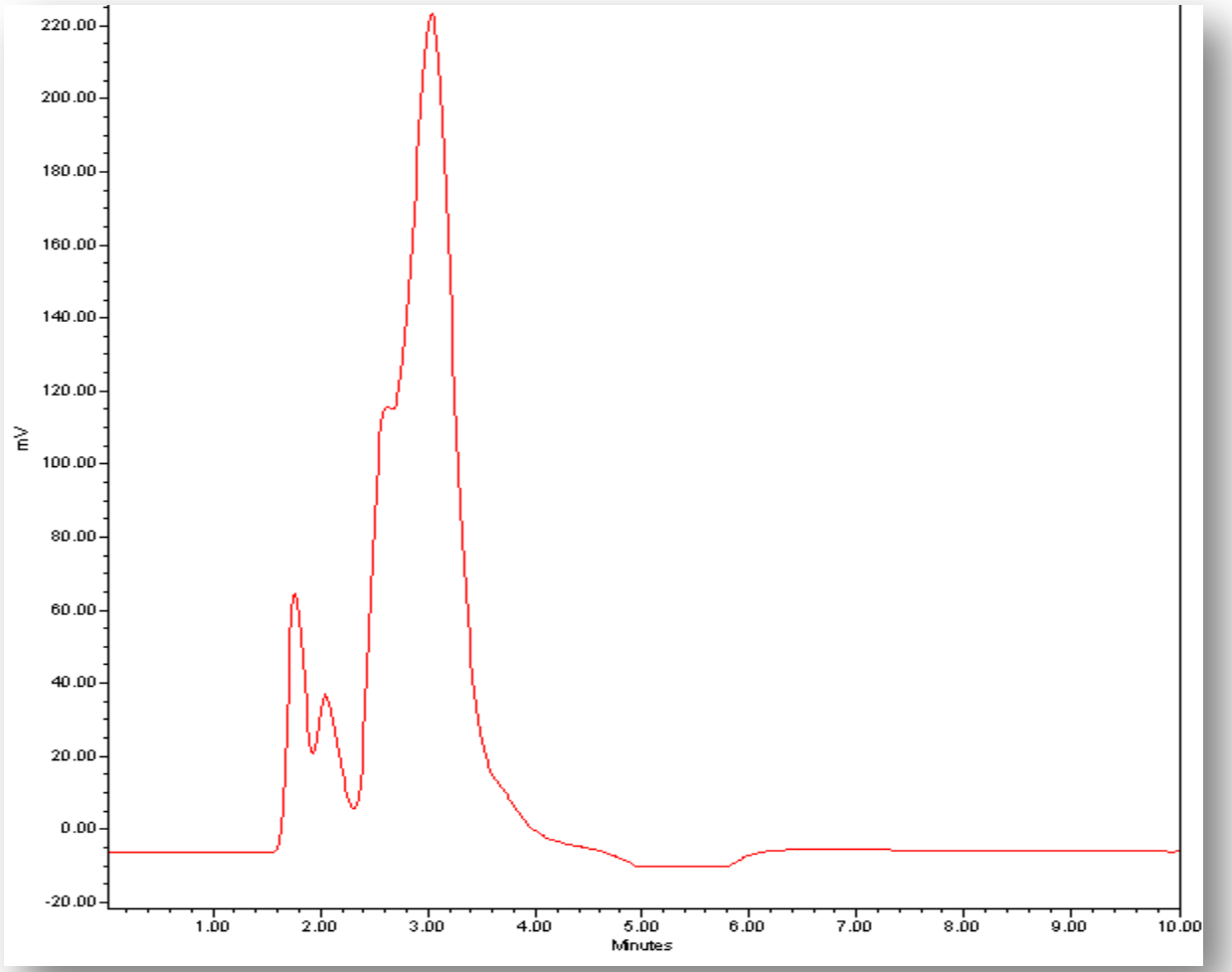

Figure 4-23. HPLC chromatogram for 3.2 mM 5-HMF incubated in human hepatic cytosol for 80 minutes.

4.4 Discussion and Conclusions

The NAD^+-dependent oxidation of all ADH/ALDH model-substrates (ethanol, acetaldehyde, and DN) in human hepatic cytosol were adequately characterized by Michaelis Menten kinetics as indicated by the goodness of fit of the non-linear regression. This validated the hepatic cytosolic system and confirmed the presence of active ADH and ALDH enzymes. The estimated K_m values for all these substrates was similar to these reported previously in the literature, as listed in Table 4.2. Similarly, the NAD^+-dependent oxidation of 5-HMF in human hepatic cytosol was described by Michaelis Menten kinetics, indicating 5-HMF metabolism by ALDH and ADH enzymes. This was further supported by the observed formation of the metabolite, HMFA, in human hepatic cytosol.

Overall, low-affinity (K_m: 218 mM)/high capacity (v_{max}: 33.2 nmol/min/mg) metabolism was observed for 5-HMF relative to ethanol (1.3 mM/0.7 nmoles/min/mg) and DN and acetaldehyde (3.5 nM/3.6 nmol/min/mg and 149 μM/2.8 nmol/min/mg). However, the K_m estimation for 5-HMF is limited by the fact that 5-HMF concentrations greater than K_m could not be achieved experimentally since the UV absorption saturated the instrument and 5-HMF solubility was exceeded.

The observed increase in the absorbance is a result of NADH production. Since this a common product for ALDH and ADH, the following reactions might be involved:

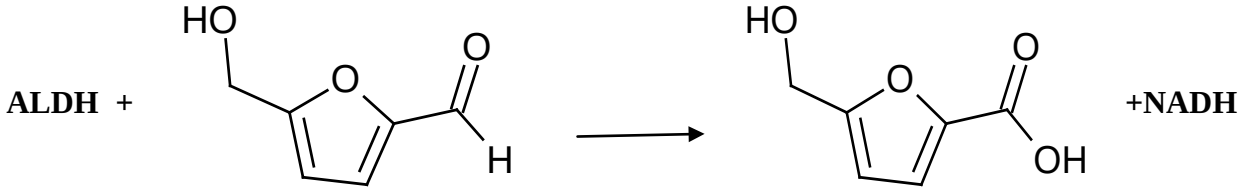

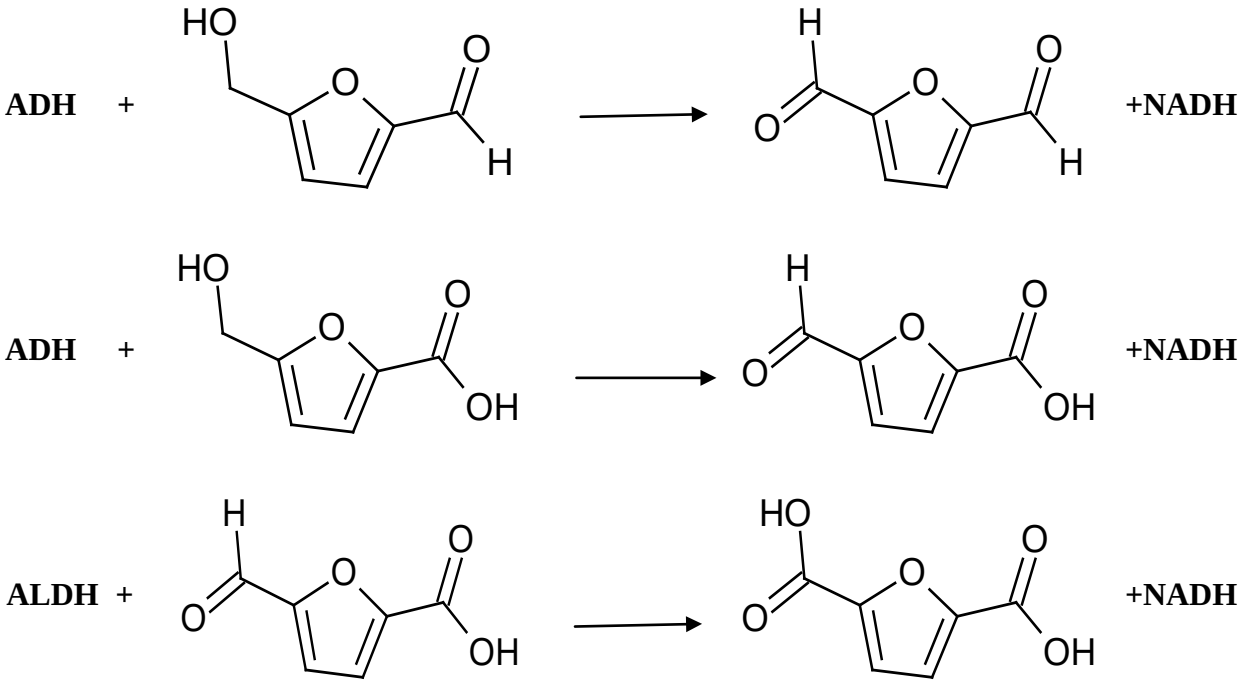

The effect of the selective ALDH and ADH inhibitors was demonstrated by the inhibition of ethanol and acetaldehyde metabolism by 4-methylpyrazole and disulfiram, respectively, ethanol metabolism by ADH was inhibited mainly by 4-methylpyrazole, while acetaldehyde metabolism by ALDH was inhibited to a large extent by disulfiram.

Relative to the control, the activity of 5-HMF in the presence of disulfiram declined to 40% of the control activity, indicating a significant role of ALDH enzyme in its metabolism. On the other hand, 5-HMF metabolism was inhibited to a lesser extent (33%) by 4-methylpyrazole. This suggests that ALDH-mediated oxidation of 5-HMF to HMFA (a human metabolite identified *in-vivo*) is the major route of hepatic metabolism.

In concordance with the conclusion of ADH and ALDH-mediated oxidation of 5-HMF, Modig and co-workers investigated 5-HMF in isolated yeast ADH and ALDH enzymes (Modig 2002). This study involved 5-HMF concentrations up to 32 mM, which is lower than that used in

this research, and studied NAD^+ conversion into NADH. However, the investigators were interested in 5-HMF interaction with another ALDH and ADH substrate rather than the characterization of the metabolic parameters for 5-HMF (Modig 2002).

When linearization-graphing methodologies were used to fit ethanol metabolism in human hepatic cytosol and 5-HMF metabolism in different species hepatic cytosol, the best linear fits were achieved for ethanol metabolism in human hepatic cytosol and 5-HMF metabolism in mouse hepatic cytosol. The involvement of multiple enzymes in the metabolism of 5-HMF might cause the observed deviation from linearity. In our case, it is assumed that the enzyme involved are both ADH and ALDH. Furthermore, the non-linearity might be due to the inherent errors in these methods as mentioned below:

- The errors associated with small concentration are exaggerated in the Lineweaver-Burk (double-reciprocal) due to the use of concentration reciprocal on the x-axis. In addition to the aggregation of the points at the left side of the plot with high concentrations.
- The x-axis in the Eadie-Hofstee is not independent since it contains the dependent variable (velocity).

Furthermore, 5-HMF oxidative metabolism in the hepatic cytosol of mouse, rat, dog, and human was described well by Michaelis Menten kinetics, with the most precise v_{max} and K_m estimates observed in the mouse. While v_{max} values/enzyme capacity in the four animal species were relatively similar (per mg protein of hepatic cytosol), the enzyme affinity was more variable - with the highest affinity observed in the dog and the lowest in humans. This suggests involvement of ALDH and/or ADH in 5-HMF metabolism in all animal species, however, with quantitative differences in their intrinsic clearance. The highest intrinsic clearance (per kg body

weight) was predicted for the mouse (2.3 ml/min/kg), while the lowest intrinsic clearance was predicted for humans (0.18 ml/min/kg). The use of Equation 4-5 to estimate the intrinsic clearance entails the assumption of therapeutic concentrations lower than the K_m value and similarity between the substrate concentration at the enzyme site and the unbound plasma concentration (Houston 2008).

Despite the quantitative differences in the intrinsic clearance, in all animal species studied, 5-HMF is predicted to be subject to low hepatic extraction and thus to show high oral bioavailability *in-vivo*. The actual *in-vivo* oral bioavailability is unknown since no IV reference dose was administered concurrently with an oral dose.

In-vivo systemic exposure predictions (AUC and $t_{1/2}$) using the respective IVIVE parameter estimates in the mouse were within two-fold of those reported for *in-vivo* exposures after oral administration of 100 mg/kg of 5-HMF. In dogs, the IVIVE-predicted $t_{1/2}$ is approximately two-fold longer than that reported *in-vivo* after I.V. infusion of 5-HMF (397 mg/kg for 1 hr). In both cases, the IVIVE predictions may have underestimated CL_{met} for 5-HMF, possibly due to other (minor) routes of metabolism, e.g., hepatic mitochondrial oxidation. Nevertheless, the IVIVE exposure predictions were reasonable for dogs and mice.

On the other hand, the IVIVE-predicted $t_{1/2}$ for humans is more than 30-fold longer than the reported plasma $t_{1/2}$ of the (presumed) primary metabolite, HMFA after oral administration of approximately 7.5 mg/kg of 5-HMF. This major discrepancy most likely implies a significant involvement of other hepatic fractions and/or extrahepatic metabolism of 5-HMF in humans, most likely oxidative, ALDH-mediated metabolism in RBCs (see Chapter 5).

As observed from the IVIVE, all the prediction were underestimated to some extent in comparison to *in-vivo* data. Under-prediction is a common issue that is encountered when

dealing with different *in-vitro* systems. Considering the average inaccuracy, it was reported that IVIVE for human microsomes and hypatocytes were 9-fold and 5-fold lower than their corresponding *in-vivo* values and were associated with low precision of 30 -150 fold (Houston 2008) (Hallifax 2009). On the other hand, our observation of higher bias in human vs. other species IVIVE is a common annotation in the literature. The IVIVE was reported to mispredict rat *in-vivo* data by 1.4- and 2.2-fold using microsomes and hepatocytes, respectively (Houston 2008). When the repeatability of *in-vitro* estimates was investigated in hepatocytes, 28% variation was found using midazolam as a substrate (Hallifax 2009). Unfortunately, a definite mechanistic understanding of this misprediction is not always available (Hallifax 2009).

In-vivo predictions from *in-vitro* systems suffers from inaccuracy if the *in-vivo* data was collected from a population with different genetic characteristic in comparison to those used in the generation of the *in-vitro* data (Hallifax 2009). Both of ALDH and ADH enzymes, involved in this research, were reported to have extensive polymorphism among ethnic groups (Goedde 1983). The hepatic cytosol is pooled from different donors, which introduces variability in age, gender, disease, medications, smoking, drinking, and cause of death. In contrast, these variability factors are well-controlled in the *in-vivo* studies (Hallifax 2009). In addition, errors from experimental procedures and extrapolation using the physiological values, which are subject to inter-individual variability, contribute to random error associated with IVIVE leading to the uncertainty in the hepatic clearance prediction (Hallifax 2009). For instance, the human cytosolic protein recovery per gram liver was reported with a significant variation, 45 -134 mg/g liver vs. 78-105 mg/g liver in rats.

In the experiments conducted in this research project, the total added concentration of 5-HMF was used and the unbound fraction in the *in-vitro* system was assumed to be one. This may

contribute to under-prediction if the drug was non-specifically bound in the hepatic cytosol *in-vitro* and was less bound in the physiological system. In addition, diffusion into the subcellular fraction, increasing or decreasing the concentration available to enzymes, is not accounted for with the use of hepatic cytosol.

Moreover, the activity of the enzymes might have decreased because of the procedures associated with liver resection and cellular fractionation (Hallifax 2009). The speed, at which subcellular fractions are obtained from different species, can be different leading to a variation in the accuracy of IVIVE among species (Hallifax 2009). Furthermore, endogenous activators or inhibitors might exist in the physiological setting but not in *in-vitro* system (Hallifax 2009). In addition, errors are introduced at the metabolic pharmacokinetics model level due to the inability to reach saturation due to high background absorbance and substrate solubility (Hallifax 2009).

CHAPTER 5

5-HMF METABOLISM IN HUMAN RBCS

5.1 Introduction

ALDH was first extracted from human erythrocytes by Inoue and co-workers in 1979 as a tetrameric protein (Inoue 1979). Unfortunately, the literature is sparse with studies investigating this ALDH enzyme in RBCs. This might be a result of the low number of drugs with an aldehyde moiety that are administered to humans therapeutically. As discussed in Chapter 1, the ALDH isoenzyme present in RBCs has similar properties as the ALDH isoenzyme in hepatic cytosol (Goedde 1983) (Inoue 1979). It was shown by Goedde et al. that the ALDH isoenzyme in RBCs corresponds to ALDH1 enzyme present in the liver. This fact together with the discrepancy in the IVIVE prediction with the observed $t_{1/2}$ (Chapter 4), suggest that 5-HMF may be metabolized in human RBCs. Consequently, 5-HMF metabolism was investigated in human RBCs.

The same methodology used in studying 5-HMF metabolic stability in the hepatic cytosol was used to study the metabolism of 5-HMF in human RBCs. NADH production was spectrophotometrically monitored to investigate 5-HMF oxidation.

5.2 Methods

5.2.1 Materials and Reagents

1. BD Gentest™ TRIS Buffer 0.5 M, pH 7.5 (BD Bioscience, San Jose, CA).
2. 5-Hydroxymethyl-2-furfural (5-HMF) Solution:

   - 5-Hydroxymethyl-2-furfural (Sigma, St. Louis, MO).

   - BD Gentest™ TRIS buffer 0.5 M, pH 7.5 (BD Bioscience, San Jose, CA).
3. Ethanol Solution:

   - Ethanol 99.5%, 200 proof (Aldrich, Milwaukee, WI)

   - BD Gentest™ TRIS buffer 0.5 M, pH 7.5 (BD Bioscience, San Jose, CA).
4. 4-Methylpyrazole (4-MP) Solution:

   - 4-MP, 99% (Sigma-Aldrich, Milwaukee, WI).

   - BD Gentest™ TRIS buffer 0.5 M, pH 7.5 (BD Bioscience, San Jose, CA).
5. Tetraethylthiuram Disulfide (disulfiram) Solution:

   - Disulfiram, purum 97% (Sigma-Aldrich, Milwaukee, WI).

   - BD Gentest™ TRIS buffer 0.5 M, pH 7.5 (BD Bioscience, San Jose, CA).
6. Human Blood:

   - Human: mixed gender, pool of three black females, two black males, and one white male (35.3 ± 13.5 years).

   - Water (BD Bioscience, San Jose, CA).
7. Cofactor Solution, β-Nicotinamide Adenine Dinucleotide (NAD^+) Solution:

   - NAD^+ from yeast (Sigma, St. Louis, MO).

   - BD Gentest™ TRIS buffer 0.5 M, pH 7.5 (BD Bioscience, San Jose, CA).

5.2.2 Equipment

1. 25-µl, 50-µl, and 250-µl positive displacement pipettes and corresponding pipette tips (Microman, Rainin Instruments, Oakland, CA).
2. 10-µl, 100-µl, and 1000-µl VWR pipettes and corresponding pipette tips (VWR, West Chester, PA).
3. 0.5-5 ml Finnpipette (Thermo Scientific, Waltham, MA).
4. Vortex (Vortex-Genie, VWR, West Chester, PA).
5. Sonicator (American Brand Products C6450-11, VWR, West Chester, PA).
6. pH meter (Corning, Glendale, AZ).
7. Balance (Fisher Scientific A 250, Pittsburgh, PA).
8. Synergy™ 2 multi-mode microplate reader (BioTek, Winooski, VT).
9. Falcon assay plate, 96 reaction wells (VWR, West Chester, PA).

5.2.3 Preparation of Solutions

- Cofactor solution, β-nicotinamide adenine dinucleotide (β-NAD^+) solution

22.3 g of NAD^+ (M.W.: 663.43 Da) was dissolved in 3 ml of Tris buffer to prepare 1.4 mM solution.

- Diluted human RBCs

RBCs were obtained after centrifugation of whole blood. The RBCs were lysed and diluted 625-fold with water on two stages.

- Substrates solution

Solutions of different concentrations (12-142 mM) of 5-HMF (M.W. 126.11 Da) were prepared in Tris buffer. The estimation of NADH at low substrate was limited by the assay sensitivity in some cases. In addition, the estimation of NADH at high substrate was limited by the high baseline absorbance of 5-HMF and its solubility.

- Inhibitors solution

Solutions of inhibitors, 0.03-281 µM 4-methylpyrazole (M.W. 82.10 Da) and 0.03-33.8 µM disulfiram (M.W. 296.54 Da) were prepared to achieve maximum inhibition of the relevant enzymes taking into consideration their reported K_i, as stated in Chapter 4.

5.2.4 Procedures

Diluted RBCs, NAD^+ cofactor, and 5-HMF at different concentrations were mixed at a final volume of 0.2 ml. The reaction was initiated by the addition of diluted RBC solutions after allowing the mixture to equilibrate for approximately 5 minutes. The increase in the absorbance at 340 nm at 37 °C was monitored over time. The change in the absorbance was converted to an NADH concentration using Beer's law, as discussed in the method section of Chapter 4.

5.2.5 Concentration Dependency Studies

When the initial velocities were plotted against their corresponding concentrations, they did not reach saturation. Consequently, the initial velocities were related to their corresponding concentrations by the intrinsic clearance, which was represented by the slope.

$$v_i = CL_{int}^{in-vitro} \times C + v_0 \quad \text{Equation } 5-1$$

Where

v_i: the observed velocity

v_0: the baseline velocity observed in the absence of the substrate

C: the substrate concentration

$CL_{int}^{in\text{-}vitro}$: *in-vitro* intrinsic clearance

5.2.6 Inhibition Studies

Taking into consideration their reported K_i value, different concentrations of disulfiram and 4-methylpyrazole were used. All reaction components except for 5-HMF were incubated for approximately 15 minutes and 25 minutes with 4-methylpyrazole and disulfiram, respectively, after which 5-HMF, 26 mM, was added. At each concentration, a minimum of duplicate reactions were considered in the data analysis.

The data were modeled using non-linear regression as discussed in the methods section of Chapter 4.

5.2.7 *In-Vitro-In-Vivo* Extrapolation

$CL_{int}^{in\text{-}vitro}$ in Equation 5-2 is a measure of the innate ability of each milliliter of RBCs to clear a substrate. This *in-vitro* measure was extrapolated to *in-vivo* clearance (CL_{RBCs}) using the RBCs fraction of blood (0.4) and the total blood volume (5000 ml) according to Equation 5-2. Consequently, CL_{RBCs} refers to the innate ability of whole RBCs volume to clear 5-HMF.

$$\mathrm{CL_{RBCs}} = \mathrm{CL_{int}^{in-vitro}} \times 0.4 \times 5000 \ldots\ldots\ldots\

- 5-HMF has negligible renal excretion.
- Fraction unbound of 5-HMF in plasma (f_u)= 1.

The bases for these assumptions are stated in Chapter 4. Consequently, Equation 5-3 was used to estimate the total clearance.

$$\mathrm{CL_{tot}} = \mathrm{CL_{hep}} + \mathrm{CL_{RBC}} \quad \text{Equation } 5-3$$

IVIVE exposure predictions were calculated as described in the methods section of Chapter 4.

5.3 Results

An increase in the absorption was not observed when ethanol was incubated in the RBC system. This is expected since ADH expression in human RBCs was not reported. On the other hand, upon the incubation of 5-HMF with diluted RBCs, an increase in absorbance at 340 nm was observed, indicating the production of NADH in conjunction with 5-HMF oxidation. Initial velocities (v_i) were estimated from the slopes of the linear portion, representing the pseudo-zero order increase in the absorbance for each concentration within a ten-minute frame of spectrophotometric monitoring. When these initial velocities were plotted against their corresponding concentrations, they resulted in a linear relationship that was modeled by linear regression, as shown in Figure 5-1. The *in-vitro* intrinsic clearance, expressed in ml/min/ml RBCs, is shown in Table 5-1. The estimated metabolic activity of 5-HMF was partially inhibited by disulfiram as demonstrated in Figure 5-2. The parameters of the non-linear regression inhibition model are shown in Table 5-2.

The IVIVE results are summarized in Table 5-3, including CL_{RBCs}, CL_{tot}, and $t_{1/2}$. The predicted half-life by the IVIVE (41 minutes) was 0.6 of that obtained from *in-vivo* studies (69 minutes) after oral administration of 5-HMF (Prior 2006). In addition, Table 5-4 summarizes the modified predictions of AUC_{∞} after oral administration of 5-HMF FTIM study.

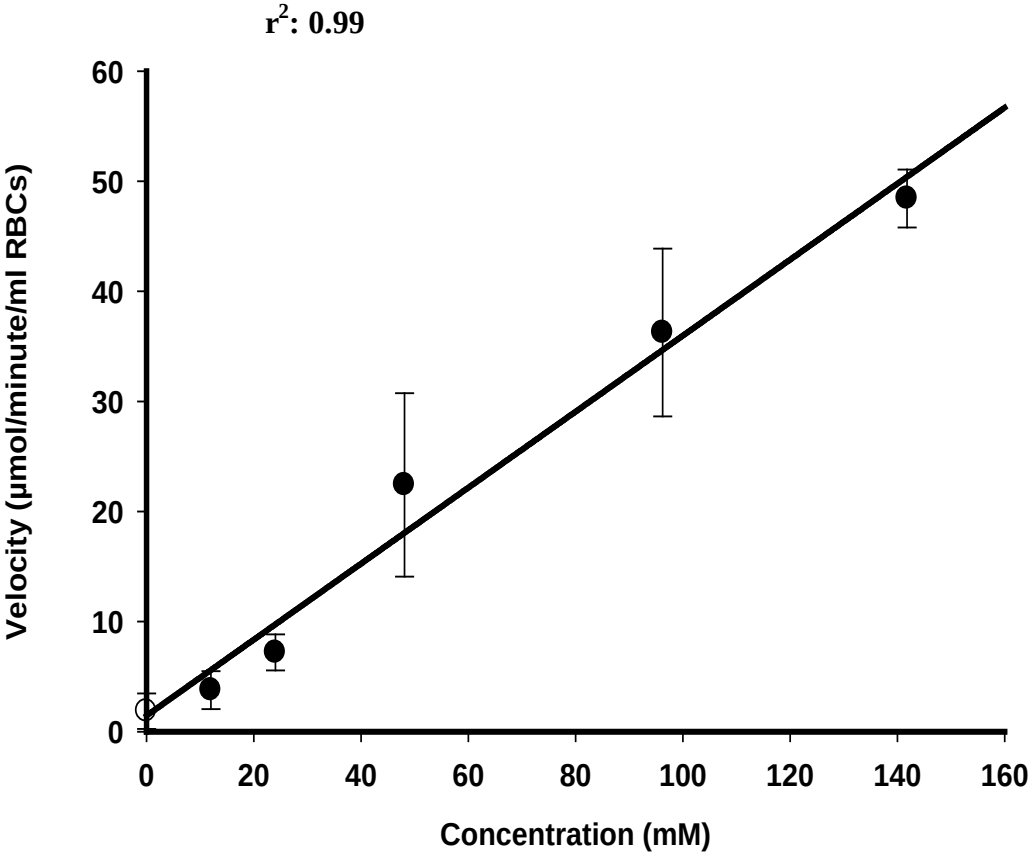

Figure 5-1. Concentration-dependent human RBC metabolism of 5-HMF.

Table 5-1. Final metabolic parameter estimates (SE) for 5-HMF in human RBC.

v_0 (µmol/min/ml RBCs)	1.4 (1.8)
$CL_{int}^{in\text{-}vitro}$ (ml/min/ml RBCs)	0.35 (0.02)

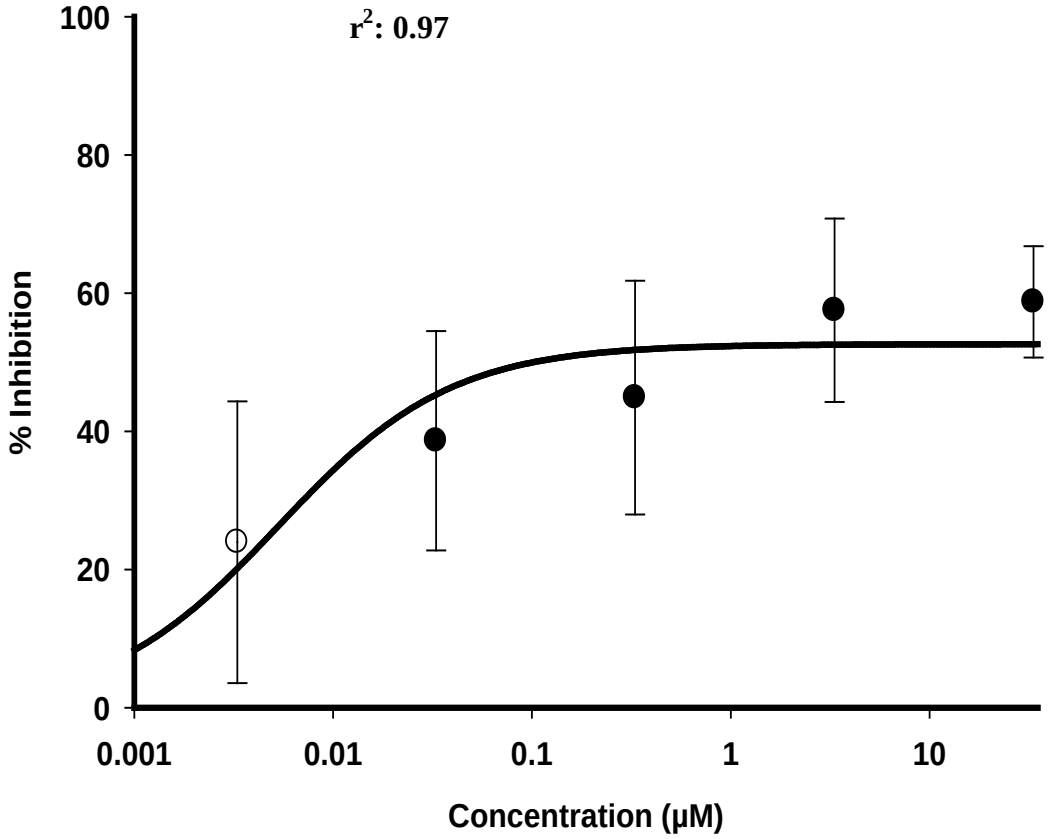

Figure 5-2. Inhibition of NADH-mediated human RBC metabolism of 5-HMF by disulfiram.

.

Table 5-2. Inhibition of NADH-mediated human RBC of 5-HMF metabolism by disulfiram (SE).

Maximum inhibition (%)	52.6 (3.62)
IC_{50} (µM)	0.0053 (0.0027)

Table 5-3. Modified IVIVE predictions for 5-HMF in humans.

CL_{hep} (ml/min)	12
CL_{RBCs} (ml/min)	690
CL_{tot} (ml/min)	702
$t_{1/2}$ (min)	41.5

Table 5-4. Modified predictions of AUC∞ for oral administration of 5-HMF FTIM study.

Dose (mg)	Projected AUC_{∞} (mg/ml.min)
100	0.14
300	0.41
1000	1.4
3000	4.2
6000	8.3
10000	14

5.4 Discussion and Conclusions

Significant NAD^+-dependent oxidation of 5-HMF was observed in RBCs. Overall, low-affinity metabolism was observed for 5-HMF, where K_m estimation for 5-HMF was not possible due to the fact that 5-HMF concentrations greater than K_m could not be achieved experimentally due to saturation in the instrument response and limitations in 5-HMF solubility.

The failure to observe NAD^+-dependent oxidation of ethanol and 5-HMF inhibition by 4-methylpyrazole indicated the absence of ADH enzyme in RBCs. On the other hand, 5-HMF metabolism and inhibition by disulfiram was in concordance with the presence of ALDH in RBCs, as reported in the literature suggesting ALDH-mediated oxidation of 5-HMF in RBCs. The use of the slope to estimate the intrinsic clearance entailed the assumption of therapeutic concentrations lower than the K_m value and similarity between the substrate concentration at the enzyme site and the unbound plasma concentration (Houston 2008).

The IVIVE-predicted $t_{1/2}$ for humans is similar to the reported plasma $t_{1/2}$ of the (presumed) primary metabolite, HMFA after oral administration of approximately 7.5 mg/kg of 5-HMF. This resolves the discrepancy noted in Chapter 4 that suggested the involvement of extrahepatic metabolism of 5-HMF in humans and led the study of RBC metabolism.

As discussed in Chapter 4, *in-vivo* predictions from *in-vitro* systems suffers from inaccuracy if different genetic characteristic were associated with the *in-vivo* data population in comparison to those used in the generation of the *in-vitro* data (Hallifax 2009). Ueshima et al. studied ALDH activity in the blood of an individual with normal ALDH1 homozygote after the addition of 1 mM of acetaldehyde for 14 minutes and found that approximately 80% of the added acetaldehyde disappeared, while approximately 30% of the acetaldehyde disappeared in the blood taken from an individual with ALDH1 deficiency (Ueshima 1993). Moreover, errors from

experimental procedures and extrapolation using blood volume and hematocrit value, which are subject to inter-individual variability, contribute to IVIVE inaccuracy in this research project.

CHAPTER 6

5-HMF *IN-VITRO* PROTEIN BINDING

6.1 Introduction

As stated in Section 1.2.2 in Chapter 1, the pharmacological activity of 5-HMF has been shown to be a consequence of the increased oxygen affinity to hemoglobin upon the formation of a Schiff adduct between the aldehyde group of 5-HMF and α-valine (Safo 2004). This valine amino acid is located in the hemoglobin water cavity, as shown in Figure 6-1.

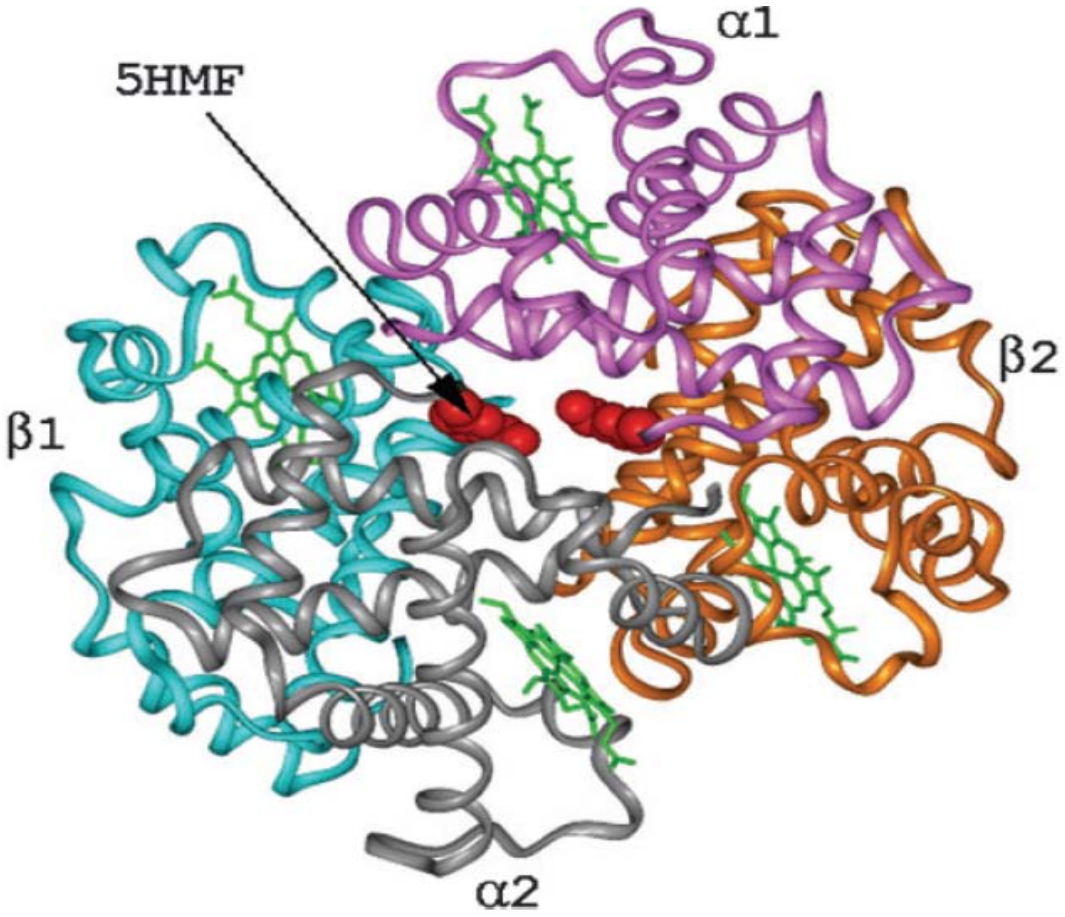

Figure 6-1. 5-HMF binding to a hemoglobin molecule. **(Abdulmalik 2005)**

Likewise, Schiff base formation has been reported between hemoglobin and other endogenous moieties. An example of a clinically relevant Schiff base adduct with hemoglobin is HbA_{Ic}. The normal blood glucose concentration, 3.6-7.0 mM, is associated with 5.0-8.5% glycosylated hemoglobin in healthy non-fasting humans (John 1988). Glucose interacts with hemoglobin, forming a Schiff base that undergoes further rearrangement to form a stable ketoamine linkage at the amino terminus of the β chain (Higgins 1981) (Bunn 1981). This interaction results in a slow formation of HbA_{Ic} throughout the life cycle of RBCs (Higgins 1981). Moreover, albumin also undergoes non-enzymatic glycosylation (Day 1979). The principal site for this glycosylation is the lysine amino acid at the 525 position (Garlick 1983).

In 1977, Zaugg et al. investigated Schiff base adducts between aldehydes and hemoglobin at the amino terminals as a potential approach to decrease HbS polymerization (Zaugg 1977). In that study, 31 compounds with carbonyl groups were incubated with a 20% RBC suspension, whole blood, and 6% of cell free hemoglobin (Zaugg 1977). The compounds included twenty five aromatic aldehydes, most of which were benzaldehyde derivatives, such as salicylaldehyde, vanillin, and carboxybenzaldehydes (Zaugg 1977). In addition, four aliphatic aldehydes were studied, namely, glyceraldehydes, cyclohexanecarbxaldehyde, glucose, and valeraldehyde (Zaugg 1977). Although Schiff base is reversible, it is considered as a relatively stable adduct since it could be characterized by isoelectric focusing (Zaugg 1977). A hemoglobin molecule with a Schiff base is slightly more anionic than the unmodified hemoglobin. These studies showed that aromatic aldehydes have higher affinity towards hemoglobin (typical association constant (K_A) value of 220 M^{-1}) than aliphatic aldehydes (typical K_A value of 70 M^{-1}) (Zaugg 1977). These observed association constants are higher than those obtained for small amine molecules, possibly due to water exclusion by the microenvironment that hemoglobin tetramer

provides favoring the formation of adduct (Zaugg 1977). In general, ketones and aliphatic aldehydes (including glucose) binding to hemoglobin did not affect oxygen affinity (Zaugg 1977).

It is noteworthy, that 5 mM of *o*-vanillin demonstrated 75% left shift of the control P_{50} value in 20% suspension of normal erythrocytes. This result was followed-up by Abraham and coworkers, where they incubated different concentrations (2.5, 5, and 10 mM) of vanillin in whole blood with homozygote sickle hemoglobin (Abraham 1991). With all of the above concentrations more than 85% of HbS molecules were modified to adducts with vanillin in less than an hour without affecting the hydration of RBCs (Abraham 1991). Nevertheless, vanillin was found to possess low oral bioavailability, which hindered its development (C. L. Zhang 2004).

This chapter presents the results of *in-vitro* binding studies of 5-HMF to human HbA and HSA. Time–dependency studies were designed to characterize the protein interaction and to estimate the appropriate rate constants, while concentration-dependency studies were performed to estimate the binding affinity and capacity of these proteins.

Various methods can be used to perform the physical separation of bound and unbound concentration of drugs to protein. Equilibrium dialysis is a commonly used method that employs semipermeable membrane, with a suitable molecular cutoff, to separate two chambers (Cheng 2004). The plasma spiked with the drug is added to one of the chambers while the other chamber contains a buffer. Despite its widespread use, equilibrium dialysis takes is time-consuming, which might be problematic to unstable drugs (Pacifici 1992). In addition, non-specific binding of the drug to the apparatus and volume shift between the compartments are disadvantages of equilibrium dialysis (Pacifici 1992).

HPLC using immobilized HSA is a recently developed method that can be used to determine protein binding (Cheng 2004). However, this method is hindered by the availability of the column and the drug since a large amount of drug is needed for the analysis (Cheng 2004).

Ultrafiltration uses a semipermeable membrane and forces the plasma or buffer with the unbound (ultrafiltrate) into a separate compartment using centrifugation that causes a pressure gradient (Bowers 1984). As with other protein binding determination methodologies, it suffers from non-specific binding to the instrument and membrane. In addition, centrifugation is usually performed at room temperature, which might disturb the equilibrium that might have been initiated at 37 °C (Pacifici 1992).

As a simple and rapid technique in protein binding determination, ultrafiltration was used in this study. Non-specific binding was determined in the absence of proteins to overcome this disadvantage. The molecular weight of HSA and Hb were considered in selecting the cutoff of the semipermeable membrane to avoid protein leakage. The temperature of the centrifuge was set to 37 °C.

6.2 Methods

6.2.1 Materials and Reagents

1. Phosphate-Buffered Saline (PBS), pH 7.4:

   - Phosphate-buffered saline tablets, pH 7.4 (Sigma, St. Louis, MO).

   - Milli-Q® water (Virginia Commonwealth University, PK/PD Laboratory).

2. Human Hemoglobin Solution:

   - Human hemoglobin lyophilized powder (Sigma, St. Louis, MO).

   - Phosphate-buffered saline, pH 7.4.

3. Human Serum Albumin Solution (Sigma, St. Louis, MO):

   - Human hemoglobin, fatty acid free, lyophilized powder (Sigma, St. Louis, MO).

   - Phosphate-buffered saline, pH 7.4.

4. 5-Hydroxymethyl-2-furfural (5-HMF) Solution:

   - 5-Hydroxymethyl-2-furfural (Sigma, St. Louis, MO).

   - Milli-Q® water (Virginia Commonwealth University, PK/PD Laboratory).

5. Mobile Phase for 5-HMF Assay Method:

   - 93.5% Milli-Q® water (Virginia Commonwealth University, PK/PD Laboratory).

   - 6.2% Methanol, HPLC grade (Burdick and Jackson, Morristown, NJ).

   - 1% Acetic acid glacial, > 99% (Sigma, Milwaukee, WI).

   - 0.3 % Tetrahydrofuran HPLC grade (Burdick and Jackson, Morristown, NJ).

6. SPE Conditioning:

   - Methanol, HPLC grade (Burdick and Jackson, Morristown, NJ).

   - Milli-Q® water (Virginia Commonwealth University, PK/PD Laboratory).

7. SPE Washing Solution: Phosphate-buffered Saline (PBS), pH 7.4:

   - Phosphate-buffered saline tablets, pH 7.4 (Sigma, St. Louis, MO).

   - Milli-Q® water (Virginia Commonwealth University, PK/PD Laboratory).

8. SPE Eluting Solution: 50% Methanol:

   - Methanol, HPLC grade (Burdick and Jackson, Morristown, NJ).

   - Milli-Q® water (Virginia Commonwealth University, PK/PD Laboratory).

6.2.2 Equipment

1. 25-µl, 50-µl, and 250-µl positive displacement pipettes and corresponding pipette tips (Microman, Rainin Instruments, Oakland, CA).
2. 10-µl, 100-µl, and 1000-µl VWR pipettes and corresponding pipette tips (VWR, West Chester, PA).
3. 0.5-5 ml Finnpipette (Thermo Scientific, Waltham, MA).
4. Vortex (Vortex-Genie, VWR, West Chester, PA).
5. Sonicator (American Brand Products C6450-11, VWR, West Chester, PA).
6. pH meter (Corning, Glendale, AZ).
7. Balance (Fisher Scientific A 250, Pittsburgh, PA).
8. Centrifuge 5804-R (Eppendorf, Hauppauge, NY).
9. Amicon® Ultra-4 centrifugal filter units with Ultracel-10 and Ultracel-50 membranes (Millipore, Billerica, MA).
10. Glass vials with caps, 1 ml (Waters, Milford, MA).
11. UV detector (Shimadzu, AV-10, Columbia, MA).
12. C_{18} Zorbax Rx column, 4.6 X 150 mm (Agilent, Santa Clara, CA).
13. C_{18} guard column, 12.5 mm x 4.6 mm (Agilent, Santa Clara, CA).
14. 717 plus autosampler (Waters, Milford, MA).
15. 600 Multisolvent controller (Waters, Milford, MA).
16. Empower 2 software (Waters, Milford, MA)
17. Forma Scientific incubator.

6.2.3 Preparation of Solutions

- Mobile Phase for 5-HMF Assay Method (1 L)

  935 ml water, 62 ml methanol, 10 ml acetic acid glacial, and 3 ml tetrahydrofuran were mixed to prepare the mobile phase.

- 5-Hydroxymethyl-2-furfural Solution (5-HMF)

  5-hydroxymethyl-2-furfural **(**M.W.: 126.11 Da) was dissolved in PBS.

- Phosphate-buffered Saline (PBS), pH 7.4

  One tablet of phosphate-buffered saline was added to 200 ml of water.

- SPE Eluting Solution: 50% Methanol

  25 ml of methanol was mixed with 25 ml of water.

- Human Hemoglobin Solution

  Human hemoglobin powder (M.W.: 64,677 Da) was dissolved in PBS.

- Human Serum Albumin Solution

  Human serum albumin powder (M.W.: 66,478 Da), was dissolved in PBS.

6.2.4 Procedures

5-HMF was added to human serum albumin or hemoglobin solutions in PBS at different concentrations. The solution was incubated at 36.5 ± 1 °C. Two milliliter samples were transferred to Amicon® Ultra-4 and centrifuged (5,000 rpm) for 20 minutes at 36.5 ± 1 °C. 50 kDa and 10 kDa were chosen as the molecular cut-off values for the membranes used in the ultrafiltration of human serum albumin and hemoglobin solutions, respectively. The ultrafiltrate was transferred to HPLC for analysis to quantitate the unbound 5-HMF concentrations (UC). The difference between the initial concentration and the measured 5-HMF concentration was assumed to represent the total 5-HMF binding to both the protein and the ultrafiltration system (TB). Non-specific binding was determined, in unicate, after ultrafiltration of 5-HMF solutions in the absence of proteins (NSB).

The chemical stability of 5-HMF was investigated at 36.5 ± 1 °C for 30 hours; where samples of 5-HMF solution at 16 μM in PBS were analyzed by HPLC in unicate. In all of the experiments, calibration curves of 5-HMF in PBS (0.2 – 80 μM) were established in PBS in parallel with the analysis of the samples in various experiments in order to estimate the unbound concentration of 5-HMF.

6.2.4.1 Time-Dependency Studies

5-HMF was pre-incubated in the suspension of RBCs containing HbS in the experiments reported by Abdulmalik. This was justified by the notion that Hb adduct needed some time to form (Abdulmalik, 2005). This rationale triggered this research to investigate time-dependency

in 5-HMF binding to hemoglobin. Therefore, studies were conducted with 5-HMF in concentrations ranging from 8 μM to 0.3 mM, incubated in Hb (217 μM) or HSA (63 and 202 μM) solutions in PBS at 37°C. Serial samples (unicate, mostly) for up to 30 hours were taken and ultra-filtered using the Amicon® Ultra-4 centrifugal filter unit with Ultracel-10 and Ultracel-50 membranes for Hb and HSA, respectively, by centrifugation for 20 minutes at 5,000 rpm at 37 °C.

6.2.4.2 Concentration-Dependency Studies

Studies were conducted with various concentrations of 5-HMF ranging from 5 μM to 5 mM and incubated in Hb (217 μM) or HSA (63 and 202 μM) solutions at 37 °C. Duplicate samples at 24 hours (Hb solution) and 6 hours (HSA solution) were taken and ultrafiltered. Unbound 5-HMF concentrations were measured by HPLC. Specific binding was estimated after the correction for non-specific binding using the equations discussed in the Data Analysis section.

6.2.5 Data Analysis

The general scheme for the binding reaction, which leads to the formation of 5-HMF Schiff base adduct with the amino group of a protein (human hemoglobin or serum albumin), is described by Figure 6-2. In this scheme, k_1 is the Schiff base formation rate constant, following second-order kinetics, while k_{-1} is the adduct degradation constant that follows first-order kinetics (Ge 1997). Any rearrangement of the aldimine bond in 5-HMF adduct to a stable covalent bond (as it is the case for glucose) was assumed to be negligible.

The rate of change in the concentration of the adduct [Adduct] at any time in the binding reaction is estimated according to Equation 6-1:

$$\frac{\mathrm{d[Adduct]}}{\mathrm{dt}} = \mathrm{k_1} \times [5\mathrm{HMF}](\mathrm{t}) \times [\mathrm{Protein}\,](\mathrm{t}) - \mathrm{k_{-1}} \times [\mathrm{Adduct}](\mathrm{t}) \ldots\ldots\ldots\ldots \text{Equation } 6-1$$

where

$[5\mathrm{HMF}](\mathrm{t})$: the concentration of free 5-HMF at time (t)

$[\mathrm{Protein}](\mathrm{t})$: the concentration of free protein at time (t)

$[\mathrm{Adduct}](\mathrm{t})$: the concentration of the adduct between 5-HMF and the protein at time (t)

In these studies, free (i.e. unbound) 5-HMF at a certain time point $(\mathrm{t_i})$, namely $[5\mathrm{HMF}](\mathrm{t_i})$, was measured using the validated HPLC method. On the other hand, Equations 6-2 and 6-3 were used to estimate the adduct formed, $[\mathrm{Adduct}](\mathrm{t_i})$, and the concentration of free protein, $[\mathrm{Protein}](\mathrm{t_i})$, at the relevant time point, $\mathrm{t_i}$:

$$[\text{Adduct}](t_i) = [5\text{HMF}](t_0) - [5\text{HMF}](t_i) \ldots\ldots\ldots\ldots\ldots\ldots\ldots\ldots\ldots\ldots\ldots\ldots\ldots\ldots \text{Equation } 6-2$$

$$[\text{Protein}](t_i) = [\text{Protein}](t_0) - \left([5\text{HMF}](t_0) - [5\text{HMF}](t_i)\right) \ldots\ldots\ldots\ldots\ldots\ldots\ldots \text{Equation } 6-3$$

where $[5\text{HMF}](t_0)$ and $[\text{Protein}](t_0)$ are the initial concentrations of 5-HMF and the protein, respectively. At equilibrium, the rate of change is zero, as described by Equations 6-4 and 6-5:

$$k_1 \times [5\text{HMF}]_{eq} \times [\text{Protein}]_{eq} = k_{-1} \times [\text{Adduct}]_{eq} \ldots\ldots\ldots\ldots\ldots\ldots\ldots\ldots\ldots\ldots\ldots\ldots \text{Equation } 6-4$$

$$K_A = \frac{k_1}{k_{-1}} = \frac{[\text{Adduct}]_{eq}}{[5\text{HMF}]_{eq} \times [\text{Protein}]_{eq}} \ldots\ldots\ldots\ldots\ldots\ldots\ldots\ldots\ldots\ldots\ldots\ldots\ldots\ldots\ldots\ldots \text{Equation } 6-5$$

where K_A is association equilibrium constant, while $[5\text{HMF}]_{eq}$, $[\text{Protein}]_{eq}$, and $[\text{Adduct}]_{eq}$ are the concentrations of free 5-HMF, free protein, and protein adduct, respectively, at equilibrium.

As a measure of affinity, the dissociation constant, K_D, can be estimated, as an inverse of K_A as described by Equation 6-6:

$$K_D = \frac{1}{K_A} \ldots\ldots\ldots\ldots\ldots\ldots\ldots\ldots\ldots\ldots\ldots\ldots\ldots\ldots\ldots\ldots\ldots\ldots\ldots\ldots\ldots\ldots\ldots\ldots\ldots\ldots\ldots\ldots\ldots\ldots \text{Equation } 6-6$$

After performing the non-linear regression of the time dependency studies, the final estimates for the forward and backward rate constants (k_1 and k_{-1}) were used to estimate an

apparent first-order equilibration rate constant, k_{eq} (assuming that 5-HMF concentrations are lower than the protein concentration, i.e., [5-HMF]<<[Protein]) as described in Equation 6-7.

$$k_{eq} = k_{-1} + (k_1 \times [\text{Protein}]t_0) \quad \text{Equation } 6-7$$

k_{eq} (apparent first-order rate constant) was estimated for 7.9 and 19.8 μM 5-HMF incubated with Hb and HSA, respectively, using the rate constant estimates. k_{eq} was compared to the actual rate constant, k_{obs}, obtained from the slope when the natural logarithmic value for difference between the adduct concentration at steady-state (Css) and the concentration of the adduct at different time points (Ct), i.e. (ln (Css-Ct)), was plotted against time.

In addition, the final estimates of the rate constants were compared to those reported for glucose and the equilibration rate for 5-HMF-Hb adduct was extrapolated to physiological blood concentrations of Hb (2.3 mM) and the expected clinically relevant concentrations of 5-HMF (1-2 mM). In addition, the overall results of this study were put in context with the previously reported data (Abdulmalik 2005).

In the data analysis performed, specific binding (SB) was estimated from the nominal concentration (NC) and nonspecific binding (NSB), as follows:

Total Concentration Bound (TB) = NC – Ultrafiltrate (=Unbound) Concentration (UC)

Specific Binding (SB) = TB - NSB

Fraction Specifically Bound (f_{SB}) = SB/(NC – NSB)

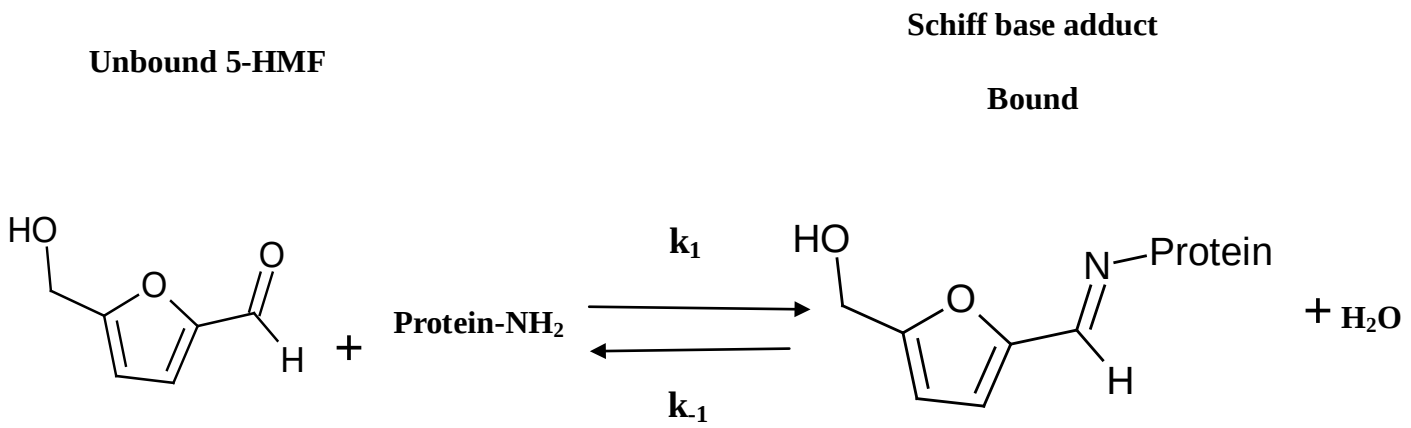

Figure 6-2. Schiff base interaction between 5-HMF and protein.

6.2.6 Modeling

For all models, goodness of fit was assessed by r^2. Parameter estimates are reported along with their standard errors.

6.2.6.1 Time-Dependency Studies

6.2.6.1.1 INITIAL ESTIMATES

To obtain initial estimates for the rate constants, shown in Figure 6-3, Equation 6-1 was combined with Equation 6-5. The reaction was rewritten as shown in Equations 6-9 and 6-10 using K_A and k_{-1} to express k_1.

$$\frac{d[\text{Adduct}]}{dt} = k_{-1} \times K_A \times [5\text{HMF}](t) \times [\text{Protein}](t) - k_{-1} \times [\text{Adduct}](t) \ldots \text{Equation } 6-8$$

$$\frac{d[\text{Adduct}]}{dt} = k_{-1} \times (K_A \times [5\text{HMF}](t) \times [\text{Protein}](t) - [\text{Adduct}](t)) \ldots\ldots\ldots \text{Equation } 6-9$$

The above differential equation was approximated by Equations 6-10 and 6-11:

$$\frac{\Delta[\text{Adduct}]}{\Delta t} = k_{-1} \times (K_A \times [5\text{HMF}](t) \times [\text{Protein}](t) - [\text{Adduct}](t)) \ldots\ldots\ldots \text{Equation } 6-10$$

$$B = k_{-1} \times A \ldots\ldots\ldots\

Where B represents the left side of the equation and A is the right side of the equation divided by k_{-1}.

An initial estimates of K_A was obtained according to Equation 6-5 by measuring the steady state concentration of 5-HMF and estimating the steady-state concentration of the adduct and the protein in accordance with Equations 6-2 and 6-3. Consequently, k_1 was estimated using Equation 6-5.

6.2.6.1.2 FINAL ESTIMATES

Equation 6-1 describes the rate of adduct formation using forward and backward reaction rate constants. However, the adduct was not directly measured experimentally, alternatively, unbound 5-HMF was measured. Therefore, nonlinear regression, (Scientist®, version 2.1, Micromath), was fitted to the data across initial 5-HMF concentrations, and the initial model estimates (k_1 and k_{-1}) were optimized using non-linear regression using Equation 6-12.

$$\frac{d[5HMF]}{dt} = k_{-1} \times [Adduct](t) - k_1 \times [5HMF](t) \times [Hb](t) \ldots\ldots\ldots\ldots\ldots\ldots\ldots \text{Equation } 6-12$$

The above equation assumes that all of the lost 5-HMF is involved in the adduct formation after the correcting for the NSB. The final model parameter estimates were compared to those reported for the Schiff adduct of glucose and Hb. The built Scientist model is shown in Appendix C.

6.2.6.2 Concentration-Dependency Studies

After correction for nonspecific binding, specific binding was used to estimate steady-state binding affinity (K_D) and the maximum binding capacity or that which can be attained at a very high concentration of 5-HMF (binding capacity, B_{max}) by nonlinear regression (SigmaPlot® 10.0, Systat), using the hyperbolic relationship described by Equation 6-13. B_{max} was expressed as a molar ratio of 5-HMF bound to the total protein.

$$C_B = \frac{B_{max} \times C_u}{K_D + C_u} \quad \text{Equation } 6-13$$

Where saturable binding was not observed, linear regression was employed using Equation 14.

$$C_B = SB \times C_u + Y_0 \quad \text{Equation } 6-14$$

where C_B is 5-HMF concentration bound to the protein, SB is the specific binding coefficient, Y_0 is the y-axis intercept, and C_u is the concentration of unbound 5-HMF.

6.3 Results

6.3.1 Non-Specific Binding Studies

In the hemoglobin study, non-specific binding to Amicon® Ultra-4 centrifugal filter units with Ultracel-10 membrane was fitted to a quadratic equation, as shown in Figure 6-3. This model was used to estimate the specific binding to hemoglobin at different concentrations. On the other hand, non-specific binding to Amicon® Ultra-4 centrifugal filter units with Ultracel-50 membrane was fitted to a linear equation, as shown in Figure 6-4. This model was used to estimate the specific binding to albumin at different concentrations. The goodness of fit of these models was assessed through the coefficient of determination r^2 as shown the corresponding figures.

6.3.2 Time-Dependency Studies

The concentration of 5-HMF was constant when incubated in PBS in the absence of protein for 30 hours, as shown in Figure 6-5, indicating that it was chemically stable under the experimental conditions. However, 5-HMF concentration decreased in the ultrafiltate when incubated in the protein (Hb or HSA) solutions as demonstrated in Figures 6-6, 6-7, 6-8, 6-9, 6-10, 6-11, 6-12. The extent of decrease was higher in the presence of hemoglobin in comparison to serum albumin, as demonstrated in Figures 6-6 and 6-10. Since only a small fraction of 5-HMF was bound to albumin, the y-axis scale in Figures 6-9, 6-10, and 6-11 was changed to make the decrease in the free concentration of 5-HMF more visible.

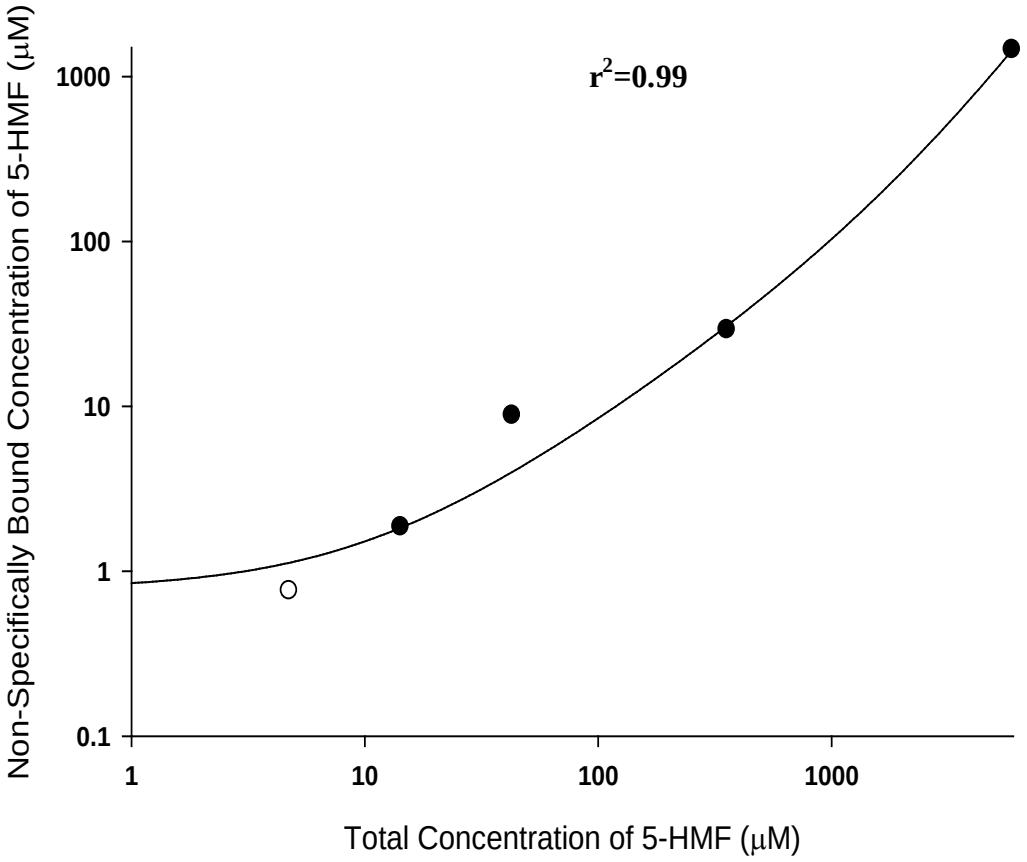

Figure 6-3. Non-specific binding of 5-HMF in Amicon® Ultra-4 centrifugal filter units with Ultracel-10 membrane.

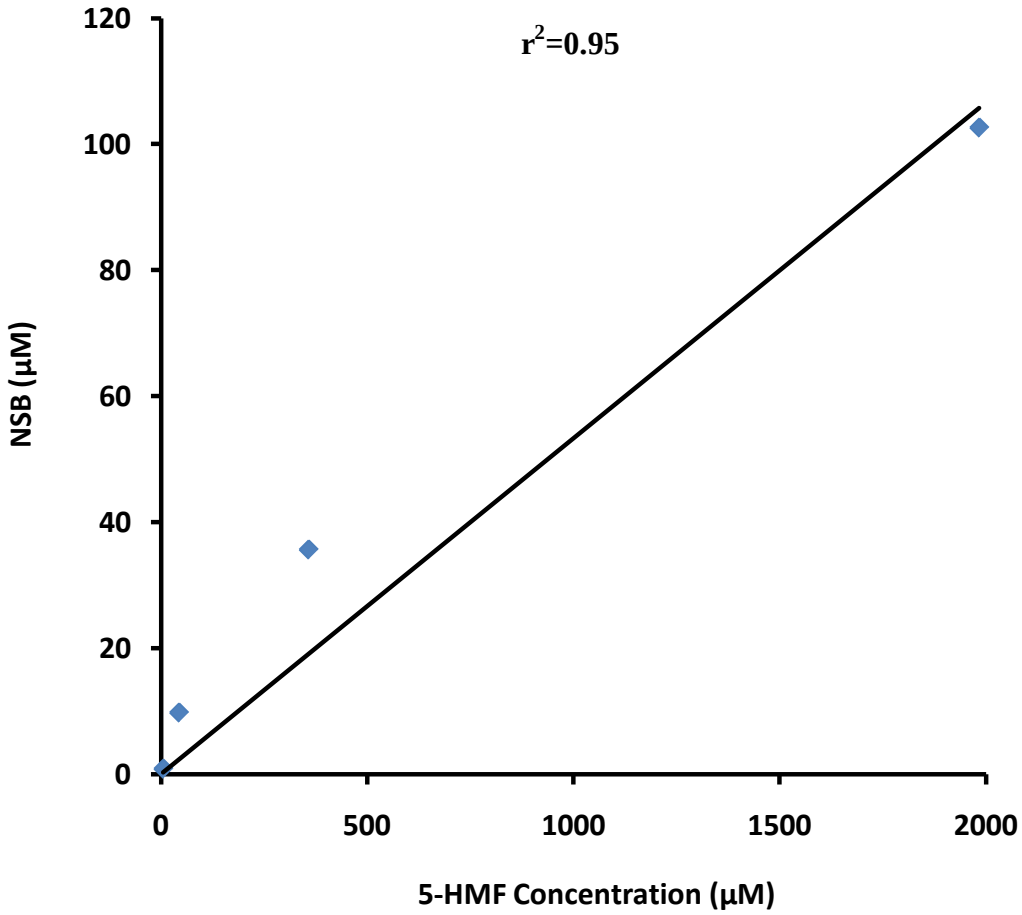

Figure 6-4. Non-specific binding of 5-HMF in Amicon® Ultra-4 centrifugal filter units with Ultracel-50 membrane.

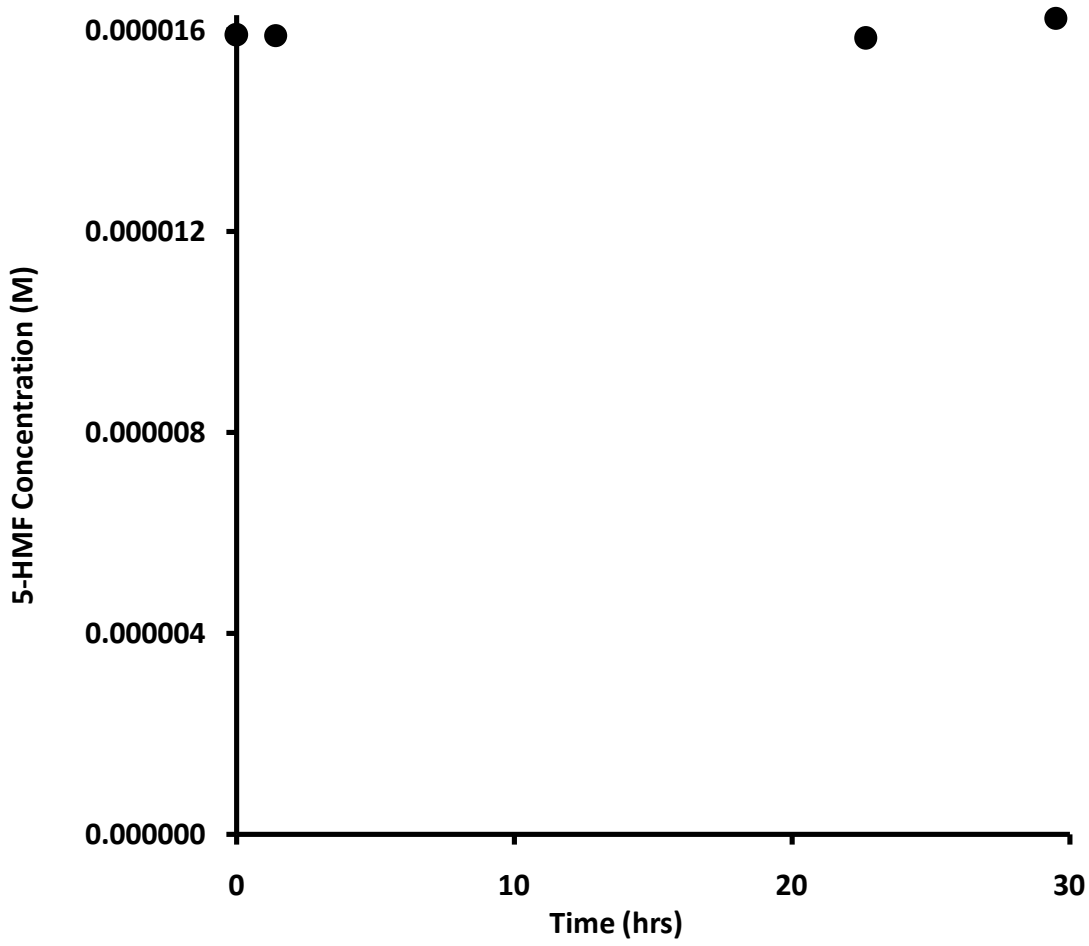

Figure 6-5. 5-HMF (16 μM) stability in PBS.

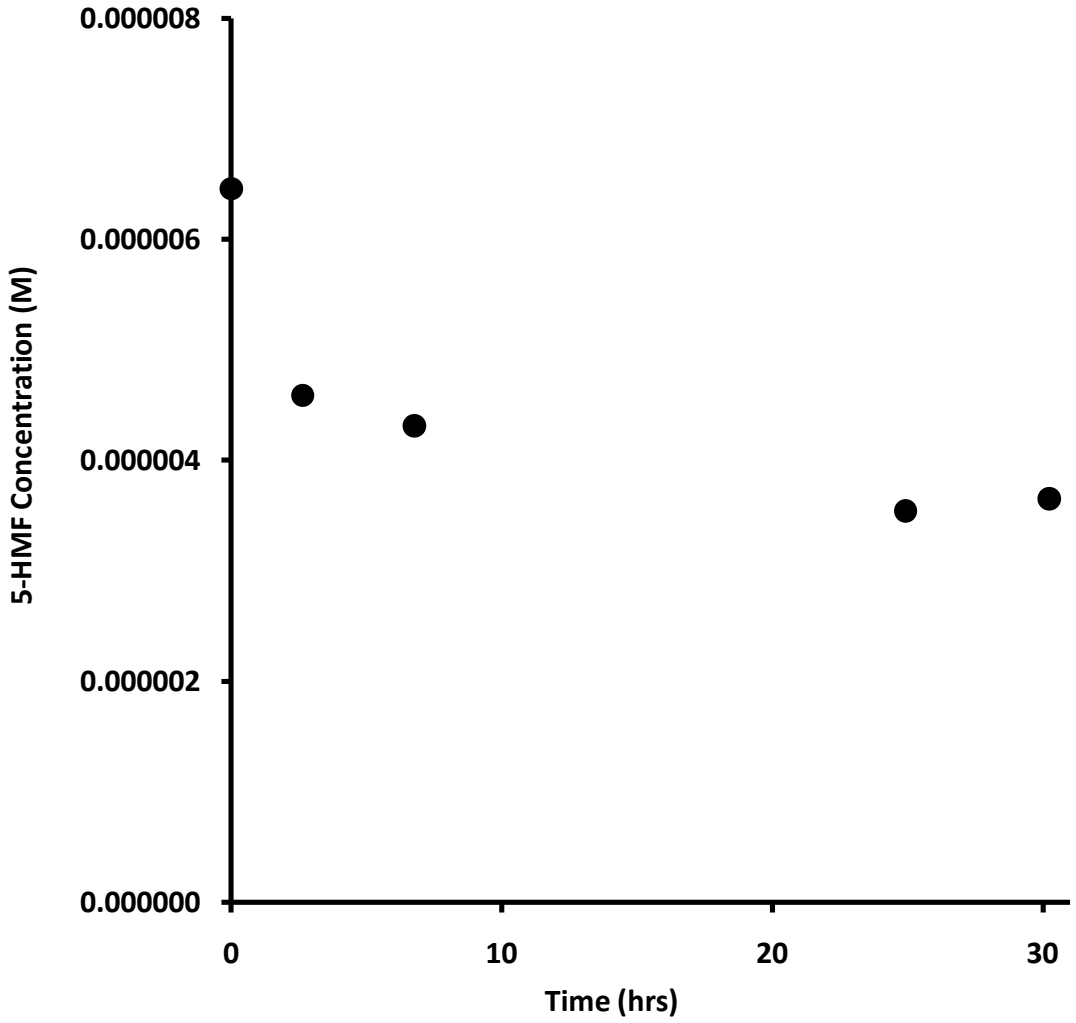

Figure 6-6. Time-dependency of 5-HMF (7.9 µM) binding to hemoglobin (217 µM).

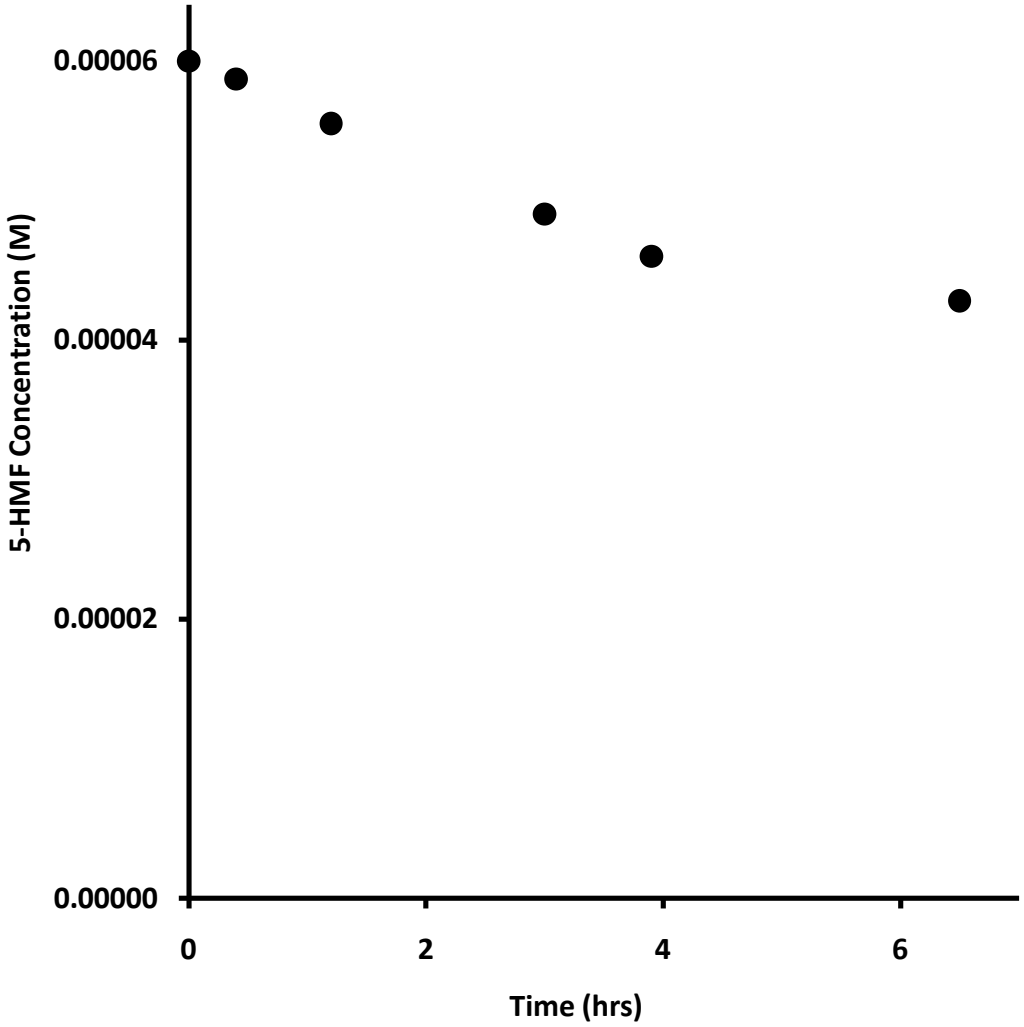

Figure 6-7. Time-dependency of 5-HMF (63 µM) binding to hemoglobin (217 µM).

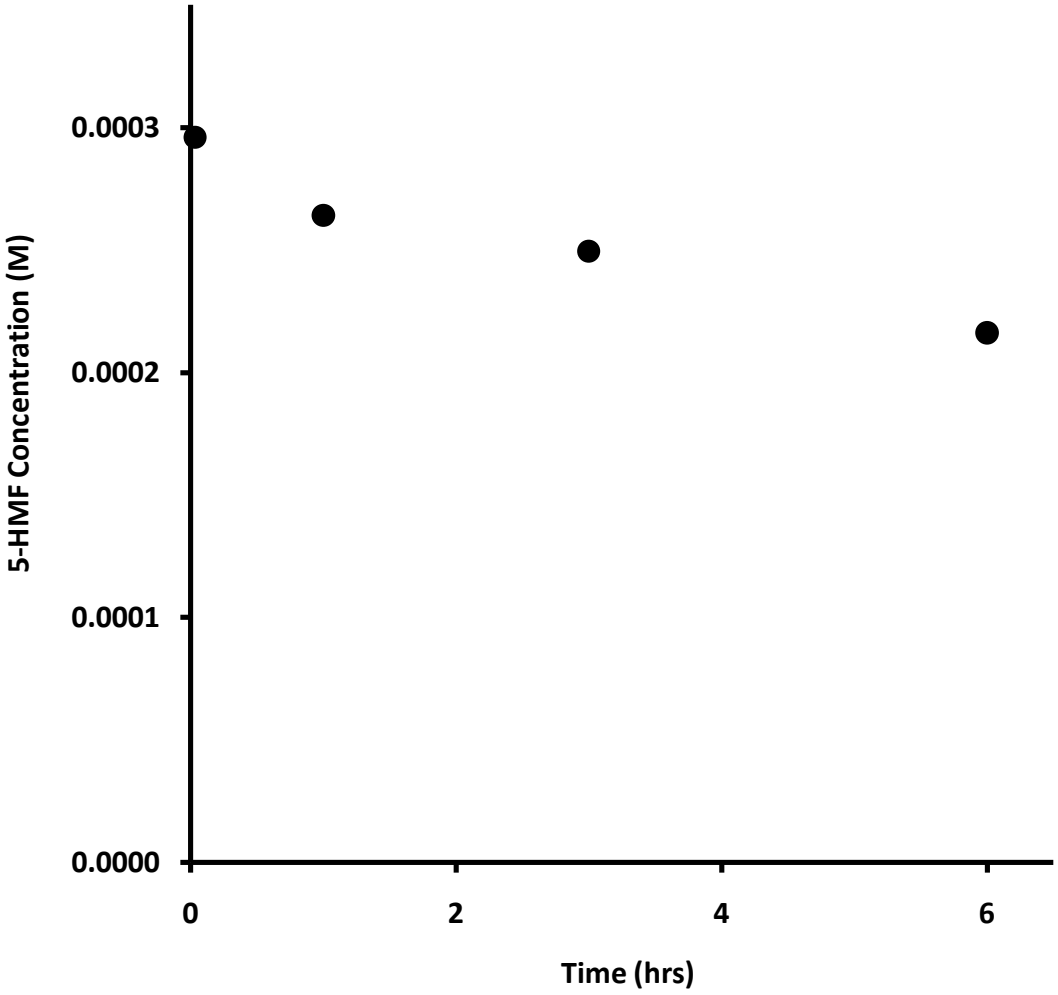

Figure 6-8. Time-dependency of 5-HMF (397 µM) binding to hemoglobin (217 µM).

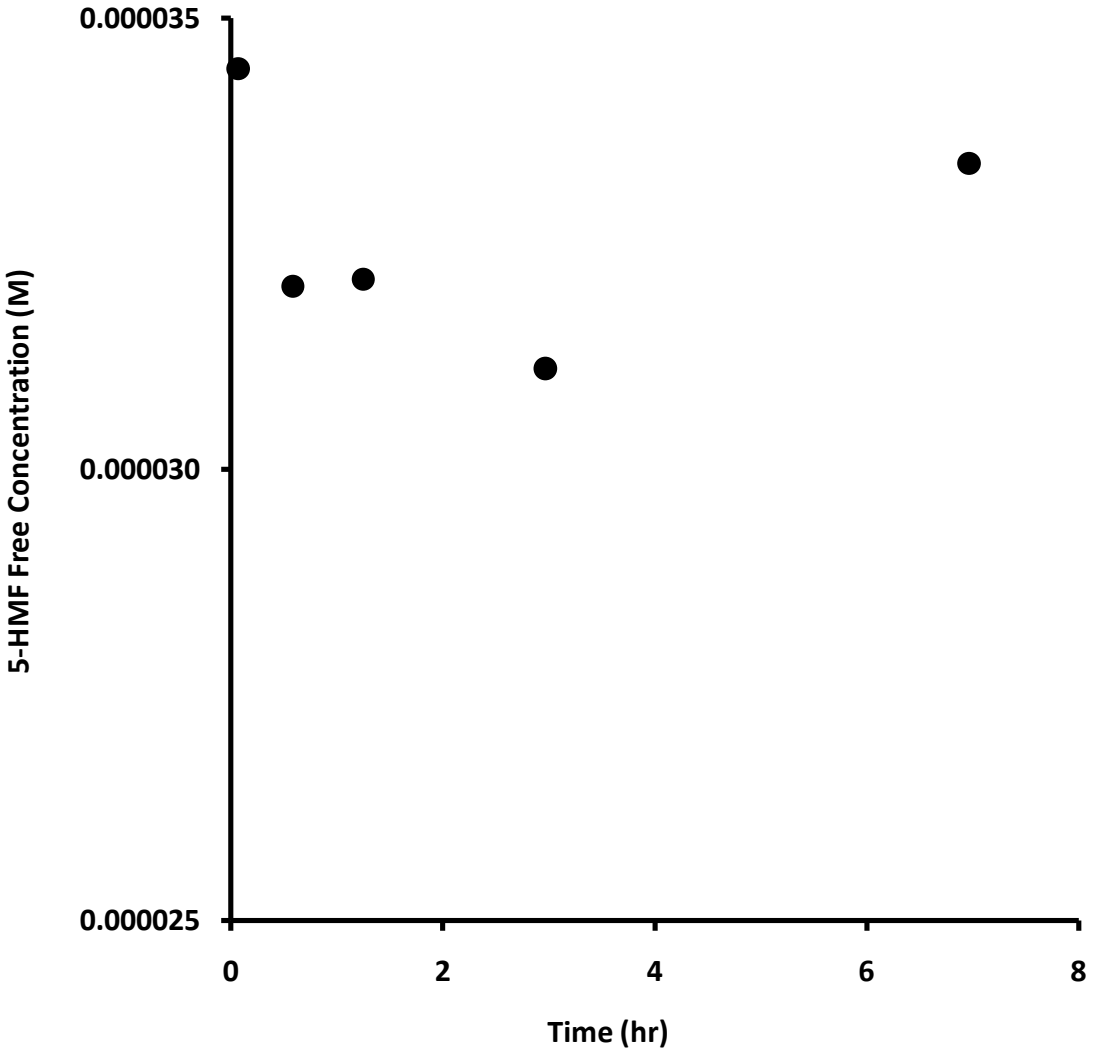

Figure 6-9. Time-dependency of 5-HMF (37 µM) binding to HSA (202 µM).

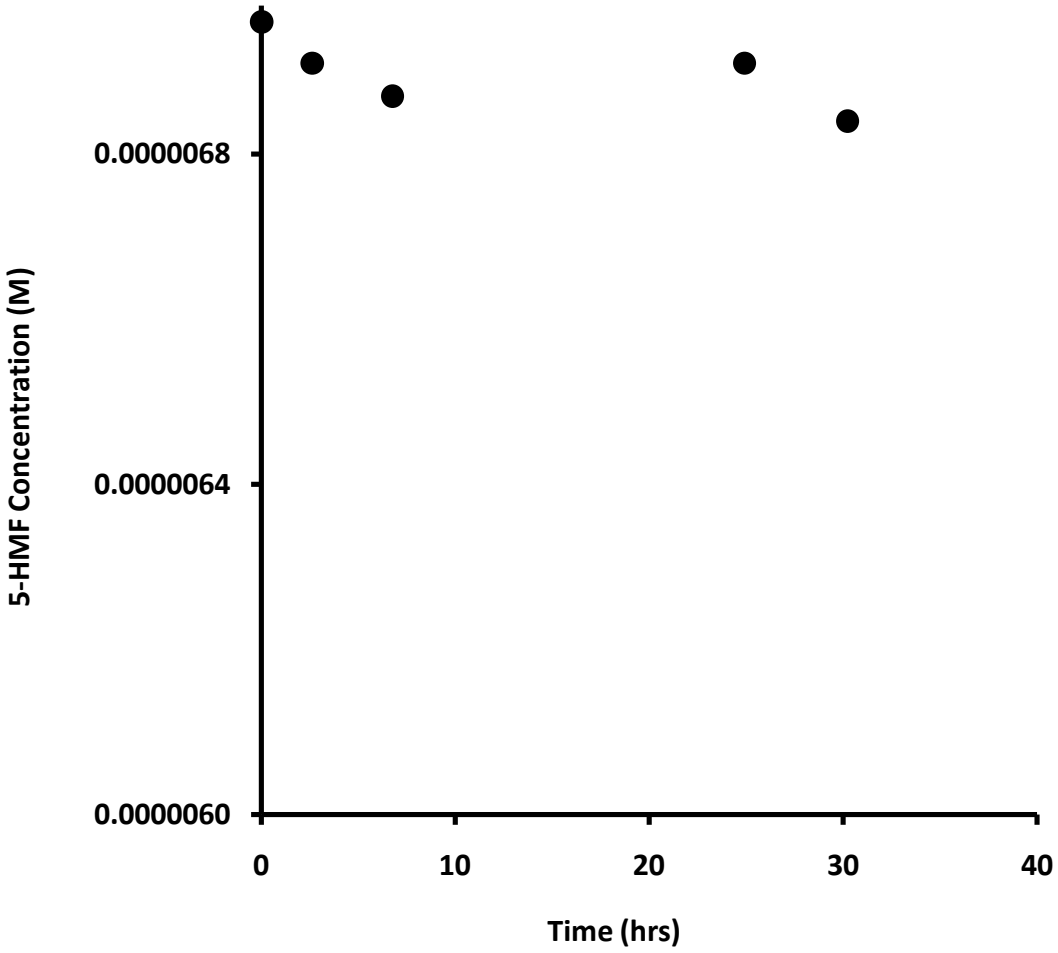

Figure 6-10. Time-dependency of 5-HMF (7.9 µM) binding to HSA (63 µM).

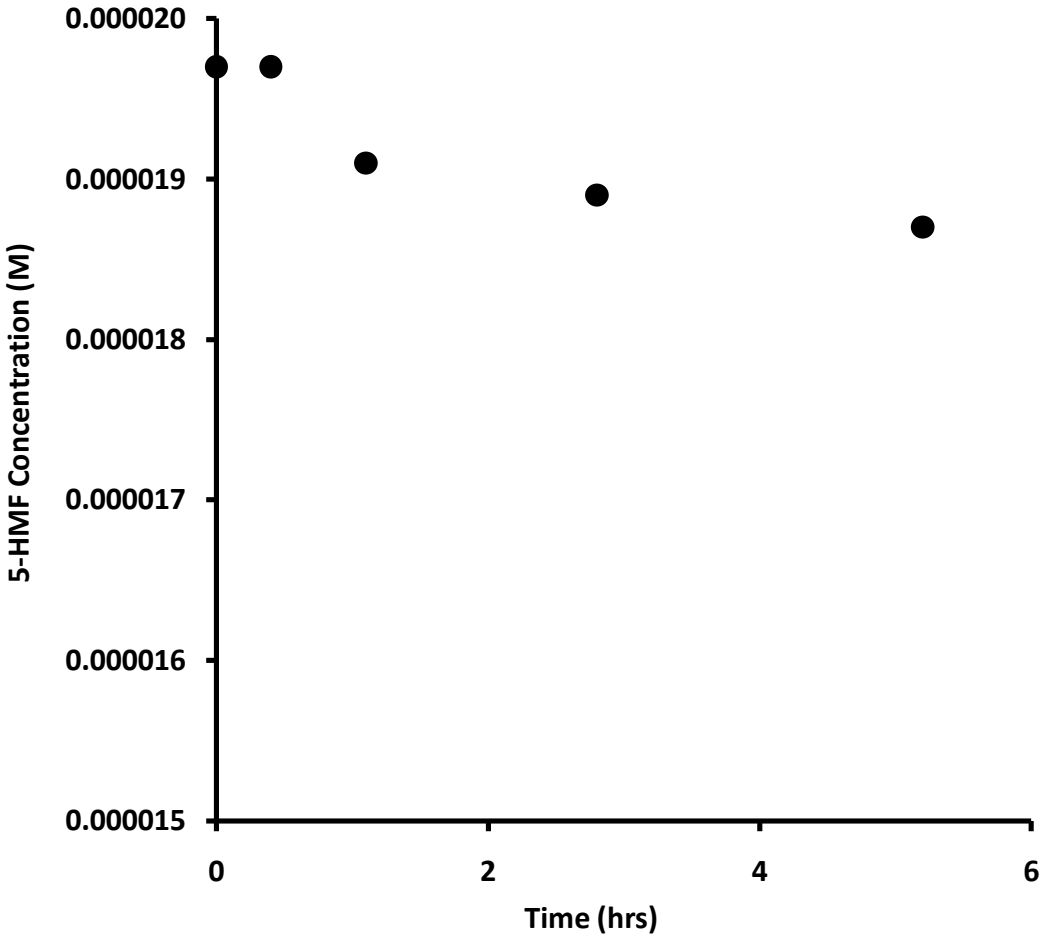

Figure 6-21. Time-dependency of 5-HMF (20 µM) binding to HSA (63 µM).

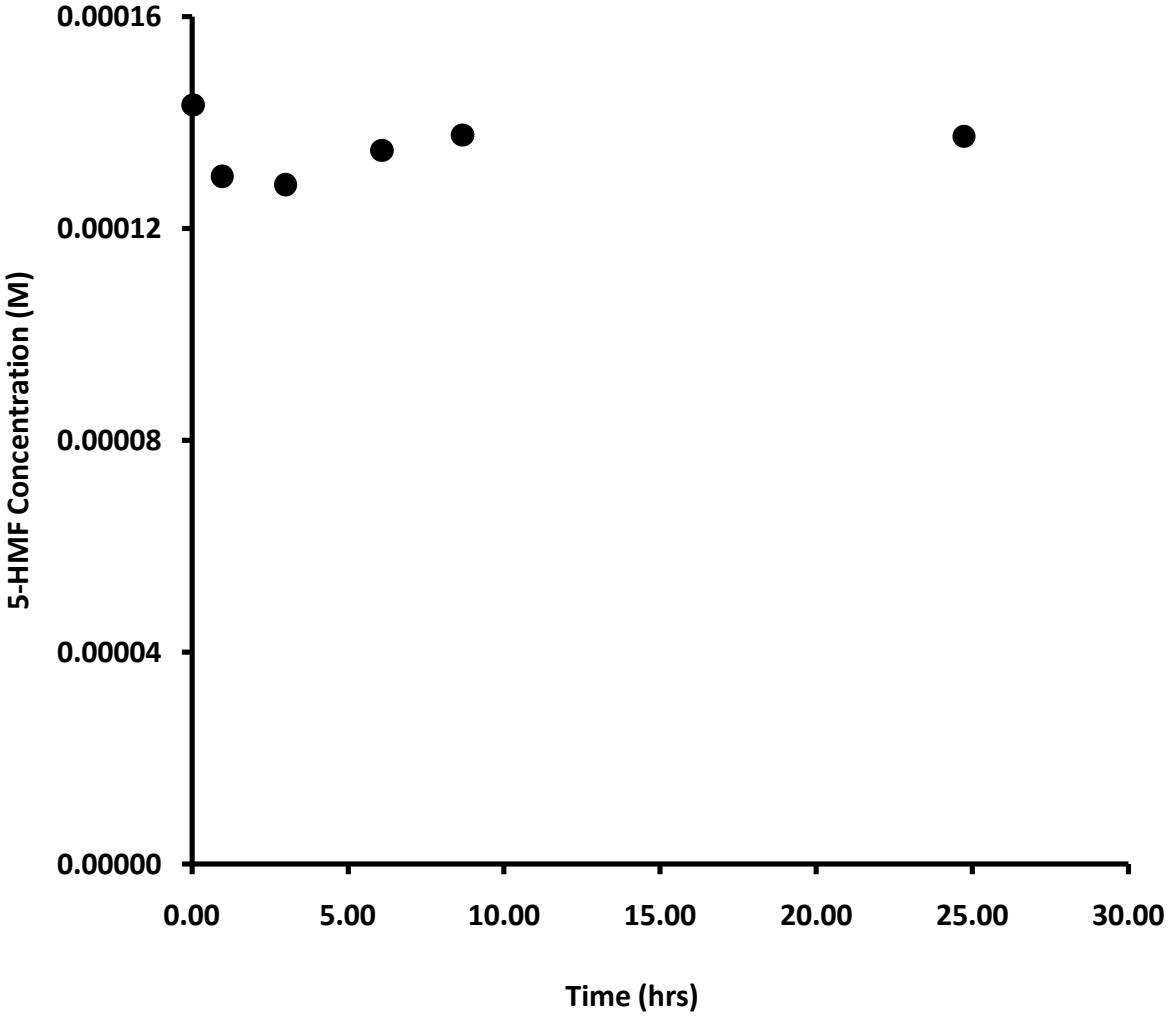

Figure 6-12. Time-dependency of 5-HMF (150 µM) binding to HSA (63 µM).

It appears from Figure 6-6 that equilibrium between 5-HMF and hemoglobin was achieved in this experiment. According to Equation 6-5, the average of last two points were used in estimating the equilibrium constant (K_A) for the purpose of obtaining the initial estimates as follows:

$$= \frac{2.86\ (0.08)}{3.60\ (0.08) \times 214\ (0.08)} \times 10^6$$

$$= 3711 \pm 128\ M^{-1}$$

After that, the data from the experiment shown in Figure 6-7 were used for the purpose of obtaining an initial estimate of the backward constant (k_{-1}) as per Equation 6-11. Consequently, the slope, $0.099 \pm 0.025\ hr^{-1}$, in Figure 6-13 represents k_{-1} for 5-HMF binding to hemoglobin. This approach in estimating k_{-1} and k_1 was previously reported by (Ge 1997). The values of A and B are shown in Table 6-1. The initial estimate for k_1 was calculated using Equation 6-5:

$$= 3711\ (128)\ X\ 0.099\ (0.025)$$

$$= 367 \pm 93.6\ M^{-1}hr^{-1}$$

The same approach was used in obtaining initial estimates for the rate constants of 5-HMF binding to human serum albumin. The equilibrium between 5-HMF and albumin was achieved in the experiment shown in Figure 6-10. Consequently, the initial estimate of K_A for 5-HMF binding to human serum albumin was:

$$= \frac{0.09\ (0.03)}{6.87\ (0.03) \times 62.9\ (0.03)} \times 10^6$$

$$= 208 \pm 69\ M^{-1}$$

Plotting Equation 6-11, as shown in Figure 6-14, k_{-1} was obtained from the slope and estimated to be 0.61 ± 0.12 hr^{-1}. The values of A and B are shown in Table 6-2. Using Equation 6-5, k_1 was estimated

$$= 208\ (69)\ X\ 0.61\ (0.12)$$

$$= 127 \pm 49\ M^{-1}hr^{-1}$$

The initial estimates of the rate constants for both human hemoglobin and serum albumin binding were optimized through non-linear regression across various concentrations. The final parameter estimates of Equation 6-12 are shown in Table 6-3.

The final estimates of 5-HMF binding to hemoglobin were used to fit the experimental data at three different 5-HMF initial concentrations. The fitted lines vs. the observed data are shown in Figures 6-15, 6-16, 6-17.

When the natural logarithmic value for the adduct concentration yet to be formed , i.e. ln (Css-Ct), was plotted against the incubation time for 5-HMF with human hemoglobin and serum albumin, as shown in Figures 6-18 and 6-19, respectively, the observed rate constants (k_{obs}) were 0.194 ± 0.09 hr^{-1} and 0.66 ± 12 hr^{-1}, while the $t_{1/2}$ (=0.693/ k_{obs}) was equal to 3.58 hours and 1.1 hours for hemoglobin and albumin, respectively. k_{obs} is equivalent to the product of the forward and backward rate constants according to Equation 6-7. Consequently, the final estimate of the rate constants (k_1 and k_{-1}) were used to calculate k_{eq} for hemoglobin and albumin. As shown in Table 6-4, the estimated k_{eq} were similar to their corresponding k_{obs} values.

Table 6-1. Estimation of A and B for Hb-5-HMF adduct using Equation 6-11.

Time (hr)	**Free 5-HMF, [5-HMF](t) (μM)**	**Adduct Formed [Adduct](t) (μM)**	**Free Hb, [Hb](t) (μM)**	**"A" (K_A*[Hb](t) *[5-HMF](t)) - [Adduct](t)**	**"B" Δ[5-HMF](t)/ Δt (μM/hr)**
0	60.43	0	217.2		
0.4	58.75	1.68	215.5	47.1	4.59
1.2	55.53	4.90	210.6	43.7	3.86
3.0	49.03	11.4	199.2	37.0	3.75

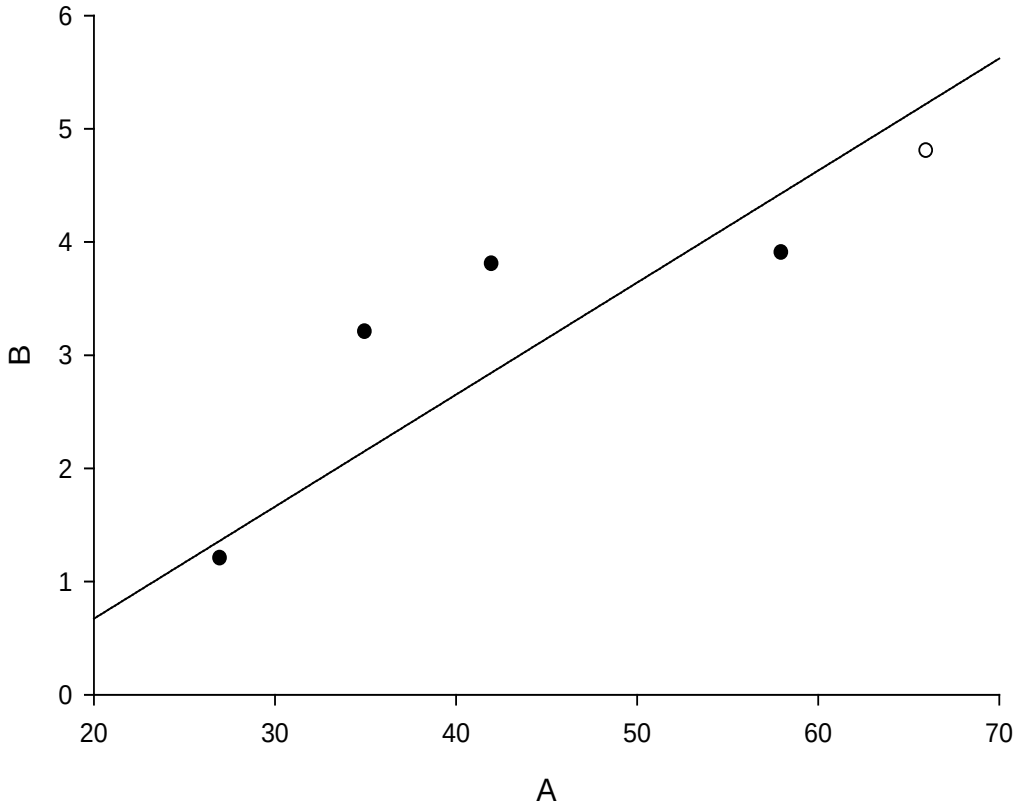

Figure 6-13. Initial estimate of k_{-1} for 5-HMF binding to hemoglobin using Equation 6-11.

Table 6-2. Estimation of A and B for HSA-5-HMF adduct using Equation 6-11.

Time (hr)	**Free 5-HMF, [5-HMF](t) (μM)**	**Adduct Formed [Adduct](t) (μM)**	**Free HSA, [HSA](t) (μM)**	**"A" (K_A*[HSA](t) *[5-HMF](t)) - [Adduct](t)**	**"B" Δ[5-HMF](t)/ Δt (μM/hr)**
0.2	19.7	0	63.0		
1.1	19.1	0.6	62.4	0.26	0.60
2.8	18.9	0.8	61.6	-0.31	0.17
5.2	18.7	1.0	60.5	-0.61	0.08

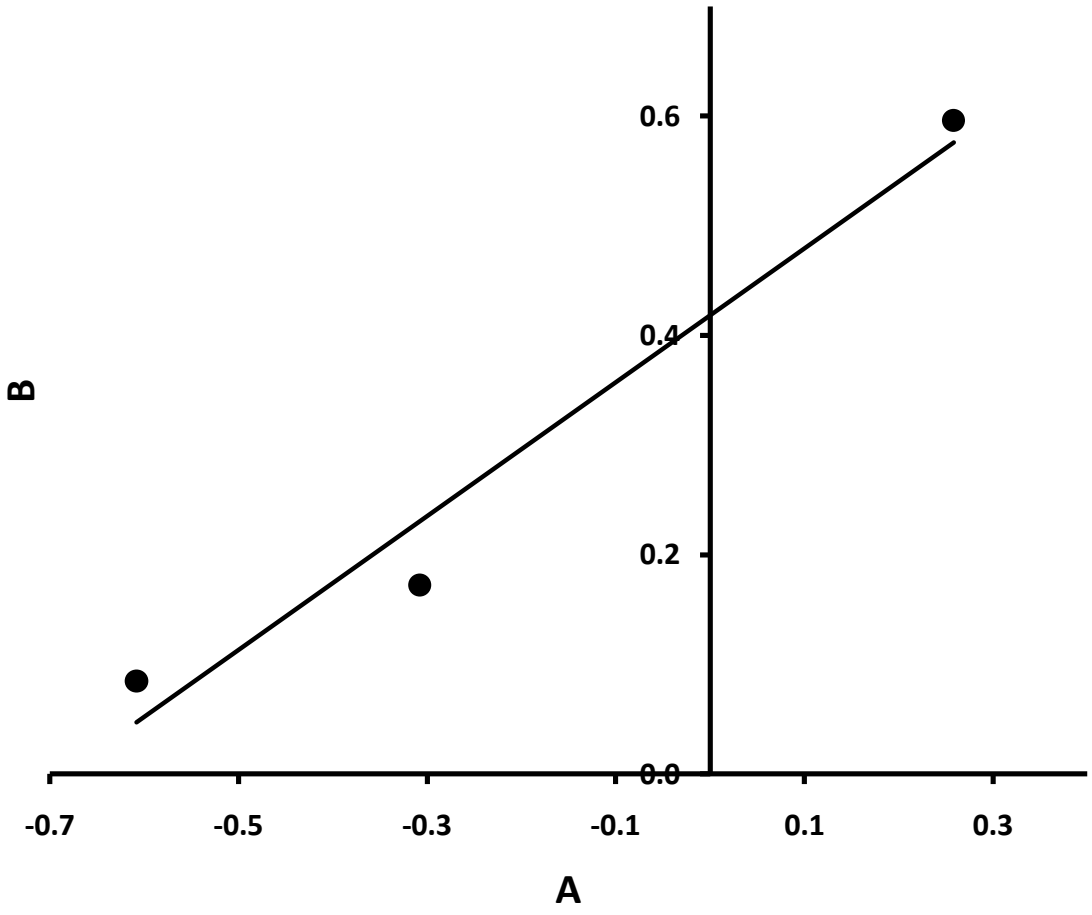

Figure 6-14. Initial estimate of k_{-1} for 5-HMF binding to albumin using Equation 6-11.

Table 6-3. Final model parameter estimates for 5-HMF with HSA and Hb.

	k_1 ($M^{-1}hr^{-1}$)	k_{-1} (hr^{-1})	K_A (M^{-1})	K_D (mM)
Human Serum Albumin	523 ± 274	0.769 ± 0.502	680 ± 569	1.5 ± 1.2
Human Hemoglobin	414 ± 35	0.107 ± 0.026	3879 ± 998	0.26 ± 0.07

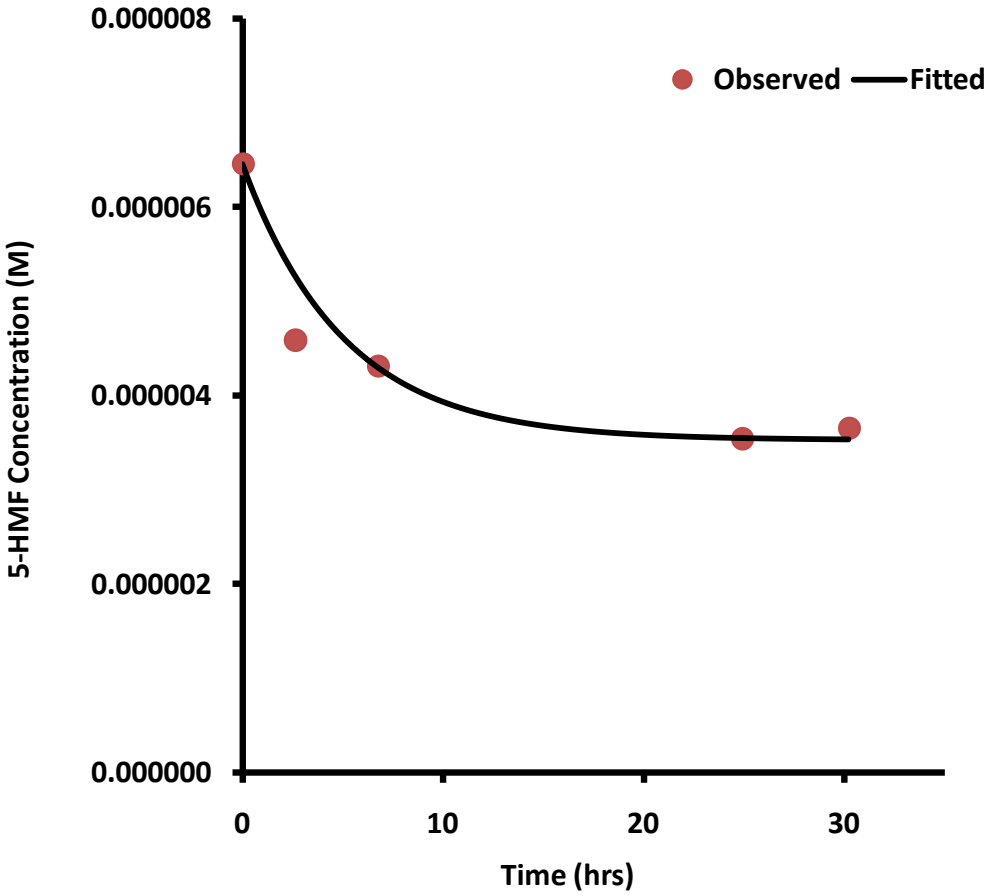

Figure 6-15. Observed vs. fitted concentration of 5-HMF (7.9 µM).

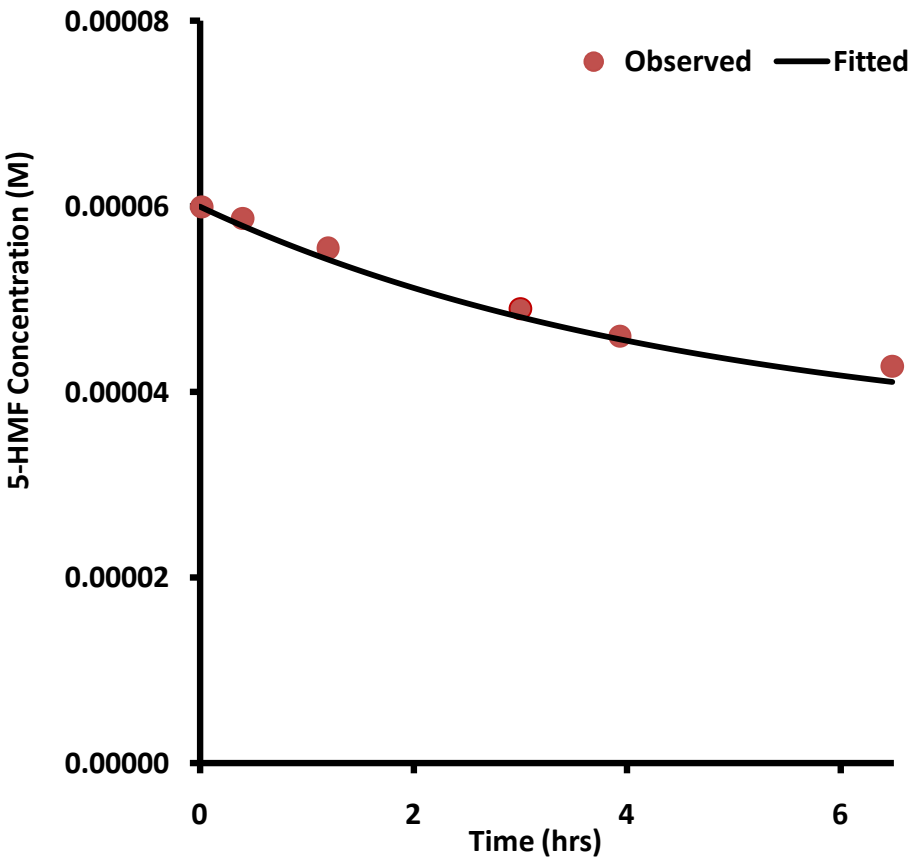

Figure 6-16. Observed vs. fitted concentration of 5-HMF (63 µM).

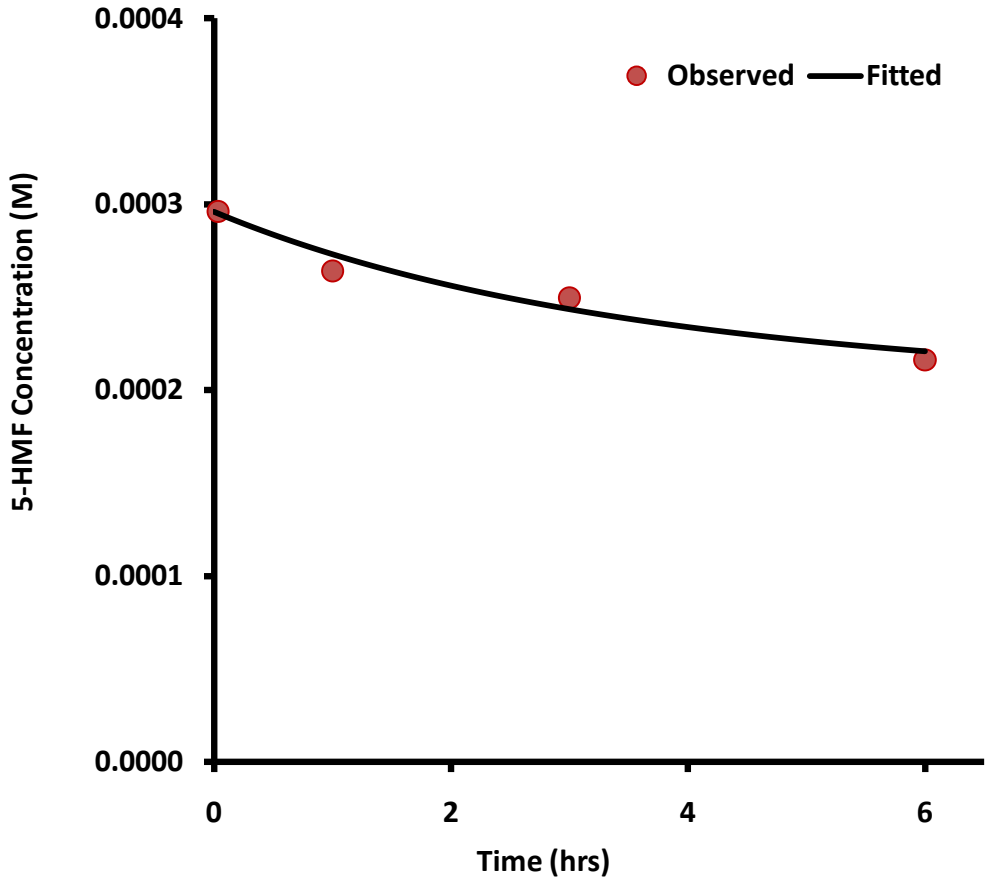

Figure 6-17. Observed vs. fitted concentration of 5-HMF (397 µM).

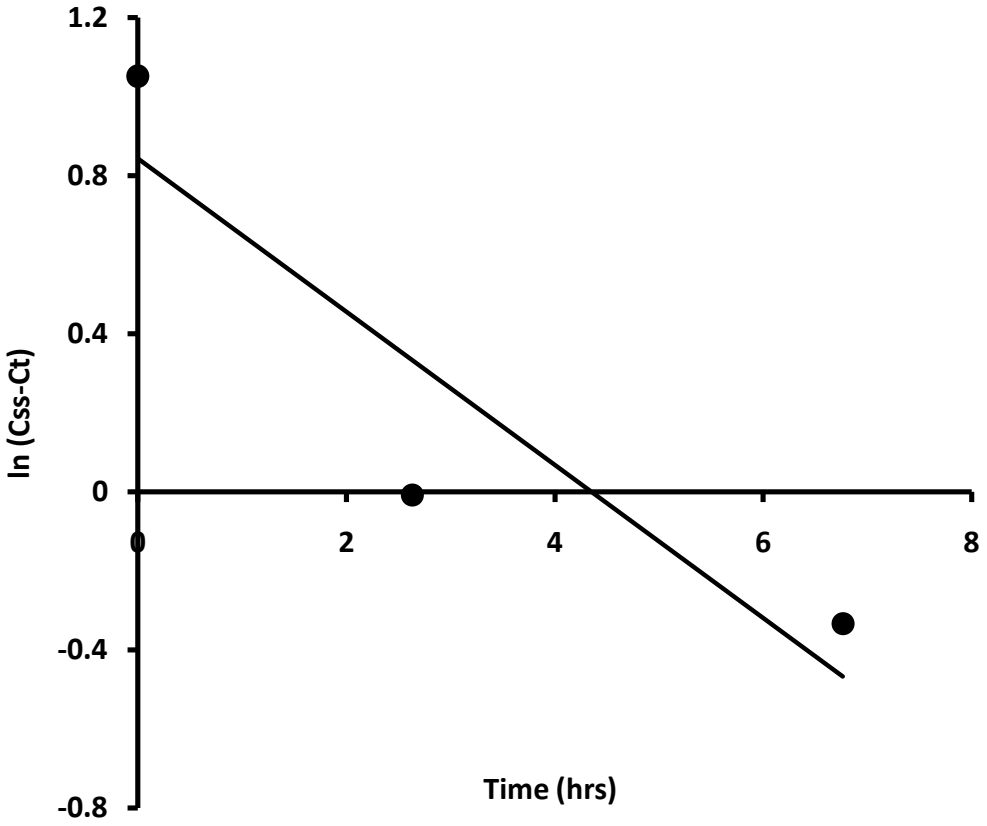

Figure 6-18. Apparent first-order decline in (Css-Ct) to estimate kobs for 5-HMF (7.9 μM) binding to hemoglobin (217 μM).

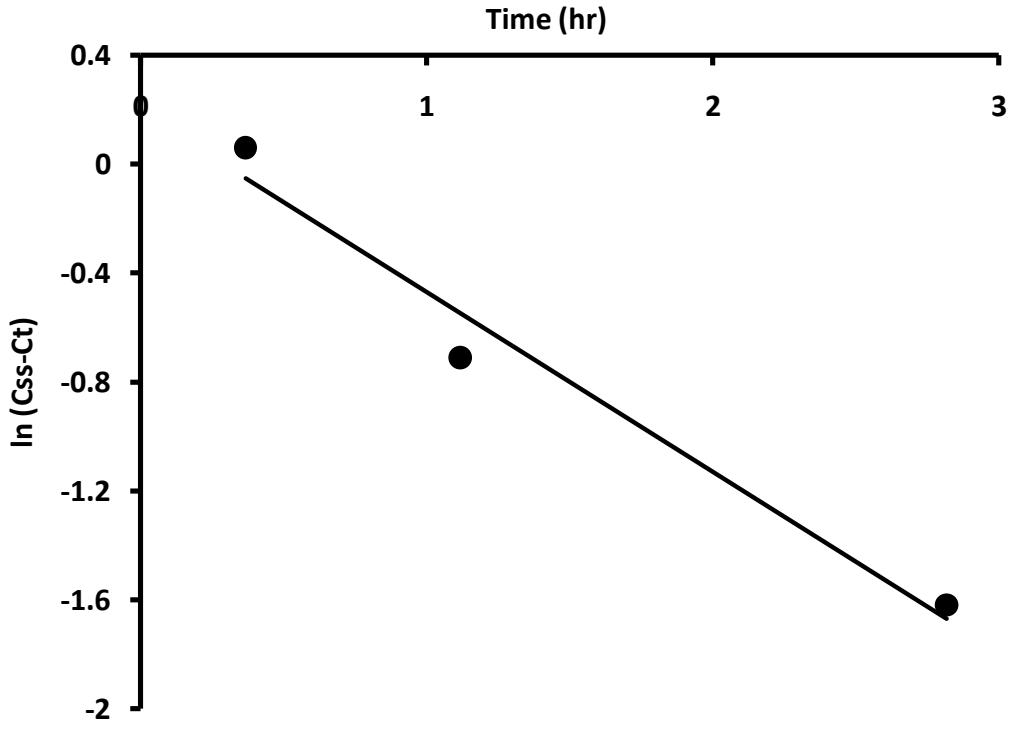

Figure 6-19. Apparent first-order decline in (Css-Ct) to estimate kobs for 5-HMF (19.8 μM) binding to human serum albumin (63 μM).

Table 6-4. Apparent first-order decline rate constant (SD) estimated from the data vs. that obtained from the model.

	Data k_{obs} (hr^{-1})	**Model k_{eq} (hr^{-1})**
Human Serum Albumin	0.66 (0.12)	0.80 (0.67)
Human Hemoglobin	0.19 (0.09)	0.20 (0.05)

6.3.3 Concentration-Dependency Studies

After correction for non-specific binding using the equations discussed in Section 6.2.5, specific binding to human hemoglobin and albumin was estimated, as summarized in Tables 6-5 and 6-7. Specific binding to hemoglobin and albumin was plotted against the unbound concentration, as shown in Figures 6-20 and 6-21. The data points represent the average of the duplicate samples and the error bars represent their associated standard deviation (hard to visualize due to their small value). The parameter estimates of 5-HMF- hemoglobin and 5-HMF-albumin binding models, are summarized in Tables 6-6 and 6-8 along with the standard error of these estimates.

Table 6-5. 5-HMF bound to hemoglobin at different initial 5-HMF concentrations ([Hb]= 217 µM, n=2 per concentration, mean (SD)).

Nominal 5-HMF Concentration (µM)	Ultrafiltrate (UC) Concentration (µM)	NSB (µM)	Specific Binding (µM)	Fraction Specifically Bound%	Bound 5-HMFmol/ Hbmol
4.76	3.12	0.758	0.882	22.1	0.004
14.3	8.72 (0.037)	1.85	3.70 (0.04)	29.8	0.017 (0.0002)
42.8	11.7 (0.279)	8.80	22.3 (0.28)	65.6	0.103 (0.001)
119	62.9 (0.983)	10.5	45.5 (0.98)	42.0	0.209 (0.005)
357	224 (2.60)	29.1	104 (2.6)	31.8	0.480 (0.012)
714	487 (1.34)	64.3	163 (1.3)	25.1	0.751 (0.006)
5952	4170	1455	328	7.29	1.51

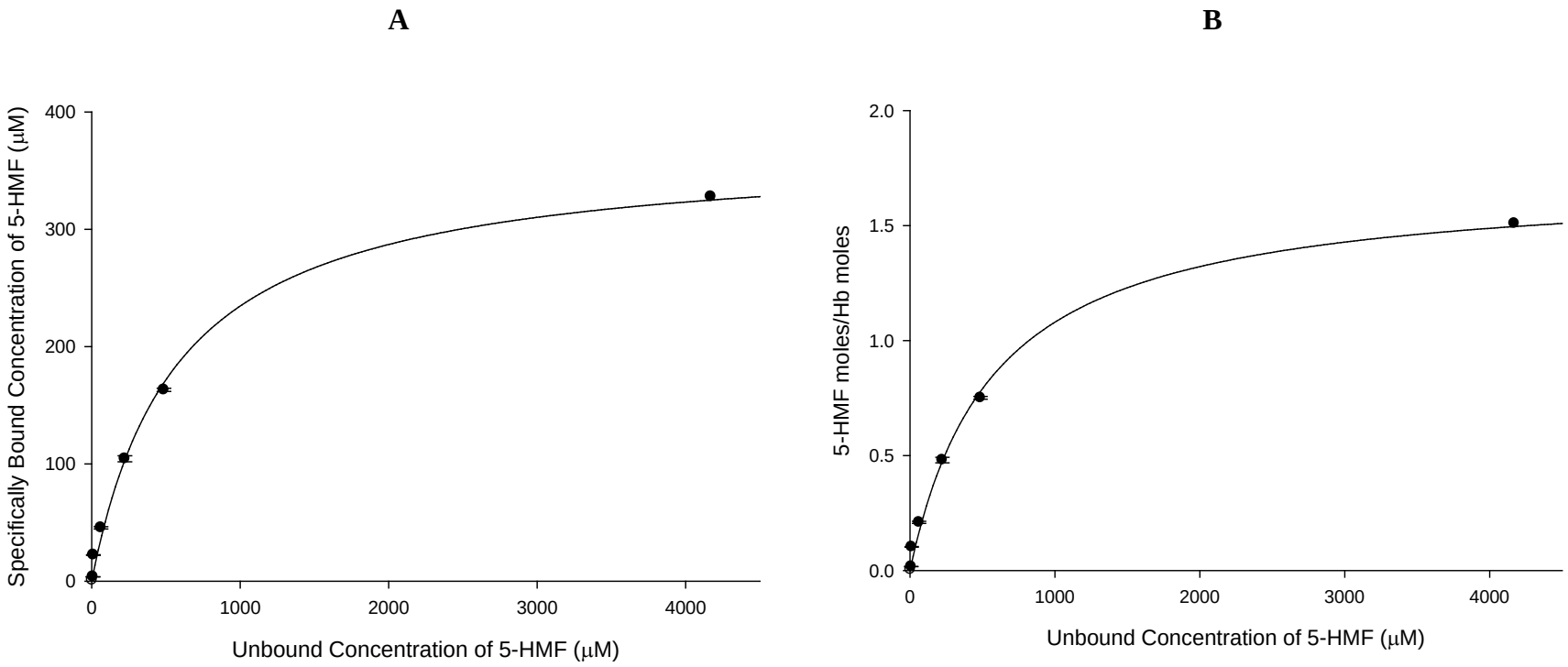

Figure 6-20. 5-HMF specific binding to human hemoglobin.

Table 6-6. Final parameter estimates of 5-HMF binding to hemoglobin (217 µM).

Parameter	Value (SE)	
	Concentration (µM)	**Molar Ratio**
$\mathbf{B_{max}}$	370 (6.93)	1.7 (0.03)
$\mathbf{K_D}$ **(µM)**	577 (32.0)	577 (32.0)
$\mathbf{r^2}$	0.993	0.993

Table 6-7. Concentration-dependency of 5-HMF binding to human serum albumin. ([HSA]= 202 µM, n=2 per concentration, mean (SD)).

Nominal 5-HMF Concentration (µM)	Ultrafiltrate (UC) Concentration (µM)	NSB (µM)	Specific Binding (µM)	Fraction Specifically Bound%	Bound 5-HMFmol/ HSAmol
12	8.8 (0.2)	1	2.9 (0.07)	32	0.014 (0.0003)
37	33 (1)	2	1.7 (0.05)	5.0	0.008 (0.0003)
74	66 (1)	4	3.7 (0.07)	5.6	0.018 (0.0003)
222	177 (6)	12	33 (1.1)	19	0.17 (0.005)
667	521 (52)	36	110 (11)	21	0.55 (0.05)
2000	1588 (189)	107	306 (36)	19	1.5 (1.8)

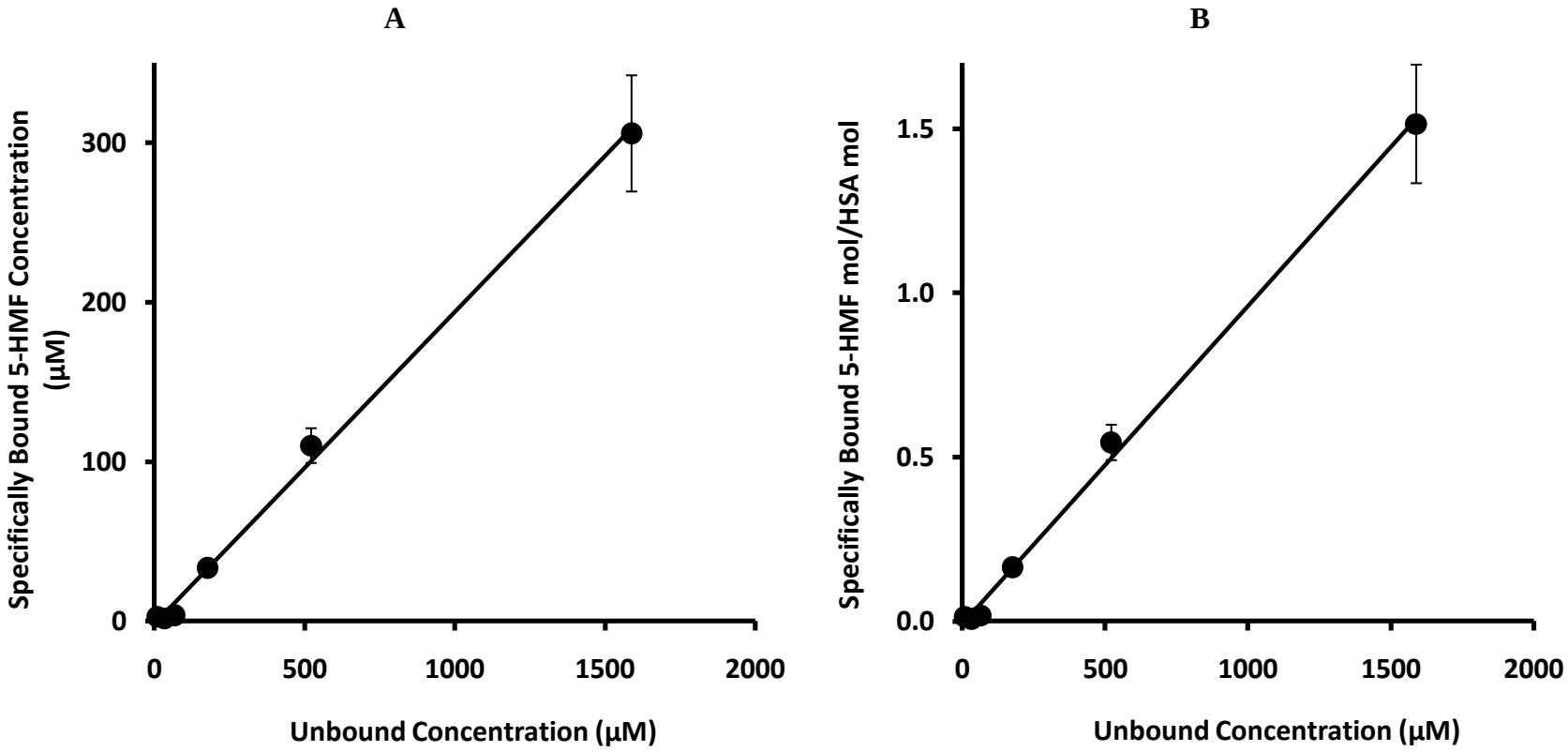

Figure 6-21. 5-HMF specific binding to human serum albumin.

Table 6-8. Final parameter estimates of 5-HMF binding to human serum albumin (202 µM).

Parameter	Value (SE)	
	Concentration (µM)	**Molar Ratio**
SB	0.197 (0.005)	0.001 (0.00002)
Y_0 (µM)	-1.82 (3.37)	-0.009 (0.016)
r^2	0.998	0.998

6.4 Discussion and Conclusions

Under the experimental conditions of the binding experiments, 5-HMF was chemically stable at 37 °C for at least 30 hours – allowing the assessment of time-dependent binding. On the other hand, binding of 5-HMF to both proteins, namely Hb and HSA, showed the expected time dependency, reflecting the "transiently covalent" nature of this Schiff base binding reaction. The time-dependency studies showed that the binding of 5-HMF to its target site of action, Hb, was characterized by a time-dependent binding reaction with a high affinity and selectivity to Hb relative to HSA. Hb had over 5-fold higher equilibrium association constant for 5-HMF than that with human serum albumin, as shown in Table 6-3, indicating that 5-HMF is a high affinity substrate for Hb.

Upon the comparison of the estimated rate constants with those estimated for glucose binding to hemoglobin (Higgins 1981), as shown in Table 6-9, 5-HMF has a faster rate constant of adduct formation (k_1= 0.9 $M^{-1}hr^{-1}$ for glucose vs. 414 $M^{-1}hr^{-1}$ for 5-HMF). In contrast, 5-HMF has a slower rate constant of the adduct degradation (k_{-1}= 0.33 hr^{-1} for glucose vs. 0.11 hr^{-1} for 5-HMF) and this coincides with the duration of action shown in Figure 1-8, Chapter 1. In addition, the affinity constant (K_D) for 5-HMF binding to Hb is 10-fold higher than that observed for a typical aromatic aldehyde (Zaugg 1977), listed in Table 6-9, which is consistent with the fact that 5-HMF has a better *in-vitro* pharmacological activity when compared to other structurally-related aromatic aldehydes (Safo 2004). Besides, because 5-HMF has a faster rate constant of Hb-adduct formation than glucose, while it has a slower rate constant of Hb-adduct degradation, 5-HMF has more than a 1,000-fold larger association constant, i.e., much higher affinity for Hb than glucose. Again, this is consistent with the observation that aromatic aldehydes (similar to 5-HMF) have higher affinity than aliphatic aldehydes (glucose) (Zaugg 1977).

At a relatively low concentrations of human serum albumin, 63 µM, only a small fraction of 5-HMF was bound to serum albumin (approximately 20% of total binding). On the other hand, non-specific binding was quite high (approx. 80% of total binding), which may have prevented better characterization of HSA binding to 5-HMF. However, at a higher human serum albumin concentration, 202 µM, binding to human serum albumin showed a non-saturable pattern. Abdulmalik et al, implied that 5-HMF does not have significant binding to plasma proteins (Abdulmalik 2005). This might be due to the fact that serum albumin has a lower physiological blood concentration compared to hemoglobin (0.6 vs. 2.3-5.3 mM), which makes hemoglobin have higher capacity of binding than that of serum albumin in addition to its higher affinity.

Both time-dependency and (steady-state) concentration-dependency studies resulted in similar affinity (K_D) estimates for Hb (0.26 mM vs. 0.59 mM). In addition, the B_{max} value for Hb is consistent with approximately two moles of 5-HMF bound per mole of hemoglobin. This observation was expected, since each Hb molecule has two 5-HMF binding sites, one at each α-chain of the hemoglobin molecule, i.e., α-valine (Safo 2004).

Table 6-9. Hemoglobin binding rate constants (SD) to different substrates.

Substrate	k_1 ($M^{-1}hr^{-1}$)	k_{-1} (hr^{-1})	K_D (mM)	Reference
Aliphatic aldehydes (Typical)			14	(Zaugg 1977)
Aromatic aldehydes (Typical)			5	(Zaugg 1977)
Glucose	0.9 (0.2)	0.33 (0.04)	367 (91)	(Higgins 1981)
5-HMF	414 (35)	0.11 (0.03)	0.26 (0.07)	

As shown in Table 6-4, the predicted first rate-order equilibrium constants for 5-HMF binding with Hb and HSA, (k_{eq}) were 102% and 121% of the observed constants (k_{obs}), respectively, obtained from the decline in the concentration of the adduct to be formed (Css-Ct). A good estimate of k_{eq}, is expected if the initial Hb concentration is much higher than 5-HMF concentration; thus, the free Hb concentration remains relatively constant during the binding/unbinding reaction.

At the physiological Hb concentration in whole blood, the presumed effective concentrations of 5-HMF (i.e., 1-2 mM, exceeding K_D, i.e., beginning to saturate Hb binding sites) are expected to show fast association with, but slow dissociation from Hb, resulting in prolonged persistence of the Hb adduct ($t_{1/2}^{eq}$ of 0.7 hrs). Thus, this unique drug-receptor interaction may lead to a prolonged *in-vivo* PD effect.

Overall, these *in-vitro* findings are consistent with the results from an *in-vivo* PK study in transgenic mice, which received single, oral 5-HMF doses of 50 to 200 mg/kg (Abdulmalik 2005). There was an initial lag-time observed between *in-vivo* plasma concentrations of 5-HMF and the "modified" Hb (adduct) concentrations, semi-quantitatively determined by Hb gel electrophoresis – consistent with the time-dependent binding of 5-HMF to hemoglobin, as shown in Figure 1-10, Chapter 1.Moreover, the results of an accompanying *in-vitro* study, assessing hypoxia-induced RBC sickling after 1 hour pre-incubation and immediate addition of 5-HMF (5 mM) demonstrated that pre-incubation enhanced the antisickling effects of 5-HMF relative to direct addition, as shown in Figure 1-8, Chapter 1 - consistent with time depending binding and an equilibration half-life of 0.7 hours, as reported above.

CHAPTER 7

IN-VITRO DISPOSITION IN HUMAN BLOOD

7.1 Introduction

As discussed in Chapters 5 and 6, 5-HMF is subject to human hemoglobin and serum albumin binding, as well as being metabolized in human RBCs. Consequently, studies were carried-out to investigate 5-HMF concentration changes in the presence of blood proteins and enzymes at their physiological concentration. The studies were performed in RBC hemolysate suspension and in whole blood. Models were built combining both binding and metabolism processes to examine their ability in predicting the free concentration of 5-HMF and the fraction bound to hemoglobin, its site of action. In addition, studies were designed to verify whether the validated HPLC method in Chapter 3 is measuring the total concentration of 5-HMF (bound and unbound fractions) or only the free (unbound) fraction. Moreover, this project aimed to explore the sensitivity of 5-HMF metabolism to inhibitors in order to estimate the contribution of RBC metabolism to the observed 5-HMF disappearance rate in human blood.

7.2 Methods

7.2.1 Materials and Reagents

1. Milli-Q® Water (Virginia Commonwealth University, PK/PD Laboratory).
2. 4-Methylpyrazole (4-MP) Solution:

   - 4-MP, 99% (Sigma-Aldrich, Milwaukee, WI).

   - Milli-Q® water (Virginia Commonwealth University, PK/PD Laboratory).
3. Tetraethylthiuram Disulfide (Disulfiram) Solution:

   - Disulfiram, purum 97% (Sigma-Aldrich, Milwaukee, WI).

   - BD Gentest™ TRIS buffer 0.5 M, pH 7.5 (BD Bioscience, San Jose, CA).
4. Human Blood:

   From a single female caucasian individual.
5. Phosphate-Buffered Saline (PBS), pH 7.4:

   - Phosphate-buffered saline (PBS) tablets, pH 7.4 (Sigma, St. Louis, MO).

   - Milli-Q® water (Virginia Commonwealth University, PK/PD Laboratory).
6. Phosphate-Buffered Saline (PBS), pH 7.4:

   -Sodium phosphate dibasic (Sigma, St. Louis, MO).

   -Potassium phosphate (Sigma, St. Louis, MO).

   -Sodium chloride (Sigma, St. Louis, MO).

   -Potassium chloride (Sigma, St. Louis, MO).

   -Milli-Q® water (Virginia Commonwealth University, PK/PD Laboratory).

7. 5-Hydroxymethyl-2-furfural (5-HMF) Solution:

   - 5-Hydroxymethyl-2-furfural (Sigma, St. Louis, MO).

   - Milli-Q® water (Virginia Commonwealth University, PK/PD Laboratory).

8. Mobile Phase for 5-HMF Assay Method in Plasma and RBCs:

   - 93.5% Milli-Q® water (Virginia Commonwealth University, PK/PD Laboratory).

   - 6.2% Methanol, HPLC grade (Burdick and Jackson, Morristown, NJ).

   - 1% Acetic acid glacial, > 99% (Sigma, Milwaukee, WI).

   - 0.3 % Tetrahydrofuran HPLC grade (Burdick and Jackson, Morristown, NJ).

9. SPE Conditioning:

   - Methanol, HPLC grade (Burdick and Jackson, Morristown, NJ).

   - Milli-Q® water (Virginia Commonwealth University, PK/PD Laboratory).

10. SPE Washing Solution: Phosphate-buffered Saline (PBS), pH 7.4:

    - Phosphate-buffered saline (PBS) tablets, pH 7.4 (Sigma, St. Louis, MO).

    - Milli-Q® water (Virginia Commonwealth University, PK/PD Laboratory).

11. SPE Eluting Solution: 50% Methanol:

    - Methanol, HPLC grade (Burdick and Jackson, Morristown, NJ).

    - Milli-Q® water (Virginia Commonwealth University, PK/PD Laboratory).

7.2.2 Equipment

1. 25-µl, 50-µl, and 250-µl positive displacement pipettes and corresponding pipette tips (Microman, Rainin Instruments, Oakland, CA).
2. 10-µl, 100-µl, and 1000-µl VWR pipettes and corresponding pipette tips (VWR, West Chester, PA).
3. 0.5-5 ml Finnpipette (Thermo Scientific, Waltham, MA).
4. Vortex (Vortex-Genie, VWR, West Chester, PA).
5. Eppendorf vials (VWR, West Chester, PA).
6. Sonicator (American Brand Products C6450-11, VWR, West Chester, PA).
7. pH meter (Corning, Glendale, AZ).
8. Balance (Fisher Scientific A 250, Pittsburgh, PA).
9. Centrifuge 5804-R (Eppendorf, Hauppauge, NY).
10. Amicon® Ultra-4 centrifugal filter units with Ultracel-10 membrane (Millipore, Billerica, MA).
11. Oasis HLB cartridge, 1 cc/ 30 mg (Waters).
12. Glass vials with caps, 1 ml (Waters, Milford, MA).
13. UV detector (Shimadzu, AV-10, Columbia, MA).
14. C_{18} Zorbax Rx column, 4.6 X 150 mm (Agilent, Santa Clara, CA).
15. C_{18} guard column, 12.5 mm x 4.6 mm (Agilent, Santa Clara, CA).
16. 717 plus autosampler (Waters, Milford, MA).
17. 600 Multisolvent controller (Waters, Milford, MA).
18. Empower 2 software (Waters, Milford, MA).
19. Forma Scientific incubator.

7.2.3 Solution Preparation

- Mobile Phase for 5-HMF Assay Method in Plasma and RBCs (1 L)

  935 ml water, 62 ml methanol, 10 ml acetic acid glacial, and 3 ml tetrahydrofuran were mixed to prepare the mobile phase.

- 5-Hydroxymethyl-2-furfural Solution (5-HMF) Stock Solution (381 mM)

  48 mg of 5-hydroxymethyl-2-furfural, M.W.: 126.11 Da, was dissolved in 1 ml of PBS.

- Phosphate-buffered Saline (PBS), pH 7.4

  One tablet of phosphate-buffered saline was added to 200 ml of water.

- SPE Eluting Solution: 50% Methanol

  25 ml of methanol was mixed with 25 ml of water.

7.2.4 Procedures

Human blood was collected from a healthy female volunteer using heparinized vacutainer.

7.2.4.1 Total vs Free 5-HMF Concentration in Hemolyzed RBCs.

After centrifuging the whole blood, plasma layer was removed and RBCs were washed with PBS. RBCs were re-suspended in Milli-Q® water (0.4 RBCs: 0.6 water) and hemolyzed by centrifugation. Concentrated PBS mixture was added to the hemolyzed RBCs together with 5-HMF to achieve a concentration of 2 mM of 5-HMF. The suspension was then incubated at 36.5±1 °C for approximately 3 hours. Two sets, each with duplicate samples, taken at different time points, were analyzed by the validated HPLC method after extracting the samples using either solid phase extraction as described in Chapter 3 or by ultrafiltration using Amicon® Ultra.

7.2.4.2 5-HMF Metabolism in Hemolyzed RBCs.

Hemolyzed RBCs were processed using the same approach stated above. However, water was replaced by 4-methylpyrazole and disulfiram solution in Milli-Q® water (0.4 RBCs: 0.6 inhibitors solution). The final concentrations of 4-methylpyrazole and disulfiram were 375 µM and 40.5 µM, respectively. After incubation for 30 minutes, 5-HMF was added to the mixture to achieve a concentration of 2 mM and the suspension was incubated at 36.5±1 °C for approximately 3 hours. Duplicate samples, taken at different time points, were analyzed by the validated HPLC method using solid phase extraction as described in Chapter 3.

7.2.4.3 5-HMF in Whole Blood

5-HMF was incubated in whole blood and RBC suspension at concentrations of 2 mM and 0.3 mM at 36.5 ± 1 °C over 2 hours. Duplicate samples, taken at different time points, were analyzed by the validated HPLC method after separating plasma and RBCs using centrifugation for 12 minutes at 3500 rpm, 3 °C.

7.2.5 Data Analysis and Modeling Assumptions

The first-order rate constants (k) for the disappearance of 5-HMF in different studies were obtained as the negative value of the slope when the natural logarithmic values of 5-HMF concentrations were plotted vs time. Consequently, the half-life ($t_{1/2}$) was estimated using Equation 7-1:

$$t_{1/2} = \frac{0.693}{k} \quad \text{Equation } 7-1$$

These rate constants and half-lives were compared to:

1. Verify the fraction of 5-HMF measured by the validated HPLC method, where the samples were extracted using solid phase extraction. Only the unbound fraction of 5-HMF was assumed to survive sample extraction using ultrafiltation.
2. Investigate the sensitivity of 5-HMF metabolism in RBCs to inhibition by disulfiram and 4-methylpyrazole.
3. Explore any difference in 5-HMF decline-rate between plasma and RBCs.

In the non-linear regression carried-out for 5-HMF disappearance in human blood, the concentration of hemoglobin was fixed, considering that the average hematocrit in females is 42% and is associated with an Hb concentration of 14 g/dl (Dixon 1997) (Rhoades 1996). In this study, the hematocrit was adjusted to 40% and the Hb concentration was assumed to be 13.3 g/dl. Having a molecular weight of 64,677 g/mol, the concentration of Hb in this study was equivalent to 2.06 mM.

The intrinsic clearance was estimated in Chapter 5 as 0.35 ml/min/ml RBCs, which is equivalent to 21 ml/hr/ml RBCs. In this part of the research project, studies were carried-out in whole blood or in RBCs suspension. Hence, the RBCs intrinsic clearance was diluted with PBS or with plasma. With the RBCs accounting for approximately 40% in these matrices, the metabolic activity of the enzymes was decreased by a factor of 2.5. Accounting for this dilution factor, the intrinsic clearance was scaled by the volume of RBCs in the body resulting in a metabolic rate constant of 8.3 hr^{-1}, which was used as an initial model parameter. The data of the ultrafiltrate of the RBCs hemolysate was selected for modeling purposes since it is believed to reflect the free fraction of 5-HMF.

7.2.6 Modeling

In blood, 5-HMF is subject to simultaneous hemoglobin binding and enzyme metabolism in RBCs, as shown in Figure 7-1. Considering these processes, Equation 7-2 was used to simulate the change of free 5-HMF in RBCs over time as follows:

$$\frac{d[5-HMF]}{dt} =$$

$$-k_{met}\,[5HMF](t) + k_{-1} \times [Adduct](t) - k_1 \times [5HMF](t) \times [Hb](t) \ldots\ldots\ldots \text{Equation } 7-2$$

where

$[5HMF](t)$: the concentration of free 5-HMF at time (t)

$[Protein](t)$: the concentration of free protein at time (t)

$[Adduct](t)$: the concentration of the adduct between 5-HMF and the protein at time (t)

k_{met}: the metabolic rate constant

Moreover, 5-HMF might be prone to binding to RBCs membrane. Hence, a factor was added to account for this binding in the initial concentration of 5-HMF available for hemoglobin binding and metabolism in RBCs. This value was estimated using the difference between the nominal and the observed initial 5-HMF concentration. The simulation was performed assuming four scenarios:

Scenario (1): 5-HMF binding to hemoglobin is the sole contributor to 5-HMF disappearance over time.

Scenario (2): Concurrent metabolism and binding of 5-HMF contribute to 5-HMF disappearance over time.

Scenario (3): In the third scenario, the metabolic rate constant was re-estimated since it is assumed to involve higher inter-individual variability than hemoglobin binding.

Scenario (4): In whole blood: in addition to hemoglobin binding and RBC metabolism, 5-HMF can bind to serum albumin. Consequently, a second term in the initial conditions of the model was added to account for human serum albumin binding.

The parameters used in the simulation are summarized in Table 7-1. The model parameters were used in the simulations of 5-HMF free concentration in RBC hemolysate suspension and whole blood using non-linear regression of Equation 7-2. Scientist non-linear regression models are shown in Appendix C.

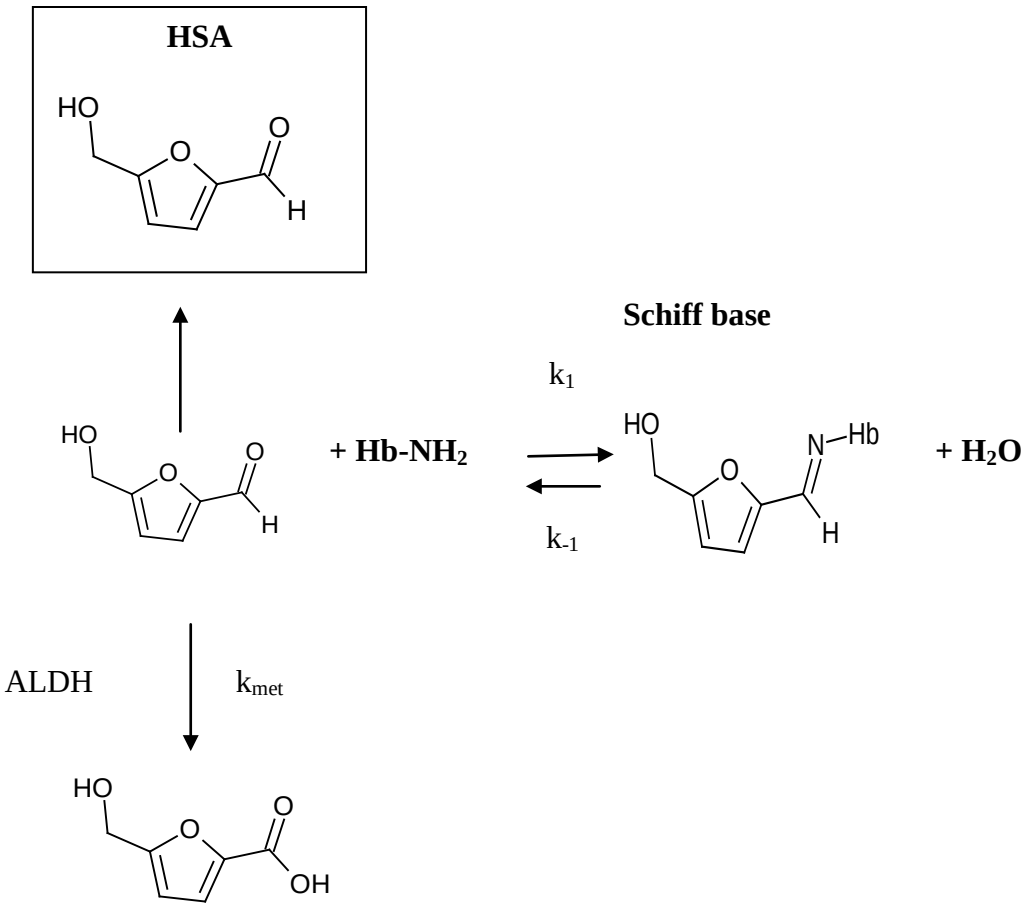

Figure 7-1. Concurrent 5-HMF binding and metabolism in blood.

Table 7-1. Model parameters.

Parameter	Scenario (1)	Scenario (2)	Scenario (3)	Scenario (4)
HB0 (M)	0.00206	0.00206	0.00206	0.00206
HMF0 (M)	0.002	0.002	0.002	0.002, 0.0003
k_1 ($M^{-1}hr^{-1}$)	414	414	414	414
k_{-1} (hr^{-1})	0.107	0.107	0.107	0.107
k_{met} (hr^{-1})	0	8.3	0.174	0.174
k_{hsa}	0	0	0	0.2

7.3 Results

The concentrations of 5-HMF over time in the RBC hemolysates, which were analyzed using solid phase extraction and by ultrafiltration, are shown in Figure 7-2. In addition, the concentrations of 5-HMF in the presence of inhibitors, are shown in Figure 7-3. The concentration of 5-HMF in the samples prepared by ultrafiltraton and that prepared by solid phase extraction were found to be similar. The same was observed when 5-HMF concentration was compared in the presence of inhibitors and in their absence. In addition, the concentration of 5-HMF over time when incubated in whole blood is shown in Figures 7-4 and 7-5. For all of these studies, the first-order disappearance rate constant and the half-life are summarized in Table 6-2.

The simulation for hemoglobin binding using the physiological concentration of hemoglobin is shown in Figure 7-7. When the metabolism process was added to the process, the fitted line underestimated the observed concentrations as shown in Figure 7-8. Upon optimizing the metabolic rate constant, the k_{met} was estimated as 0.174 ± 0.047 hr^{-1} and the fit is shown in Figure 7-9.

When the optimized metabolic and binding parameters were used in the simulation of 5-HMF in whole blood, it fitted better to the data of higher 5-HMF concentration, 2 mM, than that of the lower concentration, 0.3 mM, as demonstrated in Figures 7-10 and 7-11.

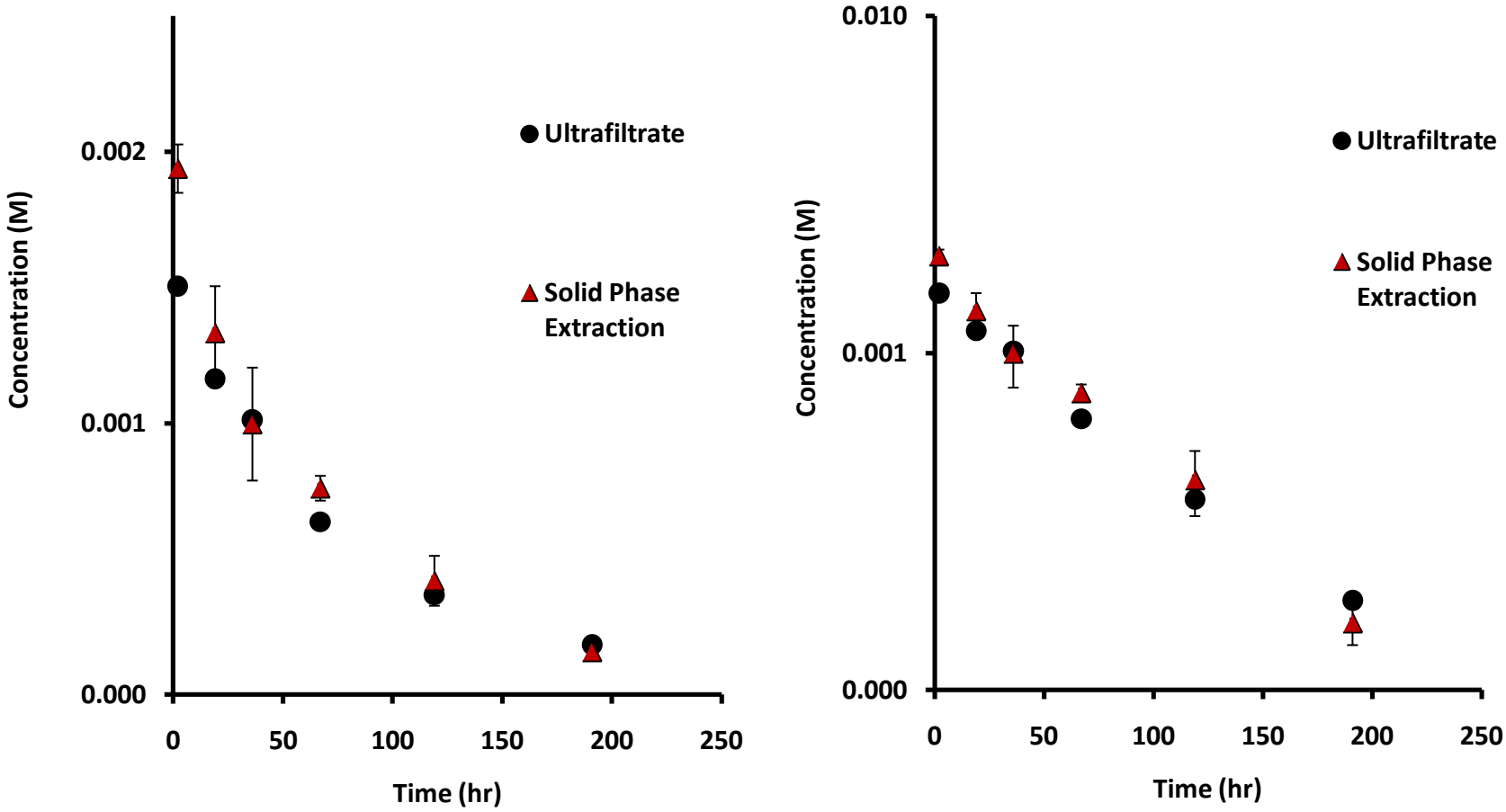

Figure 7-2. Decline in 5-HMF concentration (2 mM) in RBC hemolysate measured after SPE or ultrafiltration.

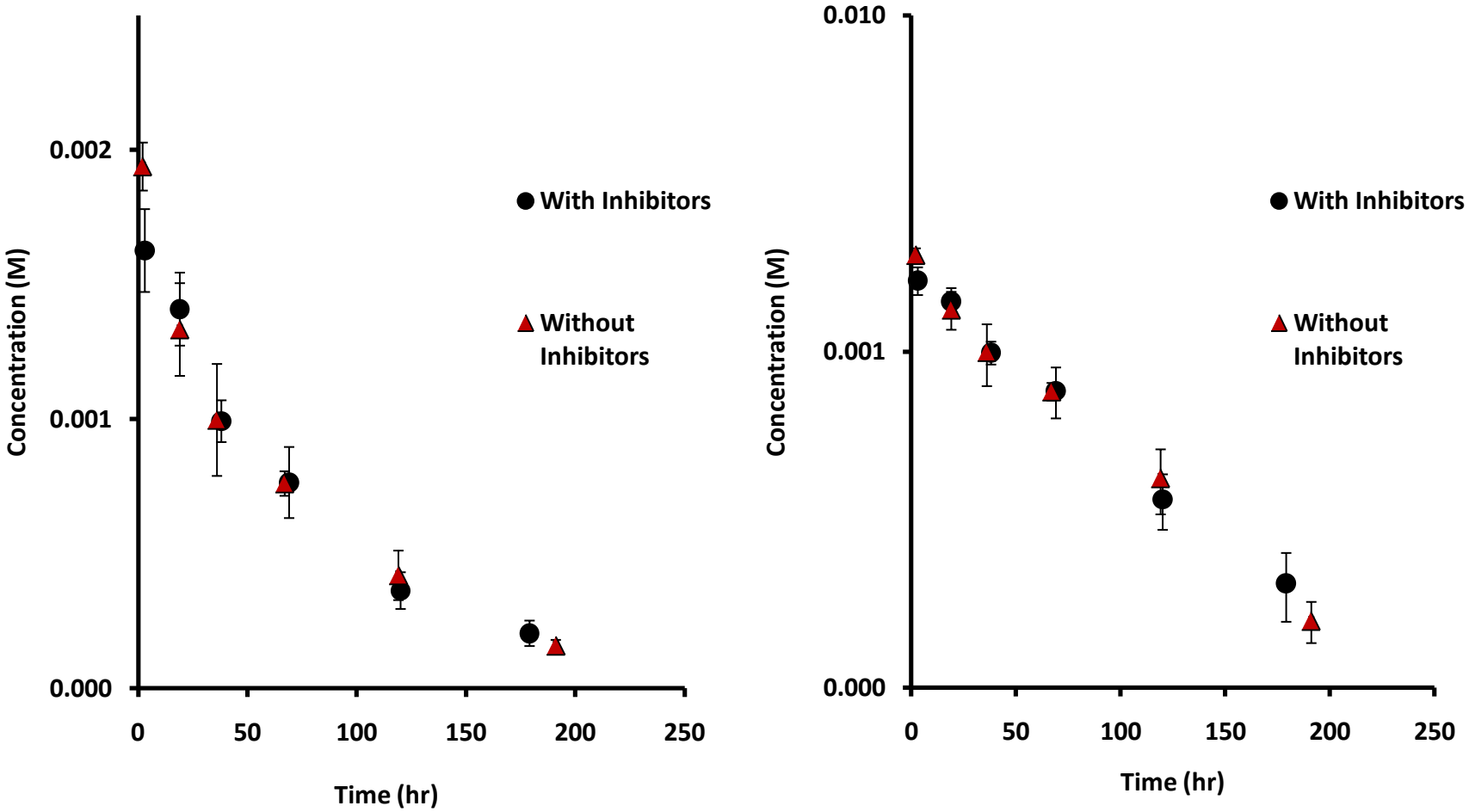

Figure 7-3. Decline in 5-HMF concentration (2 mM**)** in RBC hemolysate in the presence or absence of inhibitors.

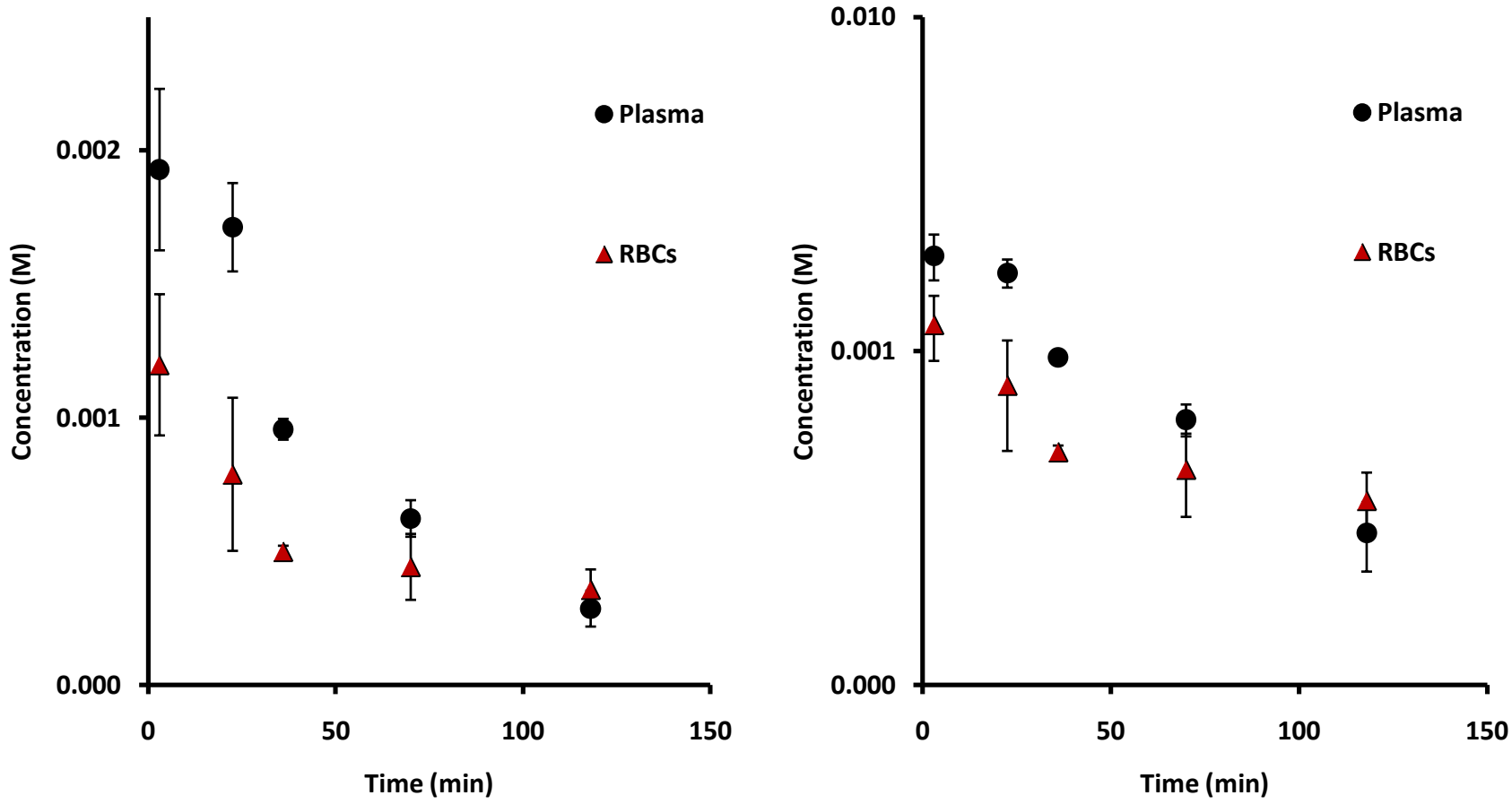

Figure 7-4. Decline in 5-HMF concentration (2 mM) in whole blood.

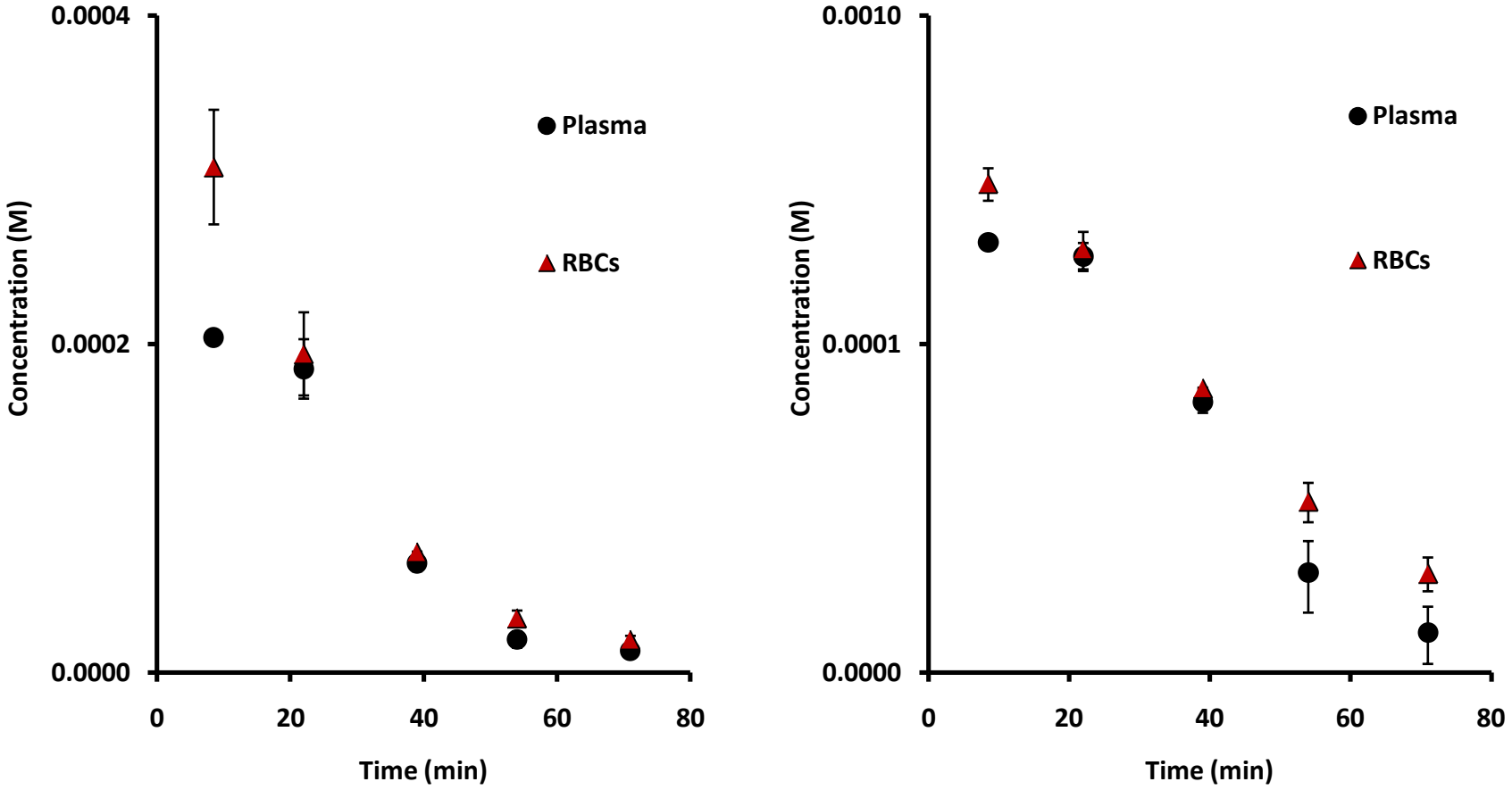

Figure 7-5. Decline in 5-HMF concentration (0.3 mM) in whole blood.

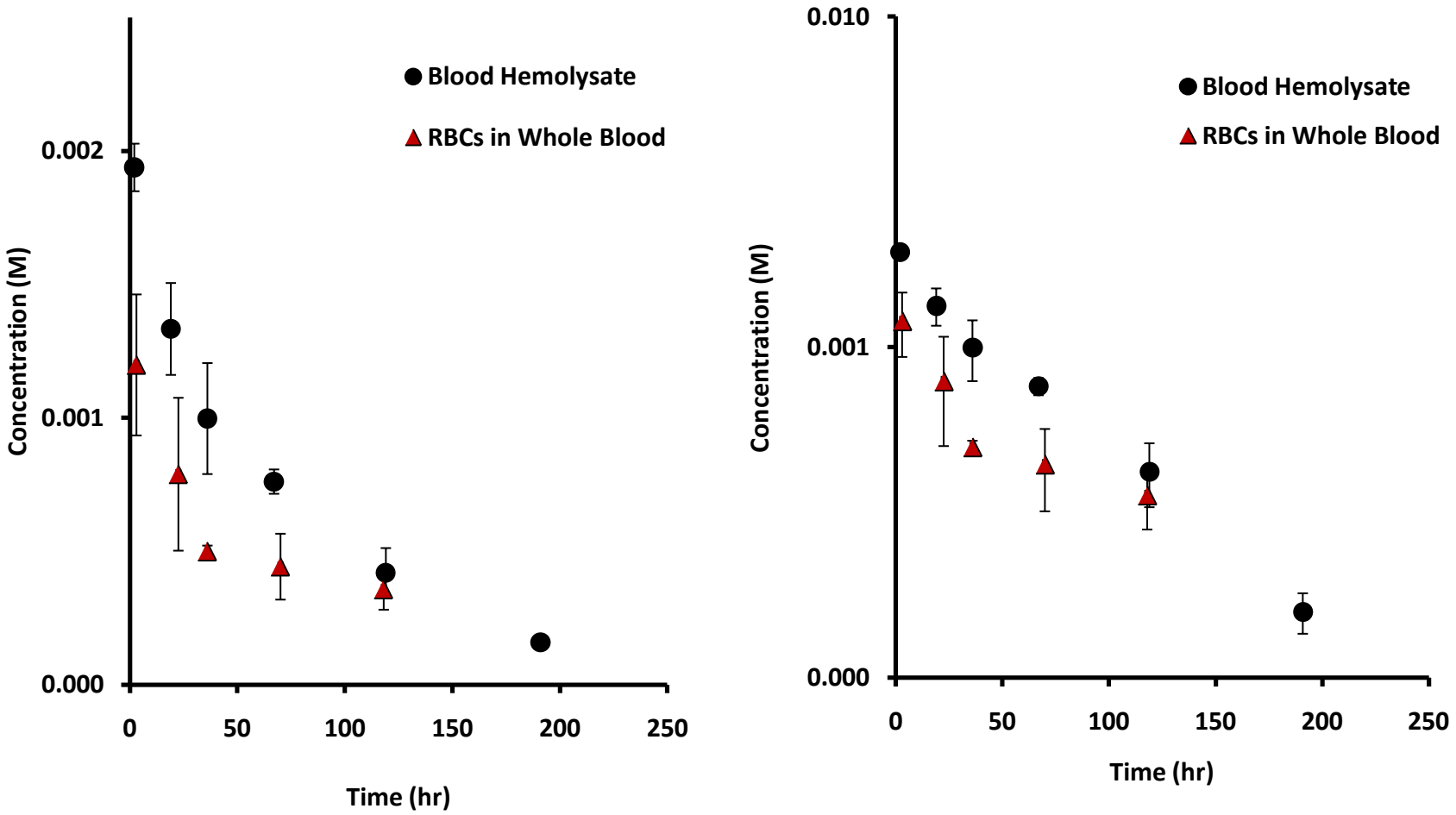

Figure 7-6. Decline in 5-HMF concentration (2 mM) in RBCs of whole blood and RBCs hemolysate suspension.

Table 7-2. Disappearance rate constants (SD) and t1/2 of 5-HMF in various matrices.

Matrix	Sample Preparation	Presence of Inhibitors	k (hr^{-1})	$t_{1/2}$ (hour)	r^2
Hemolysate Suspension (2 mM)	Ultrafiltration	Absent	0.67 (0.02)	1.0	0.99
	SPE		0.76 (0.04)	0.9	0.99
		Present	0.72 (0.03)	1.0	0.99
RBCs of Whole Blood (2 mM)		Absent	0.58 (0.17)	1.2	0.80
RBCs of Whole Blood (0.3 mM)			2.8 (0.17)	0.3	0.99
Plasma (2 mM)			1.0 (0.10)	0.7	0.97
Plasma (0.3 mM)			2.9 (0.38)	0.2	0.95

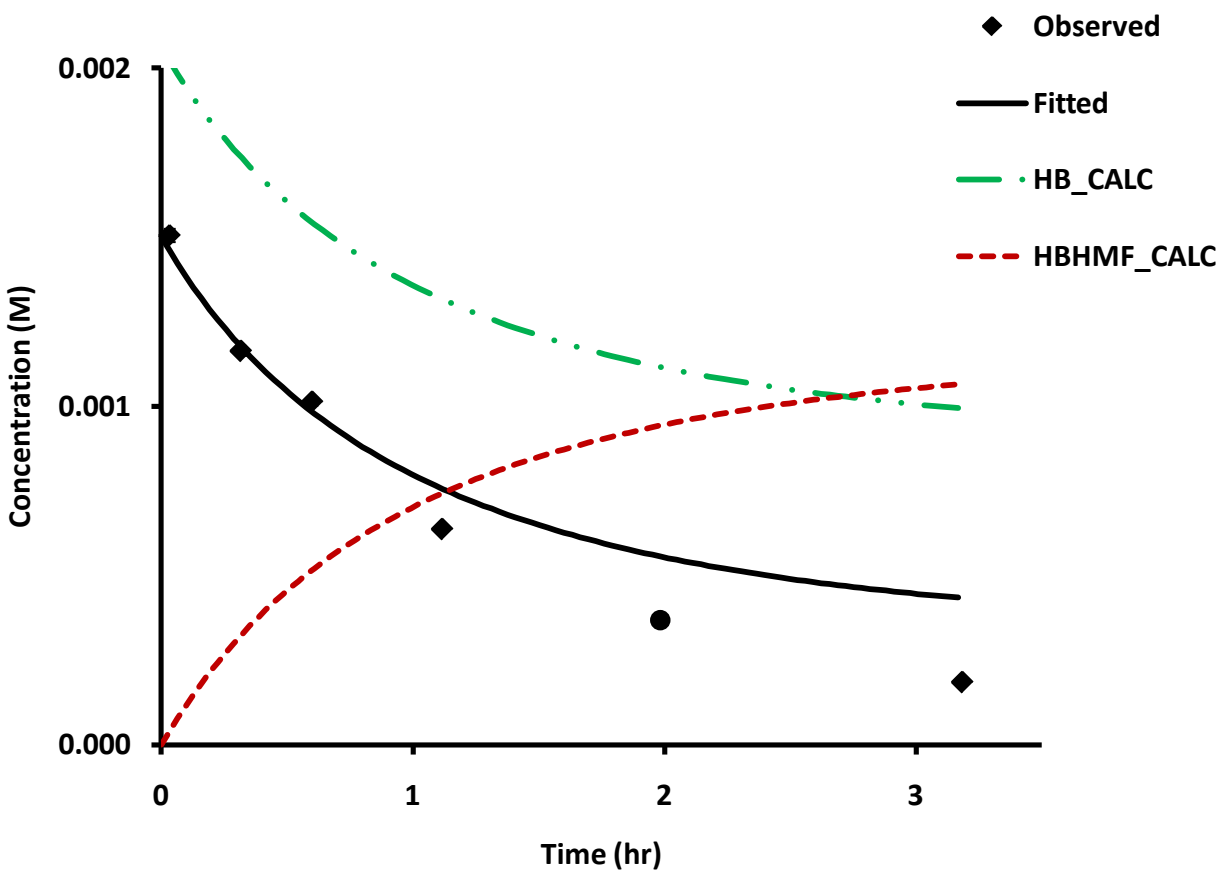

Figure 7-7. Simulated 5-HMF free concentration in RBCs hemolysate using Scenario (1) with no metabolism included.

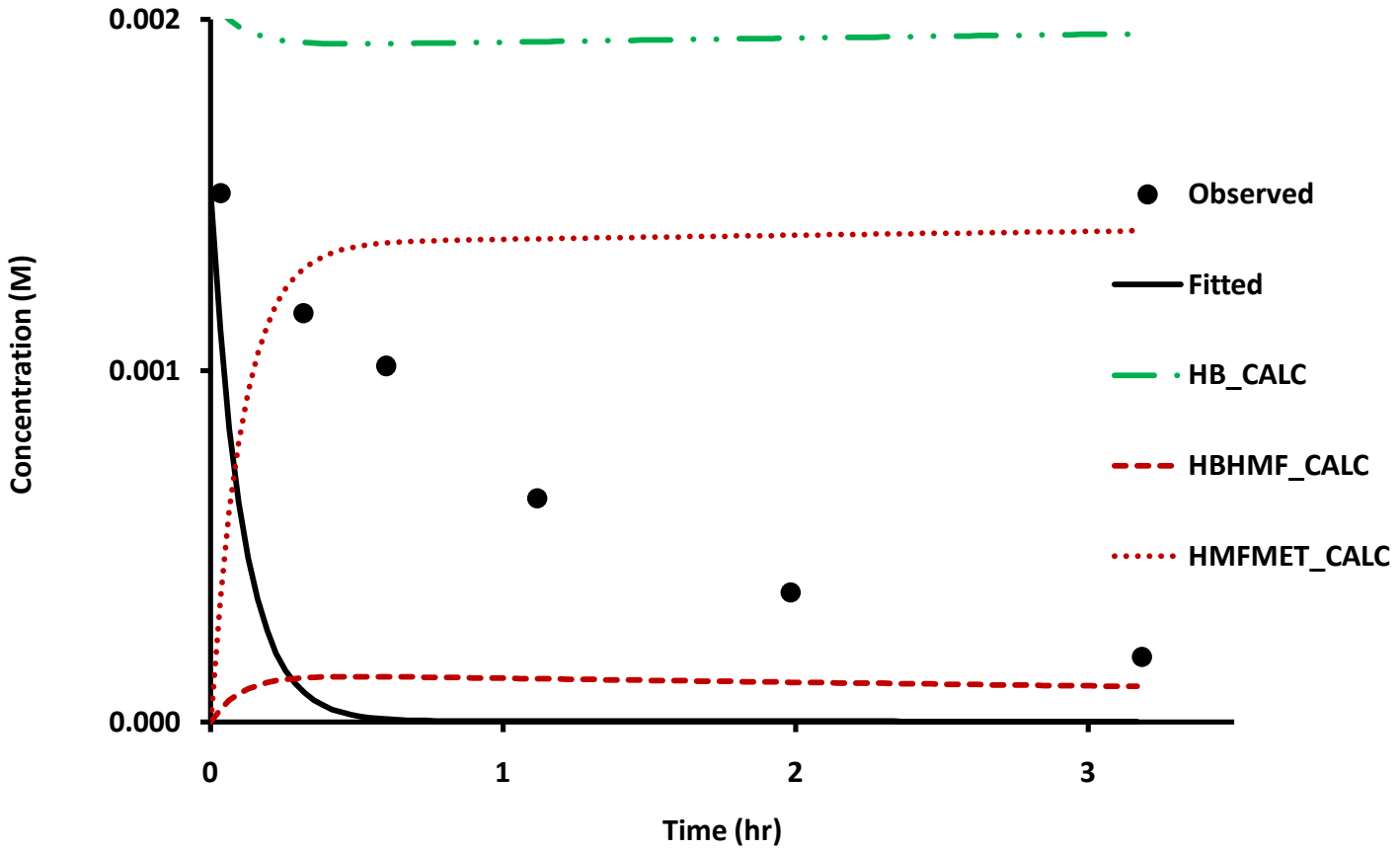

Figure 7-8. Simulated 5-HMF free concentration in RBCs hemolysate using Scenario (2) including k_{met}= 8.3 hr^{-1}.

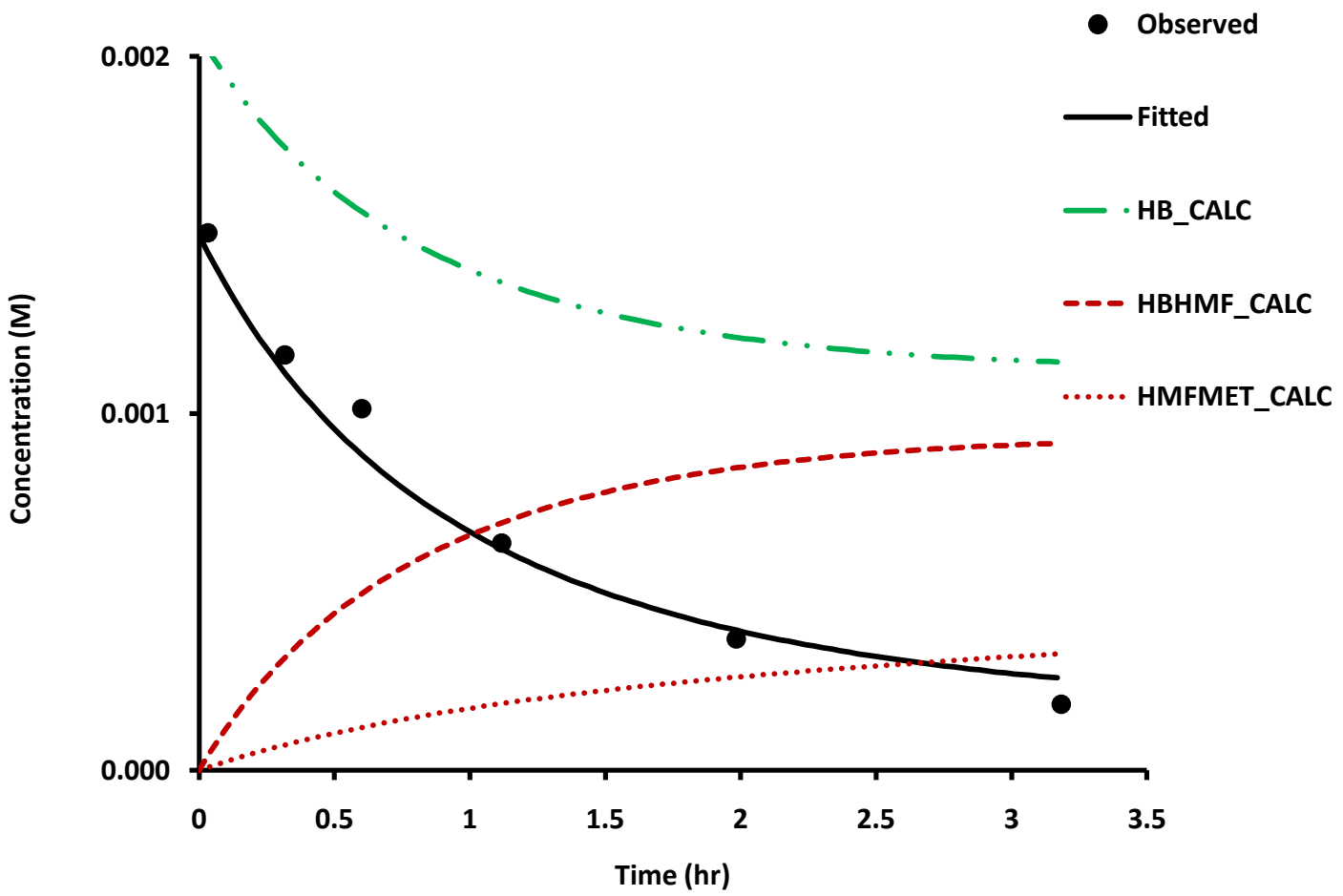

Figure 7-9. Simulated 5-HMF free concentration in RBCs hemolysate using Scenario (3) including k_{met}= 0.174 hr^{-1}.

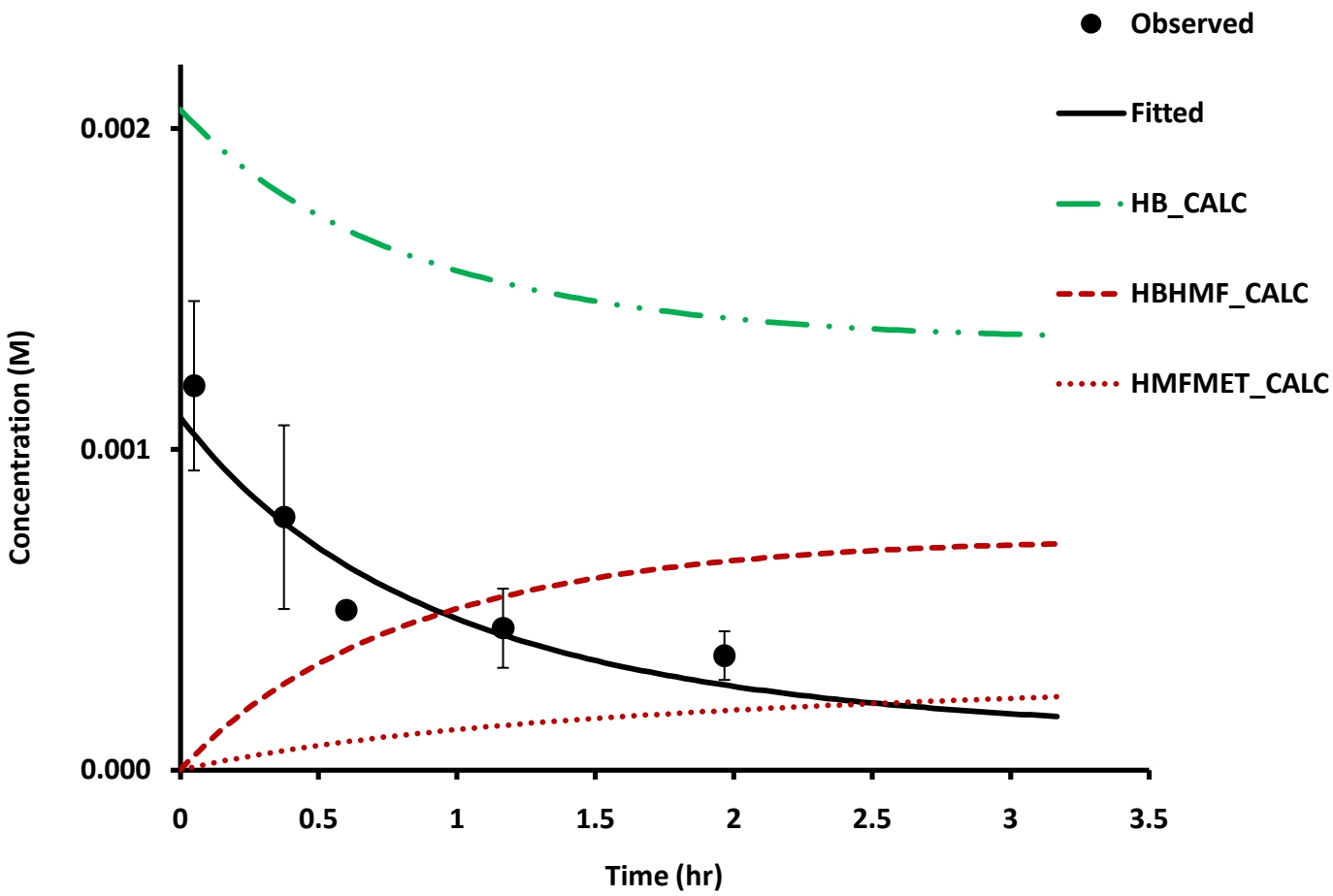

Figure 7-10. Simulated 5-HMF free concentration (2 mM) in RBCs of whole blood using Scenario (4) including HSA binding.

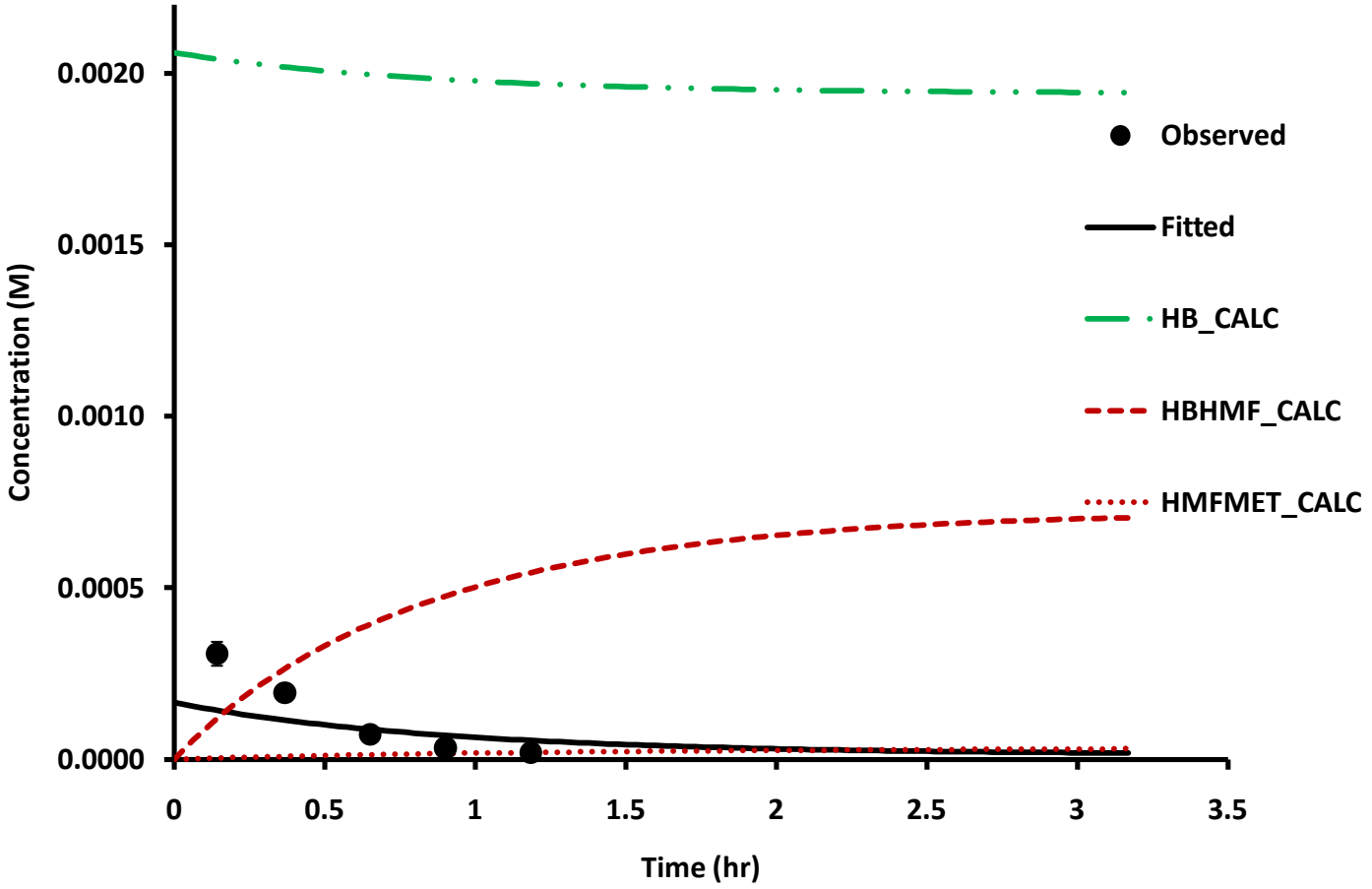

Figure 7-11. Simulated 5-HMF free concentration (0.3 mM) in RBCs of whole blood using Scenario (4) including HSA binding.

7.4 Discussion and Conclusions

Due to the small difference in the concentration between 5-HMF in the ultrafiltrate and 5-HMF exposed to solid phase extraction, it seems that the extraction method developed in Chapter 3 is unable to dissociate the bound 5-HMF from proteins and that HPLC determination reflects mainly the free, i.e. the unbound, fraction of 5-HMF. This is further supported by the similar rate constants for 5-HMF decline, shown in Table 7-2. In addition, there was no significant difference in 5-HMF concentrations (or the determined decline rate constants) measured in the presence of inhibitory concentrations of the inhibitors, as discussed in Chapter 4, and 5-HMF concentrations measured in their absence. This indicates the absence of significant metabolic activities that are sensitive to these inhibitors. The metabolic enzymes might have their activity decreased or diminished during the experiment.

The rate constant for 5-HMF decline in the plasma was higher than that for 5-HMF decline in the RBCs. This might be attributed to a higher rate of distribution of 5-HMF from the plasma into the RBCs compartment in comparison to the redistribution rate. Higher capacity of RBCs for 5-HMF versus that of the plasma may justify this difference in the distribution and redistribution rates.

However, the higher rate constant for 5-HMF decline with lower initial 5-HMF concentration was not expected. At the concentration of hemoglobin employed in these studies, saturation of its binding sites is not anticipated at 2 mM. On the other hand, binding of 5-HMF to blood components (other than hemoglobin) is assumed to be instantaneous, hence, it contributes only to the initial decline of 5-HMF but not to the decline of 5-HMF over time. This might not be true with low concentrations of 5-HMF that can show some time-dependency in its 5-HMF

binding and increase the overall observed rate of 5-HMF decline over time. This coincides with what is demonstrated in Figure 7-12, where the model initially underpredicts the free 5-HMF concentration and overpredict it later in the experiment for the 0.3 mM 5-HMF concentration.

The simulations showed that 5-HMF binding to hemoglobin alone overestimated the free concentration of 5-HMF in RBCs hemolysate suspension. This might be attributed to modifications in the binding kinetics in the physiological setting that is affected by the unique environment of RBCs, conformational changes of hemoglobin, and/or 5-HMF binding to other proteins, such as RBC membranes.

On the other hand, the 5-HMF free concentration was underpredicted in the simulations including concurrent RBC metabolism. The two simulation scenarios indicated that 5-HMF metabolism may have existed in the matrix, however, not to the extent observed in the metabolic studies discussed in Chapter 5. Here, the optimized metabolic rate constant was significantly lower than that estimated from the RBC metabolism studies in Chapter 5. This observation coincides with the absence of inhibitor activity due to the loss of enzyme viability during the study. In addition, the metabolic studies in Chapter 5 were performed in a blood pooled from different individuals, while in this study the blood was taken from a single Caucasian female. Consequently, the activity of the enzyme might be different in these two studies. This is further supported by Table 7-3. As demonstrated in this table, the activity of ALDH enzyme in RBCs varies between individual as much as 10 fold. In addition, as stated in Chapter 1, 1 out of 16 persons had a deficiency in RBCs ALDH enzyme. Hence, this may have contributed to the failure of observing significant metabolism in the current study. Moreover, Equation 7-2 assumes that the activity of enzymes remains fully functional over the incubation time, which might not

be the case. Furthermore, the cofactor for the metabolic enzymes might have diminished during the period of the experiment.

Table 7-3. Erythrocyte ALDH activity in mU/ml **(Goedde 1983)**

	Number of Individuals		
Erythrocyte ALDH Activity (mU/ml)	**Healthy Controls**	**Alcoholics**	**Psychiatric Patients (Non-Alcoholic)**
0.3	9	41	6
0.9	29	17	3
1.5	23	6	13
2.1	5	1	9
2.7	1	0	3

As shown in Figures 7-10 and 7-11, the fit using the optimized parameters matches the observed data for the 2 mM of 5-HMF incubated in whole blood, which validates the optimized model parameter estimates. On the other hand, the fit was less perfect for the 0.3 mM concentration of 5-HMF incubated in whole blood. This discrepancy was explored above through the discussion of the rate constant for 5-HMF decline over time.

The inclusion of albumin binding in the initial conditions of the model assumes that a steady-state (equilibrium) was instantaneous. While this might be valid in the case of 2 mM, this might not be the case with lower concentrations such as 0.3 mM. In addition, in the model, the factor correcting for RBCs membrane binding was estimated at 2 mM concentration rather than at 0.3 mM.

Overall, the built model demonstrated a persistence of the adduct concentration in the RBCs in comparison to the free concentration of 5-HMF in plasma. Consequently, the plasma concentration of 5-HMF does not reflect the concentration of 5-HMF in its biophase in contrast to the assumption made to most of the drugs in the market. Due to the time-dependency in 5-HMF binding to hemoglobin, there is a lag time between the peak plasma concentration and the peak adduct concentration. In addition, the covalent bond in the adduct will hinder the clearance of the bound 5-HMF leading to the persistence of the pharmacodynamics effects of 5-HMF.

Since binding and metabolic parameters were not obtained in an *in-vivo* settings, the following factors may contribute to a different behavior of 5-HMF when compared to *in-vitro* studies:

1. The unique environment of RBCs, including the presence of organic phosphate 2,3-diphosphoglycerate (2,3-DG), cationic, and anionic species might affect the binding and the metabolic reactions. It was reported that the presence of 2,3-DG, CO, CO_2, and O_2 affected the rate constants for the Schiff base in HbA_{1c} **Invalid source specified.**.
2. Inter-individual variation in hemoglobin concentration.
3. Genetic variation in the metabolic enzymes.
4. Sample preparation used in the analysis might disturb the equilibrium of binding and metabolism.
5. Conformational changes of hemoglobin upon oxygenation and deoxygenation, which makes the binding site for 5-HMF more or less accessible **Invalid source specified.**.
6. 5-HMF might be bound to other proteins. Lens crystalline, peripheral nerve proteins, and erythrocytes membranes are examples of proteins that are susceptible to Schiff base adduct formation with aldehydes **Invalid source specified.** (Bucala 1982).
7. The cofactor steady-state concentration in the physiological setting might be different from that used in the conducted-studies.

Nevertheless, the parameters obtained from the performed studies were able to describe 5-HMF behavior in blood. Accordingly, 5-HMF free concentration and that bound to its site of action can be acceptably predicted using Equation 7-2.

In a human body, 5-HMF is exposed to metabolism by the liver and RBCs. This metabolism is not expected to undergo saturation since the determined K_m value in hepatic cytosol (218 mM) was much higher than the proposed therapeutic concentration (1-2 mM). Likewise, the metabolism in the RBCs was not saturated with 5-HMF concentration up to 142 mM. Consequently, non-linear PK of 5-HMF in the plasma are not expected due to 5-HMF metabolism. On the other hand, 5-HMF binding to hemoglobin is saturable due to the finite binding sites to 5-HMF, which are equivalent to the concentration of Hemoglobin dimmers (4.6 mM in blood). Consequently, 5-HMF binding to hemoglobin result in non-linear PK of 5-HMF in plasma (supra-propotional) at high concentration of 5-HMF.

CHAPTER 8

OVERALL RESULTS AND CONCLUSIONS

In this research project, the available literature on the physiochemical properties, pharmacokinetics, and pharmacodynamics of 5-HMF was reviewed. 5-HMF is found constitutively in food and is an adulteration product in honey, beer, fruit juice, and glucose infusion solutions (Janzowski 2000) (Godfrey 1999). Although 5-HMF was administered orally to human in three clinical studies, its PK properties were not described (Prior 2006) (Matzi 2007) (M. P. Murkovic 2006). In different species, 5-HMF was shown to be extensively metabolized and the metabolites were mainly excreted in urine (Godfrey 1999) (Germond 1987). On the other hand, gaps were identified in human pharmacokinetics. Consequently, this research project was carried out to explore the differences in 5-HMF pharmacokinetics between and among species and to estimate its oral bioavailability.

An HPLC assay method for the quantitation of 5-HMF in neat solution, human plasma, and human RBCs was developed and validated. 5-HMF was detected using UV absorbance at 285 nm. The mobile phase was mainly aqueous with more than 90% water

in addition to acetic acid, methanol, and tetrahydrofuran. The mobile phase had a flow rate of 0.75 ml/minute through C_{18} guard and analytical columns.

The experimental conditions needed to investigate 5-HMF metabolism in human hepatic cytosol were optimized to determine the metabolic pathways of the oxidative metabolism of 5-HMF. NADH production was monitored at 340 nm as an indicator of 5-HMF oxidative metabolism. In human hepatic cytosol, selective substrates validated the presence of active ALDH and ADH enzymes. In addition, selective inhibitors demonstrated that 5-HMF was metabolized by ALDH enzyme and to a lesser extent by ADH enzyme in human hepatic cytosol.

In addition to human hepatic cytosol, oxidative metabolism was also demonstrated in mouse, rat, and dog hepatic cytosol and was described by Michaelis Menten kinetics. The *in-vitro* metabolic capacities (per mg protein of hepatic cytosol) were relatively similar in mouse, rat, and dog hepatic cytosol. On the other hand, affinities were more variable - with the highest affinity observed in the dogs and the lowest in humans. Consequently, quantitative differences were predicted in the intrinsic clearance (per kg body weight) among species with the lowest intrinsic clearance in humans.

In-vitro-in-vivo extrapolations of 5-HMF metabolism in mouse, rat, dog, and human hepatic cytosol were performed and compared with published data. In all animal species studied, 5-HMF is predicted to be subject to low hepatic extraction and clearance and show high oral bioavailability *in-vivo*. *In-vivo* systemic exposure predictions using the respective *in-vitro-in-vivo* extrapolations parameter estimates in mouse and dog were reasonable and were within two-fold of those reported for *in-vivo* exposures. On the other

hand, the *in-vitro-in-vivo* extrapolated $t_{1/2}$ for humans was more than 30-fold longer than the reported plasma $t_{1/2}$ of the (presumed) primary metabolite, HMFA, after oral administration of 5-HMF. This major discrepancy implied the involvement of extrahepatic metabolism of 5-HMF in humans.

In-vitro 5-HMF metabolism was observed in human RBCs. Nevertheless, metabolic saturation was not achieved in that system due to experimental limitations. The intrinsic clearance was determined from the slope of the velocities vs. the concentration. The failure to observe NAD^+-dependent oxidation of ethanol and 5-HMF inhibition by 4-methylpyrazole indicated the absence of ADH enzyme in RBCs. 5-HMF clearance by RBCs, estimated through *in-vitro-in-vivo* extrapolations, was added to the hepatic clearance, estimated previously from human hepatic cytosol, resulting in a total 5-HMF clearance in human. The *in-vitro-in-vivo* extrapolated half-life was similar to the reported plasma $t_{1/2}$ of the (presumed) primary metabolite, HMFA, after oral administration of 5-HMF. This resolved the discrepancy observed in human hepatic cytosol studies.

Time-dependency was observed in 5-HMF binding to human hemoglobin and to a lower extent in 5-HMF binding to serum albumin. The kinetics of this binding indicated a fast binding reaction rate with a slow dissociation rate. When 5-HMF binding to hemoglobin was compared to glucose binding to hemoglobin, 5-HMF had a faster rate constant of Hb-adduct formation than glucose, while it had a slower rate constant of Hb-adduct degradation. At physiological Hb concentrations in whole blood, 5-HMF is expected to show fast association with, but slow dissociation from Hb, resulting in

prolonged persistence of the Hb adduct ($t_{1/2}^{eq}$ of 0.7 hrs). Thus, this unique drug-receptor interaction may lead to a prolonged *in-vivo* PD effect.

When the steady-state concentration-dependent kinetics were investigated, 5-HMF showed saturable binding to human hemoglobin and non-saturable binding to serum albumin. In the physiological environment, the serum albumin concentration in blood is lower than hemoglobin, which makes hemoglobin have a higher capacity and affinity of binding to 5-HMF than serum albumin.

A PK model that combined both hemoglobin and serum albumin binding together with RBCs metabolism of 5-HMF to describe its disposition in blood was developed. The fit using the optimized parameters matched the observed data for the 2 mM of 5-HMF incubated in whole blood, validating by that the optimized model parameters. Accordingly, 5-HMF free concentration and that bound to its site of action can be acceptably predicted using the developed PK model. In addition, the model demonstrated a persistence of the adduct concentration in the RBCs in comparison to the free concentration of 5-HMF in plasma. Consequently, the plasma concentration of 5-HMF does not reflect the concentration of 5-HMF in its biophase due to the time-dependency in 5-HMF binding to hemoglobin and the covalent bond in the adduct leading to the persistence of the pharmacodynamics effects of 5-HMF.

Nevertheless, since binding and metabolic studies were not carried-out in an *in-vivo* setting, a discrepancy might be observed in the behavior of 5-HMF *in-vivo* when compared to *in-vitro* studies findings.

As a conclusion, 5-HMF was found to be a low-affinity ALDH/ADH substrate in hepatic cytosol and appears to be oxidatively metabolized primarily by ALDH in humans. Across animal species, 5-HMF is expected to be a low-hepatic-extraction-ratio drug with low hepatic first-pass effect and high oral bioavailability. In addition, 5-HMF is metabolized in humans RBCs (presumably by ALDH). The presumed effective concentrations of 5-HMF are expected to show fast association with, but slow dissociation from its drug target, hemoglobin, which may lead to a prolonged *in-vivo* PD effect.

LIST OF REFERENCES

REFERENCES

Abdulmalik, O, Safo, M, Chen, Q, Yang, J, Brugnara, C, Ohene-Frempong, K, Abraham, D, Asakura, T. "5-hydroxymethyl-2-furfural modifies intracellular sickle haemoglobin and inhibits sickling of red blood cells." *British Journal of Haematology* 128 (2005): 552-61.

Abraham, D., Mehanna, A., Wireko, F., Whitney, J., Thomas, R., Orringer, E. "Vanillin, a potential agent for the treatment of sickle cell anemia." *Blood* 77, no. 6 (1991): 1334-41.

ACS. *SciFinder.* June 9, 2009.

Agarwal, D., Goedde, H. "Pharmacogenetics of alcohol metabolism and alcoholism." *Pharmacogenetics* 2, no. 2 (1992): 48-62.

Aliyu, Z., Kato, G., Taylor, J., Babadoko, A., Mamman, A. "Sickle cell disease and pulmonary hypertension in Africa: A global perspective and review of epidemiology, pathophysiology, and management." *American Journal of Hematology* 83 (2008): 63-70.

Beedham, C. "The role of non-P450 enzymes in drug oxidation." *Pharm World Sci.* 19, no. 6 (1997): 255-63.

Bestic, M., Blackford., M., Reed, M. "Fomepizole: A Critical Assessment of Current Dosing Recommendations." *J. Clin. Pharmacol.* 49 (2009): 130-137.

Bogaards, J., Freidig, A., Bladeren, P. "Prediction of isoprene diepoxide levels in vivo in mouse, rat and man using enzyme kinetic data in vitro and physiologically-based pharmacokinetic modelling." *Chemico-Biological Interactions* 138 (2001): 247-265.

Bolaños-Meade, J., Brodsky, R. "Blood and marrow transplantation for sickle cell disease: overcoming barriers to success." *Curr Opin Oncol.* 21, no. 2 (2009): 158-161.

Bowers, W., Fulton, S., Thompson, J. "Ultrafiltration vs equilibrium dialysis for determination of free fraction." *Clin Pharmacokinet.* 9, no. 1 (1984): 49-60.

Brandon, E., Raap, C., Meijerman, I., Beijnen, J., Schellens, J. "An update on in vitro test methods in human hepatic drug biotransformation research: pros and cons." *Toxicol Appl Pharmacol.* 189, no. 3 (2003): 233-246.

Bucala, R., Fishman, J., Cerami, A. "Formation of covalent adducts between cortisol and 16 alpha-hydroxyestrone and protein: possible role in the pathogenesis of cortisol toxicity and systemic lupus erythematosus." *Proc. NatL Acad. Sci.* 79 (1982): 3320-4.

Bunn, H., Higgins, P. "Reaction of monosaccharides with proteins: possible evolutionary significance." *Science.* 213, no. 4504 (1981): 222-4.

Charache, S. "Mechanism of action of hydroxyurea in the management of sickle cell anemia in adults." *Semin Hematol* 34 (1997): 15-21.

Cheng, Y., Ho, E., Subramanyam, B., Tseng, J. "Measurements of drug-protein binding by using immobilized human serum albumin liquid chromatography-mass spectrometry." *J Chromatogr B Analyt Technol Biomed Life Sci.* 809, no. 1 (2004): 67-73.

Cheung, C., Davies, N., Hoog, J., Hotchkiss, S., Pease, C. "Species variations in cutaneous alcohol dehydrogenases and aldehyde dehydrogenases may impact on toxicological assessments of alcohols and aldehydes." *Toxicology* 184, no. 2-3 (2003): 97-112.

Cheung, C., Davies, N., Hoog, J., Hotchkiss, S., Smith Pease, C. "Species variations in cutaneous alcohol dehydrogenases and aldehyde dehydrogenases may impact on toxicological assessments of alcohols and aldehydes." *Toxicology* 184, no. 2-3 (2003): 97-112.

Cheung, C., Hotchkiss, S., Pease, C. "Cinnamic compound metabolism in human skin and the role metabolism may play in determining relative sensitisation potency." *J Dermatol Sci. 2003 Feb;31(1):9-19* 31, no. 1 (2003): 9-19.

Clark, M. "Mean corpuscular hemoglobin concentration and cell deformability." *Ann N Y Acad Sci.* 565 (1989): 284-94.

Cocchi, M., Consonni, R., Durante, C., Grandi, M., Manzini, S., Marchetti, A., Sighinolfi, S. "Changes in the chemical composition of reduced cooked musts during the heating process." *J Agric Food Chem.* 56, no. 15 (2008): 6397-407.

Coco, F., Valentini, C., Novelli, V., Ceccon, L. "High-performance liquid chromatographic determination of 2-furaldehyde and 5-hydroxymethyl-2-furaldehyde in honey." *Journal of Chromatography A* 749 (1996): 95-102.

Corti, M., Guralnik, J., Salive, M., Sorkin, J. "Serum albumin level and physical disability as predictors of mortality in older persons." *JAMA. 1994 Oct 5;272(13):1036-42* 272, no. 13 (1994): 1036-1042.

Czok, G. "Tolerance of 5-hydroxymethylfurfural (HMF). 2d communication: pharmacologic effects." *Z Ernahrungswiss.* 10, no. 2 (1970): 103-10.

Czok, G. "Tolerance of 5-hydroxymethylfurfural (HMF). 2d communication: pharmacologic effects." *Z Ernahrungswiss.* 10, no. 2 (1970): 103-110.

Davies, B., Morris, T. "Physiological parameters in laboratory animals and humans." *Pharm Res.* 10, no. 7 (1993): 1093-1095.

Day, J., Thorpe, S., Baynes, J. "Nonenzymatically glucosylated albumin. In vitro preparation and isolation from normal human serum." *JBC* 254, no. 3 (1979): 595-7.

Deitrich, R., Petersen, D., Vasiliou, V. "Removal of acetaldehyde from the body." *Novartis Found Symp.* 285 (2007): 23-40.

Delgado-Andrade, C., Seiquer, I., Navarro, M., Morales, F. "Estimation of hydroxymethylfurfural availability in breakfast cereals. Studies in Caco-2 cells." *Food Chem Toxicol.* 46, no. 5 (2008): 1600-7.

Delgado-Andrade, C., Seiquer, I., Navarro, M., Morales, F. "Maillard reaction indicators in diets usually consumed by adolescent population." *Mol Nutr Food Res.* 51, no. 3 (2007): 341-51.

Di Santo, R., Maga, G. "Human terminal deoxynucleotidyl transferases as novel targets for anticancer chemotherapy." *Curr Med Chem* 13, no. 20 (2006): 2353-68.

Dixon, L. "The complete blood count: physiologic basis and clinical usage." *J Perinat Neonatal Nurs.* 11, no. 3 (1997): 1-18.

Drifield, M., Chan, D., Macarthur, D., MacDonald, S., Brereton, P., Wood, R. "Single laboratory validation of a method for the determination of hydroxymethylfurfural in honey by using solid-phase extraction cleanup and liquid chromatography." *Journal of AOAC International* 88, no. 1 (2005): 121-127.

Driscoll, M. "Sickle Cell Disease." *Pediatrics in Review* 28, no. 7 (2007): 259.

Druteika, D., Zed, P., Ensom, M. "Role of fomepizole in the management of ethylene glycol toxicity." *Pharmacotherapy* 22, no. 3 (2002): 365-372.

Fallico, B., Arena, E., Zappala, M. "Degradation of 5-hydroxymethylfurfural in honey." *J Food Sci.* 73, no. 9 (2008): C625-31.

FDA. *www.fda.gov.* 2000. http://www.fda.gov/cder/guidance/3618fnl.pdf (accessed August 2, 2008).

Ferrer, E., Alegr´ıa, A., Farre´, R., Abella´n, P., Romero, F. "High-performance liquid chromatographic determination of furfural compounds in infant formulas Changes during heat treatment and storage." *Journal of Chromatography A* 947 (2002): 85-95.

Field, J., Knight-Perry, J., Debaun, M. "Acute pain in children and adults with sickle cell disease: management in the absence of evidence-based guidelines." *Curr Opin Hematol.* 16, no. 3 (2009): 173-178.

Garlick, R., Mazer, J. "The principal site of nonenzymatic glycosylation of human serum albumin in vivo." *J. Biol. Chem., Vol. 258, Issue 10, 6142-6146* 258, no. 10 (1983): 6142-6.

Gaspar, E., Lopes, J. "Simple gas chromatographic method for furfural analysis." *J Chromatogr A. 2009* 1216, no. 14 (2009): 2762-7.

Ge, S., Lee, T. "Kinetic Significance of the Schiff Base Reversion in the Early-Stage Maillard Reaction of a Phenylalanine−Glucose Aqueous Model System." *J. Agric. Food Chem.* 45, no. 5 (1997): 1619–23.

Germond, J., Philippossian, G., Richli, U., Bracco, I., Arnaud, M. "Rapid and complete urinary elimination of [14C]-5-hydroxymethyl-2-furaldehyde administered orally or intravenously to rats." *J Toxicol Environ Health.* 22, no. 1 (1987): 79-89.

Godfrey, V., Chen, L., Griffin, R., Lebetkin, E., & Burka, L. "Distribution and Metabolism of (5-Hydroxymethyl) Furfural in Male F344 Rats and B6C3F1 Mice after Oral Administration." *Journal of Toxicology and Environmental Health, Part A* 57, no. 3 (1999): 199-210.

Goedde, H., Agarwal, D., Harada, S. "The role of alcohol dehydrogenase and aldehyde dehydrogenase isozymes in alcohol metabolism, alcohol sensitivity, and alcoholism." *Isozymes Curr Top Biol Med Res.* 8 (1983): 175-193.

Gupta, Pankaj. *Pharmacokinetic scaling and metabolism of alcohols and glycols.* Richmond: Virginia Commonweatlh University, 2006.

Hallifax, D., Houston, J. "Methodological uncertainty in quantitative prediction of human hepatic clearance from in vitro experimental systems." *Curr Drug Metab.* 10, no. 3 (2009): 307-321.

Hatake, K., Taniguchi, T., Ouchi, H., Sakaki, N., Hishida, S., Ijiri, I. "Possible involvement of kinins in cardiovascular changes after alcohol intake." *Pharmacol Biochem Behav.* 35, no. 2 (1990): 437-42.

Hebbel, R. "Beyond hemoglobin polymerization: the red blood cell membrane and sickle disease pathophysiology." *Blood* 77, no. 2 (1991): 214-37.

Higgins, P., Bunn, H. "Kinetic analysis of the nonenzymatic glycosylation of hemoglobin." *J Biol Chem.* 256, no. 10 (1981): 5204-8.

Houston, J., Galetin, A. "Methods for predicting in vivo pharmacokinetics using data from in vitro assays." *Curr Drug Metab.* 9, no. 9 (2008): 940-951.

Howard, J, Thomas, V., Rawle, H. "Pain management and quality of life in sickle cell disease." *Expert Rev Pharmacoecon Outcomes Res.* 9, no. 4 (2009): 347-52.

Hurst, S., Loi, C., Brodfuehrer, J., El-Kattan, A. "Impact of physiological, physicochemical and biopharmaceutical factors in absorption and metabolism mechanisms on the drug oral bioavailability of rats and humans." *Expert Opin Drug Metab Toxicol.* 3, no. 4 (2007): 469-489.

Husøy, T., Haugen, M., Murkovic, M., Jöbstl, D., Stølen, L., Bjellaas, T., Rønningborg, C., Glatt, H., Alexander, J. "Dietary exposure to 5-hydroxymethylfurfural from Norwegian food and correlations with urine metabolites of short-term exposure." *Food Chem Toxicol.* 46, no. 12 (2008): 3697-702.

Inoue, K., Nishimukai, H., Yamasawa, K. "Purification and partial characterization of aldehyde dehydrogenase from human erythrocytes." *Biochim Biophys Acta. 1979 Aug 15;569(2):117-23* 569, no. 2 (1979): 117-23.

Janzowski, C., Glaab, V., Samimi, E., Schlatter, J., Eisenbrand, G. "5-Hydroxymethylfurfural: assessment of mutagenicity, DNA-damaging potential and reactivity towards cellular glutathione." *Food Chem Toxicol.* 38, no. 9 (2000): 801-809.

Jellum, E., Borresen, H., & Elujarn, L. "The Presence of Furan Derivatives in Patients Receiving Fructose-Containing Solutions Intravenously." *Clin Chim Acta.* 47 (1973): 191-201.

Jellum, E., Borresen, H., Elujarn, L. "The Presence of Furan derivatives in patients receiving fructose-containing solutions intravenously." *Clinica Chimica Acta* 47 (1973): 191-201.

John, G., Scott, K., Hawcroft, D. "Glycated haemoglobin and glycated protein and glucose concentrations in necropsy blood samples." *J Clin Pathol.* 41, no. 4 (1988): 415-8.

Johnson, R., Bahnisch, J., Stewart, B., Shearman, D., Edwards, J. "Optimized spectrophotometric determination of aldehyde dehydrogenase activity in erythrocytes." *Clin Chem.* 38, no. 4 (1992): 584-8.

Kahoun, D., Rezková, S., Veskrnová, K., Královský, J., Holcapek, M. "Determination of phenolic compounds and hydroxymethylfurfural in meads using high performance liquid chromatography with coulometric-array and UV detection." *J Chromatogr A.* 1202, no. 1 (2008): 19-33.

Kelly, S., Glynn, P., Madden, S., Grayson, D. "Impurities in a morphine sulfate drug product identified as 5-(hydroxymethyl)-2-furfural, 10-hydroxymorphine and 10-oxomorphine." *J Pharm Sci.* 92, no. 3 (2003): 485-493.

Keung, W., Vallee, B. "Daidzin: a potent, selective inhibitor of human mitochondrial aldehyde dehydrogenase." *Proc Natl Acad Sci U S A.* 90, no. 4 (1993): 1247-51.

Kitson, T. "The effect of disulfiram on the aldehyde dehydrogenases of sheep liver." *Biochem J.* 151, no. 2 (1975): 407-412.

Klimmek, V. "Wirkung von 5-hyroxymethylfurfural auf atmung, krieslauf, blutgase und klinisch-chemische parameter beim hund." *Wehrmed Mschr. Heft* 2 (1978): 44-47.

Klyosov, A. "Kinetics and specificity of human liver aldehyde dehydrogenases toward aliphatic, aromatic, and fused polycyclic aldehydes." *Biochemistry* 35, no. 14 (1996): 4457-67.

Klyosov, A., Rashkovetsky, L., Tahir, M., Keung, W. "Possible role of liver cytosolic and mitochondrial aldehyde dehydrogenases in acetaldehyde metabolism." *Biochemistry* 35, no. 14 (1996): 4445-4456.

Klyosov, A., Rashkovetsky, L., Tahir, M., Keung, W. "Possible Role of Liver Cytosolic and Mitochondrial Aldehyde Dehydrogenases in Acetaldehyde Metabolism." *Biochemistry* 35 (1996): 4445-4456.

Kulkarni, A., Yokota, T., Suzuki, S., Etoh, H. "Subcritical Water Extraction of Barley to Produce a Functional Drink." *Bioscience, Biotechnology, and Biochemistry* 72, no. 1 (2008): 236-239.

Lang, K., Kieckebusch, W., Bässler, K., Griem, W., Czok, G. "Tolerance of 5-hydroxymethylfurfural (HMF). 1st communication: chronic administration of HMF and metabolites of the substance." *Z Ernahrungswiss. 1970 Dec;10(2):97-101* 10, no. 2 (1970): 97-101.

Lanzkron, S., Strouse, J., Wilson, R., Beach, M., Haywood, C., Park, H., Witkop, C., Bass, E., Segal, J. "Systematic review: Hydroxyurea for the treatment of adults with sickle cell disease." *Ann Intern Med.* 148, no. 12 (2008): 939-955.

Li, Y., Lu, X. "Investigation on the origin of 5-HMF in Shengmaiyin decoction by RP-HPLC method." *J Zhejiang Univ Sci B.* 6, no. 10 (2005): 1015-21.

Liao, C., Lin, J., Chang, C., Chao, T., Chao, Y., Cheng, T., Wu, C., Yin, S. "Stomach and duodenal alcohol and aldehyde dehydrogenase isozymes in Chinese." *Proc Natl Sci Counc Repub China B.* 15, no. 2 (1991): 92-6.

Lin, A., Qian, K., Usami, Y., Lin, L., Itokawa, H., Hsu, C., Morris-Natschke, S., Lee. K. "5-Hydroxymethyl-2-furfural, a clinical trials agent for sickle cell anemia, and its mono/di-glucosides from classically processed steamed Rehmanniae Radix." *Nat Med (Tokyo)* 62, no. 2 (2008): 164-167.

Liu, Z. "Genomic adaptation of ethanologenic yeast to biomass conversion inhibitors." *Appl Microbiol Biotechnol.* 73, no. 1 (2006): 27-36.

Manzer, R., Qamar, L., Estey, T., Pappa, A., Petersen, D., Vasiliou, V. "Molecular cloning and baculovirus expression of the rabbit corneal aldehyde dehydrogenase (ALDH1A1) cDNA." *DNA Cell Biol.* 22, no. 5 (2003): 329-38.

Marchitti, S., Brocker, C., Stagos, D., Vasiliou, V. "Non-P450 aldehyde oxidizing enzymes: the aldehyde dehydrogenase superfamily." *Expert Opin Drug Metab Toxicol.* 4, no. 6 (2008): 697-720.

Matzi, V., Lindenmann, J., Muench, A., Greilberger, J., Juan, H., Wintersteiger, R., Maier, A., & Smolle-Juettner, F. "The Impact of Preoperative Micronutrient Supplementation in Lung Surgery. A Prospective Randomized Trial of Oral Supplementation of Combined Alpha-Ketoglutaric Acid and 5-Hydroxymethylfurfural." *European Journal of Cardio-thoracic Surgery* 32 (2007): 776-782.

Menez, J., Berthou, F., Meskar, A., Picart, D., Le Bras, R., Bardou, L. "Glycosylated Haemoglobin: High-performance liquid chromatographic determination of 5-(hydroxymethyl)-2-furfuraldehyde after haemoglobin hydrolysis." *Journal of Chromatography* 297 (1984): 339-350.

Michail, K., Matzi, V., Maier, A., Herwig, R., Greilberger, J., Juan, H., Kunert, O., Wintersteiger, R. "Hydroxymethylfurfural: an enemy or a friendly xenobiotic? A Bioanalytical Approach." *Anal Bioanal Chem* 387 (2007): 2801-2814.

Minkin, S. "Statistical analysis of aberrant crypt assays for colon cancer promotion studies." *Biometrics.* 50, no. 1 (1994): 279-88.

Miura, S., Izuta, S. "DNA polymerases as targets of anticancer nucleosides." *Curr Drug Targets* 5, no. 2 (2004): 191-5.

Mizushina, Y., Yagita, E., Kuramochi, K., Kuriyama, I., Shimazaki, N., Koiwai, O., Uchiyama, Y., Yomezawa, Y., Sugawara, F., Kobayashi, S., Sakaguchi, K., Yoshida, H. "5-(Hydroxymethyl)-2-furfural: a selective inhibitor of DNA polymerase lambda and terminal deoxynucleotidyltransferase." *Arch Biochem Biophys.* 446, no. 1 (2006): 69-76.

Modig, T., Lidén, G., Taherzadeh, M. "Inhibition effects of furfural on alcohol dehydrogenase, aldehyde dehydrogenase and pyruvate dehydrogenase." *Biochem J.* 363, no. 3 (2002): 769-776.

Monien, B., Frank, H., Seidel, A., Glatt, H. "Conversion of the common food constituent 5-hydroxymethylfurfural into a mutagenic and carcinogenic sulfuric acid ester in the mouse in vivo." *Chem Res Toxicol.* 22, no. 6 (2009): 1123-1128.

Mrochek, J., Rainey, W. "Identification and biochemical significance of substituted furans in human urine." *Clin Chem.* 18, no. 8 (1972): 821-8.

Murkovic, M., Bornik, M. "Formation of 5-hydroxymethyl-2-furfural (HMF) and 5-hydroxymethyl-2-furoic acid during roasting of coffee." *Mol Nutr Food Res. 2007 Apr;51(4):390-4* 51, no. 4 (2007): 390-4.

Murkovic, M., Pichler, N. "Analysis of 5-hydroxymethylfurfual in coffee, dried fruits and urine." *Mol Nutr Food Res.* 50, no. 9 (2006): 842-6.

Nässberger, L. "Influence of 5-hydroxymethylfurfural (5-HMF) on the overall metabolism of human blood cells." *Hum Exp Toxicol.* 9, no. 4 (1990): 211-4.

Niscola, P., Sorrentino, F., Scaramucci, L., de Fabritiis, P., Cianciulli, P. "Pain syndromes in sickle cell disease: an update." *Pain Med.* 10, no. 3 (2009): 470-480.

NTP. "National Toxicology Program at NIH." *http://ntp.niehs.nih.gov/ntp/htdocs/Chem_Background/ExSumPdf/Hydroxymethyl.pdf.* 12 1994. (accessed April 4, 2009).

—. "TR-554 Toxicology and Carcinogenesis Studies of 5-(Hydroxymethyl)-2-Furfural (CAS No. 67-47-0) in F344/N Rats and B6C3F1 Mice (Gavage Studies)." *NTP Database Search Application.* 2008. (accessed July 2008).

Pacifici, G., Viani, A. "Methods of determining plasma and tissue binding of drugs. Pharmacokinetic consequences." *Clin Pharmacokinet. 1992 Dec;23(6):449-68.* 23, no. 6 (1992): 449-68.

Perez Locas, C., Yaylayan, V. "Isotope labeling studies on the formation of 5-(hydroxymethyl)-2-furaldehyde (HMF) from sucrose by pyrolysis-GC/MS." *J Agric Food Chem.* 56, no. 13 (2008): 6723.

Plapp, B., Leidal , K., Smith, R., Murch, B. "Kinetics of inhibition of ethanol metabolism in rats and the rate limiting role of alcohol dehydrogenase." *Archives of Biochemistry and Biophysics* 230, no. 1 (1984): 30-38.

Porter, J. "Concepts and goals in the management of transfusional iron overload." *Am. J. Hematol.* 2007 (2007): 1136–1139.

Prior, R., Wu, X., Gu, L. "Identification and Urinary Excretion of Metabolites of 5-(Hydroxymethyl)-2-funural in Human Subjects following Consumption of Dried Plums or Dried Plum Juice." *Agric. Food Chem. 2006* 54 (2006): 3744-3749.

Rasmussen, A., Hessov, I., Bojsen-Møller, M. "General and local toxicity of 5-hydroxymethyl-2-furfural in rabbits." *Acta Pharmacol Toxicol (Copenh).* 50, no. 2 (1982): 81-4.

Rawles, J., Rhodes, D., Potter, J., Mezey, E. "Characterization of human erythrocyte aldehyde dehydrogenase." *Biochem Pharmacol.* 36, no. 21 (1987): 3715-22.

Rhoades, R., Pflanzer, R. *Human Physiology.* Third. Saunders College Publishing, 1996.

Ricciardi, B., Saunders, J., Williams, R., Hopkinson, D. "Hepatic ADH and ALDH isoenzymes in different racial groups and in chronic alcoholism." *Pharmacol Biochem Behav.* 18, no. 1 (1983): 61-5.

Riggs, A. "Self-association, cooperativity and supercooperativity of oxygen binding by hemoglobins." *J Exp Biol. 1998 Apr;201(Pt 8):1073-84.* 201, no. 8 (1998): 1073-1084.

Routledge, P. "The plasma protein binding of basic drugs." *Br J Clin Pharmacol.* 22, no. 5 (1986): 499-506.

Safo, M., Abdulmalik, O., Danso-Danquah, R., Burnett, C., Nokuri, S., Joshi, G., Musayev, F., Asakura, T., & Abraham, D. "Structural Basis for the Potent Antisickling Effect of a Novel Class of Five-Membered Heterocyclic Aldehydic Compounds." *J. Med. Chem* 47 (2004): 4665-4676.

Sahi, J., Khan, K., Black, C. "Aldehyde oxidase activity and inhibition in hepatocytes and cytosolic fractions from mouse, rat, monkey and human." *Drug Metab Lett.* 2, no. 3 (2008): 176-183.

Sampietro, T., Lenzi, S., Giampietro, O., Cecchetti, P., Masoni, A., Navalesi, R. "A sensitive High performance liquid chromatographic method for determining small amounts of glycosylproteins." *Clin. Physiol. Biochem* 5 (1987): 49-56.

Satre, M., Zgombić-Knight, M., Duester, G. "The complete structure of human class IV alcohol dehydrogenase (retinol dehydrogenase) determined from the ADH7 gene." *J Biol Chem.* 269, no. 22 (1994): 15606-15612.

Sharma, V., Choi, J., Sharma, N., Choi, M., Seo, SY. "In vitro anti-tyrosinase activity of 5-(hydroxymethyl)-2-furfural isolated from Dictyophora indusiata." *Phytother Res.* 18, no. 10 (2004): 841-4.

Shena, M., Johnson, K., Maysa, D., Lipskya, J., Naylora, S. "Determination of in vivo adducts of disulfiram with mitochondrial aldehyde dehydrogenase." *Biochemical Pharmacology* 61 (2001): 537-545.

Sigma-Aldrich. *http://sigma-aldrich.custhelp.com/.* (accessed June 15, 2009).

Sládek, N. "Human aldehyde dehydrogenases: potential pathological, pharmacological, and toxicological impact." *J Biochem Mol Toxicol* 17, no. 1 (2003): 7-23.

Sladen, R. "The oxyhemoglobin dissociation curve." *Int Anesthesiol Clin.* 19, no. 3 (1981): 39-70.

Smiley, D., Dagogo-Jack, S., Umpierrez, G. "Therapy insight: metabolic and endocrine disorders in sickle cell disease." *Nat Clin Pract Endocrinol Metab.* 4, no. 2 (2008): 102-109.

Sophos, N., Vasiliou, V. "Aldehyde dehydrogenase gene superfamily: the 2002 update." *Chem Biol Interact. 2003 Feb 1;143-144:5-22.* 143-144 (2003): 5-22.

Standefer, J., Eaton, R. "Evaluation of a colorimetric method for determination of glycosylated hemoglobin." *Clin. Chem.* 29, no. 1 (1983): 135-140.

Stevens, V., Vlassara, H., Abati, A., Cerami, A. "Nonenzymatic glycosylation of hemoglobin." *JBC* 252, no. 9 (1977): 2998-3002.

Surh, Y., Tannenbaum, S. "Activation of the Maillard reaction product 5-(hydroxymethyl)furfural to strong mutagens via allylic sulfonation and chlorination." *Chem Res Toxicol.* 7, no. 3 (1994): 313-8.

Thomasson, H., Edenberg, H., Crabb, D., Mai, X., Jerome, R., Li, T., Wang, S., Lin, Y., Lu, R., Yin, S. "Alcohol and aldehyde dehydrogenase genotypes and alcoholism in Chinese men." *Am J Hum Genet.* 48, no. 4 (1991): 677-81.

Tomita, Y., Haseba, T., Kurosu, M., Watanabe, T. "Effects of acute ethanol intoxication on aldehyde dehydrogenase in mouse liver." *Arukoru Kenkyuto Yakubutsu Ison.* 25, no. 2 (1990): 116-28.

Turk, Z., Misur, I., Turk, N. "Temporal association between lens protein glycation and cataract development in diabetic rats." *Acta Diabetol.* 34, no. 1 (1997): 49-54.

Ueshima, Y., Matsuda, Y., Tsutsumi, M., Takada, A. "Role of the aldehyde dehydrogenase-1 isozyme in the metabolism of acetaldehyde." *Alcohol Alcohol Suppl.* 1, no. B (1993): 15-9.

Ulbricht, R., Northup, S., Thomas, J. "A review of 5-hydroxymethylfurfural (HMF) in parenteral solutions." *Fundam Appl Toxicol.* 4, no. 5 (1984): 843-53.

Usta, M., Tuncer, M., Baykal, A., Ciftçioğlu, M., Erdoğru, T., Köksal, I., Ersoy, F., Baykara, M. "Impact of chronic renal failure and peritoneal dialysis fluids on advanced glycation end product and iNOS levels in penile tissue: an experimental study." *Urology* 59, no. 6 (2002): 953-7.

Vasiliou, V., Nebert, D. "Analysis and update of the human aldehyde dehydrogenase (ALDH) gene family." *Hum Genomics* 2, no. 2 (2005): 138-143.

Vasiliou, V., Pappa, A. "Polymorphisms of human aldehyde dehydrogenases. Consequences for drug metabolism and disease." *Pharmacology.* 61, no. 3 (2000): 192-8.

Vekilov, P. "Sickle-cell haemoglobin polymerization: is it the primary pathogenic event of sickle-cell anaemia?" *Br J Haematol.* 139, no. 2 (2007): 173-184.

Venitz, J. "5-HMF clinical pharmacology/development plan-proposal." 2006.

Wagner, F., Burger, A., Vallee, B. "Kinetic properties of human liver alcohol dehydrogenase: oxidation of alcohols by class I isoenzymes." *Biochemistry. 1983 Apr 12;22(8):1857-63* 22, no. 8 (1983): 1857-63.

Wahl, S., Quirolo, K. "Current issues in blood transfusion for sickle cell disease." *Curr Opin Pediatr.* 21, no. 1 (2009): 15-21.

Wu, C., Benet, L. "Predicting drug disposition via application of BCS: transport/absorption/ elimination interplay and development of a biopharmaceutics drug disposition classification system." *Pharm Res.* 22, no. 1 (2005): 11-23.

Xu, Q., Li, Y., Lü, X. "Investigation on influencing factors of 5-HMF content in Schisandra." *J Zhejiang Univ Sci B.* 8, no. 6 (2007): 439-45.

Yamamoto, K., Ueno, Y., Mizoi, Y., Tatsuno, Y. "Genetic polymorphism of alcohol and aldehyde dehydrogenase and the effects on alcohol metabolism." *Arukoru Kenkyuto Yakubutsu Ison.* 28, no. 1 (1993): 13-25.

Yan, R., Zhu, C., Chen, J. "Oxidation product(s) in acetaldehyde reacts with NAD(P)H and interferes with assay of alcohol dehydrogenase." *Anal Biochem.* 164, no. 2 (1987): 362-6.

Yin, S. "Alcohol dehydrogenase: enzymology and metabolism." *Alcohol Alcohol Suppl.* 2 (1994): 113-9.

Yong, G., Zhang, Y., Ying, J. "Efficient catalytic system for the selective production of 5-hydroxymethylfurfural from glucose and fructose." *Angew Chem Int Ed Engl.* 47, no. 48 (2008): 9345-8.

Zaugg, R., Walder, J., Klotz, I. "Schiff base adducts of hemoglobin. Modifications that inhibit erythrocyte sickling." *JBC* 252, no. 23 (1977): 8542-8548.

Zhang, C., Li, X., Lian, L., Chen, Q., Abdulmalik, O., Vassilev, V., Lai, C., Asakura, T. "Anti-sickling effect of MX-1520, a prodrug of vanillin: an in vivo study using rodents." *Br J Haematol. 2004 Jun;125(6):788-95.* 125, no. 6 (2004): 788-95.

Zhang, X., Chan, C., Stamp, D., Minkin, S., Archer, M., Bruce, W. "Initiation and promotion of colonic aberrant crypt foci in rats by 5-hydroxymethyl-2-furaldehyde in thermolyzed sucrose." *Carcinogenesis.* 14, no. 4 (1993): 773-5.

APPENDIX A

DATA FOR CONCENTRATION DEPENDENCY KINETICS USING HEPATIC CYTOSOL

Table A- 1. Ethanol concentration-dependency metabolic curve in human hepatic cytosol.

Concentration (mM)	Velocity (nmol/min/mg)
0.000	0.112 (0.013)
0.255	0.256 (0.008)
0.510	0.363 (0.023)
1.53	0.496 (0.032)
3.06	0.613 (0.013)
6.12	0.708 (0.031)
12.2	0.736 (0.001)
24.5	0.835 (0.042)

Table A- 2. DN concentration-dependency metabolic curve in human hepatic cytosol.

Concentration (nM)	Velocity (nmol/min/mg)
0.000	0.083 (0.199)
3.30	2.03 (0.110)
8.25	2.07 (0.082)
24.8	3.21 (1.94)
66.0	3.46 (0.543)

Table A- 3. Acetaldehyde concentration-dependency metabolic curve in human hepatic cytosol.

Concentration (µM)	**Velocity (nmol/min/mg)**
4.12	1.92 (0.309)
12.4	2.39 (0.317)
37.0	2.08 (0.424)
111	2.62 (1.13)
333	4.38 (2.24)
33333	4.41 (0.603)

Table A- 4. 5-HMF concentration-dependency metabolic curve in human hepatic cytosol.

Concentration (mM)	Velocity (nmol/min/mg)
0.000	1.86 (0.622)
1.50	2.01 (0.155)
3.01	2.40 (0.340)
6.02	2.23 (0.050)
12.0	3.78 (0.723)
24.1	4.89 (0.297)
48.1	7.90 (0.584)
96.3	11.9 (0.918)

Table A- 5. 5-HMF concentration-dependency metabolic curve in mouse hepatic cytosol.

Concentration (mM)	Velocity (nmol/min/mg)
0.000	0.815 (0.511)
1.50	1.49 (0.284)
3.01	2.02 (0.357)
6.02	2.83 (1.13)
12.0	4.48 (1.98)
24.1	7.78 (1.12)
48.1	9.54 (0.633)
96.3	12.6 (2.83)

Table A- 6. 5-HMF concentration-dependency metabolic curve in rat hepatic cytosol.

Concentration (mM)	Velocity (nmol/min/mg)
6	2.49 (0.682)
12	2.34 (0.788)
16	7.07 (2.69)
24	5.67 (0.637)
32	7.23 (1.71)
48	10.7 (2.59)
64	13.8 (1.35)
96	14.9 (2.13)

Table A- 7. 5-HMF concentration-dependency metabolic curve in dog hepatic cytosol.

Concentration (mM)	Velocity (nmol/min/mg)
0.000	1.36 (1.25)
1.50	2.28 (0.819)
3.01	4.31(3.98)
6.02	4.47 (3.10)
12.0	4.02 (0.482)
24.1	8.43 (1.97)
48.1	9.90 (0.259)
96.3	13.4 (1.61)

APPENDIX B

DATA FOR 5-HMF *IN-VITRO* PROTEIN BINDING

Table B- 1. Time-dependency of 5-HMF (0.0000079) binding to hemoglobin (0.000217 M).

Time (hours)	Unbound 5-HMF (M)
0	0.0000065
2.6	0.0000046
6.8	0.0000043
25	0.0000035
30	0.0000037

Table B- 2. Time-dependency of 5-HMF (0.000063 M) binding to hemoglobin (0.000217 M).

Time (hours)	Unbound 5-HMF (M)
0	0.000060 (0.00000002)
0.40	0.000059 (0.00000043)
1.2	0.000056 (0.00000025)
3.0	0.000049 (0.00000005)
3.9	0.000046
6.5	0.000043

Table B- 3. Time-dependency of 5-HMF (0.000397 M) binding to hemoglobin (0.000217 M).

Time (hours)	Unbound 5-HMF (M)
0.03	0.000296
1.0	0.000264
3.0	0.000250
6.0	0.000216

Table B- 4. Time-dependency of 5-HMF (0.000037 M) binding to albumin (0.000202 M).

Time (hours)	Unbound 5-HMF (M)
0.07	0.000034
0.58	0.000032
1.3	0.000032
3.0	0.000031

Table B- 5. Time-dependency of 5-HMF (0.0000079 M) binding to albumin (0.000063 M).

Time (hours)	Unbound 5-HMF (M)
0.0	0.00000696
2.6	0.00000691
6.8	0.00000687
24.9	0.00000691
30.2	0.00000684

Table B- 6. Time-dependency of 5-HMF (0.0000198 M) binding to albumin (0.000063 M).

Time (hours)	Unbound 5-HMF (M)
0.0	0.0000197
0.4	0.0000197
1.1	0.0000191
2.8	0.0000189
5.2	0.0000187

Table B- 7. Time-dependency of 5-HMF (0.000150 M) binding to albumin (0.000063 M).

Time (hours)	Unbound 5-HMF (M)
0.03	0.000143
0.97	0.00013
3.0	0.000128
6.1	0.000135
8.7	0.000138
25	0.000137

APPENDIX C

SCIENTIST MODELS

```
// In-Vitro 5-HMF Binding to Hemoglobin
//  Version 1.0
//  JV, TO, July 29, 2009
//
//  Assuming bimolecular, reversible interaction
//  concentrations in M
//   k1 in M*hr-1
//   k-1 in hr-1
//
IndVars: T
DepVars: HMF, Hb, HbHMF
Params: k1, kmin1, Hb0, HMF0
// Diff Equations
HMF'=kmin1*HbHMF-k1*Hb*HMF
HbHMF'=k1*Hb*HMF-kmin1*HbHMF
// Mass Balance
Hb=Hb0-HbHMF
// IC
t=0
HMF=HMF0
HbHMF=0
***
```

```
// In-Vitro 5-HMF in RBC suspension
//  Version 1.0
//  JV, TO, Dec 27, 2009
//
//  Assuming bimolecular, reversible interaction
//  concentrations in M
//   k1 in M*hr-1
//   k-1 in hr-1
//   kmet in hr-1
//   kmembrane in fraction
//
IndVars: T
DepVars: HMF, Hb, HbHMF, HMFmet
Params: k1, kmin1, Hb0, HMF0, kmet, kmembrane
// Diff Equations
HMF'=kmin1*HbHMF-k1*Hb*HMF-kmet*HMF
HbHMF'=k1*Hb*HMF-kmin1*HbHMF
HMFmet'=kmet*HMF
// Mass Balance
Hb=Hb0-HbHMF
// IC
t=0
HMF=HMF0-kmembrane*HMF0
HbHMF=0
HMFmet=0
***
```

```
// In-Vitro 5-HMF in Blood
//  Version 1.0
//  JV, TO, Dec 28, 2009
//
//  Assuming bimolecular, reversible interaction
//  concentrations in M
//   k1 in M*hr-1
//   k-1 in hr-1
//   kmet in hr-1
//   kmembrane and khsa in fraction
//
IndVars: T
DepVars: HMF, Hb, HbHMF, HMFmet
Params: k1, kmin1, Hb0, HMF0, kmet, kmembrane, khsa
// Diff Equations
HMF'=kmin1*HbHMF-k1*Hb*HMF-kmet*HMF
HbHMF'=k1*Hb*HMF-kmin1*HbHMF
HMFmet'=kmet*HMF
// Mass Balance
Hb=Hb0-HbHMF
// IC
t=0
HMF=HMF0-kmembrane*HMF0-khsa*HMF0
HbHMF=0
HMFmet=0
***
```

VITA

Taghrid Obied was born in Amman, Jordan, on April 28, 1980, and she is holding a Jordanian nationality. She received her B.Sc. in Pharmacy with an excellent GPA, 3.94, from the University of Jordan in 2003. During her high school and undergraduate study, Taghrid was honored with DMS high school and the University of Jordan awards for her excellent performance. Taghrid worked in the pharmaceutical industry for two years (2003-2005) as a regulatory affairs officer. In 2005, Taghrid was granted a Fulbright pre-doctoral scholarship (sponsored by the US Department of State) to pursue her MS degree at Virginia Commonwealth University, which she received in 2007 with an excellent GPA, 3.90. In addition, in 2009 Taghrid was awarded VCU Graduate Student Travel Grant to attend the ACCP 2009 Annual Meeting and Exposition and Amgen Travel Award to attend the AAPS 2009 Annual Meeting and Exposition. Five of Taghrid's posters were accepted for national meetings presentation. She is a member of the American Association of Pharmaceutical Scientists (AAPS), the American College of Clinical Pharmacology (ACCP), American Society of Clinical Pharmacology and Therapeutics (ASCPT), and the Phi-Kappa-Phi Honor Society.